



National Library
of Canada

Acquisitions and
Bibliographic Services Branch

395 Wellington Street
Ottawa, Ontario
K1A 0N4

Bibliothèque nationale
du Canada

Direction des acquisitions et
des services bibliographiques

395, rue Wellington
Ottawa (Ontario)
K1A 0N4

Your file / Votre référence :

Our file / Notre référence :

NOTICE

The quality of this microform is heavily dependent upon the quality of the original thesis submitted for microfilming. Every effort has been made to ensure the highest quality of reproduction possible.

If pages are missing, contact the university which granted the degree.

Some pages may have indistinct print especially if the original pages were typed with a poor typewriter ribbon or if the university sent us an inferior photocopy.

Reproduction in full or in part of this microform is governed by the Canadian Copyright Act, R.S.C. 1970, c. C-30, and subsequent amendments.

AVIS

La qualité de cette microforme dépend grandement de la qualité de la thèse soumise au microfilmage. Nous avons tout fait pour assurer une qualité supérieure de reproduction.

S'il manque des pages, veuillez communiquer avec l'université qui a conféré le grade.

La qualité d'impression de certaines pages peut laisser à désirer, surtout si les pages originales ont été dactylographiées à l'aide d'un ruban usé ou si l'université nous a fait parvenir une photocopie de qualité inférieure.

La reproduction, même partielle, de cette microforme est soumise à la Loi canadienne sur le droit d'auteur, SRC 1970, c. C-30, et ses amendements subséquents.

UNIVERSITY OF ALBERTA

**GEOPHYSICAL WELL LOG ANALYSIS IN SHALY SANDSTONE FOR
HYDROGEOLOGICAL PURPOSES**

BY

LIANE SCHLICKENRIEDER



A THESIS

**SUBMITTED TO THE FACULTY OF GRADUATE STUDIES AND RESEARCH
IN PARTIAL FULFILLMENT OF THE REQUIREMENTS FOR THE DEGREE OF
MASTER OF SCIENCE**

DEPARTMENT OF GEOLOGY

EDMONTON, ALBERTA

SPRING 1994



National Library
of Canada

Bibliothèque nationale
du Canada

Acquisitions and
Bibliographic Services Branch

Direction des acquisitions et
des services bibliographiques

395 Wellington Street
Ottawa, Ontario
K1A 0N4

395, rue Wellington
Ottawa (Ontario)
K1A 0N4

Author's name - Votre référence

Author's name - Votre référence

The author has granted an irrevocable non-exclusive licence allowing the National Library of Canada to reproduce, loan, distribute or sell copies of his/her thesis by any means and in any form or format, making this thesis available to interested persons.

L'auteur a accordé une licence irrévocable et non exclusive permettant à la Bibliothèque nationale du Canada de reproduire, prêter, distribuer ou vendre des copies de sa thèse de quelque manière et sous quelque forme que ce soit pour mettre des exemplaires de cette thèse à la disposition des personnes intéressées.

The author retains ownership of the copyright in his/her thesis. Neither the thesis nor substantial extracts from it may be printed or otherwise reproduced without his/her permission.

L'auteur conserve la propriété du droit d'auteur qui protège sa thèse. Ni la thèse ni des extraits substantiels de celle-ci ne doivent être imprimés ou autrement reproduits sans son autorisation.

ISBN 0-612-11357-4

Canada


UNIVERSITY OF ALBERTA

RELEASE FORM

NAME OF AUTHOR: Liane Schlickenrieder
TITLE OF THESIS: Geophysical Well Log Analysis
in Shaly Sandstone for
Hydrogeological Purposes
DEGREE: Master of Science
YEAR THIS DEGREE GRANTED: 1994

Permission is hereby granted to the University of Alberta Library to reproduce single copies of this thesis and to lend or sell such copies for private, scholarly or scientific research purposes only.

The author reserves all other publication and other rights in association with the copyright in the thesis, and except as hereinbefore provided neither the thesis nor any substantial portion thereof may be printed or otherwise reproduced in any material form whatever without the author's prior written permission.




184 Willow Way
Edmonton, Alberta
Canada T5T 1C8

March 9, 1994

UNIVERSITY OF ALBERTA

FACULTY OF GRADUATE STUDIES AND RESEARCH

The undersigned certify that they have read, and recommend to the Faculty of Graduate Studies and Research for acceptance, a thesis entitled *Geophysical Well Log Analysis in Shaly Sandstone for Hydrogeological Purposes* submitted by *Liane Schlickenrieder* in partial fulfillment of the requirements for the degree of Master of Science.



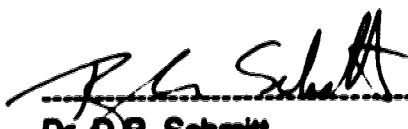
Dr. J. Tóth,
Supervisor



Dr. C.A. Mendoza



Dr. T.F. Moslow



Dr. D.R. Schmitt

Date: 1996 March 9

Dedication

**gewidmet
meinen Eltern
(to my parents)**

Abstract

Geophysical well logs are continuous records of physical parameters of the fluid-filled rock formation beyond the borehole. The measurements may be interpreted in terms of lithology, or transformed into shale volume, porosity, permeability, or other petrophysical properties. This study reviewed and compared a selection of conventional methods of acquisition and analysis of geophysical well logs to examine their potential use for hydrogeological investigations in shaly sandstone.

The numerical algorithms and cross-plotting methods involved logs of total gamma radiation, natural gamma ray spectroscopy, neutron porosity, bulk density, density porosity, photoelectric cross-section index, sonic traveltime and free fluid index, complemented by core measurements of porosity and permeability. These analytical tools were applied to two suites of well logs recorded in south-eastern Alberta over an Upper Cretaceous section of sandstone, shaly sandstone and shale. The procedures of implementation were modified to cope with the 700 m long interval of continuous data records in digitized format with the aid of computer spreadsheet programmes. The empirical algorithms were applied above the limits of shale volume or clay content implied by the original derivations.

Comparisons of methods, on theoretical basis and in terms of computed results of porosity, proved the empirical relationships containing the same input parameters as closely related. Excessive clay mineralogy did not invalidate the analytical algorithms. All seven core-calibrated, log-derived porosity profiles compared well with each other over the full range of calculated magnitudes of 3 to 27 %, and also with porosities measured on core samples from adjacent townships. However, more detailed comparative data sets are necessary for the reliable evaluation of accuracy. Two unrelated methods of determination were used to generate closely related, continuous permeability profiles with calculated values ranging from 10^{-2} to 10^3 md. The method based on the free fluid index was favoured over the one relying on statistical calibration with limited core porosity and core permeability, because the more direct approach of calculation allows for fewer uncertainties and recurring errors. The accuracy of the permeability profiles could also not be evaluated unambiguously due to an insufficient number of core values for comparison.

In conclusion, geophysical well logging methods may definitely contribute qualitative and quantitative information to hydrogeological investigations in shaly sandstone. To accommodate the specific conditions of geology or data availability, the conventional methods of analysis and interpretation may require adaptations.

Acknowledgements

First and foremost I would like to express my sincere gratitude and appreciation to my supervisor, Dr. József Tóth, for providing me with the opportunity to study the basics of hydrogeology and to learn overcome the challenges of independent research. I have greatly valued Dr. Tóth's inspiration and enthusiasm for my thesis project, the objectives of which were believed by many to be impossible to achieve.

I would also like to thank my committee members, Dr. Tom Moslow, Dr. Doug Schmitt and especially Dr. Carl Mendoza for the time and effort invested in improving my thesis.

A big Thank You goes to Ross Crain of Spectrum 2000 Mindware Ltd. in Rocky Mountain House, who offered a big hand when I first plunged into the "real" world of well log interpretation. In the last stages of the project, Ross drew upon his immense experience as well log analyst and instructor to provide much appreciated criticism.

Billy-Dean Gibson of Schlumberger of Canada provided the final link in the search for an appropriate suite of well logs, and also introduced me to the potentials of the nuclear magnetism log.

AEC Oil and Gas Company of Calgary graciously released the then confidential data set.

Funding was supported by the Department of Geology in form of Teaching and Research Assistantships and by NSERC grants held by my supervisor.

Over the years, I enjoyed sharing fun and frustrations with my colleagues of the Hydrogang. Dan Berson proved that all is well that ends well; Allan Fryar served as a model for a determined student aiming for nothing less but perfection; John Horgan shared some dry English humour and moist homemade baking; Morris Maccagno introduced me to an addictive brew called espresso and to South African music; Claus Otto was always there for a gossip session in good old German; Debashish Paul provided encouragement and listening ears when most needed, and added to the international flair at the office; Ben Rostron was my personal advisor for scientific and administrative problems of any sort, and took the worst brunt of friendly abuse; Kriengsak Srisuk spent many late nights at the office entertaining me with Corel Draw magic, Hank Williams tapes, and munchies; David Toop was a challenging class mate for all the courses in first year; and Kent Wilkinson was just a fun guy to have around.

I treasured highly the companionship which fellow Pembinites and friends all over the world provided through the sunny, the rainy and the dark days.

This thesis would not have happened, were it not for my parents' adventurous spirit and optimism which took me to Alberta. My parents made certain, however, to send me equipped with good helpings of Bavarian perseverance, optimism and humour - black and white!

Thank you all!

Table of Contents

1. Introduction.....	1
2. Theory and Background Information	4
2.1. Hydraulic Conductivity, Permeability and Porosity	4
2.2. Principles of Well Logging.....	9
2.3. Clay Minerals	24
2.4. Data Base	29
2.5. Local Geology.....	32
3. Data Analysis and Interpretation	39
3.1. Data Preparation	41
3.1.1. Well Logs	41
3.1.2. Core Analyses.....	46
3.2. Stratigraphic Correlation.....	49
3.3. Lithology.....	51
3.4. Shale Volume	65
3.5. Porosity.....	72
3.6. Permeability.....	100
4. Discussion	108
5. Conclusions.....	120
References.....	122
Appendices.....	130
Appendix A: Digitized Log Parameters.....	131
Appendix B: Original Core Data.....	153
Appendix C: Computed Parameters.....	157

List of Tables

Table 2.1: Information and data included in the core of this study's data base (available from the Energy Resource Conservation Board in Calgary, Alberta).....	31
Table 3.1: Core measurements of porosity and maximum permeability of 5-7 and 6-35 averaged with equations 3.1.1 and 3.1.2 over one-metre intervals corresponding to digitizing intervals of logs.....	50
Table 3.2: Depths of tops of stratigraphic units defined on logs of 5-7 and 6-35.....	52
Table 3.3: Depth intervals in which the characteristic signatures of lithology shown in Figure 3.3 are displayed on the logs of 5-7 and 6-35.....	54
Table 3.4: Logging tool responses for a selection of water-wet sedimentary minerals	58
Table 3.5: Shale and sandstone base values used for shale volume analysis	69
Table 3.6: Shale base values used for porosity analysis	74
Table 3.7: Results of regression analyses by the least-squares method for log-derived porosities, expressed in terms of the correlation statistic R-squared, and the y-intercept and slope of the best-fit straight line.....	84
Table 3.8: Comparison of log-derived porosities and core porosity in cored intervals of 5-7	87
Table 3.9: Comparison of log-derived porosities and core porosity in cored intervals of 6-35.....	88
Table 3.10: Results of regression analyses by the least-squares method to establish the dependence of log-derived porosities on core based porosity (independent variable).....	89
Table 3.11: Results of regression analyses by the least-squares method for calibrated log-derived porosities, expressed in terms of the correlation statistic R-squared, and the y-intercept and slope of the best-fit straight line	97
Table 3.12: Collection of porosity and permeability measurements available from core analyses conducted for boreholes in townships adjacent to 017-07W4M and 017-08W4M, and ranges of the log-derived PND2, PND3, PDA, PDC and PBWV (one enveloping range).....	98

Table 3.13: Results of regression analyses by the least-squares method to establish the dependence of the logarithm of the maximum value of core permeability on the core porosity (independent variable), expressed in terms of the correlation statistic R-squared, and the y-intercept and slope of the best-fit straight line.....	102
--	-----

List of Figures

Figure 2.1: Schematic illustration of the apparatus used by H. Darcy for experiments on fluid flow (modified after de Marsily, 1986, p. 59)	5
Figure 2.2: Schematic illustration of the apparatus used by K. Hubbert to study fluid flow through permeable material (modified after Hubbert, 1940, p. 788).....	6
Figure 2.3: Schematic illustration of (a) shale (Nernst, membrane) potential; and (b) liquid-junction (diffusion) potential (modified after Telford et al., 1976, p. 782)	12
Figure 2.4: Schematic illustration of the electrode configuration and current distribution for a dual laterolog in an infinite homogeneous isotropic medium. The sonde is split into two halves for the purpose of presentation; the deep (LLD) and shallow (LLS) systems operate at different frequencies allowing simultaneous recording (modified after Suau et al., 1972, p. 3).....	13
Figure 2.5: (a) Characteristic emission spectra produced by the nuclear disintegration of naturally occurring elements of the ^{238}U and ^{232}Th series, and the ^{40}K isotope (approximate adaptation after Tittman, 1986, p. 51)	16
Figure 2.6: Schematic illustrations of the three modes of interaction between gamma rays and electrons: (a) Compton scattering, (b) photo conversion, and (c) electron-positron pair production (modified after Helander, 1983, p. 172).....	17
Figure 2.7: Schematic illustration of the borehole compensated sonic tool in the borehole showing the arrangement of transmitters and receivers, and fastest travel paths of P-waves (modified after Tittman, 1986, p. 154).....	20
Figure 2.8: Schematic illustration of the motions undergone by a proton as a strong external magnetic field is applied, prompting the proton's axis of magnetic moment to leave its position of alignment with the Earth's magnetic field for a new position of alignment with the external magnetic field (modified after Wessells and Hopson, 1988).....	22
Figure 2.9: Schematic illustrations of (a) clean sandstone, and the three types of shale distribution in sandstone: (b) laminar shale, (c) structural shale, and (d) dispersed shale and the associated formation models (modified after Bateman, 1985, p. 537)	26

Figure 2.10: Schematic illustrations of the three modes of dispersion of authigenic clay minerals: (a) pore lining, (b) pore filling, and (c) pore bridging (modified after Ellis, 1987, p. 445).....	27
Figure 2.11: Location maps of the two study wells 5-7 and 6-35 at 05-07-017-07W4M and 06-35-017-09W4M, respectively	30
Figure 2.12: Geological time scale showing relative position of Cretaceous period (adapted in part from Press and Siever, 1982, inside cover)	33
Figure 2.13: Representative stratigraphic section compiled of units defined on well logs for locations 05-07-017-07W4M and 06-35-017-09W4M (modified after Rudkin, 1970; and Williams and Burk, 1970)	35
Figure 3.1: Illustration showing true log values recorded in thick beds, and apparent log values recorded in thin beds whose thickness is less than the vertical resolution of the logging tool.....	43
Figure 3.2: Comparison of the original and the digitized signatures over an arbitrary interval of the neutron porosity, density porosity and photoelectric cross-section curves of 5-7	44
Figure 3.3: Schematic illustration of the well logs at 05-017-07W4M and 06-35-017-09W4M in response to lithology and gas. Depth ranges at which these signatures are seen on the actual logs are listed in Table 3.3.....	53
Figure 3.4: Cross plots of (a) potassium concentration (K) versus photoelectric cross-section index (Pe), and of (b) the ratio of thorium to potassium concentration (Th/K) versus photoelectric cross-section index (Pe) for the identification of clay types at 05-07-017-07W4M (identification cross-plots adapted after Schlumberger, 1968, p. 52).....	60
Figure 3.5: Cross plots of neutron porosity versus density porosity showing (a) reference lines for three types of shale distribution (after Brock, 1966, p. 193), and data of 5-7 for intervals corresponding to the definition of shale base values.....	63
Figure 3.6: Cross plots of neutron porosity versus density porosity showing (a) reference lines for three types of shale distribution (after Brock, 1966, p. 193), and data of 6-35 for intervals corresponding to the definition of shale base values.....	64
Figure 3.7: Comparative cross plots of shale volumes determined from the total gamma radiation log (VSHG) and the separation between the neutron porosity and density porosity curves (VSHND), for (a) 5-7 and (b) 6-35	70

Figure 3.8: Cross plots of core based porosity versus log-derived porosities for the cored interval of the Bow Island Formation of 5-7	90
Figure 3.9: Cross plots of core based porosity versus log-derived porosities for the cored interval of the Basal Colorado Sandstone of 5-7	91
Figure 3.10: Cross plots of core based porosity versus log-derived porosities for the cored interval of the Bow Island Formation of 6-35	93
Figure 3.11: Cross plots of core based porosity versus log-derived porosities for the cored interval of the Basal Colorado Sandstone of 6-35	94

List of Logs

(in back pocket)

Set A1: Digitized versions of raw data logs for 5-7:

- GR, SP
- PHID, PHIN, PEF
- FFI, DENS
- DTL
- LLD, LLS

Set A2: Digitized versions of raw data logs for 6-35:

- GR, SP
- PHID, PHIN, PEF
- FFI, DENS
- DTL
- LLD, LLS

Set A3: Digitized versions of representative shallow logs:

- SP
- GR

Set B1: Computed curves for 5-7:

- VSH
- PHIEDA, PHIEDC
- PHIES, PHIEBVW
- PHIEND2, PHIEND3, PHIENDS
- PDA, PDC
- PS, PBVW
- PND2, PND3, PNDS
- KCN, KNML, KCA

Set B2: Computed curves for 6-35:

- VSH
- PHIEDA, PHIEDC
- PHIES, PHIEBVW
- PHIEND2, PHIEND3, PHIENDS
- PDA, PDC
- PS, PBVW
- PND2, PND3, PNDS
- KCN, KNML, KCA

List of Symbols

Only the symbols applied in equations for spreadsheet computations are included.

BVWSH	= bulk volume water attached to clay minerals in shale
DELTMA	= assumed sonic traveltime in formation matrix
DELTSH	= approximated sonic traveltime in shale
DELTW	= assumed sonic traveltime in mud filtrate
DENS	= digitized bulk density
DENSDC	= assumed density of clay
DENSMA	= assumed density of formation matrix
DENSSH	= approximated bulk density of shale
DENSW	= approximated density of mud filtrate
D_i	= thickness of core represented by an individual porosity measurement
DTL	= digitized sonic traveltime
GR	= digitized total gamma radiation
GR0	= sandstone base value of total gamma radiation
GR100	= shale base value of total gamma radiation
K_{avg}	= core measurement of maximum permeability averaged over one-metre digitizing interval
KCA	= K _{avg} in log form
KCN	= permeability derived from core based transformation of log-derived porosity PND2
KCP	= correction factor for compaction effects on sonic traveltime
K_{maxd}	= individual measurement of maximum permeability on core sample
KNML	= permeability derived from the free fluid index and density porosity
P_{avg}	= core porosity measurement averaged over one-metre digitizing interval
PBWV	= PHIEBVW calibrated with core based porosity values
PDA	= PHIEDA calibrated with core based porosity values
PDC	= PHIEDC calibrated with core based porosity values
PHID	= digitized density porosity
PHIDC	= shale corrected density porosity
PHIDDC	= approximated density porosity of dry clay
PHIDSH	= shale base value of density porosity
PHIEBVW	= porosity derived from the bulk volume water method
PHIEDA	= porosity derived from bulk density log, corrected for shale effects
PHIEDC	= porosity derived from bulk density log, corrected for shale effects
PHIEND2	= porosity derived from cross plot of neutron porosity and density porosity, corrected for shale effects
PHIEND3	= porosity derived from cross plot of neutron porosity and density porosity, corrected for shale effects
PHIENDS	= porosity derived from cross plot of neutron porosity and density porosity, corrected for shale effects
PHIES	= porosity derived from sonic traveltime log, corrected for shale effects and compaction

PHIN	= digitized neutron porosity
PHINC	= shale corrected neutron porosity
PHINDC	= approximated neutron porosity of dry clay
PHINSH	= shale base value of neutron porosity
PHISC	= porosity derived from sonic traveltime log, corrected for shale effects
PHIT	= total porosity derived from the bulk volume water method
P_i	= individual measurement of porosity on core sample
PND2	= PHIEND2 calibrated with core based porosity values
PND3	= PHIEND3 calibrated with core based porosity values
PNDS	= PHIENDS calibrated with core based porosity values
PS	= PHIES calibrated with core based porosity values
S	= slope of best-fit line for PND2 versus KCN, derived from regression analysis of P_{avg} versus K_{avg}
VSH	= final shale volume
VSHG	= shale volume determined from the total gamma radiation log
VSHND	= shale volume determined from the combination of neutron porosity and density porosity
Y	= y-intercept of best-fit line for PND2 versus KCN, derived from regression analysis of P_{avg} versus K_{avg}

1. Introduction

The science of well logging dates back at least to September 5, 1927. On that day Conrad Schlumberger, accompanied by his brother Marcel, applied his adaptation of an electrical surface exploration method in the first series of measurements of resistivity in a borehole in the Pechelbronn Field of France (Johnson, 1962). These measurements were recorded at fixed intervals and the values plotted manually on graph paper against depth. This first and subsequent logs were used primarily by oil prospectors and their drillers for correlation and depth control purposes. To the present, petroleum explorationists have been directly and indirectly responsible for the most significant developments in the acquisition, processing, analysis and interpretation of well logs.

At this time, no geophysical well logging methods exist to directly determine flow parameters like porosity and permeability of the rock volume surrounding the borehole. The application of well logs is restricted to providing in-situ measurements of parameters which are subsequently used in interpretation algorithms solving for approximations of porosity and permeability.

From a hydrogeological point of view, geophysical well log analysis may be employed most effectively in studies involving investigations of cross-formational hydraulic communication. For such studies it is necessary to examine the hydraulic continuity of rock formations, ranging in size up to basinal scales on the order of tens and hundreds of kilometres. A subsurface rock body is said to be hydraulically continuous on a given time scale, if a change in pressure in any of its points can cause a change in any other point, within a time interval measurable on the specified time scale (Tóth, 1980). It

may be extremely difficult to prove hydraulic continuity or to quantify the degree of cross-formational hydraulic communication corresponding to a specified time scale. With interconnected pore space being the primary requirement for hydraulic communication, however, continuous permeability profiles spanning the entire depth of the stratigraphic column under investigation, including tight beds, would allow the evaluation of the potential for hydraulic communication.

Computer modelling is generally employed for thorough investigations of cross-formational hydraulic communication in sedimentary basins. Both porosity and permeability profiles, as well as continuous records of shale volume, may contribute significantly to the definition of boundary conditions and various input parameters to enhance the quality of the final model of flow systems. By considering some of the primary effects of moving groundwater such as dissolution, transport and deposition of inorganic and organic matter, transport of heat and modification of pore pressures, such models find a broad scope of applications in the mining and petroleum industries, hazardous waste containment agencies, groundwater resource developers, etc. (Tóth, 1984).

The petroleum industry is largely responsible for numerous technological advances and analytical techniques of well logging, which serve its specific needs for approximations of porosity and permeability for purposes of formation evaluation. Thus, exploration projects concerned with potential petroleum accumulations tend to be focussed on sandstone or carbonate reservoirs where rock properties can be defined within certain limits and geophysical measurements can be calibrated with reliability and precision. Environmental studies or large-scale basinal studies, for example, commonly lack such spatial uniformity as they incorporate broad ranges of possible lithologies, and specific lithologic endpoints of the calibrations are difficult to define (Paillet and

Crowder, 1993). Such is the case for this thesis project. The mathematical algorithms and the interpretation procedures used have been generated predominantly by or for the petroleum industry; their applicability in hydrogeology is potentially challenged most prominently by an abundance of clay minerals.

In this investigation of the potential use of geophysical well logging in hydrogeology, the objectives are:

- (1) to provide a review and comparison of the most conventional qualitative and quantitative methods of geophysical well log analysis for shaly sandstone lithology, and**
- (2) to apply these methods in the analysis and interpretation of two suites of well logs for lithology and formation correlation, as well as for the generation of continuous shale volume, porosity and permeability profiles.**

2. Theory and Background Information

Some basic theory must be introduced before any actual analysis or interpretation may be performed. Sections 2.1 and 2.2, therefore, provide definitions of key words used in subsequent discussions, and explain scientific principles upon which the majority of analytical and interpretational methods of well logging are based. Section 2.3 draws attention to some particular mineralogical and sedimentary characteristics of clay minerals and the influence of these on well logging. Sections 2.4 and 2.5 contain necessary background information, such as the type of data available for application in this study and the geological setting, for Chapter 3.

2.1. Hydraulic Conductivity, Permeability and Porosity

After experimentation with an apparatus similar to that illustrated in Figure 2.1, Henry Darcy established the following expression (Darcy, 1856):

$$q = k \frac{s}{e} (h + e) . \quad (2.1.1)$$

He defined the variables as: q is the flow rate of water, k is a coefficient of proportionality depending on the permeability of the sand layer, s is the surface area (cross-section) of the sand layer, e is the thickness of the sand layer, and h is the height of water above the sand layer.

Hubbert (1940) proposed that Darcy's proportionality coefficient not only depends on the properties of the medium through which the fluid flows, but also on the properties of the fluid itself. Following experimentation (Figure 2.2) and mathematical derivations, Hubbert introduced Darcy's Law as

$$q = - K \frac{dh}{dl} \quad (2.1.2)$$

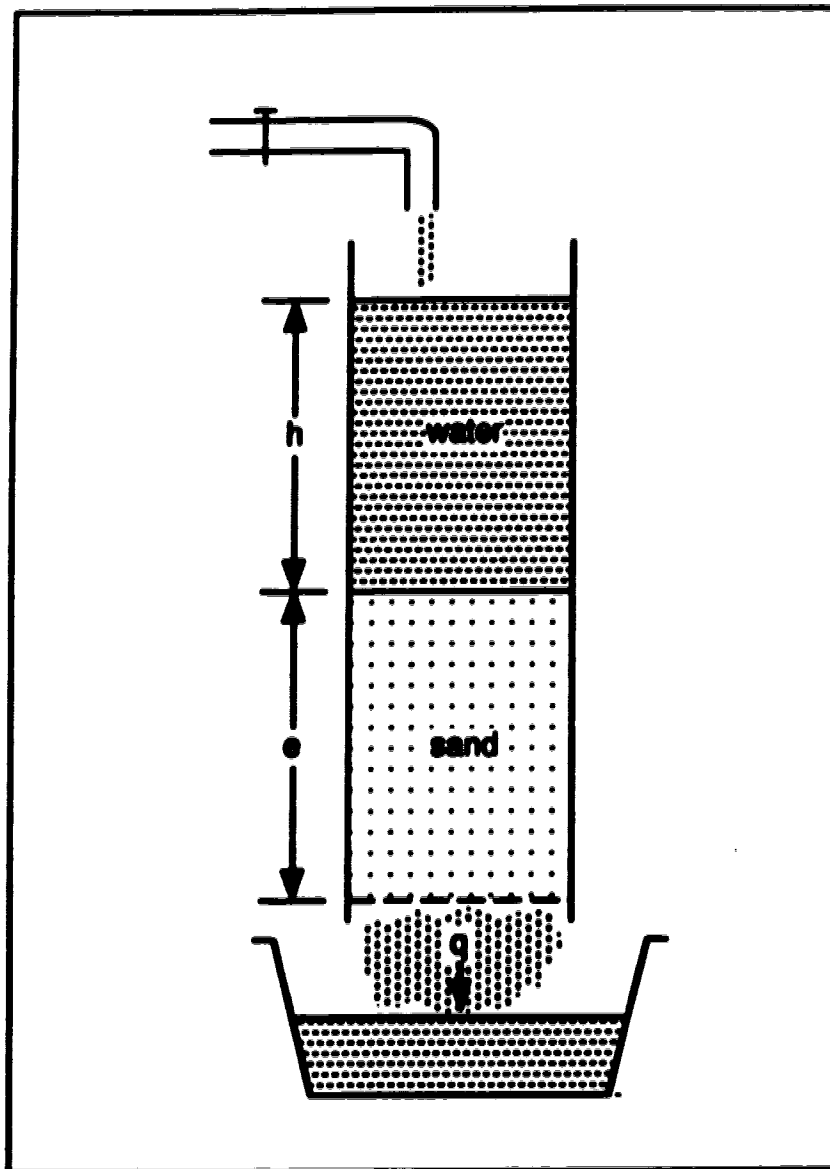


Figure 2.1: Schematic illustration of the apparatus used by H. Darcy for experiments on fluid flow (modified after de Marsily, 1986, p. 59).

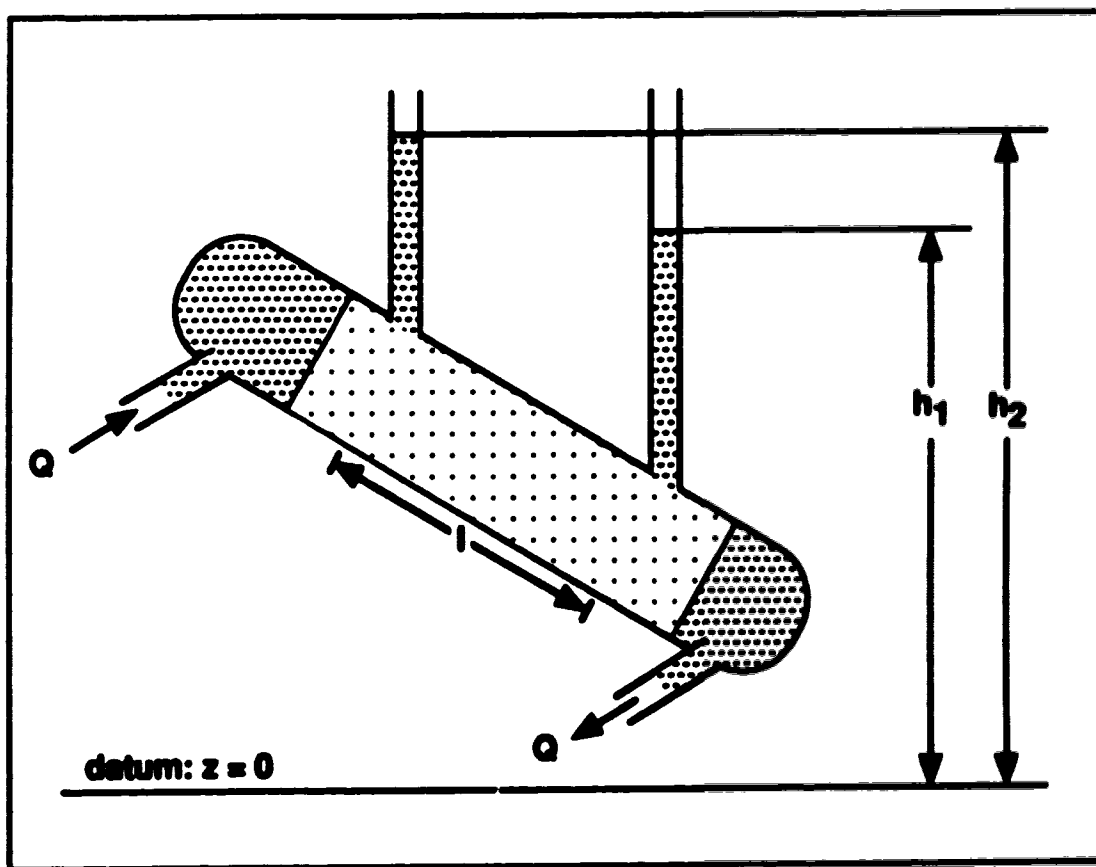


Figure 2.2: Schematic illustration of the apparatus used by K. Hubbert to study fluid flow through permeable material (modified after Hubbert, 1940, p. 788).

$$\text{where } K = \frac{k\rho g}{\mu} . \quad (2.1.3)$$

q is the specific volume discharge, i.e., volume of discharge per unit area, of a fluid of density ρ and dynamic viscosity μ ; $\frac{dh}{dl}$ is the hydraulic gradient expressed as a differential representing the ratio of $(h_2 - h_1)$ to l in Figure 2.2; K is the hydraulic conductivity, sometimes referred to as coefficient of permeability; k is the intrinsic permeability, also called specific permeability or simply permeability; and g is the acceleration due to gravity (de Marsily, 1986). The constant Q in Figure 2.2 represents the inflow and outflow rates or fluxes. The dimension of permeability k is that of a surface area:

$$\begin{aligned} [k] &= \frac{[q] [\mu]}{\left[\frac{dh}{dl}\right] [\rho] [g]} \quad (2.1.4) \\ &= \frac{(\text{length time}^{-1}) (\text{mass length}^{-1} \text{time}^{-1})}{(\text{length length}^{-1}) (\text{mass length}^{-3}) (\text{length time}^{-2})} \\ &= (\text{length}^2) . \end{aligned}$$

Rather than in m^2 , k is commonly measured in darcys (d), where "One darcy is equal to $0.987 \times 10^{-12} \text{ m}^2$, and is defined by a medium for which a flow of $1 \text{ cm}^3/\text{s}$ is obtained through a section of 1 cm^2 , for a fluid of viscosity 1 cP , and a pressure gradient of 1 atm/cm (760 mm Hg/cm)" (de Marsily, 1986, p. 60).

When Darcy's Law is taken from the controlled environment of the laboratory to the rock formations in the field, permeability, and therefore hydraulic conductivity, may show variations in space and with direction of measurement (Freeze and Cherry, 1979). A formation has a homogeneous permeability distribution if permeability is independent of the position within the medium. In contrast, a formation has a heterogeneous permeability distribution if permeability is dependent on the position within the medium. The formation is

isotropic if permeability, at any point within it, is independent of the direction of measurement. If the permeability varies with the direction of measurement, the formation is anisotropic at that point. Any medium of flow may show one of four possible combinations of these properties: (1) homogeneous, isotropic; (2) homogeneous, anisotropic; (3) heterogeneous, isotropic; (4) heterogeneous, anisotropic. Knowledge of the absolute and directional distribution of permeability in a rock formation is important because the distribution influences the geometry and rate of fluid flow.

Considering a model in which the total volume of rock is separated into the volume of the solid portion and the volume of the voids, the total porosity ϕ is defined as

$$\phi = \frac{\text{volume of the voids}}{\text{volume of the rock}} \quad (2.1.5)$$

(de Marsily, 1986). Porosity is a scalar quantity, generally expressed as a dimensionless decimal fraction or a percent.

As a sedimentary rock quality, porosity may be divided further (Sheriff, 1991): primary porosity is the porosity remaining after the sediments have been compacted; additional porosity generated by changes, for example those caused by subsequent chemical action or flow of water through the sediments, is called secondary porosity. In terms of grain size and shape (Freeze and Cherry, 1979), porosity is enhanced in well-sorted sedimentary rocks made of grains of approximately equal size, as well as grains of somewhat spherical shape. A mixture of grain sizes and platy grains tend to lower porosity.

To investigate fluid flow in the rock, the total porosity as defined above must be differentiated from effective porosity (de Marsily, 1986). Water attached to the surface of grains through molecular attraction, water bound in the

molecular structure of minerals, and water contained in dead-end and unconnected pores does not circulate in the rock volume. The complement, free water, may move under the influence of an external force like gravity or a pressure gradient. Effective porosity, also called kinematic porosity, is the ratio of the volume occupied by free fluid to the total volume of rock.

2.2. Principles of Well Logging

A geophysical well log is a record of one or more physical measurements as a function of depth in a borehole (Sheriff, 1991). In this study, as in general log analysts' jargon, the noun 'log' is applied in three senses. Firstly, 'log' refers to an individual curve showing one particular measurement. Secondly, 'log' represents an entire record which may contain curves of several measurements. Thirdly, 'log' is a synonym for 'tool' or 'sonde', i.e., the measuring device. The reader is assured that context here will convey the appropriate meaning.

Logging involves the measuring of physical properties of the material around the borehole (Sheriff, 1991). Although the measurements are made under in-situ conditions, they are affected by disturbances introduced by such processes as drilling, hole maintenance, and previous logging activity. The disturbance caused by invasion has played a role in the development of the majority of acquisition and analysis techniques of well logging. Invasion refers to the penetration of drilling fluid from the well bore into the rock, or in other words, to the displacement of formation fluids as a result of the excess pressure of the mud column with respect to the pressure of the formation fluids (Sheriff, 1991).

As the mud enters permeable zones, its solid particles tend to build a so-called mud cake on the borehole wall, limiting further penetration of the water portion, known as mud filtrate, into the formation. The zone directly behind the mud cake, from which almost all the formation fluids have been displaced by mud filtrate, is called the flushed zone (Telford et al., 1976; Sheriff, 1991). Acquisition and analysis techniques incorporate the effects of invasion on the rock and the fluids it contains, and the depth of the invaded zone. For example, different configurations of the measurement devices inside the logging sonde achieve different depths of investigation. Also referred to as depth of penetration, the depth of investigation is the radius about the logging sonde which contains the material whose properties dominate the measurements (Telford et al., 1976; Sheriff, 1991).

A large number of well logging methods have been developed based on different physical principles. A brief introduction is provided on the basic physical concepts and some specifics on the tools with which the logs used in this study were recorded.

Electrical methods record either the electrical conductivity or resistivity, and the self potential of the formation around the borehole.

The source of the naturally occurring, or spontaneous, potentials in the borehole are electrochemical (shale potential, liquid-junction potential and mineralization potential) and electrokinetic (streaming potential) activities prompted partially by the presence of, and the ionic composition of, formation fluids. Only two processes are of significance in sedimentary lithology without sizable heavy mineral deposits. (1) The shale (Nernst or membrane) potential is a result of shale's permeability to sodium cations (Na^+) and relative impermeability to chloride anions (Cl^-). Sodium cations pass from saline

formation water in permeable beds into adjacent shales which act as membranes, then into the fresh-water mud - or vice versa from mud to formation water if their relative salinities are the reverse (Figure 2.3 a)). (2) The liquid-junction (diffusion) potential is generated at the interface between the mud filtrate in the invaded zone and the formation water beyond. Because of the greater mobility of chloride anions than sodium cations, a net ionic flow will result from the more saline fluid to the fresher fluid. (Figure 2.3 b)). The customary self-potential device records the difference between the potential of a movable electrode down-hole and a fixed reference electrode at the surface. (Telford et al., 1976; Tittman, 1986; Sherrif, 1991)

Sedimentary rock minerals, e.g., silicates, oxides and carbonate, are practically non-conductive, i.e., highly resistive (mostly 1 to $10^6 \Omega\cdot\text{m}$ - ohm-metres). Distilled water, too, is non-conductive. Formation waters are saline solutions, however, containing anions and cations which allow electrical currents to flow. As a result, the conductive properties of shale and sandstone formations are dominated by the rock porosity and the ionic composition of the fluids filling the rock pores. Additional conductivity is introduced by clay minerals. Most resistivity logging methods involve the introduction of currents into the formation around the borehole and the measuring of a potential or voltage. In order to best approximate the true formation resistivity beyond the invaded zone, the dual laterolog, a member of the group of focussed or guard logs, uses two sets of two bucking or guard electrodes plus two sensing electrodes arranged in mirror-image style vertically about the central current emitting electrode. The emitted current is focussed into a horizontal disc which penetrates the formation laterally (Figure 2.4). Two measurements are recorded, the deep laterolog and the shallow laterolog. Both utilize the same physical electrodes and have the same current-beam thickness. The deep

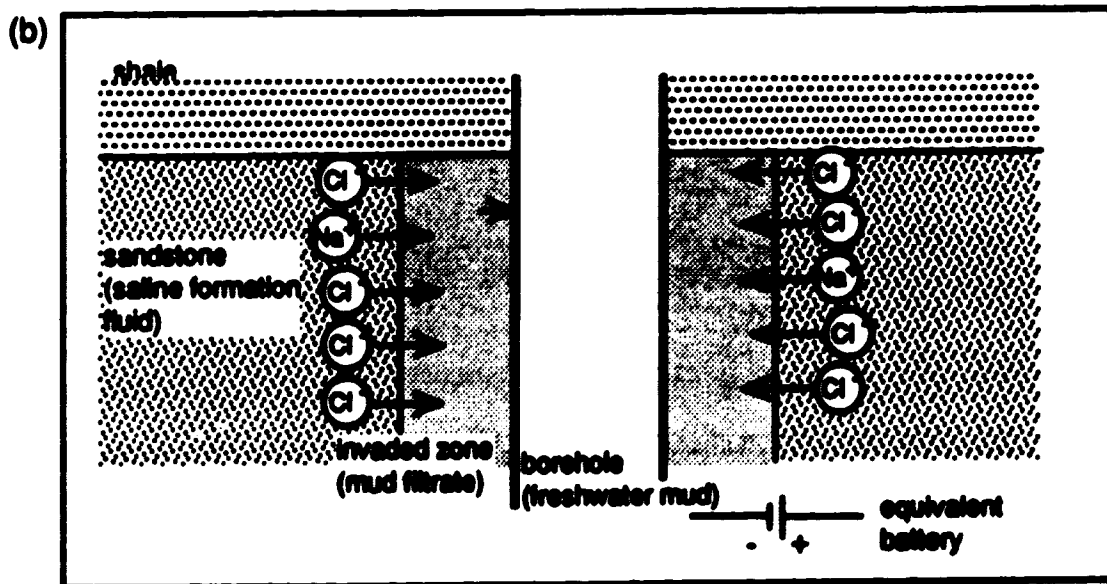
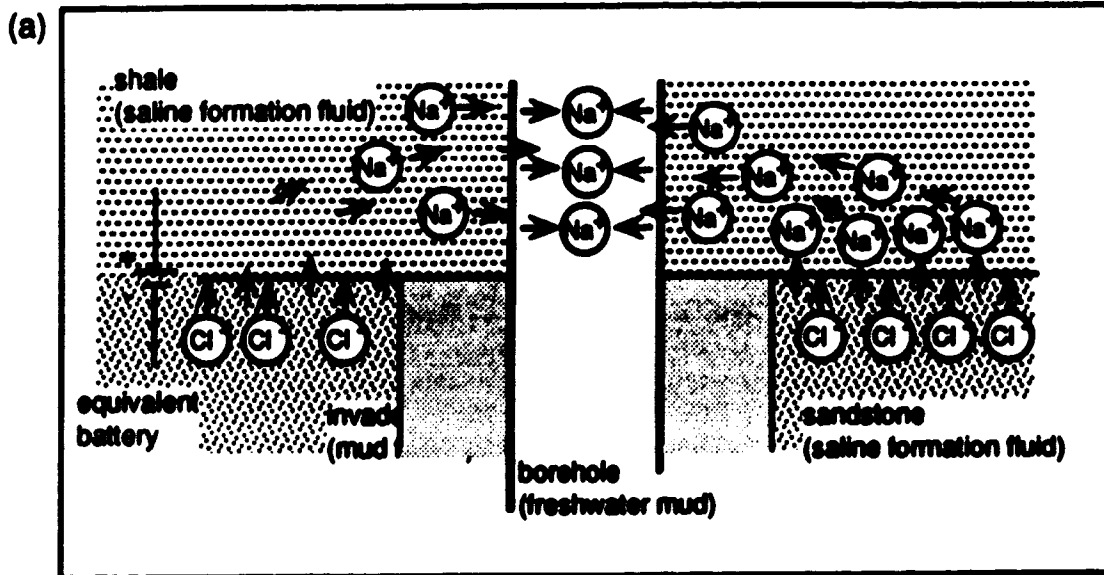


Figure 2.3: Schematic illustration of (a) shale (Nernst, membrane) potential; and (b) liquid-junction (diffusion) potential (modified after Telford et al., 1976, p.782).

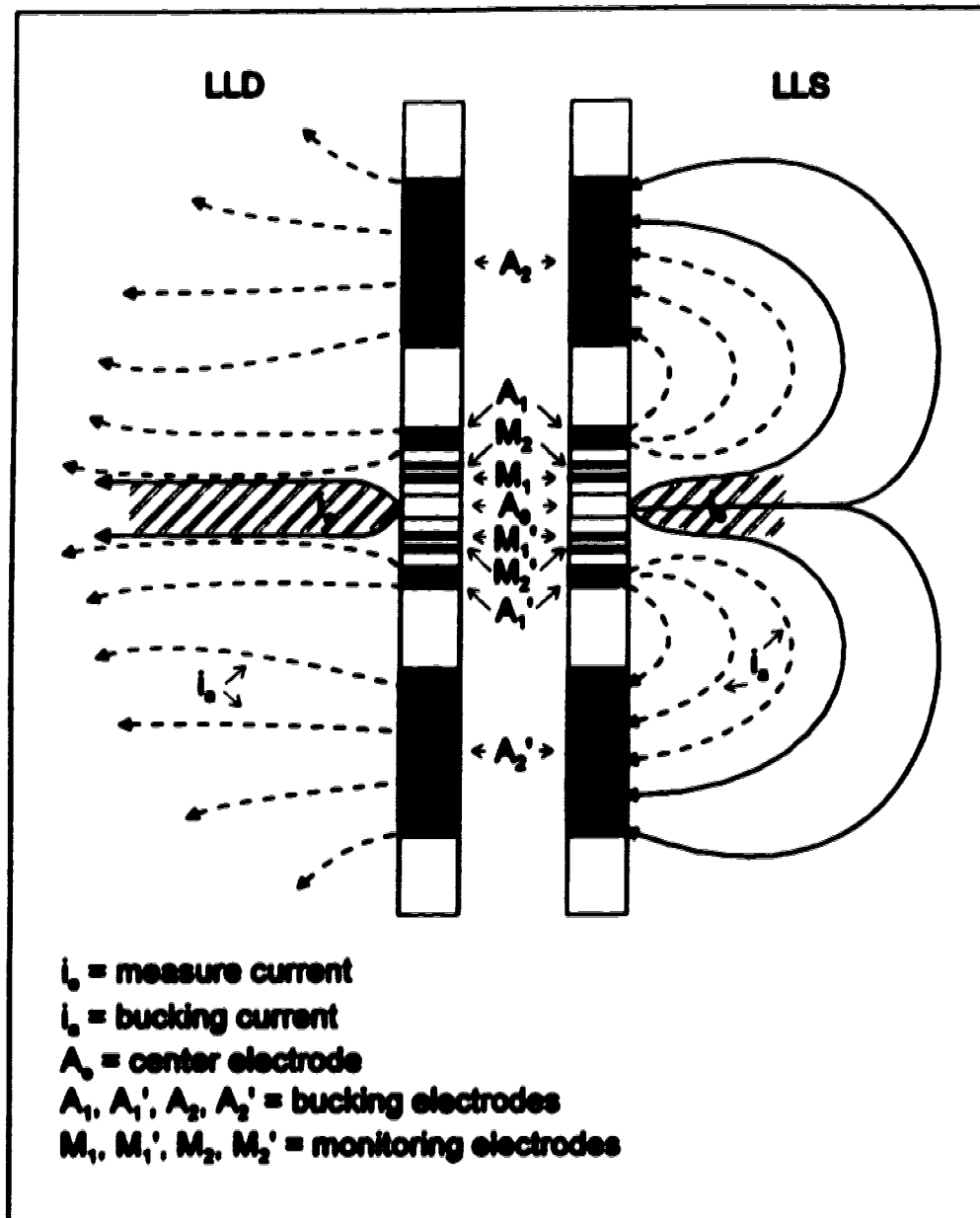


Figure 2.4: Schematic illustration of the electrode configuration and current distribution for a dual laterolog in an infinite homogeneous isotropic medium. The sonde is split into two halves for the purpose of presentation; the deep (LLD) and shallow (LLS) systems operate at different frequencies allowing simultaneous recording (modified after Suau et al., 1972, p. 3).

laterolog uses A_2 and A_2' as long focussing electrodes while the shallow laterolog employs them as return electrodes. By operating at different frequencies, the electrodes are used in different circuit configurations to achieve different depths of penetration. The deep laterolog measurement may penetrate as deeply as 3 m and, thus, generally extends beyond the invaded zone while the shallow laterolog measurement usually records potential in the invaded zone. The microspherically focussed log is frequently attached to the dual laterolog tool to measure the resistivity of the flushed zone. Its shallow depth of penetration is attained with a miniature laterolog-style electrode configuration mounted on a small pad which is forced against the borehole wall. (Tittman, 1986; Sheriff, 1991)

Radioactivity methods represent the largest group of common logging methods. The instruments are designed to measure either natural or induced radiation in the formations surrounding the borehole.

Nearly all of the natural radioactivity encountered in the earth is due to naturally occurring elements of the uranium and thorium series, and the potassium isotope of atomic mass 40 (^{40}K). During nuclear disintegrations ^{40}K , and daughter products of uranium (^{238}U) and thorium (^{232}Th), emit pure electromagnetic radiation of a certain band of wavelength, namely gamma rays. The energy level of the gamma ray represents excess energy and is thus characteristic of a certain decay or nuclear disintegration from one particular isotope to the next in the series. ^{40}K decays directly to the stable isotope argon 40, while ^{238}U and ^{232}Th decay sequentially through a series of isotopes or daughter products before reaching stable lead isotopes (^{206}Pb and ^{208}Pb , respectively). The decay of ^{40}K emits gamma rays of 1.46 MeV. The two decay series emit gamma rays producing entire spectra of energy levels with distinct

peaks at 2.62 MeV (thallium 208 of the ^{232}Th series) and 1.76 MeV (bismuth 214 of the ^{238}U series) (Figure 2.5 a)). The conventional gamma ray log measures the total undifferentiated gamma energy, i.e., abundance of gamma rays of all energy levels. In contrast, natural gamma ray spectroscopy logs employ spectral analysis to identify the presence and abundance of isotopes in discrete energy windows (Figure 2.5 b)). The results are displayed as logs of K (%), U (ppm) and Th (ppm) (all % and ppm by weight) and total gamma energy (API units). The gamma ray sonde contains a scintillation counter to measure the gamma radiation emitted by the surrounding rock volume. The depth of penetration is approximately 0.30 m in sedimentary rock formations. (Telford et al., 1976; Schlumberger, 1989; Sheriff, 1991)

The density or gamma-gamma logging tool emits monoenergetic gamma rays from a concentrated source, e.g., cesium 137 at 0.66 MeV, and records the intensity of gamma rays back-scattered from the formation, with a scintillation counter. The emitted gamma rays interact with the electrons (the negatively charged outer atomic constituents) in the formation materials by three possible mechanisms. (1) The dominant of these is Compton scattering, whereby the incident gamma ray is deflected in its path by an atomic electron and is available for repeated scattering with diminished energy (Figure 2.6 a)). (2) The photoelectric effect (photoconversion) involves the liberation of bound atomic electrons, initiated by the absorption of the incident gamma ray (Figure 2.6 b)). (3) If cobalt 60 serves as source in the tool, some pair production may occur. This is the annihilation of the gamma ray into an electron-positron pair (Figure 2.6 c)). The gamma ray intensity measured by the density tool is proportional to the electron density of the formation and, thus, proportional to bulk formation density. The tool may penetrate up to about 0.15 m beyond the soft surface of the mud cake; however, most of the incoming signal is generated within the first

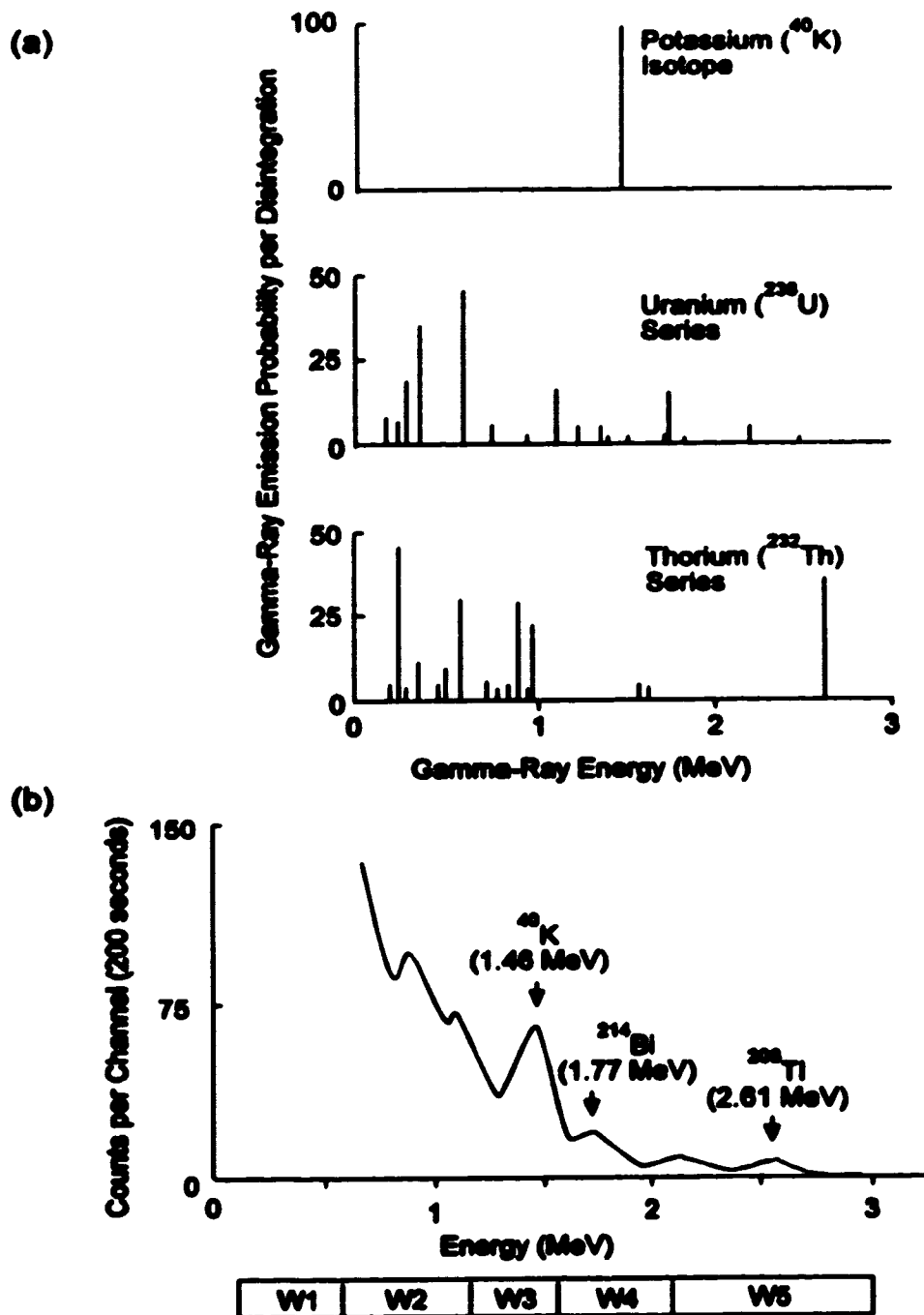


Figure 2.5: (a) Characteristic emission spectra produced by the nuclear disintegration of naturally occurring elements of the ^{238}U and ^{232}Th series, and the ^{40}K isotope (approximate adaptation after Tittman, 1986, p. 51). (b) Natural gamma-ray pulse-height spectrum recorded with a scintillation detector showing distinct energy peaks corresponding to potassium isotope ^{40}K , and daughter products ^{214}Bi and ^{208}Tl of the ^{238}U and ^{232}Th decay series, respectively (approximate adaptation after Tittman, 1986, p. 52). Also shown are approximate energy ranges of windows used for spectral analysis.

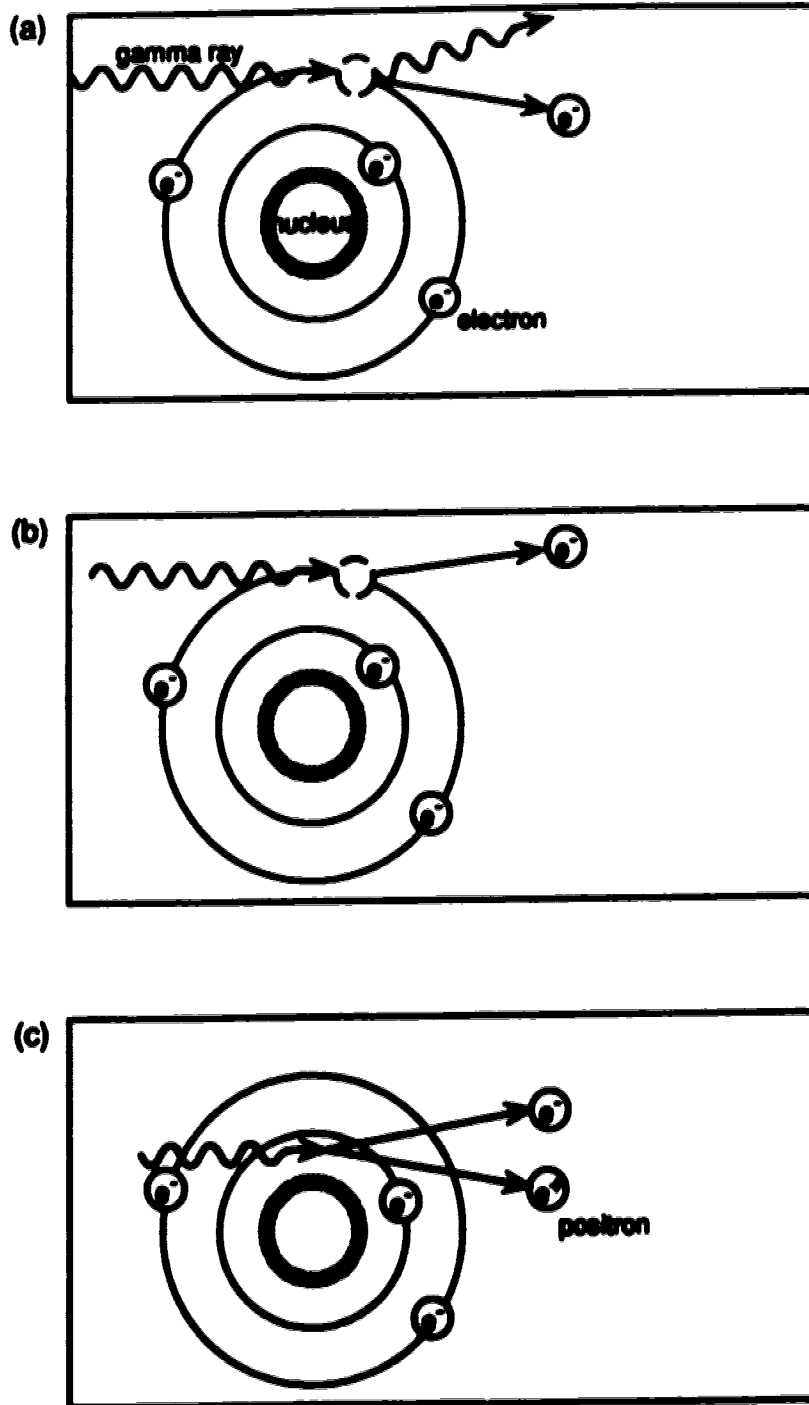


Figure 2.6: Schematic illustrations of the three modes of interaction between gamma rays and electrons: (a) Compton scattering, (b) photo conversion, and (c) electron-positron pair production (modified after Helander, 1983, p. 172).

0.08 to 0.10 m. The compensated formation density log is corrected for mud cake and borehole-wall irregularities. (Telford et al., 1976; Sheriff, 1991)

Because the bulk formation density (ρ_b) is dependent on the density of the matrix of the formation (ρ_{ma}), the density of the fluids contained in the rock framework (ρ_f) and the formation porosity (ϕ), the density log is commonly converted to a density porosity log. The process is purely computational in that the density porosity log is the continuous solution to the equation

$$\phi = \frac{(\rho_{ma} - \rho_b)}{(\rho_{ma} - \rho_f)} . \quad (2.2.1)$$

ρ_{ma} and ρ_f are assumed values for sandstone, limestone or dolomite and fresh water, respectively (Schlumberger, 1989).

The photoelectric absorption log is a curve of the photoelectric absorption cross-section index. An advanced version of the compensated formation density tool, the Litho-Density tool (Mark of Schlumberger; similar tools have been developed by other service companies) records the photoelectric absorption cross-section index in addition to the formation density. The scintillation detector measures radiation in two energy windows which allows discrimination between radiation resulting from Compton scattering (above 0.6 MeV) and photoelectric absorption (below 0.6 MeV). As the photoelectric effect is strongly dependent on the atomic number of elements, the photoelectric absorption cross-section index curve contributes greatly to the identification of lithology. (Telford et al., 1976; Schlumberger, 1989; Sheriff, 1991)

The last tool in the group of radioactivity methods is the neutron logging tool. A source in the neutron logging tool bombards the rock formation with high energy neutrons, i.e., constituents with zero charge which share the nucleus of atoms with protons. Collisions with nuclei of the formation materials slow the

neutrons down to thermal energies. The energy loss is greatest for encounters with nuclei of mass comparable to the neutron mass, mainly hydrogen atoms. The compensated neutron log uses two detectors spaced at different distances from the source to count the thermal neutrons. Subsequent processing of the recorded counts - including correction for borehole effects - produces a continuous porosity index log for a particular matrix lithology (limestone, dolomite or sandstone). Included in this porosity is the effect not only of the hydrogen atoms of fluids which fill the pore space, but also of those bound in the elemental matrix of minerals such as clays. The depth of penetration of the compensated neutron device depends on the formation density: it may be up to about 0.30 m from the borehole if porosity is zero, and as little as 0.20 m in fluid-filled high porosity formations. (Telford et al., 1976; Schlumberger, 1969; Sheriff, 1991)

Elastic-wave propagation methods measure one or several parameters of acoustic wave trains travelling through the formation.

The sonic log (acoustic velocity log, slowness log or continuous-velocity log) records traveltime (transit time) for seismic waves per unit distance, i.e., the reciprocal of velocity. The transmitter in the sonde emits bursts of sonic energy which are propagated by various modes such as P-waves (primary waves, compressional waves, longitudinal waves, etc.), S-waves (secondary waves, shear waves, transverse waves, etc.), and tube or Stoneley waves, i.e., surface waves in a borehole (e.g., Love and Rayleigh waves). The borehole compensated sonic tool consists of two transmitters, which are pulsed alternately and are positioned above and below the two pairs of receivers (Figure 2.7). The fastest travel path in the formation surrounding the borehole is for P-waves. It is only for these "first arrivals" that traveltimes are measured.

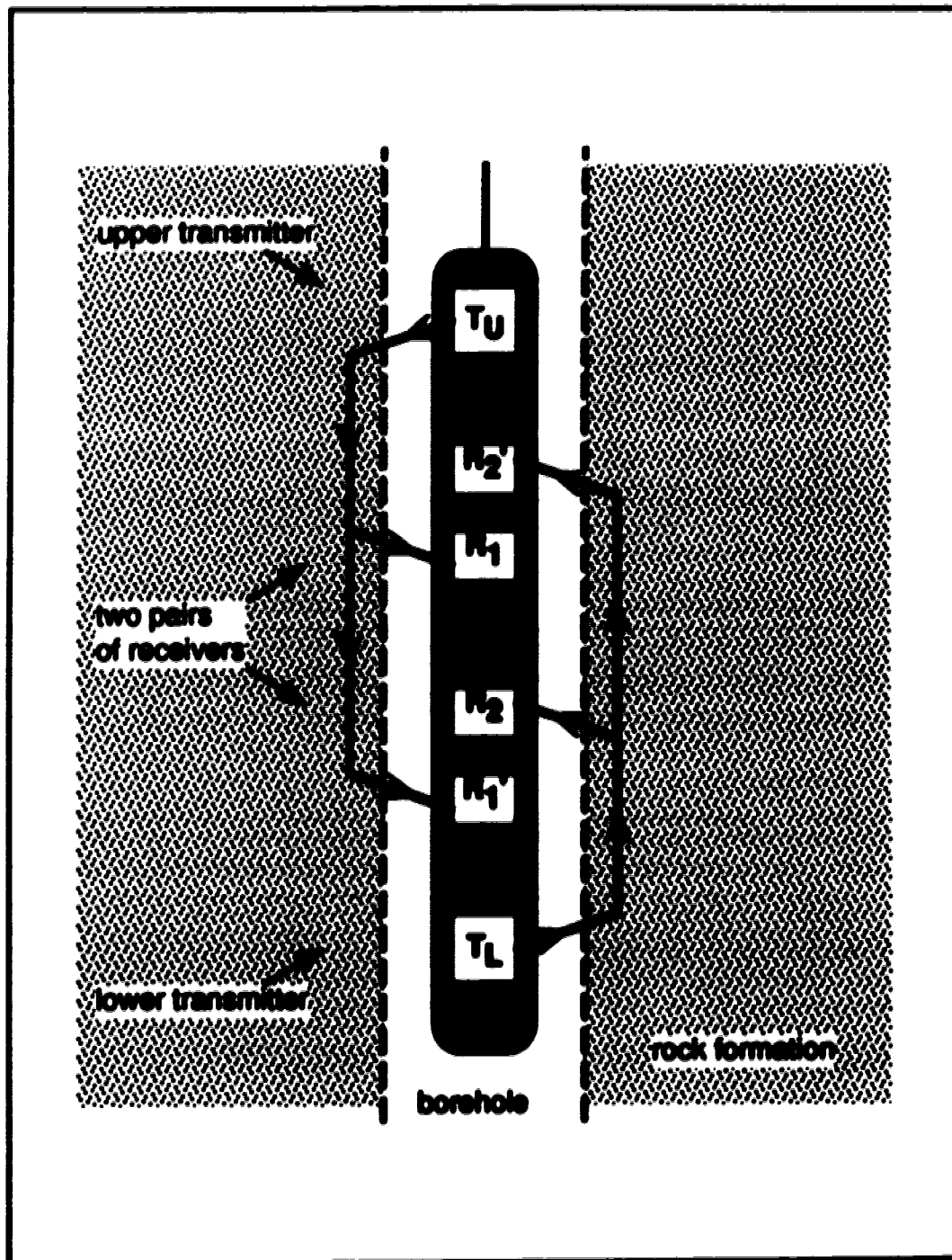


Figure 2.7: Schematic illustration of the borehole compensated sonic tool in the borehole showing the arrangement of transmitters and receivers, and fastest travel paths of P-waves (modified after Tittman, 1966, p. 154).

Compensation for borehole rugosity and tilting of the sonde is attained by averaging the traveltimes values obtained from the two sets of measurements. In the same processing operation, interval traveltimes are integrated to produce a log of total traveltimes. A continuous porosity log may be computed with the empirical time-average equation (also referred to as Wyllie relationship; enunciated in Wyllie et al., 1956):

$$\Delta t = \frac{1}{V} = \frac{(1-\phi)}{V_m} + \frac{\phi}{V_f} \quad (2.2.2)$$

$$\text{or, } \phi = \frac{(\Delta t - \Delta t_{ma})}{(\Delta t_f - \Delta t_{ma})} \quad (2.2.3)$$

where Δt is the recorded formation transit time per unit distance, V is the computed formation velocity, $V_f = \frac{1}{\Delta t_f}$ = velocity in the fluid which fills the pore spaces, $V_m = \frac{1}{\Delta t_{ma}}$ = velocity in the matrix material, and ϕ = matrix porosity.

(Telford et al., 1976; Tittman, 1986; Sheriff, 1991)

A magnetic method, the nuclear magnetism log or free-fluid log is based on the fact that water readily exhibits nuclear magnetic polarization. Since it corresponds to a single proton, hydrogen possesses a magnetic moment or dipole, which tends to align itself with the magnetic field impressed upon the formation by a source in the tool approximately perpendicular to the Earth's magnetic field. In addition, hydrogen possesses an angular momentum coaxial with the magnetic moment. The interaction between the magnetic moment and the applied field causes a torque, which is resisted by the angular momentum vector. The result is a precession of the angular momentum vector about the axis of the applied field (Figure 2.8). The precession frequency (also called Larmor frequency) depends on the intrinsic magnetic moment and the imposed

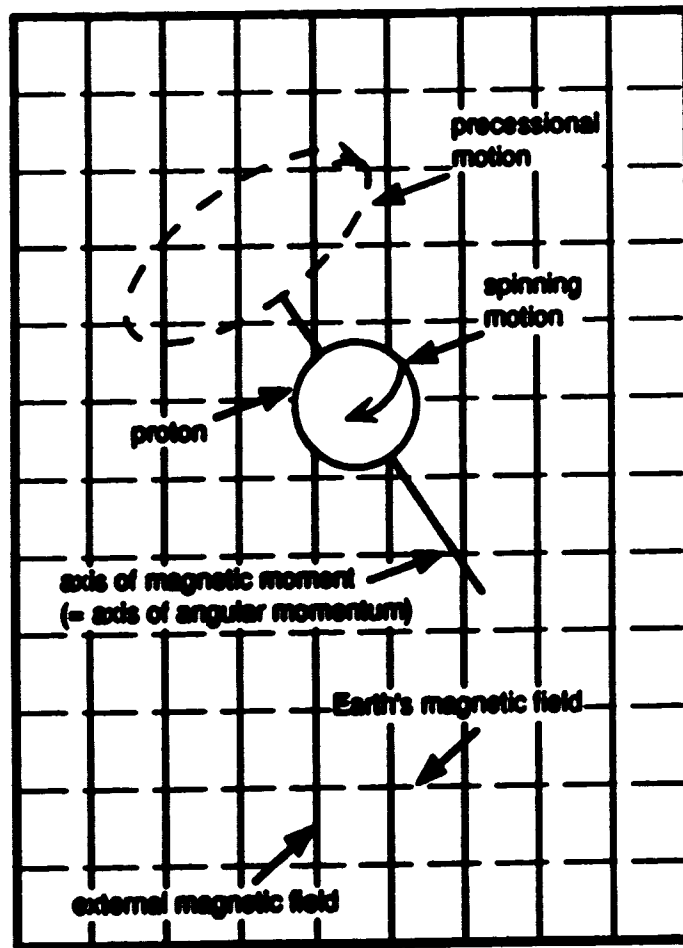


Figure 2.8: Schematic illustration of the motions undergone by a proton as a strong external magnetic field is applied, prompting the proton's axis of magnetic moment to leave its position of alignment with the Earth's magnetic field for a new position of alignment with the external magnetic field (modified after Wessells and Hopeon, 1988).

magnetic field. After a sufficient length of time, on the order of seconds, protons do align with the external field. Once the field is turned off, the polarization process is re-started with a torque and Larmor frequency influenced by the Earth's magnetic field. While gradually returning to the original state, the protons' precession produces a radio-frequency signal whose measured amplitude is proportional to the number of protons in the formation. The constant which characterizes the exponential rate of change of magnetization of a substance with time in the presence of a constant external field is called the spin-lattice relaxation time (T_1). The other time constant, of importance in the second phase of the measuring process, is the thermal relaxation time (T_2^*). As the protons re-align with the primary field, slight inhomogeneities in the Earth's magnetic field cause the spins to dephase. Consequently, T_2^* , the constant governing the rate of polarization decay is less than or equal to T_1 , the constant characterizing the rate of magnetization. T_1 depends on the interaction of the hydrogen protons with their nuclear and atomic environment. For example, T_1 , and hence T_2^* , is very short for protons bound in solids and to surfaces, e.g., water to clay minerals, and contained in doped mud, but relatively long for protons in bulk fluids in the pore space. By delaying the recording of the incoming signal after removing the polarizing field, only the signal generated by precessing protons in bulk fluids is observed. The signal is corrected for effects like magnetic inclination, temperature and borehole size before an extrapolation technique produces the free fluid index. The free fluid index represents the bulk volume occupied by fluids which are free to flow. Since oil and water have similar proton contents, both contribute to the free fluid index. Actually, with the tool's shallow depth of investigation of 0.06 to 0.15 m, the free fluid index responds mostly to filtrate and possibly remaining oil in the invaded zone (Straley et al., 1991). (Ellis, 1967; Schlumberger, 1969; Sheriff, 1991)

The caliper log is a mechanical device which is attached to most logging sondes to measure borehole diameter. Depending on the number of "arms" of the tool, the recorded log may show one or several curves representing the diameter in one or several directions. For comparison, the bit size, i.e., the diameter of the bit on the end of the drill stem, is commonly displayed as a constant on the same grid scale.

2.3. Clay Minerals

In view of the predominantly sandstone and shale lithology in the study area, clay minerals require particular attention as agents affecting logging measurements and permeability distribution.

To avoid a commonly encountered confusion, it is stated explicitly that the terms shale and clay are not to be treated synonymously. Shale is a grain size definition of a fine grained rock of unknown mineral content (Cannon and Coates, 1990, p. 2). "Clay" may also represent particles of particular size ($2.43 \cdot 10^{-1}$ to $3.9 \cdot 10^{-6}$ m particle diameter according to the Wentworth particle size classification; McQuillin et al., 1984, p. 134). However, in this study, the term "clay" refers exclusively to clay minerals. In addition to precipitates and fine clastic particles (feldspars, quartz, etc.), clay minerals normally constitute an average of about 60% of the volume of shales (Kukul and Hill, 1986). The clay minerals are hydrous aluminum silicates with small amounts of magnesium, iron, potassium and other elements arranged in stacked layered platelet structure (Asquith, 1990). The layers or sheets of atoms consist of either octahedral units of oxygen or hydroxyl around aluminum, or of silicon and oxygen in tetrahedral units (Dickey, 1986). Based on the structure of these sheets and the expanded chemical composition, a multitude of clay minerals

have been lumped into four groups: kaolinite, smectite (also referred to as montmorillonite), illite and chlorite.

Clay minerals are distributed in the rock formation in various modes either as individual particles or as constituents of shale (Figure 2.9). Laminar shales are strata (i.e., discrete interspersed layers) of shale a fraction of a centimetre to several centimetres thick, interbedded with sand or sandstone. They occupy both matrix and pore space, thereby reducing effective permeability and porosity. Structural shales occur as shale and clay mineral particles along with sand grains. As the particles remain clear of pore space, they have little effect on permeability and porosity. The most significant decrease in effective permeability and porosity is associated with dispersed shales, where small amounts of authigenic (formed in place) clay minerals are dispersed throughout the system reducing effective permeability and porosity by replacing fluid volume. The three modes of dispersion identifiable with the aid of the scanning electron microscope are pore lining, pore filling and pore bridging (Figure 2.10). (Ellis, 1987; Asquith, 1990)

For the purpose of log interpretation, only those aspects of clay minerals are discussed which influence logging measurements adversely or, in turn, may be detectable and aid analysis. In general, all measurements are affected by the quantity or volume fraction of clay minerals present in the formation.

The chemical composition of the clay minerals causes perturbations of logging measurements. Hydrogen, a prominent member in the form of hydroxyls, as well as in form of trapped water, strongly contributes to the neutron porosity response. The effect may be subdued or even completely masked, however, by the presence of large neutron absorbers commonly associated with clays (e.g., iron, potassium and boron). Primarily through the

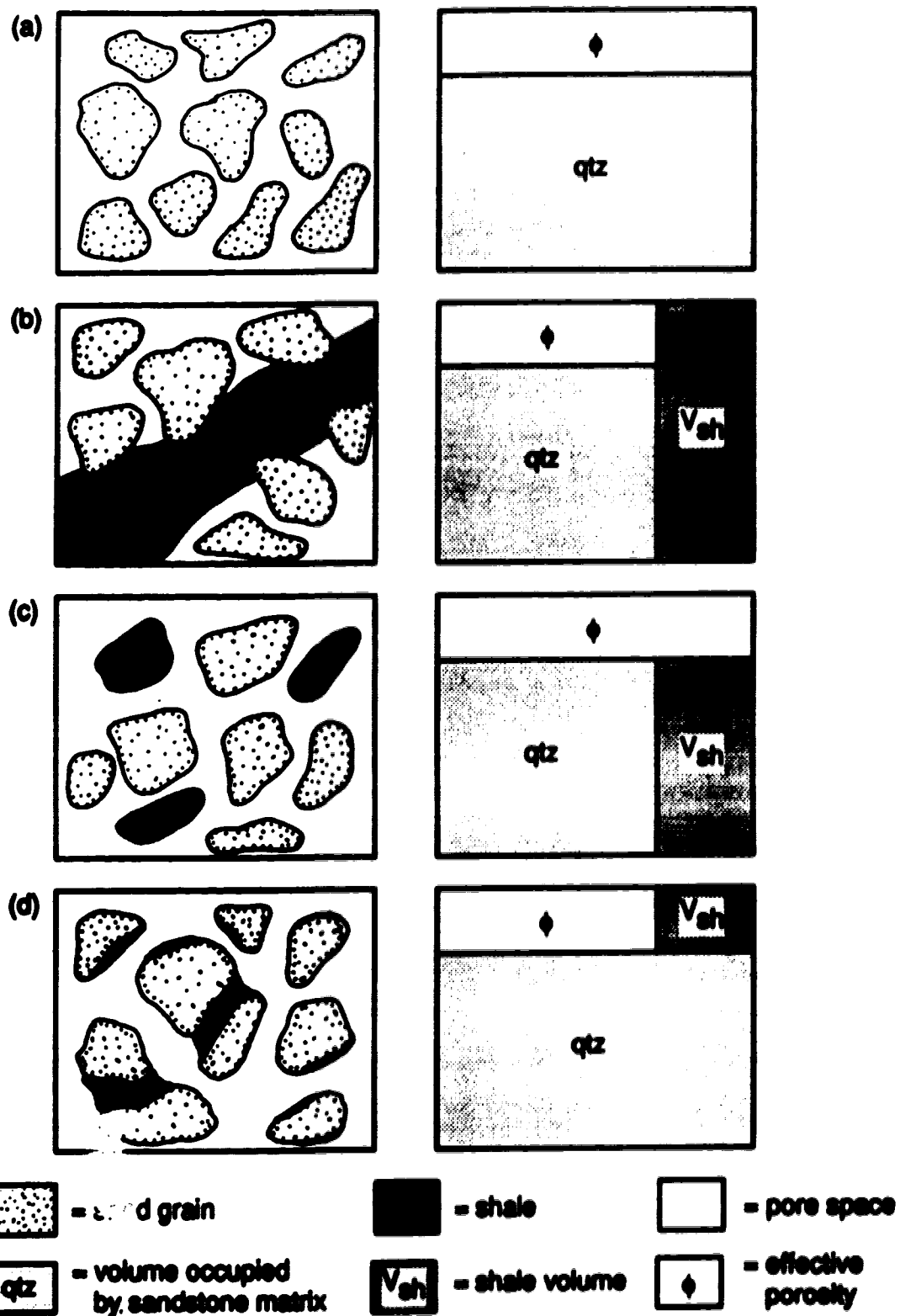


Figure 2.9: Schematic illustrations of (a) clean sandstone, and the three types of shale distribution in sandstone: (b) laminar shale, (c) structural shale, and (d) dispersed shale and the associated formation models (modified after Bateman, 1965, p. 537).

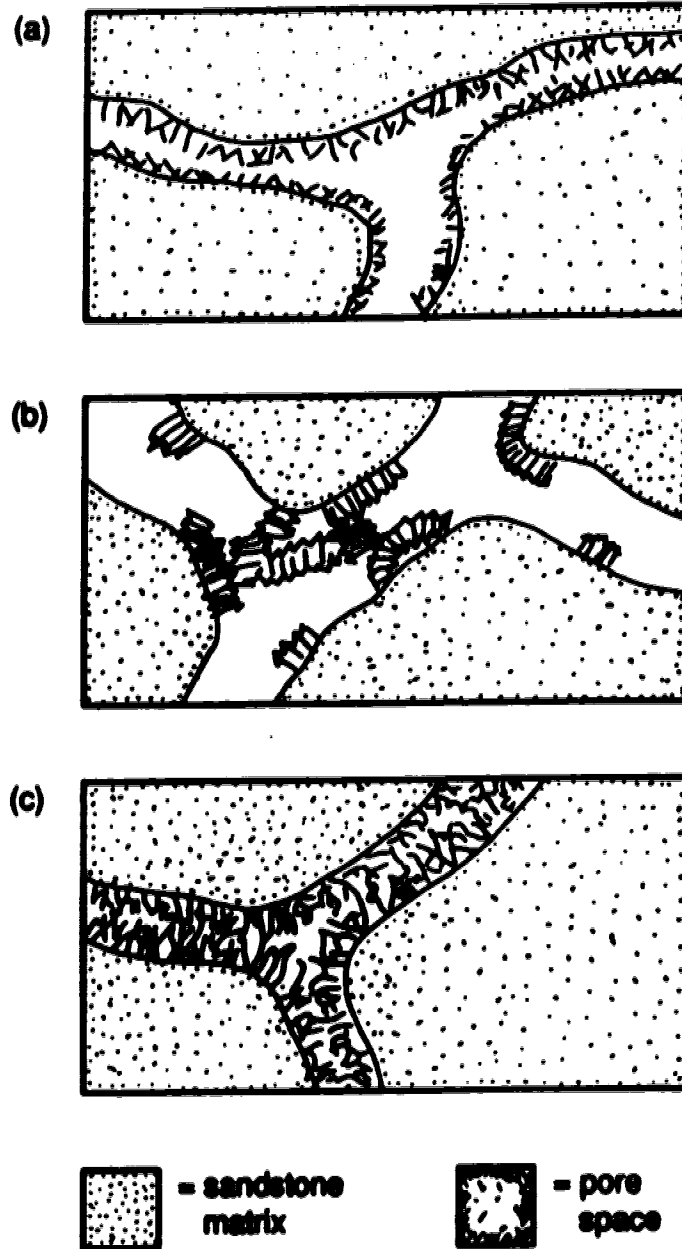


Figure 2.10: Schematic illustrations of the three modes of dispersion of authigenic clay minerals: (a) pore lining, (b) pore filling, and (c) pore bridging (modified after Ellis, 1967, p. 445).

substitution of iron for aluminum in the sheet structure, chemical composition has a noticeable impact on the photoelectric cross-section index because the photoelectric cross-section index of iron is significantly higher than the photoelectric cross-section index of most commonly encountered elements. Gamma ray spectroscopy identifies the percentage of deflection on the gamma ray log which is due to the potassium and thorium in clay minerals and, thus, aids in the discrimination of clays from other lithological assemblages. (Ellis, 1967; Cannon and Coates, 1990)

Another unique feature of clay minerals responsible for log perturbations is associated with the platy or sheetlike structure of the minerals. As mentioned above, water released during compaction or resulting from mineralogical reactions may be trapped between the plates of clay minerals. This water reduces the resistivity reading and increases the neutron porosity reading without contributing to effective porosity. The ability to adsorb ions, primarily cations, is also a result of the structure of clay minerals. A negative surface charge is produced because of substitution at the surface of the clay crystals with atoms of lower positive valence. The adsorbed ions may be radioactive, accounting for additional gamma ray activity. In the presence of an electrolyte like formation water, the adsorbed cations can move and exchange with dissolved ions in the solution, thereby reducing the recorded resistivity. (Dickey, 1966; Ellis, 1967)

Finally, the type of clay distribution causes perturbations in logging measurements. Again, the most prominent effect is evident in the formation resistivity as the accessible surface for adsorption for the same volumes of dispersed clays and laminated shales, for example, may be rather different. To a lesser degree, the clay grains of dispersed and laminated shales may have different densities, affecting density measurements. Commonly, the density of

the clay is less than the reservoir's pseudo-matrix density (sandstone, limestone or dolomite), resulting in too high conversions to density porosity from equation 2.2.1. The distribution of clay minerals also has a mild effect on P-wave traveltimes. Most commonly, the low velocity of clay increases the interval transit time recorded, thereby causing the calculated sonic porosity to be too high. (Ellis, 1987; Asquith, 1990)

2.4. Data Base

Most of the data and information used in this project was originally measured, recorded and processed for petroleum exploration purposes. The availability and suitability of this data set, in particular of the comprehensive suites of well logs, determined the location of the test holes (Figure 2.11) and to some extent the scope of the study.

Of primary interest are the geophysical well logs. Table 2.1 lists some drilling information and all logs included in the two suites of well logs for locations 05-07-017-07W4M and 06-35-017-09W4M in the Suffield exploration field of south-eastern Alberta, Canada. A complete collection of logs is available from the Energy Resources Conservation Board (ERCB) in Calgary, Alberta. The core analysis records used in this study may also be obtained from the ERCB. In addition, the AEC Oil and Gas Company (Calgary, Alberta) provided copies of the geological reports prepared from drilling observations. For easy identification, information and data pertaining to one of the two test holes will be referred to as belonging to '5-7' or '6-35'.

Well records and production records from the ERCB indicate that both wells were drilled for the purpose of obtaining gas production from the Basal Colorado Sandstone. The 5-7 well was perforated in the Bow Island Formation (772.0 to 773.0 m below KB) and in the Basal Colorado Sandstone (867.8 to

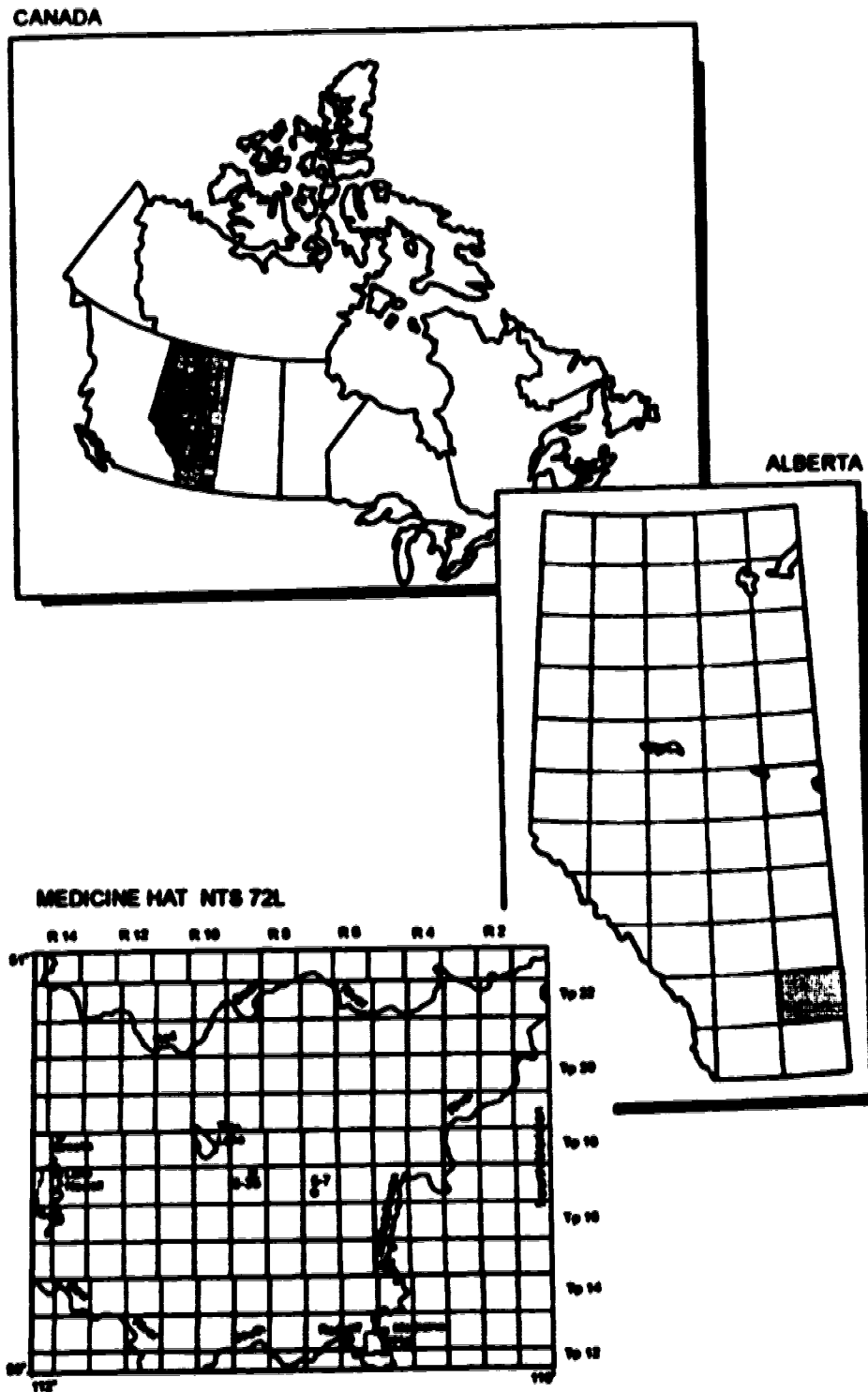


Figure 2.11: Location maps of the two study wells 5-7 and 6-35 at 05-07-017-07W4M and 06-35-017-08W4M, respectively.

Table 2.1: Information and data included in the core of this study's data base (available from the Energy Resource Conservation Board in Calgary, Alberta)

	66-97-917-97W-001	66-95-917-99W-001
Core Log		
Kelly Bushing (KB) (m above mean sea level)	789.0	789.0
Ground Level (m above mean sea level)	784.5	784.5
RT Slip (m)	0.20	0.20
Total Depth drilled (m below KB)	910.0	1025.0
Top of Casing (m below KB)	153.0	157.0
Tool	KCI	KCI
Density (g/cm ³)	1180	1140
API	6.5	7.2
Simultaneous Compensated Neutron-Litho-Density*	153.0-905.4	156.7-1020.0
Simultaneous Dual Lateration Micro-SFL*	153.0-904.0	156.7-1016.3
Nuclear Magnetism Log*	329.0-550.0 630.0-711.0 740.0-853.0 830.0-900.0	212.0-245.0 245.0-510.0 400.0-1020.0
NAL Permeability Outlook*	329.0-550.0 630.0-711.0 740.0-853.0 830.0-900.0	not available
Borehole Compensated Sonic*	153.0-901.5	not available
Acoustic	not available	156.7-1015.1
Resonated Shear Analysis*	not available	300.0-914.1
Geotechnical Log*	325.0-991.3	not available
#1 in New Island Formation*	789.0-770.4	781.0-779.0
#2 in Broad Colorado Sandstone*	867.0-876.4	868.0-868.0
#3 in Marcella Group*	not available	867.0-863.0

* depth intervals in metres below Kelly Bushing ** recorded between 1989 November 20 and 1989 December 20

871.8 m below KB). Production commenced on 1990 March 2. Until the suspension of the well on 1991 October 1, a total of $989.9 \cdot 10^3 \text{ m}^3$ of gas and 2.4 m^3 of water had been produced. The 6-35 well was abandoned on 1989 December 21 because testing and logging failed to disclose evidence of commercially recoverable hydrocarbons.

The data base was supplemented as necessary with well logs and core analyses from the ERCB. Shallow well information was obtained from the Edmonton Branch of Alberta Environment.

2.5. Local Geology

The test wells are located in the Interior Plains, i.e., the eastern segment of the Western Canada Sedimentary Basin. The physiographical province is characterized by flat to subdued topography underlain by thin, extremely widespread, and nearly flat-lying Phanerozoic cratonic sedimentary rocks. (Nelson et al., 1970)

The stratigraphic section of interest contains the continental and marine strata of Cretaceous age (Figure 2.12). The environment of deposition was set by an epicontinental sea which extended into the interior of the continent from the Arctic to the Gulf of Mexico. Mostly because of tectonic activity in the Cordillera to the west and subsidence in the foreland basin area, the shoreline migrated through cycles of regression and transgression. The character of the deposits was influenced by the changing sources of sediments. (Rudkin, 1970; Williams and Burk, 1970)

For the purpose of log interpretation, the following brief stratigraphic summaries and gross lithological descriptions are provided not only for

<i>Era</i>	<i>Period</i>	<i>Mill. of years before present</i>	<i>Epoch</i>
CENOZOIC	Quaternary	.01	Recent
		2	Pleistocene
	Tertiary	7	Pliocene
		26	Miocene
		37	Oligocene
		53	Eocene
		65	Paleocene
MESOZOIC	Cretaceous	136	
	Jurassic	190	
	Triassic	225	
	Permian	280	
PALEOZOIC	Carbon- iferous	Pennsyl- vanian	320
		Missis- sippian	345
	Devonian		395
	Silurian		430
	Ordovician		500
	Cambrian		570
PRECAMBRIAN	Proterozoic	2300- 2500	
	Archean	4600- 4700	

Figure 2.12: Geological time scale showing relative position of Cretaceous period (adapted in part from Press and Siever, 1982, inside cover).

stratigraphic formations, but also for subunits and members with characteristic log signatures (Figure 2.13).

Overall, the Colorado Group deposits represent a period of relative quiescence. With minor amounts of clastic detritus being generated in the orogenic belt and generally rising sea level, the prevailing lithology of the conformable sequence of marine sediments (Williams and Burk, 1970) is shale with several intercalated sandstones (Cant, 1989). The Basal Colorado Sandstone, which forms the base of the Joli Fou Formation and thereby the base of the Colorado Group, rests disconformably upon sandstones of the Mannville Group (Rudkin, 1970; Glass, 1990). The unit consists of variably shaly, fine to coarse grained sandstone, with interbedded siltstone and mudstone (Glass, 1990). The Basal Colorado Sandstone is conformably overlain by marine shales (Stott, 1984) with minor interbedded fine and medium grained sandstones of the Joli Fou Formation (Glass, 1990). A subsequent regression of the sea provided a near shore, marine environment for the deposition of the Bow Island Formation (Rudkin, 1970; Stott, 1984). Up to three bodies of coarsening upward sandy sequences, termed First, Second and Third Bow Island Sands (Bow Island #1, Bow Island #2, Bow Island #3, respectively) in order of increasing age, may be separated in vertical succession by mudstone and shale sequences (Glass, 1990). The Bow Island Formation is succeeded by a considerable thickness of Unnamed Shale deposited during a major, basin-wide transgression (Leckie, 1989), followed in turn by a prominent log marker called the Base of Fish Scales. The marker horizon separates the lower, noncalcareous from the upper, mostly calcareous part of the Colorado Group (Glass, 1990). The Base of Fish Scales Marker is a condensed section of large amounts of organic debris, and presumably reflects a period of maximum relative sea level when sedimentation rates in the basin

Era	Period	Stratigraphic Units Defined on Well Logs	
CENOZOIC	Quaternary	Laurentide Drift	
	Tertiary	(not represented)	
MESOZOIC	Cretaceous	Judith River Formation	
		Pakowki Formation	
		Milk River Formation	
		Colorado Group	First White Speckled Shale
			Medicine Hat Sandstone
			Colorado Shale
			Second White Speckled Sandstone
			Second White Speckled Shale
			(Base of Fish Scales Marker) Unnamed Shale
			Bow Island Formation
			Bow Island #1
			Bow Island #2
			Joli Fou Formation
			Basal Colorado Sandstone
		Manville Group	

Figure 2.13: Representative stratigraphic section compiled of units defined on well logs for locations 06-07-017-07W4M and 06-35-017-09W4M (modified after Rudkin, 1970; and Williams and Burk, 1970).

were at a minimum (Cant, 1969). Fish-skeletal debris, shaly chalk and skeletal calcarenite indicating open marine conditions (Leckie, 1969) continue to be abundant in the overlying shale and mudstone of the Second White Speckled Shale. At its top, this unit incorporates a sequence of shaly sandstones and siltstones termed the Second White Speckled Sandstone (Glass, 1990). Between the Second White Speckled Shale and the First White Speckled Shale rests a unit of noncalcareous shale and mudstone (Glass, 1990), commonly referred to as Colorado Shale (Hankel et al., 1969), which was most likely deposited during a regressive phase of the sea (Stott, 1964). The First White Speckled Shale, which constitutes the top of the Colorado Group, is the result of another major transgression and is lithologically very similar to the Second White Speckled Shale. A muddy sandstone and siltstone unit, known as the Medicine Hat Sandstone (Glass, 1990), has been interpreted as a localized shelf deposit (Hankel et al., 1969). It shows a basal contact lithologically gradational (Glass, 1990) with underlying shales. Glass (1990) stated that the Medicine Hat Sandstone is incorporated within the First White Speckled Shale, while other authors (Male and Pacholko, 1982; Hankel et al., 1969) positioned it below the base of the unit. Since the log signatures in the study wells above the Medicine Hat Sandstone do not resemble those below, the Medicine Hat Sandstone is accepted as a unit separating the First White Speckled Shale and Colorado Shale.

The Milk River Formation conformably overlies the Colorado Group (Williams and Burk, 1970). Deposited in a shelf setting, the formation consists of marine shales with occasional thin beds and lenses of argillaceous sand and silt (Male and Pacholko, 1982; Moirard et al., 1983). The abrupt, conformable contact to the succeeding Pakowki Formation is generally marked by a thin chert pebble bed (Williams and Burk, 1970). The lithology of the Pakowki

Formation is dominated by the marine shales of another major marine transgression (Stott, 1984), with some thin silty sandstone and bentonite beds (Williams and Burk, 1970).

The uppermost stratum recorded partially on the well logs below surface casing is the Judith River Formation, formerly referred to as two strata, the Foremost Formation and the overlying Oldman Formation. Its lower beds are brackish water deltaic and lacustrine deposits, while the upper beds are generally considered to be nonmarine coastal plain deposits (Leckie, 1989). Overall, the Judith River Formation consists predominantly of interbedded mudstone, siltstone and sandstone in varying proportions (Glass, 1990).

According to Williams and Burk (1970), and Tokarsky (1986), the Judith River Formation forms the erosional bedrock surface in the study area. It is covered by deposits of the Quaternary period, directly related to or closely associated with the continental Laurentide icesheet (Barton et al., 1970). The latest Cretaceous Series and the Tertiary Period are not represented in the section.

Structurally, the sedimentation of these strata was affected by the Sweetgrass Arch, a positive feature which extends over the south-eastern corner of Alberta in a north-eastern trend. The arch originated in the Paleozoic (Koster et al., 1987; Cant, 1989), and was reactivated during pre-Colorado Early Cretaceous time (Williams and Burk, 1970; Leckie, 1989). Due to the effects of considerable erosion over its axial region, the arch's influence on late Cretaceous sedimentation is difficult to determine (Williams and Burk, 1970; Koster et al., 1987). Units like the Second White Speckled Sandstone and the Medicine Hat Sandstone are, however, believed to be shelf deposits localized by the topography of the Sweetgrass Arch (Hankel et al., 1989). Williams and

Burk (1970) expressed the possibility of slight upward movement during post-Colorado Cretaceous time. More recently, however, Shepard and Bartow (1986) stated that the arch was inactive during that time period. The Sweetgrass Arch acquired its present form during the Eocene Epoch of the Tertiary Period, resulting from forces exerted on the west by the Laramide orogeny and on the east by a subsiding and expanding Williston basin (Taylor et al., 1970).

3. Data Analysis and Interpretation

Both log analysis and log interpretation are forms of art mixed with science. Basic and even advanced knowledge of terminology, principles and concepts may be learned from a large assortment of literature including handbooks (Hilchie, 1978; Asquith, 1982; Dresser Atlas, 1982; Merkel, 1983; Brock, 1986; Crain, 1986; Schlumberger, 1989), well logging text books (Helander, 1983; Bateman, 1985; Hearst and Nelson, 1985; Jorden and Campbell, 1986; Tittman, 1986; Ellis, 1987), geophysical exploration textbooks (Telford et al., 1976) and technical papers (Foster and Beaumont, 1990; The Log Analyst published bi-monthly by the Society of Professional Well Log Analysts; SPE Formation Evaluation published monthly by the Society of Petroleum Engineers), as well as short courses (offered by professional societies of earth scientists and engineers, and by logging service companies). Because all methods of analysis are based at least partially on empirical relationships and the medium to be examined is that of the natural, or uncontrolled, rock formation beyond the borehole, more than just knowledge is required for in-depth analysis and interpretation. Intuition, which allows creative processing and the integration of all available information for results that most accurately describe the real conditions, is acquired through experience in the analysis and interpretation of actual data sets recorded under real-life conditions. This chapter outlines an unconventional approach, in terms of data selection and manipulation procedures, to the application of analytical equations chosen from literature.

The purpose of log analysis and interpretation is to translate the measurements of parameters recorded in the field into parameters of interest in characterizing the rock formation. Strictly speaking, analysis involves the

quantitative and qualitative examination of the measurements, the relationships between the measurements of various parameters, and the relationships between the measurements and the properties of the rock formation.

Interpretation refers to the subsequent process of explaining the results of the analysis. In log interpreters' jargon, however, the term "interpretation" is often applied in a sense which encompasses both analysis and interpretation. In this chapter both processes are discussed, with an emphasis on analysis.

Quantitative log analysis is based on a formation model in which any rock volume consists of a solid part made of minerals and their aggregates, and void space filled with fluid (Figure 2.9). An infinite number of combinations of structural arrangements, chemical compositions, physical conditions and so forth requires the division of the two principal components into subcomponents. Clay and matrix minerals constitute the solid part; bound and mobile water, gas and oil fill the void space. The relationships between these subcomponents are expressed mathematically in mostly empirically-based, algebraic equations. The constants contained in the equations are either empirically derived constants, values approximating a certain range of conditions (e.g., matrix density), or parameters which are assumed to be constant throughout the logging process (e.g., mud filtrate density). The independent variables are substituted with values of measured parameters such as natural gamma radiation. The dependent variable is the value of a parameter characterizing a formation property (e.g., effective porosity), or an intermediate value with no physical meaning, which is needed for further calculations resulting in formation parameters.

3.1. Data Preparation

3.1.1. Well Logs

The well logs were obtained in printed analog format. For the computational operations of quantitative analysis the individual curves of bulk density, density porosity, neutron porosity, total gamma radiation, photoelectric cross-section index, deep and shallow laterolog resistivities, spontaneous potential, sonic traveltime and the free fluid index for both 5-7 and 6-35 were digitized.

The IBM-PC software used to digitize the log curves (LOGDIGI) and to print the digitized parameter values in log format against depth (LOGPRINT) are products of The Logic Group (© Brown and Walsh, U.S.A., 1987). The LOGDIGI program allowed for manual tracing of the logging curve on a digitizing tablet with the logging data being output as a standard ASCII file.

A comparison of the thicknesses of the stratigraphic units in the sections against the vertical resolution of the logging tools, i.e., the bed thickness necessary for the tool to record the true formation value, was the most critical factor considered for the determination of a universal sampling interval. Core analyses of 5-7 and 6-35, and nearby wells indicate a heterogeneous lithology dominated by massive shales, sandy shales and shaly sands with bed thicknesses on the order of centimetres to many metres. Schlumberger (1989) provided the following guide lines of vertical resolution for its tools: approximately 0.60 m for both the compensated neutron log and the dual laterolog; better resolution may be expected from the photoelectric cross-section index measurement and the gamma ray tool; approximately 0.45 m for the bulk density log; a relatively poor resolution of about 1.00 m for the nuclear

magnetism log; depending on the acoustic frequency and the sediment velocity, sonic logging tools may resolve beds of a minimum thickness of 0.30 to 1.20 m. As bed thickness approaches or becomes less than the effective vertical resolution of a tool, averaging occurs in the acquisition process and the recorded value is a value between the two maximum deflections. This apparent or effective value depends not only on the thicknesses of all the units included vertically into one logging measurement, but also on the contrast between the true values associated with these individual units (Figure 3.1) (Hartmann, 1975; Ellis, 1987). Further, taking into account the 1:240 scale of the paper copies of the logs, with the exception of bulk density log at a 1:600 scale, a sampling interval of one metre was chosen. The vertical resolution of each of the digitized logs is, thus, approximately 1 m, which is equal to the digitizing interval but no greater than the vertical resolution of the original curves.

The digitized curves were checked against the original curves and edited. Corrections were made where the digitized version did not satisfactorily represent the original curve. Where information was lost which may enhance the analysis, digital values were changed manually in the computer. In general, the digitized curves appeared somewhat smoother or more homogeneous (Figure 3.2) as a result of the one-metre digitizing interval. That is, spurious variations and spikes caused by thin lithological laminae, odd heavy mineral occurrences, localized drill fluid or borehole abnormalities, mechanical inconsistencies during the initial recording, computational artifacts, etc. were "filtered out".

Occasional cycle skipping was observed on the original sonic traveltime log of 6-35. These features are produced when the first arrival is strong enough only to trigger one of the pair of receivers but not the other, which may then be triggered by a later cycle. The spikes of abnormally high traveltime were

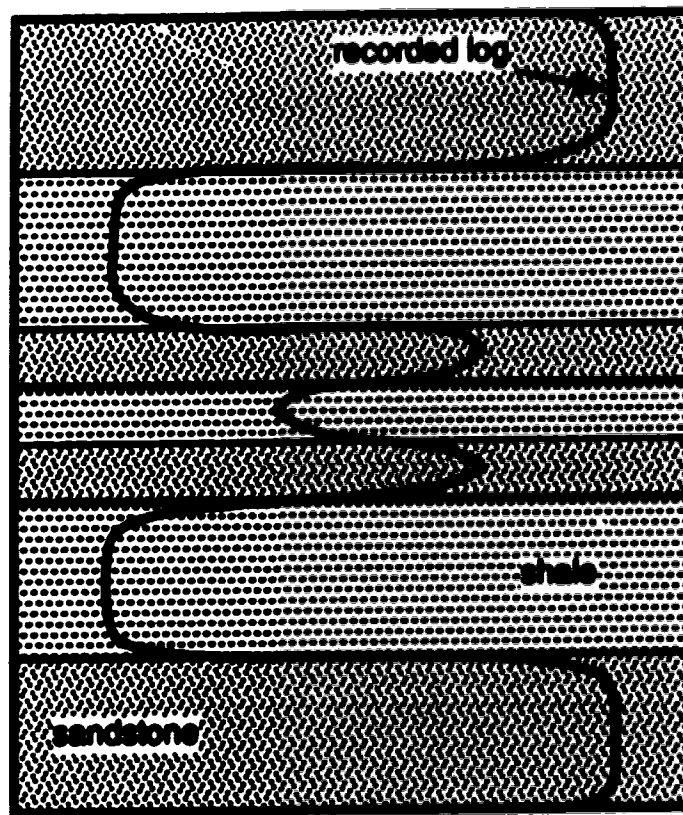


Figure 3.1: Illustration showing true log values recorded in thick beds, and apparent log values recorded in thin beds whose thickness is less than the vertical resolution of the logging tool.

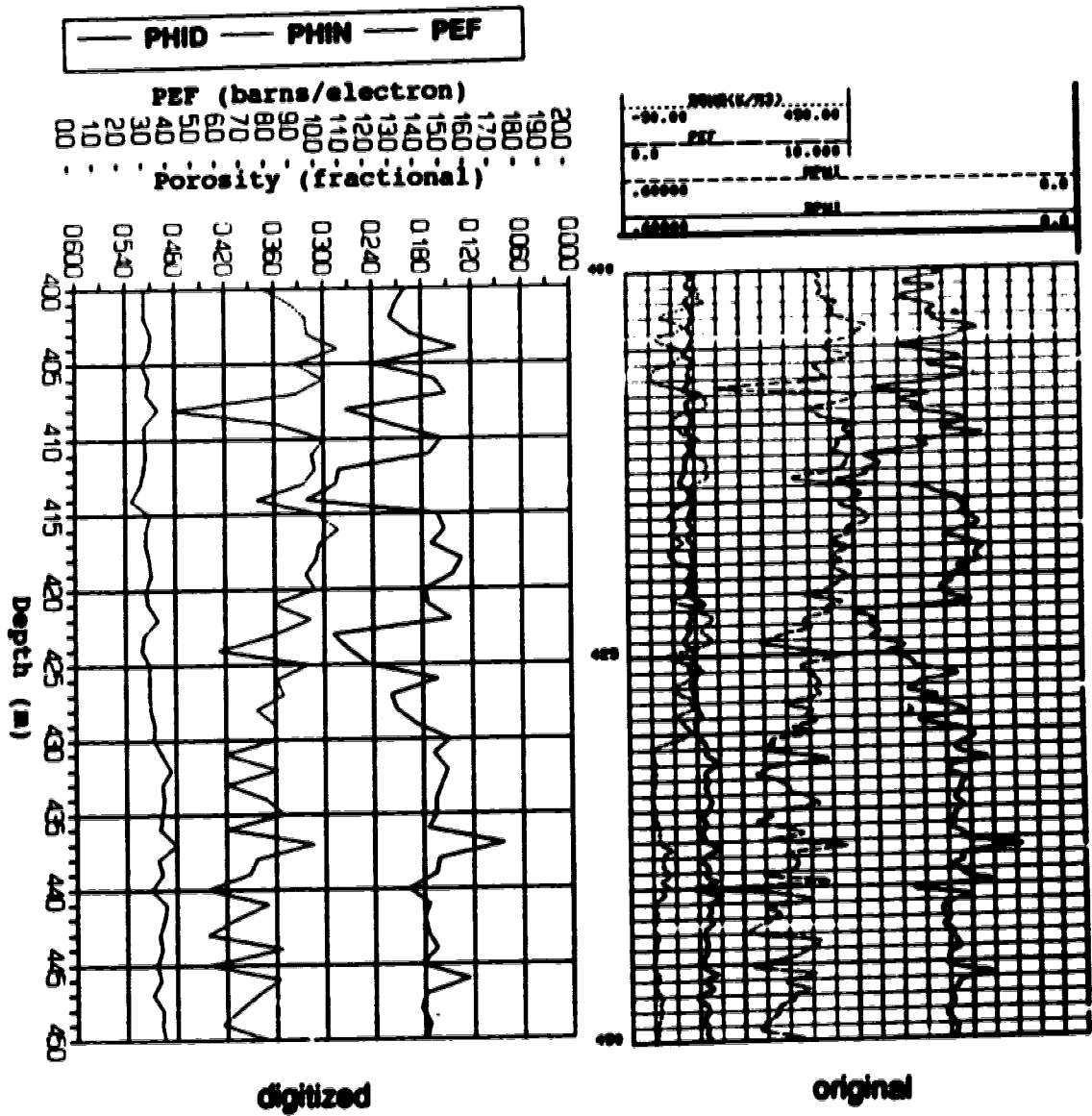


Figure 3.2: Comparison of the original and the digitized signatures over an arbitrary interval of the neutron porosity, density porosity and photoelectric cross-section curves of 5-7.

replaced by smooth curves following an estimated base log beneath the noise. The erratic curve signature from a depth of 256 to 264 m of 6-35 did not justify replacement with imaginary or assumed values because of the length of the interval and the heterogeneous sandy lithology. To represent the lack of data in the spreadsheet, the '-999' was entered instead of meaningful values of traveltime.

A more serious problem was posed by the effects of borehole rugosity on the bulk density, and therefore the density porosity. A curve of the density correction applied to the bulk density measurement by the service company to compensate for mud cake and rugosity is displayed alongside the bulk density and porosity density curves. The correction varies between -50 and +250 kg/m³ for intervals longer than 10 m in the Colorado Shale, Unnamed Shale and Joli Fou Formation of both 5-7 and 6-35. Positive density correction values correspond with increases in the density porosity to anomalously high values with respect to adjacent units for which other logs show no markedly different signature. With no guidelines available for possible correction procedures for the density porosity, the curve remained unchanged. Instead, the problem was attended to as part of the specific procedures of data analysis later on.

A zero shift was applied by the field engineer on the spontaneous potential curve of 6-35; possibly to avoid printing off-scale. At the depth of 765 m the curve jerks left by 60 mV. After digitizing had been completed, 60 mV were added to all spontaneous potential values from 766 to 882 m to correct the shift on the relative scale.

Throughout each of the two well log suites, good lateral consistency was observed for prominent log markers which affect all the curves. Therefore no depth adjustments were necessary.

The LOGDIGI output file was imported into a QuattroPro® (Borland International Inc., U.S.A., 1991) spreadsheet for the actual numerical editing and subsequent quantitative analysis. A complete listing of the parameter values may be found in Appendix A. Log Sets A1 and A2 are the digitized curves of the raw data.

No logs over shallow depth intervals were available at Alberta Environment in the immediate vicinity of 5-7 and 6-35. Instead, spontaneous potential and resistivity logs recorded at 04-04-017-10W4M and 05-10-018-10W4M for the interval between surface and the top of the Milk River Formation were combined to prepare a digitized version of representative logs. In accordance with the original logs, the curves were digitized in one-foot intervals. However, for more convenient qualitative comparison with the deep logs of 5-7 and 6-35, the shallow logs were printed in metres (Log Set A3). The original scales of resistivity and spontaneous potential were honored since the different types of measuring equipment did not warrant comparison with deep logs in absolute magnitude.

3.1.2. Core Analyses

For the purposes of comparison and calibration, the core analysis data for 5-7 and 6-35 were converted into a format similar to that of the log data. The permeability and porosity measurements corresponding to the small sample intervals of several centimetres of core were averaged over the specific one metre intervals corresponding to single digitized log values.

First, each core was depth matched to the logs. The core gamma log was compared to the digitized gamma ray log to shift the core into close

approximation of its correct vertical position. The depth match was fine tuned by comparing the digitized log bulk density to the core bulk density. Also, where siderite and pyrite are present in sufficient amounts, the photoelectric cross-section index aided the correlation. For the cores of 5-7, natural gamma ray spectroscopy curves were available as well. Particularly the thorium, and to some extent the potassium curves could be matched well with the full scale natural gamma ray spectroscopy logs. The adjustments applied to the depths of the individual cores varied from zero to one metre. Appendix B lists the raw data after depth matching.

The second step involved averaging the core permeability and porosity measurements over one metre intervals, i.e., from 0.50 m above to 0.50 m below any metre marking on the log. The averaging interval was positioned in this manner to simulate the averaging process incorporated into logging measurements. An arithmetic average function weighted by the length of the representative interval was used for the porosity values:

$$P_{avg} = \sum_{i=0}^n \frac{(D_i \cdot P_i)}{D} \quad (3.1.1)$$

where P_i is the porosity measurement, D_i is the thickness of core represented by P_i , and D is the total thickness over which the measurements are averaged. D is the sum of the thicknesses of n intervals for which porosity values are available within the designated one metre, and therefore ranges from zero (if no measurements are available) to one metre.

Core analysis may result in up to three permeability measurements from both 0.09 m full-diameter samples and drilled plugs of 0.0254 m diameter: K_{max} and K_{90} are the two horizontal measurements routinely made, one in the direction of maximum permeability (K_{max}) and one perpendicular to it (K_{90}); the

vertical permeability measured perpendicular to the horizontal plane is referred to as K_v . The analyses for the two cores of 5-7 provided all three components for all depth intervals. The analyses for the two cores of 6-35 listed mainly K_{max} values, and few corresponding K_{90} and K_v values.

The core permeability values show both heterogeneity (i.e., K_{max} , K_{90} and K_v each vary for different samples) and anisotropy (i.e., K_{max} , K_{90} and K_v are different for one sample). This numerical observation is supported by the lithology of the cored Bow Island Formation and Basal Colorado Sandstone. Thin shale laminae of little lateral continuity, and structural and dispersed shale contained in varying proportions in sandstone, cause permeability to change with position in the formation and influence the directional permeability. Heterogeneity requires that each sample interval of the core analysis be included in the averaging process. In the resulting layer cake model, which represents vertically stacked slabs of homogeneous stratigraphic units, flow direction becomes the governing factor in deriving an averaging function honoring the anisotropy of permeability. Considering the physical principles of logging and the acquisition and analysis methods, one would expect the one obtainable permeability value to be more representative of a bulk value rather than a horizontal or vertical directional value. To compare core permeabilities with log-derived permeabilities, horizontal flow parallel to the layering should therefore be treated as dominant in core data analysis. High ratios of K_{max} and K_{90} to K_v (see Appendix B) relate the relative importance of horizontal over vertical permeability, and further support the layer cake model with lateral flow. K_{max} is preferred to K_{90} because it is available for all cores. In order to better accommodate the five orders of magnitude (10^{-2} to 10^3 md) of K_{max} and to de-emphasize the importance of the smallest values, the values of K_{max} were

converted to the logarithmic scale of base 10 for the calculation. The final expression is that of a weighted geometric average:

$$K_{avg} = \text{antilog} \left(\sum_{i=0}^n \frac{(D_i \cdot \log(K_{maxi}))}{D} \right) \quad (3.1.2)$$

where K_{maxi} is the permeability measurement, D_i is the thickness of core corresponding to K_{maxi} , and D is the total thickness over which K_{max} is averaged.

The results of the core porosity and core permeability averaging calculations are listed in Table 3.1. The degree to which these results represent the actual formation properties will be discussed as part of their application in Sections 3.5 and 3.6.

3.2. Stratigraphic Correlation

Several sources were consulted to identify geological formation tops on the well logs of 5-7 and 6-35. Depths for major formation tops were listed in the well data summaries of the geological reports. These formation and marker depths were supplemented and fine-tuned with the aid of gamma ray and resistivity logs in stratigraphic cross-sections by Male and Pacholko (1982); Moinard et al. (1983); and Tokarsky (1986); and sample logs by Tizzard (1974), Hankel et al. (1989), and Martin and Yeung (1991). The log signatures of the Medicine Hat Sandstone and the Bow Island #1 and Bow Island #2 zones are not always well defined, allowing an error margin of several metres.

On the representative self-potential and resistivity logs for the shallow section, formation tops were identified using Tokarsky (1986), driller's lithological descriptions, PIX cards (© Canada Petroleum Information Exchange Ltd.), and a lexicon of stratigraphy (Glass, 1990). The relative signatures of the

Table 3.1: Core measurements of porosity and maximum permeability of 5-7 and 6-35 averaged with equations 3.1.1 and 3.1.2 over one-metre intervals corresponding to digitizing intervals of logs

05-07-017-07W4M				06-35-017-08W4M			
Depth (m below KB)	Porosity Pavg (frac.)	Permeability Kavg (md)		Depth (m below KB)	Porosity Pavg (frac.)	Permeability Kavg (md)	
Bear Island Formation Core				Bear Island Formation Core			
770	0.128	2.88		765	0.147	10.49	
771	0.148	18.23		766	0.142	2.18	
772	0.138	14.88		767	0.148	2.82	
773	0.210	320.33		768	0.166	12.74	
774	0.261	821.49		769	0.167	4.87	
775	0.241	303.74		770	0.157	0.95	
776	0.247	372.99		771	0.149	1.08	
Basal Colarado Sandstone Core				772	0.145	0.21	
868	0.183	146.99		773	NA	NA	
869	0.178	73.87		774	0.228	29.45	
870	0.144	7.97		775	0.153	4.35	
871	0.122	48.86		776	NA	NA	
872	0.102	1.97		777	0.155	1.89	
873	0.133	36.18		778	0.145	1.92	
874	0.140	11.38		Basal Colarado Sandstone Core			
875	0.090	392.01		874	0.262	212.72	
				875	0.244	128.50	
				876	0.209	22.25	
				877	0.189	8.04	
				878	0.113	0.95	
				879	0.171	17.89	
				880	0.229	312.03	
				881	0.144	0.62	
				882	0.124	0.37	

spontaneous potential and resistivity curves of the deep and shallow logs matched well for the Pakowki Formation and the top of the Milk River Formation. The contact between the Judith River Formation and glacial overburden deposits could not be unambiguously identified. It appears that the drillers set casing on or near the top of bedrock, i.e., onto the Judith River Formation itself. In other words, overburden is not recorded on logs. Approximate drift isopach values were estimated from a comparison of surface topographic to bedrock topographic maps (Carlson, 1970). Table 3.2 lists the assigned depths of all the identified log markers.

3.3. Lithology

The primary objective of the lithological analysis and interpretation is to provide a framework for later quantitative log analyses for shale volume, porosity and permeability. In other words, the determined lithological composition serves to bracket the range of expected and realistic values of these parameters. Two general approaches were taken to analyse the lithology of the rock formations beyond the boreholes of 5-7 and 6-35. First, the logging curves were inspected visually to identify signatures characteristic of sandstone, shale, bentonite, and calcite and siderite rich units. The second approach involved cross plots to identify clay types and to further clarify the distributions of clay minerals and of shale types.

The following written descriptions of signatures seen on the curves of 5-7 and 6-35 are illustrated schematically in Figure 3.3. Table 3.3 lists depth intervals in which examples of these may be seen on the curves of 5-7 and 6-35. In Section 2.5 it was established that sandstone and shale are the two main rock types in 5-7 and 6-35. The gamma ray log shows relatively high radiation

Table 3.2: Depths of tops of stratigraphic units defined on logs of 5-7 and 6-35

Stratigraphic Unit	06-07-017-07W4M		06-35-017-09W4M	
	Depth below Kelly Bushing (m)	Elevation Above Mean Sea Level (m)	Depth below Kelly Bushing (m)	Elevation Above Mean Sea Level (m)
Judith River Formation *	25	784	55	734
Palouah Formation	288	503	285	504
Milk River Formation	334	455	329	460
First White Speckled Shale	430	359	427	362
Medicine Hat Sandstone	461	328	461	328
Colorado Shale	474	315	471	318
Second White Speckled Shale	636	153	640	149
Second White Speckled Sandstone	637-643	152-146	642-648	147-141
Unnamed Shale (Base of Fish Scales Marker)	704	85	710	79
Bow Island Formation	744	45	751	38
Bow Island #1	759-771	30-18	764.5-779	24.5-10
Bow Island #2	772-784	17.5	780-786	9-3
Joli Fou Formation	829.5	-40.5	837	-48
Basal Colorado Sandstone	867	-78	874	-85
Marmville Group	878	-89	883	-93

*Cartoon, 1970

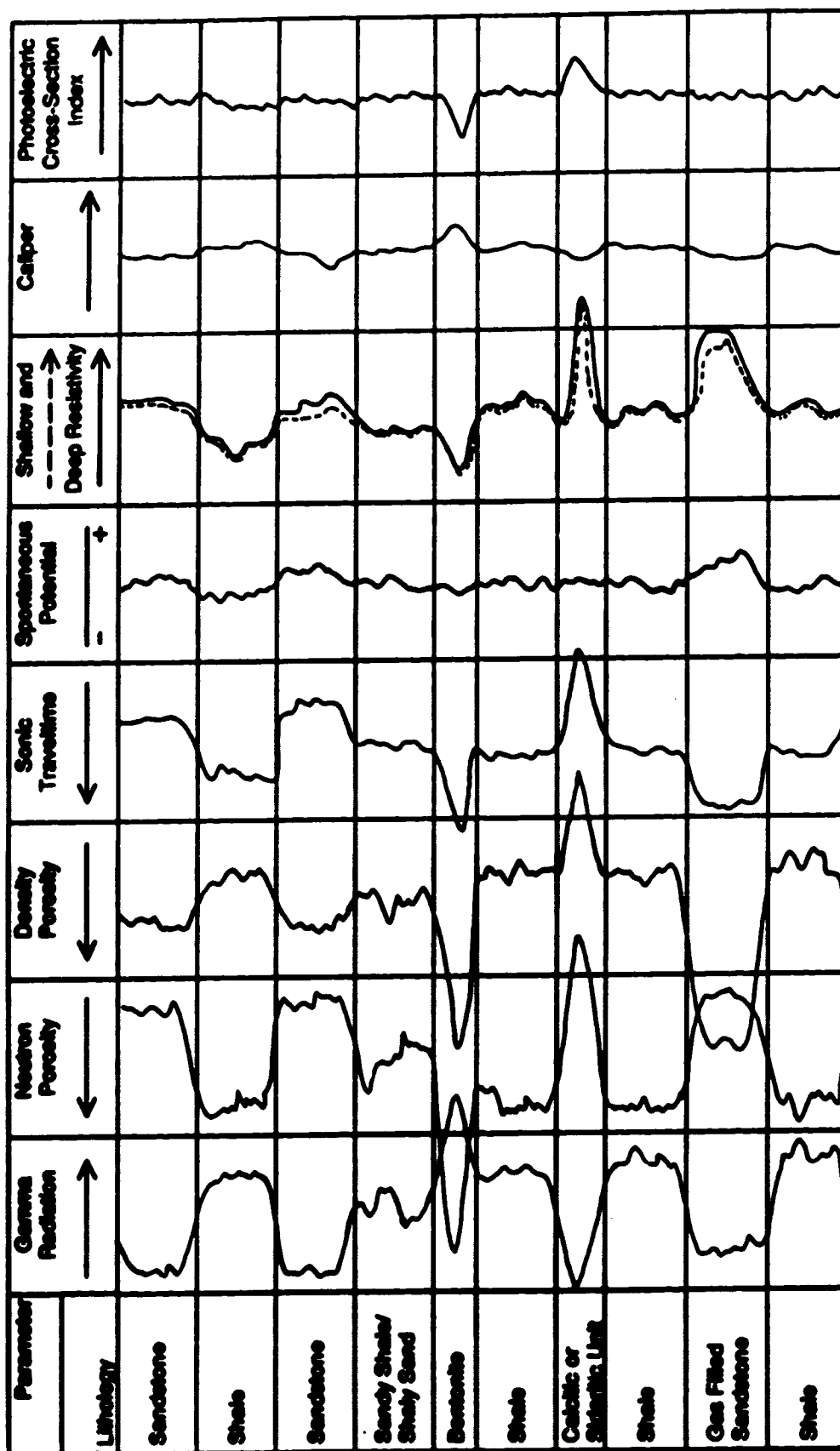


Figure 3.3: Schematic illustration of the well logs at 05-017-07W4M and 06-35-017-09W4M in response to lithology and gas. Depth ranges at which these signatures are seen on the actual logs are listed in Table 3.3.

Table 3.3: Depth intervals in which the characteristic signatures of lithology shown in Figure 3.3 are displayed on the logs of 5-7 and 6-35

Lithology	Depth Intervals on Logs (m below KB)	
	05-07-017-07W4M	06-35-017-09W4M
sandstone	199-203 227-231 775-777 638 802-803 839 869-872	224-228 258-262 643-644 646 814-816 874-877
shale	254-269 287-315 340-373 431-459 624-635 660-671 843-861	241-254 286-311 335-415 427-459 627-640 664-678 710-720 786-796
sandy shale/ shaly sandstone	233-247 462-466 535-541 642-644 776-783 807-820 837-840	217-223 266-284 597-618 753-758 761-783 831-840
bentonite	338 640 682 795	317 645 682 695 698 760 798 804
calclitic or sideritic unit	223-224 275 334 560 591 736 811	204 215 347 438 455 515 559 687 855
gas filled sandstone	772-775	no evidence

levels in shales and low levels in sandstones because radioactive elements tend to concentrate in shales in association with clay minerals. Care must be taken, however, as "All clays tend to be radioactive but all radioactivity is not necessarily clay" (Cannon and Coates, 1990, p. 3). Highly soluble uranium bearing salt precipitates, for example, may be deposited almost anywhere (Etnyre, 1993). The natural gamma ray spectroscopy log helps dissipate some uncertainty as to the origin of radiation. The uranium curve of 5-7 exceeds the relative base level, which is constant along the entire log, only in the First and Second White Speckled Shales. No evidence of uranium-induced radioactivity is observed in sandstone. Thorium and potassium are more reliable shale indicators, since concentrations of both of these elements are lower in the sandy units than in shales. The potassium in sandstone is associated primarily with feldspars and micas.

The neutron porosity log is sensitive to hydrogen atoms in the dry clay crystal structure and to the water bound to clay minerals. The associated high hydrogen index drives the derived apparent porosity above the effective porosity in clay rich shales and sandstones. The extent of the effect of clay-rich shales on the density porosity reading depends strongly on the contrast between the bulk densities of the shale and the sandstone mineralogies. The total bulk density of shale is generally higher than the density of quartz, which is assumed as sand matrix density in the computation of the density porosity log from the bulk density log with equation 2.2.1. The derived density porosity is, therefore, lower than the effective porosity. The neutron porosity and density porosity curves are usually plotted on a common scale grid to allow relative comparison. The separation between the neutron porosity and density porosity curves widens with an increase in clay content and with increases in heavy minerals. Cross-over of the curves generally indicates the presence of gas as a

low hydrogen index results in low neutron porosity while low fluid density results in high density porosity. In shaly formations the gas and clay effects can cancel, or at least negate, each other.

The sonic log reading responds to the total traveltimes associated with the minerals and pore-filling fluids. These traveltimes are longer in shales than in sandstone, due to the presence of clay minerals in the former. However, the difference is partially offset by the low sonic velocities of fluids that fill the generally higher percentages of pore space in sandstone. The sonic log is, therefore, not a reliable tool for visual lithology inspection.

The salinity or ion content of the formation waters of both 5-7 and 6-35 appears to be similar in value to the salinity of the mud filtrate because the spontaneous potential curve displays overall poor definition. As a result, the spontaneous potential curve contributes little information regarding lithology or permeable units. For the same reason of similarity in ion content, as well as the abundance of conductive clays and a lack of appreciable hydrocarbon content around the well bore, the resistivity curves are also of little value for determining lithology. In some sandy intervals there are minor separations between the deep and shallow resistivity curves, indicating invasion of mud filtrate into the formation. Slight reduction of the resistivity readings in shales with respect to adjacent sandy units in the Judith River Formation and Basal Colorado Sandstone may be due to clay effects, or may imply that the formation water is less saline than the mud filtrate.

Mud cakes, indicated by caliper log readings which are less than the bit size, build up adjacent to permeable units such as sandstones. Breakouts or washouts, i.e., caliper log readings greater than the bit size, are more common for shales.

The potential for the photoelectric cross-section index to be useful in the analysis of lithology is appreciable. Unfortunately, the index values derived from the mineral assemblages of the shales and the sandstones in 5-7 and 6-35 are rather similar, making it impossible to reliably differentiate these lithologies on the photoelectric cross-section index log. The log does, however, clearly mark horizons of "abnormal" mineral assemblages such as prominent bentonite layers, and calcareous streaks or siderite laminae.

For the mixed lithologies of shaly sandstone or sandy shale, the lithological effects on log responses are less prominently developed than for pure shale and sandstone.

Bentonite beds are identified on log curves by the high thorium radiation and low photoelectric cross-section index associated with their basic constituent, smectite (Tizzard, 1974). Also, the neutron porosity reading is relatively high due to the concentration of bound water, which is caused by smectite's particularly great potential to absorb water. According to literature (Maiklem, 1962; Tizzard, 1974; Hankel et al., 1969; Glass, 1990), bentonite is present as subordinate lithology along the entire study section. However, few occurrences are thick enough to prompt the characteristic log signature illustrated in Figure 3.3.

The logs repeatedly show a certain combination of signatures which is most likely caused by calcareous mineral deposits. Both calcite (CaCO_3) streaks and siderite (FeCO_3) laminae are characterized by low neutron and density porosities, high bulk density, short sonic traveltime, low gamma radiation, high photoelectric cross-section index (Table 3.4), and sometimes a small separation of the resistivity curves with a small increase in resistivity. The

Table 3.4: Logging tool responses for a selection of water-wet sedimentary minerals

Property	Smectite	Kaolinite	Mille	Chlorite	Quartz	Calcite	Siderite
Formula*	$(\text{Ca},\text{Na})_7(\text{Al},\text{Mg},\text{Fe})_4(\text{Si},\text{Al})_9\text{O}_{22}(\text{OH})_2(\text{H}_2\text{O})_n$	$\text{Al}_2\text{Si}_2\text{O}_5(\text{OH})_4$	$\text{K}_{1-1.5}\text{Al}_4(\text{Si}_7-8.5,\text{Al}_{1-1.5})\text{O}_{22}(\text{OH})_4$	$(\text{Mg},\text{Fe},\text{Al})_2(\text{Si},\text{Al})_4\text{O}_{10}(\text{OH})_2$	SiO_2	CaCO_3	FeCO_3
DENS (g/cc)*	2.12	2.41	2.52	2.76	2.64	2.71	3.89
PHIN (p.u.)*	0.44	0.37	0.30	0.52	-0.02	-0.01	0.12
PE (barnolec)*	2.04	1.83	3.45	6.30	1.81	5.08	14.69
GR (API units)*	150 - 200	80 - 130	250 - 300	180 - 250	0	0	0
K (%)**	0.16	0.42	4.5	0	0	0	0
Th (ppm)**	14 - 24	6 - 19	< 2	0	0	0	0
U (ppm)**	2 - 5	1.5 - 3	1.5	0	0	0	0

Bentonite***: K<0.5% Th=6-50ppm U=1-20ppm

* Schlumberger, 1968

** Fertl, 1987

log curves of 5-7 and 6-35 appear not to record the true values of the formation properties. Possible explanations are that the thicknesses of the layers are insufficient relative to the tools' vertical resolutions, or that the layers contain significant amounts of sandstone and shale minerals. According to Glass (1990), concretionary layers of calcite and siderite are present throughout the Colorado Group sedimentary sequence. The log signatures for these two minerals in their pure forms are indistinguishable from each other under the given conditions of surrounding mineralogy, available well logs, and lack of mineralogical analyses. The observed log signatures are, therefore, attributed along the entire section to concretionary layers of either calcite or siderite, or a combination of the two minerals.

The geological reports prepared for 5-7 and 6-35, lithological descriptions of the core analyses for these two and nearby wells (03-29-017-10W4M, 12-07-018-06W4M, 13-20-17-7W4M in particular), and published reports (Maiklem, 1962; Male and Pacholko, 1962; Moynard et al., 1963; Glass, 1990) have been consulted for the local lithology. The collected information has both supported and complemented the qualitative, visual lithological log interpretations.

Cross plots are two-dimensional representations of the variation of data with respect to two or more properties (Bateman, 1965). The method presented by Schlumberger (1968) for identifying the four clay types mentioned in Section 2.3 from geophysical logs is based on cross plots of photoelectric cross-section index (Pe) against potassium concentration (K) on the one hand, and against the ratio of thorium concentration to potassium concentration (Th/K) on the other (Figure 3.4). Because the natural gamma ray spectroscopy curves had not been

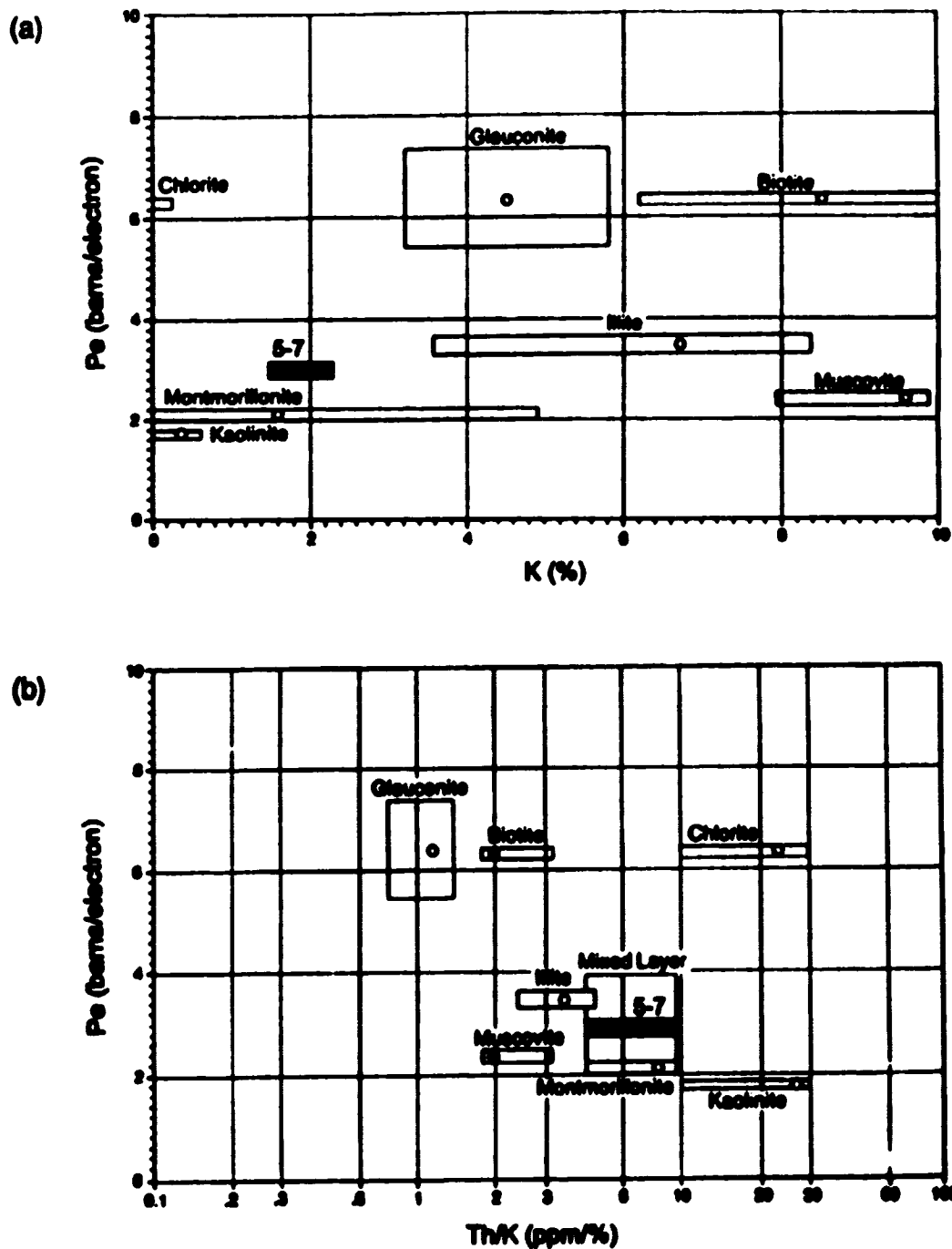


Figure 3.4: Cross plots of (a) potassium concentration (K) versus photoelectric cross-section index (Pe), and of (b) the ratio of thorium to potassium concentration (Th/K) versus photoelectric cross-section index (Pe) for the identification of clay types at 05-07-017-07W4M (identification cross-plots adapted after Schlumberger, 1968, p. 52).

digitized, only overall trends were investigated. K ranges between 1.5 and 2.3 % in shale and shaly sandstone. Pe ranges mostly from 2.8 to 3.1 barns/electron. Th/K varies between approximately 4 and 9 ppm/%.

The shaded area in Figure 3.4 a), representing the observed parameter ranges, plots between the boxes of illite and montmorillonite (smectite), permitting only ambiguous conclusions about any one or a combination of specific clay types. The shaded area in Figure 3.4 b) is contained almost completely in the "mixed layer"-area. While the thorium to potassium ratio appears to increase within the stated range with depth, a slight tendency for a decrease of the photoelectric cross-section index is observed. These vague trends may possibly indicate an overall change in clay combinations with depth, in which illite decreases, and smectite and kaolinite increase in relative weight proportion in the mixed layer clay.

No detailed mineralogical studies to sample and categorize the encountered clay minerals were conducted for this project. Some answers may be found in literature, though. Moinard et al. (1983) examined core from the Milk River Formation, the log signature of which is closely comparable to those of the study wells. These authors reported that illite and chlorite are the main types of clay, with minor amounts of kaolinite, smectite and mixed layer clays also present. Male and Pacholko (1982) stated that the clay matrix of the Second White Speckled Sandstone consists of illite, kaolinite and chlorite.

The results of the graphical analysis combined with descriptions in literature are insufficient to ascribe a single clay type to any interval, should such a layer exist. More reliably, the information supports the presence of mixed layer clays or combinations of clay types in proportions which change with depth, possibly along a continuous trend.

Layers identified as bentonite from their log signatures were not included in the cross plot analysis. The clays in bentonites were derived from volcanic ash (American Geological Institute, 1976), which differs from the sources of clays found in the sandstone and shale beds. Thus, their mineralogy may not be representative of that of adjacent layers.

Brock (1986) presented a cross plot which may be used to approximate the type of shale distribution. Figures 3.5 and 3.6 are cross plots of neutron porosity against density porosity for 5-7 and 6-35, respectively. The data pairs for the entire section are divided into depth ranges according to stratigraphic units of similar shale character, i.e., units with identical shale base values, that is neutron porosity and density porosity values assigned to represent 100 % shale. (A detailed account of the determination of the shale base values is given in Section 3.4.) Figures 3.5 a) and 3.6 a) show the general pattern of distribution of shale types on the plots. In Figures 3.5 b) to h) and Figures 3.6 b) to h) the diagonal and the trend line for laminated shales have been drawn to serve as orientation lines. Points outside the marked triangular region of the graph roughly correspond with sections where the coordinates fall outside the range between the shale baselines assigned on the curves. Upon location of these points on the log curves it becomes apparent that nearly all points below the triangle, i.e., low density porosity, are associated with previously identified sideritic or calcitic lithology. The majority of points lying to the right of the triangle, i.e., high neutron porosity, and along the trend line of structural shale are found to be associated with previously identified bentonites. Figures 3.5 e) and 3.6 e) are the most notable exceptions to both observations. For these the assigned shale baseline values are the governing factor for the abundance of points outside the marked triangle (for explanation please refer to Section 3.4).

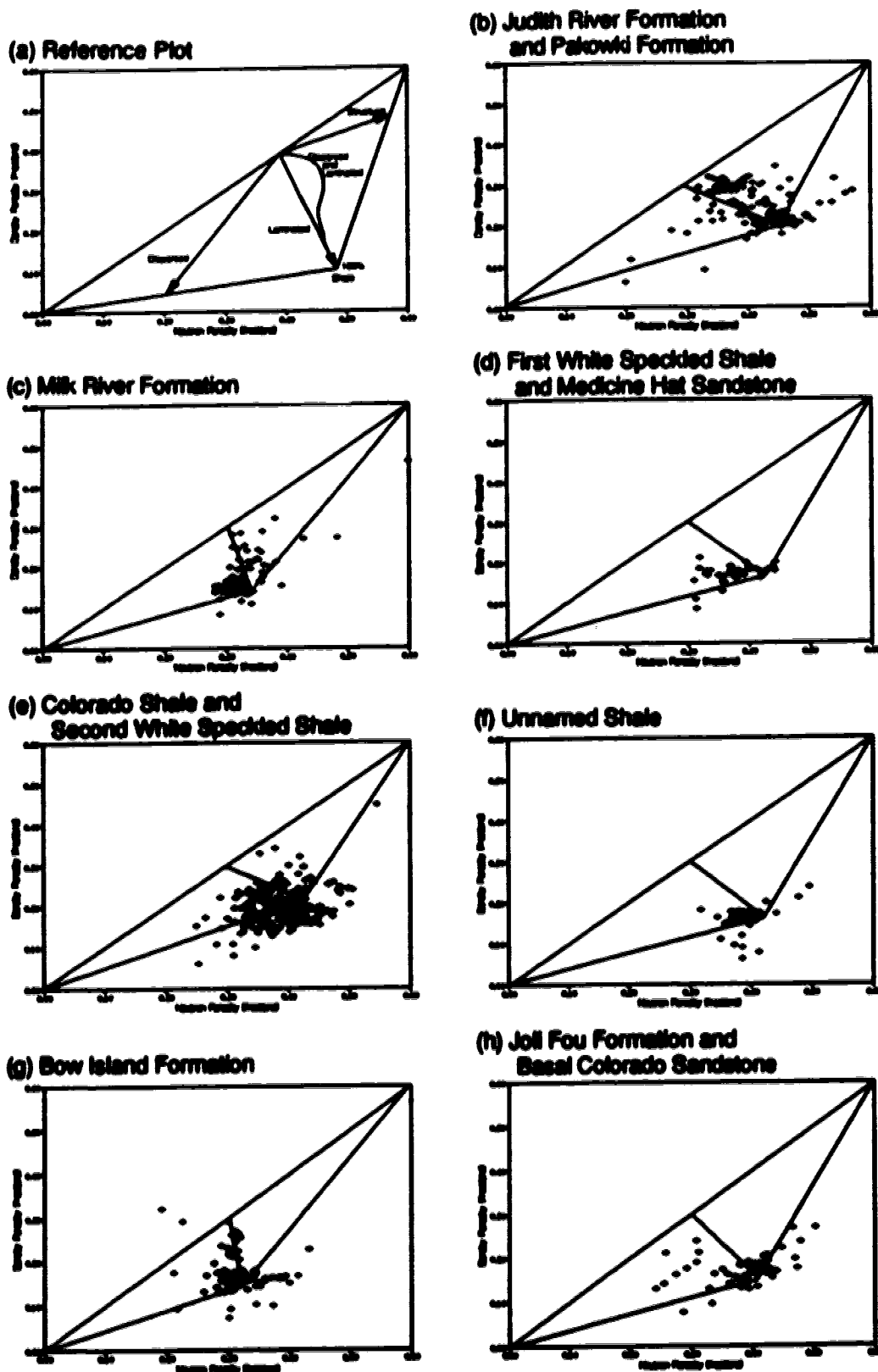


Figure 3.5: Cross plots of neutron porosity versus density porosity showing (a) reference lines for three types of shale distribution (after Brock, 1966, p. 193), and data of 5-7 for intervals corresponding to the definition of shale base values.

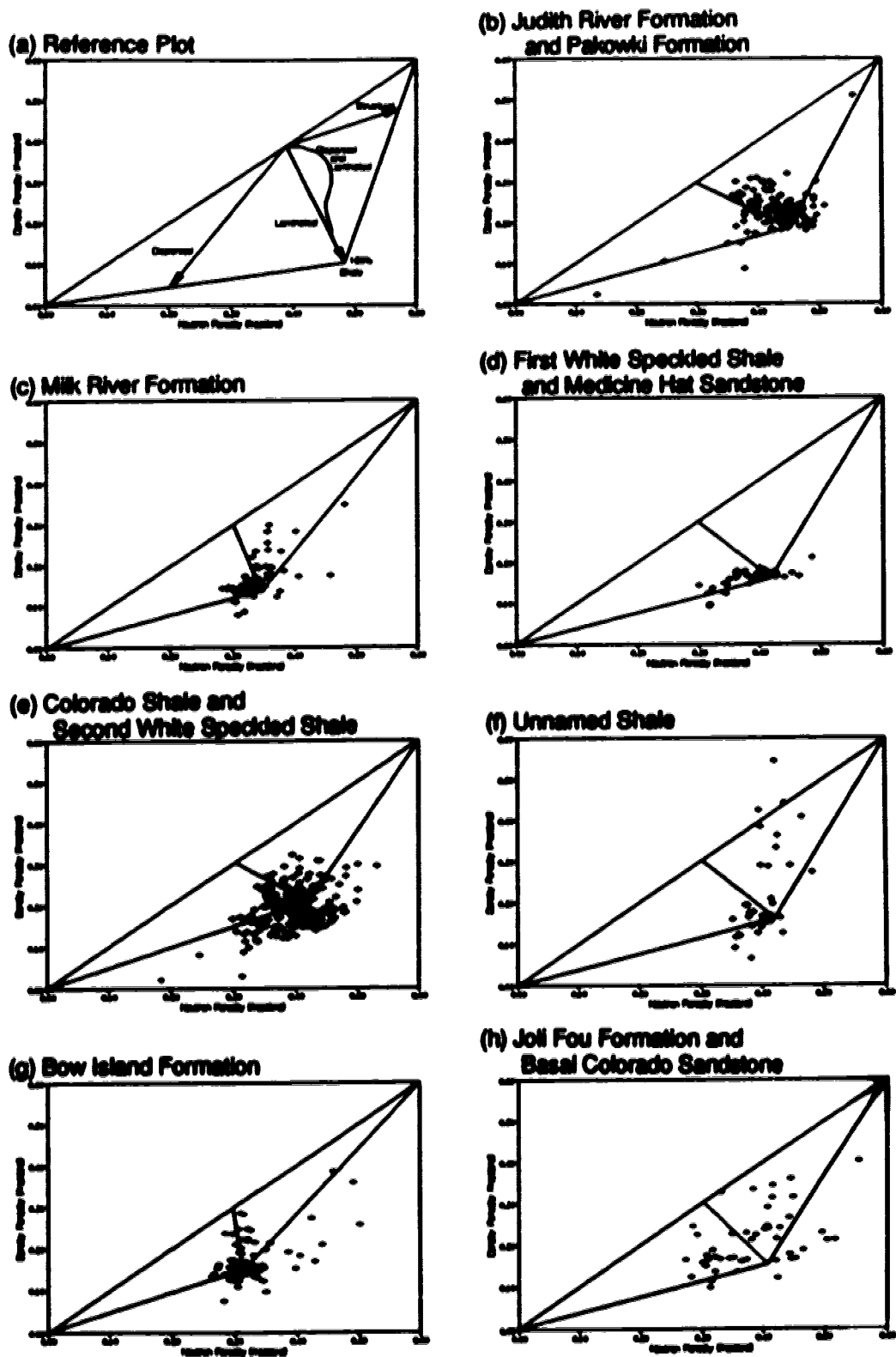


Figure 3.6: Cross plots of neutron porosity versus density porosity showing (a) reference lines for three types of shale distribution (after Brock, 1966, p. 193), and data of 6-35 for intervals corresponding to the definition of shale base values.

Unreliable density porosity data due to rough borehole conditions also contribute to points outside the designated area of the graph. In summary, the cross plots suggest mostly disseminated and laminated shales throughout the sections with some structural shale in the form of bentonites. Brock's method of shale type identification appears to fail in massive shale segments of the section, such as the Colorado Shale and Second White Speckled Shale (Figures 3.5 e) and 3.6 e)). The analysis is very approximate; nevertheless, the plots as a whole confirm generalizations about shale types in literature (Tizzard, 1974; Moinard et al., 1983) and core analyses.

More frequently used cross-plot methods include the M-N and the MID (matrix identification) plots. These have been developed primarily for complex mineral mixtures and matrix identification (Crain, 1986; Schlumberger, 1989), e.g., gypsum, anhydrite, salt, and dolomite versus limestone versus sandstone matrix. The lithology interpretation and evaluation of 5-7 and 6-35 may not be enhanced by such methods, as there are no salts or heavy minerals to be identified and the matrix has already been established to consist of sandstone and shale.

3.4. Shale Volume

Shale volume is a required quantity for porosity calculations. By itself, shale volume serves as a type of continuous lithological indicator. Although it is referred to as shale volume, the quantity actually represents the sum of effects of several formation factors including clay and bound water contents on one or a combination of two logs.

Three methods of shale-volume determination were used, involving the total gamma radiation curve, the spontaneous potential curve and a combination of the neutron porosity and density porosity curves. For each of these methods, base values or base lines, constants which represent a particular log parameter for clean sandstone or shale (i.e., no shale or sandstone inclusions, respectively) over a specified depth interval, must be picked. The indicators discussed in Section 3.3 were used to identify these lithologies on the logs. Based on distinct changes of log signatures of shale resulting from different formation characteristics and mineralogical composition, the entire log interval was divided into seven sub-intervals of one or several stratigraphic units.

On the total gamma radiation curve the shale base values (GR100) were picked at or near the maximum deflection. Exceptions were the First White Speckled Shale and the Second White Speckled Shale where uranium contributed radiation in excess of the shale-indicative thorium and potassium radiation; here the base value was picked well below the maximum deflection. Sandstone base values were more difficult to choose. There are very few clean sandstone units, all of which are probably too thin to warrant full deflections on the logs (e.g., Second White Speckled Sandstone, and thin beds in the Judith River Formation, the Bow Island Formation and the Basal Colorado Sandstone). Therefore, the total gamma radiation base value for sandstone (GR0) was picked at the very minimum deflection or even at a somewhat smaller value. GR0 is not zero because of background radiation possibly contributed by potassium feldspar, clay minerals associated with sandstone, uranium content, etc.. Bentonite and calcitic units were excluded from this procedure. The base values provide the end points for a calibration of the total gamma radiation curves in terms of fractional units of shale volume. The

underlying assumption is that all gamma radiation recorded above the sandstone base value is due solely to shale. The scale is linear and may be expressed mathematically as

$$VSHG = \frac{GR - GR0}{GR100 - GR0} \quad (3.4.1)$$

where VSHG is the shale volume as determined from the total gamma radiation curve, and GR is the recorded measurement of total gamma radiation (Crain, 1986). In the true physical sense VSHG represents clay volume rather than shale volume. GR100 is the total gamma radiation produced by the clay content of pure shale (approximately 60 % or less by volume). Error is generated if the clay content varies in volume proportion of total shale volume, or if its radiation characteristics change over the depth interval in which the base values are applied.

Attempts to pick clean sandstone and pure shale base values on the spontaneous potential curves failed due to the lack of clear definition of lithology on the curves. The mathematical expression for the calculation of shale volume would have been based on the same principle as equation 3.4.1.

For the neutron porosity and density porosity curves, only shale base values were necessary. Because shale volume is represented mainly by the separation of the two curves rather than the absolute values of each curve, separation constants were established first. Care was taken to exclude bentonite and calcitic beds, as well as intervals with disturbing borehole rugosity. As a second step, shale base values were assigned to the neutron porosity (PHINSH) and density porosity (PHIDSH) curves in accordance with the previously defined separation constants. In this case the difference between the shale base values serves as one end point for a calibration of the separation between the neutron porosity and density porosity curves. The other

end point is an assumed zero separation for clean sandstone. The assumption is shown to be practically acceptable by very small separations (less than 0.03 fractional porosity units) at several one- to three-metre intervals of probably not perfectly clean sandstone of 5-7 and 6-35. The resulting linear mathematical expression is

$$VSHND = \frac{PHIN - PHID}{PHINSH - PHIDSH} \quad (3.4.2)$$

VSHND is the shale volume in fractional units determined from the combined neutron porosity and density porosity curves; PHIN and PHID are the recorded neutron porosity and density porosity measurements, respectively (Crain, 1986).

Equations 3.4.1 and 3.4.2 were applied to the digitized measurements of total gamma radiation, neutron porosity and density porosity in separate spreadsheets for 5-7 and 6-35. The calculations were repeated for each depth entry with the appropriate constants GR0, GR100, PHINSH and PHIDSH. The VSHG and VSHND values resulting from the first round of computations did not correlate well with each other, and included numerous values outside the fractional range of zero to one. Several iterations were necessary with adjusted base values and redefined depth intervals of application. As better understanding of the signatures was gained in the process, more reasonable values were assigned to the constants. The final sets of constants and corresponding depth intervals of 5-7 and 6-35 are listed in Table 3.5.

The final sets of computed VSHG and VSHND differed for the most part by 5 to 30 %. Figures 3.7 a) and b) display the overall correlations. The largest discrepancies are found in sections where the total gamma radiation curve is affected by uranium, and where calcitic units, iron-rich cements, and

Table 3.5: Shale and sandstone base values used for shale volume analysis

Depth Range (m)	Stratigraphic Units	Gamma Ray Sand Base Value (API units)	Gamma Ray Shale Base Value (API units)	Neutron Porosity Shale Base Value (p.u.)	Density Porosity Shale Base Value (p.u.)
66-67-017-07W4M					
188 - 334	Judith River Formation and Pakowki Formation	45	75	0.450	0.200
335 - 429	Milk River Formation	45	100	0.340	0.135
430 - 473	First White Speckled Shale and Medicine Hat Sandstone	45	120	0.420	0.165
474 - 708	Colorado Shale, and Second White Speckled Sandstone and Shale	45	115	0.420	0.210
709 - 743	Unnamed Shale	45	120	0.420	0.165
744 - 828	Bow Island Formation	55	105	0.320	0.145
829 - 877	Joli Fou Formation and Basal Colorado Sandstone	55	100	0.405	0.155
66-36-017-06W4M					
188 - 328	Judith River Formation and Pakowki Formation	50	80	0.460	0.190
329 - 428	Milk River Formation	50	105	0.340	0.135
429 - 470	First White Speckled Shale and Medicine Hat Sandstone	45	120	0.420	0.165
471 - 708	Colorado Shale, and Second White Speckled Sandstone and Shale	45	120	0.420	0.210
710 - 750	Unnamed Shale	45	120	0.420	0.165
751 - 808	Bow Island Formation	45	105	0.320	0.145
809 - 882	Joli Fou Formation and Basal Colorado Sandstone	55	95	0.405	0.165

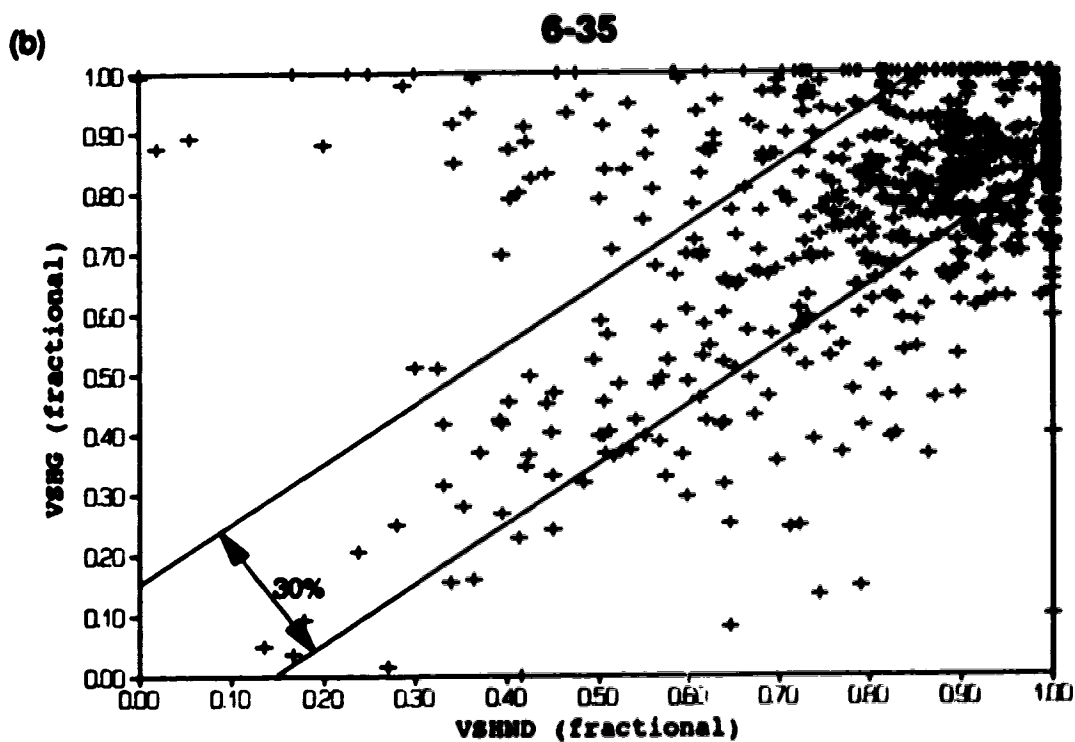
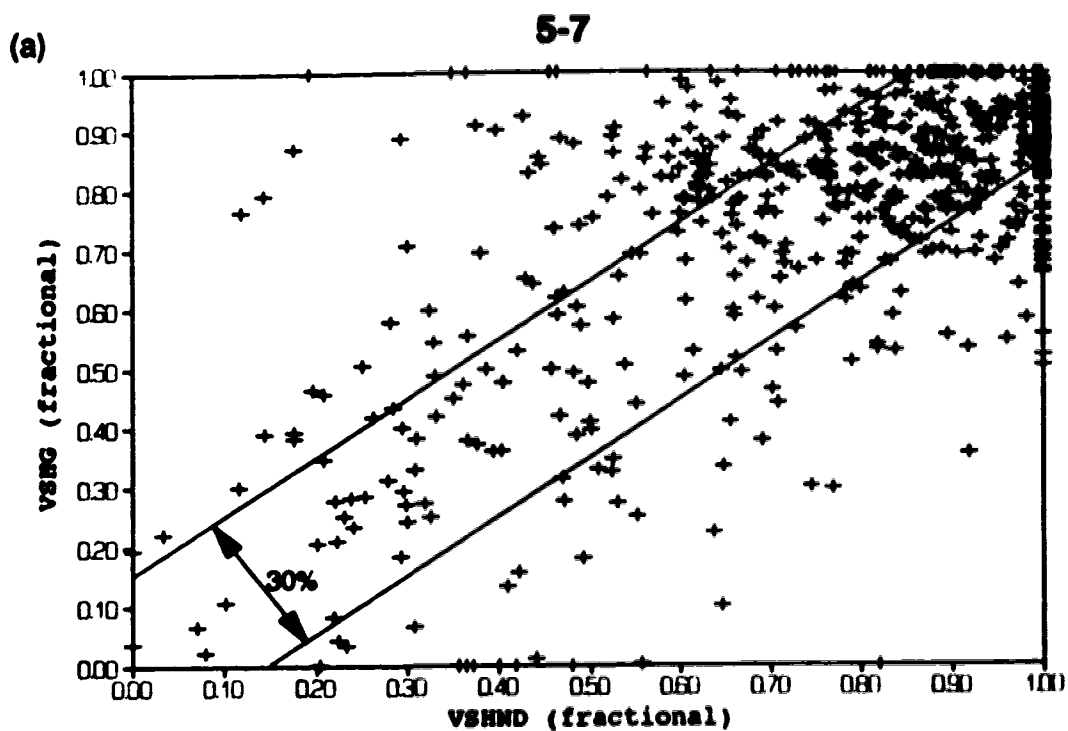


Figure 3.7: Comparative cross plots of shale volumes determined from the total gamma radiation log (VSHG) and the separation between the neutron porosity and density porosity curves (VSHND), for (a) 5-7 and (b) 6-35.

considerable borehole rugosity strongly influence the density porosity reading. The gas cross-over of the neutron porosity and density porosity curves in the Bow Island Formation in 5-7 resulted in a negative VSHND. The fine one-metre divisions may have contributed to the differences between VSHG and VSHND. Where the log responses for a 'thin' (less than or approximately equal to one metre) formation or borehole condition are offset by a digitizing interval, the values of the shale volumes are offset by the same one-metre interval.

Some discrepancy is also surely due to the difference in physical principles upon which the total gamma radiation, neutron porosity and density porosity measurements are based, and on the different spheres of investigation. Thus, the calculated shale volumes reflect different formation characteristics. For example, VSHG is largely independent of the type of shale distribution while the bound-water content associated with the three types does influence the neutron porosity measurements, and thereby VSHND.

As well, the vertical sub-intervals of logging depths for which base values were established, may have been assigned inappropriately or in insufficient number. The character and composition of shales may vary within the sub-intervals causing unrealistically high or low shale values, implying that it is not acceptable to extrapolate the defined base values from the points of definition to the entire sub-interval. However, no finer or different division was justifiable.

Manual editing was the last step in producing a single set of shale volumes for further spreadsheet operations for each location. The calculated VSHG and VSHND were used as guide values but consideration was also given to the entire log suites, and other sources of information including the core analysis reports for 5-7 and 6-35 and nearby wells, and Moinard et al. (1963). Prominent bentonites were assigned 100 % shale volume, which also usually resulted from the calculations. Prominent calcitic units resulted in low

VSHG and variable VSHND; the assigned shale values are very close in value to VSHG. In view of the moderate accuracy of the arithmetic methods involving base values and the anticipated effects associated with a change of, say 10 %, of shale volume, a 5 % precision was thought adequate for the final shale volume. A final shale volume (VSH) was assigned to each one-metre interval keeping in mind the criteria stated above as potential reasons for discrepancies. Because the process involved personal judgment, it was repeated once to improve consistency. A complete listing of the final shale volumes is included in Appendix C. Plots against depth are provided in Log Sets B1 and B2.

3.5. Porosity

Effective porosity may be derived from calculations based on different formation models, e.g., those illustrated in Figure 2.9, and involving one or more log parameters. Seven methods are introduced in this section. These contain a minimum of case- and area-specific calibration and proportionality constants, and therefore, represent the most general methods found in literature.

All methods require some type of computational transform to estimate effective porosity from recorded logging parameters. For this purpose, it is assumed that porosity associated with shales, or clay minerals in general, does not contribute to the effective porosity of the formation. The shale corrections are, therefore, attempts to filter the effects of shale and clay minerals out of log measurements and the corresponding porosities.

None of the methods presents an actual measurement of effective porosity. Since these approximations are derived from simplified models and empirical algorithms, the calculated parameter is not called "effective porosity",

a term associated with the strict definition provided in Section 2.1; rather, it is referred to as log-derived porosity.

The first pair of methods is based on the bulk density curve. The general relationship between density and porosity may be expressed as

$$\rho_b = \phi \cdot \rho_f + (1 - \phi) \cdot \rho_{ma} \quad (3.5.1)$$

ρ_b is the bulk density of the formation, ϕ is the porosity, ρ_f is the density of the fluid filling the pores, and ρ_{ma} is the matrix density. If the shale content is separated from the matrix term as was the fluid content, equation 3.5.1 becomes

$$\rho_b = \phi \cdot \rho_f + V_{sh} \cdot \rho_{sh} + (1 - \phi - V_{sh}) \cdot \rho_{ma} \quad (3.5.2)$$

which is equivalent to

$$\phi = \frac{(\rho_{ma} - \rho_b)}{(\rho_{ma} - \rho_f)} - V_{sh} \cdot \frac{(\rho_{ma} - \rho_{sh})}{(\rho_{ma} - \rho_f)} \quad (3.5.3)$$

where ρ_{sh} and V_{sh} are density and volume of shale, respectively. In terms of logging parameters equation 3.5.3 may be expressed as

$$PHIEDA = \frac{(DENSMA - DENS)}{(DENSMA - DENSW)} - VSH \cdot \frac{(DENSMA - DENSSH)}{(DENSMA - DENSW)} \quad (3.5.4)$$

where PHIEDA is a density-log derived porosity corrected for shale, DENSMA is the assumed density of the formation matrix (2650 kg/m³ for both 5-7 and 6-35), DENSW is the approximated density of the mud filtrate (1047 kg/m³ for 5-7, 1035 kg/m³ for 6-35), DENSSH is the approximated mean value of the bulk density of shale (Table 3.6), DENS is the digitized bulk density, and VSH is the shale volume (see Section 3.4). The original reference for equation 3.5.4 could not be located, however, the equation was stated by Dresser Atlas (1962).

A slightly different version of the same equation is found in Crain (1966):

Table 3.6: Shale base values used for porosity analysis

Depth Range (m)	Stratigraphic Units	Bulk Density (kg/m ³)	Sonic Traveltime (μsec/m)	Neutron Porosity (p.u.)	Density Porosity (p.u.)
06-07-017-07W4M					
188 - 394	Judith River Formation and Pakowti Formation	2325	420	0.450	0.200
395 - 429	Milk River Formation	2425	340	0.340	0.135
430 - 473	First White Speckled Shale and Medicine Hat Sandstone	2375	375	0.420	0.165
474 - 703	Colorado Shale, and Second White Speckled Sandstone and Shale	2335	375	0.420	0.210
704 - 743	Unnamed Shale	2400	375	0.420	0.165
744 - 828	Bow Island Formation	2425	375	0.320	0.145
830 - 877	Joli Fou Formation and Basal Colorado Sandstone	2400	375	0.405	0.155
06-38-017-00W4M					
193 - 328	Judith River Formation and Pakowti Formation	2325	410	0.460	0.190
329 - 426	Milk River Formation	2425	340	0.340	0.135
427 - 470	First White Speckled Shale and Medicine Hat Sandstone	2375	365	0.420	0.165
471 - 708	Colorado Shale, and Second White Speckled Sandstone and Shale	2350	365	0.420	0.210
710 - 750	Unnamed Shale	2400	365	0.420	0.165
751 - 836	Bow Island Formation	2425	365	0.320	0.145
837 - 882	Joli Fou Formation and Basal Colorado Sandstone	2375	365	0.405	0.165

$$\text{PHIEDC} = \frac{(\text{DENS} - \text{DENSMA})}{(\text{DENS} - \text{DENSMA})} - \text{VSH} \cdot \text{PHIDSH} \quad (3.5.5)$$

PHIEDC is a density-log derived porosity corrected for shale; DENSMA, DENS, and VSH are the same parameters as in equation 3.5.4; and PHIDSH is the shale base value of the density porosity curve (Table 3.6).

Just as the first fractional term of equation 3.5.4 is equal to PHID, the density porosity recording (compare to equation 2.2.1), the second fractional term - multiplied by VSH - is an equivalent PHID in a pure shale zone. Differences between PHIEDA and PHIEDC may be attributed mostly to the definition of shale base values on the bulk density and density porosity curves, and are possibly magnified by large VSH values.

The sonic traveltime may be transformed into porosity via the Wyllie relationship introduced in Section 2.2 as equation 2.2.3:

$$\phi = \frac{(\Delta t - \Delta t_{ma})}{(\Delta t_f - \Delta t_{ma})} \quad (3.5.6)$$

where Δt is the formation traveltime, Δt_{ma} is the traveltime in the matrix, and Δt_f is the traveltime in the formation fluid which fills the pores. By accounting for the log response associated with shale portions of the travel path separately, the equation becomes

$$\text{PHISC} = \frac{(\text{DELT} - \text{DELTMA})}{(\text{DELTW} - \text{DELTMA})} - \text{VSH} \cdot \frac{(\text{DELTSH} - \text{DELTMA})}{(\text{DELTW} - \text{DELTMA})} \quad (3.5.7)$$

where PHISC is the traveltime-log derived porosity corrected for shale; DELTMA is the assumed traveltime in the matrix material (180 $\mu\text{sec/m}$), DELTW is the assumed traveltime in the mud filtrate which fills the pores in the invaded zone (636 $\mu\text{sec/m}$), DELT is the digitized sonic traveltime, and VSH is the shale volume. The value of DELTSH (Table 3.6) was determined from log readings of the sonic curve in sections with VSH values equal to or greater than 0.60.

Crain (1986) suggested the application of a commonly used correction factor (KCP) in shallow stratigraphic units (generally above 900 to 1200 m in western North America) where DELTSH is greater than 328 $\mu\text{sec/m}$ (original reference in the 1960's could not be located). KCP is calculated as the ratio of DELTSH to a constant 328 $\mu\text{sec/m}$. It is an empirical factor which compensates for a characteristic of young sedimentary rocks: individual particles may not be locked rigidly into the framework of the rock due to incomplete or insufficient compaction and cementation, thus making the rock more compliant, which increases the traveltime. The correction was applied where appropriate, and the traveltime-log derived porosity corrected for shale and compaction (PHIES) was determined from the equation

$$\text{PHIES} = \frac{\text{PHISC}}{\text{KCP}} . \quad (3.5.8)$$

The second group of methods is based on combinations of two logging parameters. These are often referred to as cross-plot methods because the parameters may be plotted on the two axes of a Cartesian coordinate system and, therefore, lend themselves to graphic chart book analysis (e.g., Schlumberger, 1988). For the purpose of spreadsheet analysis, only computational equivalents are included here.

Both the neutron-porosity and density-porosity curves are records of apparent porosity, displayed in generic fractional porosity units (p.u.). Both require corrections for shale effects to derive effective porosity; additional manipulations, however, tend to improve the quality of the results.

Crain (1986) stated two versions of a quick-look method. First, shale corrections are made on the individual curves:

$$\text{PHINC} = \text{PHIN} - \text{VSH} \cdot \text{PHINSH} \quad (3.5.9)$$

$$\text{and } \text{PHDC} = \text{PHID} - \text{VSH} \cdot \text{PHIDSH}. \quad (3.5.10)$$

PHINC and PHDC are the shale corrected neutron porosity and density porosity values, respectively; PHIN and PHID are the digitized neutron porosity and density porosity, respectively; PHINSH and PHIDSH are the respective shale base values (Table 3.6); and VSH is the shale volume (see Section 3.4).

Theoretically, PHINC and PHDC are both effective porosities. By arithmetically averaging equations 3.5.9 and 3.5.10, some compensation for environmental factors may be achieved. The new shale-corrected neutron-density cross-plot derived porosity (PHIEND2) emerges as

$$\text{PHIEND2} = \frac{\text{PHINC} + \text{PHDC}}{2}. \quad (3.5.11)$$

The second version is a less optimistic variant of PHIEND2:

$$\text{PHIEND3} = \text{PHDC} + \frac{\text{PHINC} - \text{PHDC}}{3}. \quad (3.5.12)$$

When re-writing equation 3.5.11. as

$$\text{PHIEND2} = \text{PHDC} + \frac{\text{PHINC} - \text{PHDC}}{2}, \quad (3.5.13)$$

it becomes apparent that PHIEND3 is consistently 1/6 of the magnitude of the separation between PHINC and PHDC less than PHIEND2.

Schlumberger (1985) proposed a simplified mathematical expression to approximate porosity (PHIENDS) from the same two logging parameters:

$$\text{PHIENDS} = \frac{\text{PHIN} + \text{PHID}}{2} \cdot (1 - \text{VSH}). \quad (3.5.14)$$

By applying the shale correction to the arithmetic average of the neutron porosity and density porosity measurements, no shale base values need to be picked. With respect to equation 3.5.11, PHIENDS and PHIEND2 differ by an amount equal to

$$(\text{PHIENDS} - \text{PHIEND2}) = \frac{\text{VSH}}{2} \cdot [(\text{PHINSH} + \text{PHIDSH}) - (\text{PHIN} + \text{PHID})]. \quad (3.5.15)$$

The relationship shows that PHIENDS is consistently lower than PHIEND2. The difference between PHIENDS and PHIEND2 increases with increasing shale volume within depth intervals of constant shale base values. Individually, the error associated with ill-defined base values (affecting equations 3.5.11 and 3.5.12), as well as the error due to shale correcting the already scaled effective porosity (equation 3.5.14), increase with an increase in shale volume.

A different type of neutron porosity-density porosity cross-plot is the bulk volume water, or dual water, cross-plot. It is based on the dual water formation model (Clavier et al., 1984) in which the water associated with shales or shaly sand is treated as a mixture of formation and so-called clay waters. The differentiation is a result of the adsorption effects of surface charges of clay minerals on formation water. The original purpose of the model was to account for the resistivity behaviour of clayey sands and, thereby, enhance the analyses for water and hydrocarbon saturations. The derivation of a mathematical equivalent to the complex graphical representation involved the solution of simultaneous equations containing trigonometric functions (Sah, 1977).

Crain (1986) presented the series of equations required for the determination of porosity from the bulk volume water method (PHIEBVW). The recorded neutron porosity and density porosity curves in shales are assumed to be a combination of the response to the bulk volume water attached to the clay minerals in shale (BVWSH) and the response to dry clay. PHIDDC is the approximated density porosity reading in dry clay:

$$PHIDDC = \frac{DENS_{DC} - DENS_{MA}}{DENS_W - DENS_{MA}} \quad (3.5.16)$$

DENS_{MA} is the assumed value for the density of the formation matrix (2650 kg/m³) and DENS_W is the approximated density of the mud filtrate (1047 kg/m³)

for 5-7, 1035 kg/m³ for 6-35). DENSDC is the assumed density of dry clay (2900 kg/m³ for both wells). PHINDC, the neutron porosity reading in dry clay is estimated from PHIDDC and previously defined shale base values PHINSH and PHIDSH:

$$PHINDC = 1.00 - \frac{(1.00 - PHIDDC) \cdot (1.00 - PHINSH)}{(1.00 - PHIDSH)} \quad (3.5.17)$$

BVWSH is computed from the expression

$$BVWSH = \frac{(PHINDC \cdot PHIDSH) - (PHIDDC \cdot PHINSH)}{(PHINDC - PHIDDC)} \quad (3.5.18)$$

PHINSH, PHIDSH, PHINDC, PHIDDC and BVWSH are constants over the depth intervals which were defined for the purpose of picking shale base values (Section 3.4 and Table 3.6). The total porosity (PHIT) is determined with the bulk volume water method for individual one-metre digitizing intervals:

$$PHIT = \frac{(PHINDC \cdot PHID) - (PHIDDC \cdot PHIN)}{(PHINDC - PHIDDC)} \quad (3.5.19)$$

The final log-derived porosity is the solution to an equation which is familiar from one-log methods. The total porosity is adjusted for shale effects in proportion to shale volume (VSH):

$$PHIEBVW = PHIT - VSH \cdot BVWSH \quad (3.5.20)$$

Little may be said about the physical basis of the bulk volume water method in terms of porosity because some necessary background information is unavailable. Of concern is the process of assigning a value to PHIDDC.

Although the densities of the four clay minerals are well defined in theory, without mineralogical analysis it is impossible to estimate a value of DENSDC for any particular depth interval, let alone for the entire logging interval, with certainty and accuracy. DENSMA and DENSW are also mere approximations in equation 3.5.16, which is used to calculate PHIDDC. Unfortunately, the resulting PHIDDC is part of the definition of PHINDC, and both variables are

included in the equations for BVWSH and PHIT. The uncertainty associated with PHIDDC, therefore, tends to be magnified throughout the computational process to eventually affect the quality of PHIEBVW.

Plots of all log-derived porosities against depth are included in Log Sets B1 and B2.

To this point the simplified formation model has incorporated only sand matrix, shale and fluid, namely mud or mud filtrate. No adjustments have been made for hydrocarbons in the pore space. Referring to Section 2.4, gas may be expected in the section. While oils may be approximated by mud in porosity computations, gas requires special corrections of the log measurements. For the two bulk density methods, the corrections may simply be the substitution of the density of gas for the variable DENS_W in equations 3.5.4 and 3.5.5. Similarly, DELT_W in equation 3.5.7 may be replaced by the sonic traveltime in gas. Such corrections are complicated by the fact that the logging measurements reflect mostly the conditions in the invaded zone. In shaly sands, mud and mud filtrate are likely to completely or partially replace gas in the pore space. The density and traveltime of the resulting mud-gas mixture depends on factors such as the water saturation in the invaded zone, pressure, temperature, and gas and mud densities (Crain, 1966).

No adjustments of the parameter curves for gas effects are proposed for the first two neutron-porosity density-porosity cross-plot methods PHIEND2 and PHIEND3. Instead, Crain (1966) suggested PHIEND2 to be calculated as

$$\text{PHIEND2} = \sqrt{\frac{(\text{PHINC})^2 + (\text{PHIDC})^2}{2}} \quad (3.5.21)$$

where gas cross-over occurs after the shale correction has been applied (all variables are those of equation 3.5.11). PHIEND3 may be preferable to

PHIEND2 in gas-bearing zones because equation 3.5.12 is based on the premise that the neutron porosity operates with a greater depth of penetration than the density tool. The neutron porosity measurement is therefore more affected by gas, and as a result is given a less influential position in the equation than the density porosity. No further adjustments are necessary (Crain, 1986). Schlumberger (1985) states no mathematical equivalent of the suggested graphical gas correction to increase the value of PHIENDS (equation 3.5.14). For the dual water method, Crain (1986) assured that PHIEBVW (equation 3.5.20) is reasonable without special provisions for gas.

In the log suites of 5-7 and 6-35, characteristic signatures of gas (Figure 3.3) were observed only in the interval from 772 to 775 m in 5-7. According to the production records, gas may also be expected in other intervals of the Bow Island Formation and the Basal Colorado Sandstone in both 5-7 and 6-35. Evidence may be lacking in the logs because of invasion effects. Because insufficient information was available for sensible corrections of the effective porosities derived from the bulk density and sonic traveltime, PHIEND2 only was re-calculated for the section of the Bow Island Formation of 5-7 spanning from 772 to 775 m using equation 3.5.21. With respect to the porosity values obtained with equation 3.5.1, the adjusted porosities were less than 1 % higher. This difference is insignificant in view of the absolute magnitudes of PHIEND2 (9 %, 22 %, 23 %, 24 %) and their uncertainties.

The seven log-derived porosities computed for each one-metre interval of both 5-7 and 6-35 are listed in Appendix C and are included in Log Sets B1 and B2. One immediate observation was the abundance of negative results.

Negative values of porosity are alarming because they are physically meaningless. The equations involved in calculating PHIEDA, PHIEDC, PHIES,

PHIEND2, PHIEND3 and PHIFLOW produce negative answers in the case of over-correction of porosity for shale effects. In other words, the correction exceeds the total or apparent porosity. This statement holds true only in a conceptual sense, however. In actual fact, a simplified formation model consisting merely of sandstone, shale and drilling fluid, in addition to the estimated or artificially defined formation constants, was used to approximate the porosity correction for shale as the product of VSH and the associated multiplication factor in equations 3.5.4, 3.5.5, 3.5.7, 3.5.9, 3.5.10 and 3.5.20. The same criteria apply in the approximation of the minuend in the same equations. The over-correction is, therefore, not even an artifact of computational manipulations of absolute physical measurements, but of loosely defined variables already prone to uncertainty. It follows to reason that negative answers for porosity are not only alarming in terms of being physically meaningless, as said earlier; the tedious explanation for their existence leads to the more essential conclusion that the entire suite of log-derived porosities consists of pseudo-artificial values. A preliminary comparison of log-derived porosities to porosity measurements from core analyses of 5-7 and 6-35 (Section 3.1.2 and Table 3.1) confirms that they generally do not agree well in the overlapping depth intervals. The consistency aimed for in the cautious definition of constants from recorded data or from literature lends support to the speculation that the results are reliable at least in relative, if not necessarily in absolute magnitude. The speculation does not include lithologies other than sand and shale, though.

Equation 3.5.14 for PHIENDS does not permit negative porosity values based on the shale correction because the correction term $(1-VSH)$ is applied in form of a multiplication and cannot be less than zero with VSH being limited to the range zero to one. Nevertheless, the same conclusions as have been

drawn for the quality of the results of the remaining methods in terms of the reliability of the absolute and relative profile are valid for PHIENDS.

Linear regression was used to compare the seven different series of log-derived porosity statistically. In general, regression analysis is a method of finding the statistical dependence of one quantity on other quantities (Sheriff, 1991). The least-squares method (Davis, 1983) applied here is the algebraic expression of a graphic principle based on a cross-plot of quantities x and y , where x is the independent and y the dependent variable. The objective is to obtain the equation of a straight line, which may be placed in the cross-plot in a manner that minimizes the deviations of the data points from the line in terms of quantity y . In other words, the regression equation is defined to minimize the sum of the squares of the distances between the actual y -values and those predicted from the equation itself. The equation of the best-fit-line is of the form

$$y = m \cdot x + c \quad (3.5.22)$$

where m is the slope and c is the intercept at which the line crosses the y -axis. The goodness-of-fit of the line to the points is defined by R^2 . The reader is referred to Freund and Walpole (1980, pp. 419 to 451) or Davis (1983, pp. 176 to 182) for the complex equation of R^2 and its derivation. R^2 is the square of the sample correlation coefficient, which is the percentage of variation in one variable corresponding to variation in the other. An R^2 of 1.0 is optimal while an R^2 of 0.0 implies that the two variables are uncorrelated.

Table 3.7 contains the results of the regression analysis for various pairs of log-derived porosities for 5-7 and 6-35 computed with a pre-programmed spreadsheet function. The pairs of variables were chosen so that each porosity is coupled with at least one representative of each group, i.e., PHIEDA and PHIEDC, PHIEND2, PHIEND3, and PHIENDS, PHIES, and PHIEBVW. For a

Table 3.7: Results of regression analyses by the least-squares method for log-derived porosities, expressed in terms of the correlation statistic R-squared, and the y-intercept and slope of the best-fit straight line

Independent Variable (p.u.)	Dependent Variable (p.u.)	06-07-017-07WAM			06-35-017-09WAM		
		R-squared (fractional)	y-Intercept (p.u.)	Slope (fractional)	R-squared (fractional)	y-Intercept (p.u.)	Slope (fractional)
PHEND2	PHEND3	0.9916	-0.0004	0.9994	0.9832	-0.0015	0.9994
PHEND2	PHEND5	0.8203	0.0143	0.8002	0.7239	0.0148	0.7208
PHEND2	PHIES	0.7317	0.0009	0.9063	0.6316	0.0133	0.8124
PHEND2	PHIEDA	0.9021	0.0076	0.9674	0.8043	0.0088	0.9039
PHEND2	PHIEDC	0.9082	0.0028	0.9992	0.8340	-0.0007	0.9716
PHEND2	PHIESVW	0.9958	0.0004	0.9965	0.9939	0.0015	0.9883
PHEND3	PHEND5	0.8080	0.0151	0.7904	0.6583	0.0179	0.6827
PHEND3	PHIEDA	0.7382	0.0024	0.9904	0.4482	0.0141	0.7965
PHEND3	PHIEDC	0.7322	-0.0024	1.0149	0.4665	0.0049	0.8578
PHEND3	PHIESVW	0.8180	-0.0051	1.0222	0.6976	0.0017	0.9774
PHIES	PHIESVW	0.7169	0.0136	0.7981	0.5951	0.0105	0.7484
PHIEDA	PHIEDC	0.9925	-0.0049	1.0251	0.9722	-0.0082	1.0408
PHIEDC	PHIESVW	0.9024	0.0028	0.9052	0.8528	0.0029	0.8605
PHIEDC	PHIES	0.6699	0.0030	0.8256	0.4065	0.0247	0.6084

given pair of porosities, R^2 is a constant; the slope and y-intercept vary with the assignment of each porosity as either dependent or independent variable. Because R^2 is the indicator of greatest interest here, only one of the two possibilities was considered for each pair.

R^2 is a numerical indicator of how well the two curves parallel each other with depth. The absolute magnitude of the y-intercept is representative of the bulk offset in porosity units between the curves. For example, the pair of PHIEND2 and PHIEND3 results in nearly optimal R^2 's of 0.9916 and 0.9832, and very low y-intercepts of -0.0004 p.u. and -0.0015 p.u. for 5-7 and 6-35, respectively. Based on these criteria, the two curves may be expected to closely overlap. The log plots (Log Sets B1 and B2) of PHIEND2 and PHIEND3 on one common scale grid support this statistically based hypothesis.

Some observations and conclusions may be made from the analysis. PHIEND2, PHIEND3, PHIEBVW, PHIEDA and PHIEDC are very close quantitative and qualitative replicas of each other for both 5-7 and 6-35. Although they are computed with different algorithms, all are based on the same bulk density recording and shale constants, and all but PHIEDA and PHIEDC on the same neutron density measurement. The similarity is, therefore, not without reason. The correlation between PHIENDS and the log-derived porosities of the group of five identified above is likely reduced by the neglect of log responses to shale in equation 3.5.14. PHIES is an exception in that the algorithm for its calculation is based on sonic traveltime, and thereby on a different physical principle of formation evaluation than the remaining six methods.

It is not sensible to iterate the porosity calculations for the purpose of enhancing the correlation between them. By re-defining and adjusting the variables in equations 3.5.4 to 3.5.20, as would be required to increase the

R^2 's, the log-derived porosities would be calibrated against each other without reference to the actual effective porosity of the formation beyond the borehole. The resulting log-derived porosity would not have gained either accuracy or precision.

The porosities measured on core samples are representative of the formation porosity and, therefore, are more appropriate as a training set to calibrate the log-derived porosities. The processing of the porosities of the original core analysis to the log equivalent format was discussed in Section 3.1.2. Regression analysis was used to examine the correlation between the log-derived porosities and the averaged core measurements (Tables 3.8 and 3.9). For the derivation of the regression equations, core porosity was defined as the independent variable because it is based on actual measurements of rocks brought to the surface. The log-derived porosities were the dependent variables to be predicted or calibrated from the equations. The statistical parameters are listed in Table 3.10, and Figures 3.8 to 3.11 illustrate the correlations graphically.

Figure 3.8 shows the cross plot for the Bow Island Formation core interval of 5-7. The bimodal distribution (two clusters of plotted data points) of the porosities is a reflection of lithology. The cluster in the lower porosity range corresponds to shale volumes of 0.45 to 0.55, the other to shale volumes of 0.10 to 0.20. The R^2 's associated with this core interval range from 0.5835 to 0.8726.

The graphs for the Basal Colorado Sandstone core interval of 5-7 (Figure 3.9) show trendless clusters of points for every log-derived porosity. The low R^2 's confirm the lack of correlation. The original core analysis report (Appendix B) revealed several intervals of 0.02 to 0.59 m of shale throughout

Table 3.8: Comparison of log-derived porosities and core porosity in cored intervals of 5-7

Depth (m below KB)	VSH (frac.)	PHMEDA (p.u.)	PHMEDC (p.u.)	PHMES (p.u.)	PHMED2 (p.u.)	PHMED3 (p.u.)	PHMEDS (p.u.)	PHIEBVW (p.u.)	Core Porosity (p.u.)
Bow Island Formation									
770	0.50	0.1059	0.1036	0.0346	0.0994	0.0977	0.1086	0.1023	0.128
771	0.55	0.0470	0.0440	-0.0291	0.0660	0.0618	0.0685	0.0477	0.148
772	0.45	0.1220	0.1199	0.1269	0.0964	0.0942	0.1063	0.0819	0.138
773	0.10	0.3172	0.3170	0.3716	0.2330	0.2578	0.2310	0.2229	0.210
774	0.15	0.2765	0.2756	0.3077	0.2233	0.2392	0.2201	0.1961	0.261
775	0.20	0.2495	0.2486	0.2476	0.2465	0.2537	0.2368	0.2449	0.241
776	0.20	0.2415	0.2404	0.1933	0.2439	0.2433	0.2331	0.2327	0.247
Basal Colorado Sandstone									
868	0.55	0.0819	0.0825	0.0636	0.0945	0.0969	0.1056	0.0816	0.183
869	0.15	0.1287	0.1289	0.1632	0.1808	0.1675	0.1862	0.1601	0.178
870	0.50	0.0686	0.0691	0.0627	0.0759	0.0781	0.1017	0.0593	0.144
871	0.05	0.2386	0.2387	0.3143	0.2222	0.2159	0.2232	0.2193	0.122
872	0.40	0.0367	0.0391	0.0990	0.0649	0.0619	0.1121	0.0743	0.102
873	0.85	0.0093	0.0101	-0.0555	0.0129	0.0135	0.0344	-0.0078	0.133
874	1.00	-0.0172	-0.0162	-0.0366	0.0164	0.0105	0.0000	-0.0098	0.140
875	1.00	0.0227	0.0237	-0.0959	0.0261	0.0335	0.0000	0.0035	0.090

Table 3.9: Comparison of log-derived porosities and core porosity in cored intervals of 6-35

Depth (m below KB)	VSH (frac.)	PHMEDA (p.u.)	PHMEDC (p.u.)	PHMES (p.u.)	PHMED2 (p.u.)	PHMED3 (p.u.)	PHMEDS (p.u.)	PHMEBVW (p.u.)	Core Porosity (p.u.)
Bow Island Formation									
765	0.75	0.0586	0.0545	0.0396	0.0629	0.0602	0.0603	0.0704	0.147
766	0.65	0.0503	0.0468	0.0432	0.0683	0.0594	0.0779	0.0608	0.142
767	0.50	0.0846	0.0819	0.0286	0.0952	0.0905	0.1070	0.1028	0.148
768	0.65	0.0663	0.0628	-0.0123	0.0841	0.0652	0.0765	0.0673	0.166
769	1.00	0.0774	0.0717	-0.0631	0.0470	0.0540	0.0000	0.0470	0.167
770	0.75	0.0503	0.0460	-0.0279	0.0468	0.0458	0.0562	0.0527	0.157
771	0.80	0.0431	0.0366	-0.0546	0.0326	0.0325	0.0445	0.0379	0.149
772	0.85	0.0224	0.0176	-0.0714	0.0096	0.0116	0.0317	0.0133	0.145
773	0.90	0.0016	-0.0036	-0.0667	-0.0047	-0.0047	0.0209	0.0013	na
774	0.90	0.0008	-0.0043	-0.0804	-0.0025	-0.0044	0.0211	0.0051	0.228
775	0.60	0.0714	0.0680	0.0323	0.0925	0.0652	0.0940	0.1032	0.153
776	0.75	0.0408	0.0365	-0.0224	0.0523	0.0472	0.0576	0.0620	na
777	0.90	-0.0012	-0.0063	-0.0726	-0.0008	-0.0037	0.0213	0.0078	0.155
778	1.00	-0.0185	-0.0242	-0.1131	-0.0223	-0.0223	0.0000	-0.0157	0.145
Sand Colorado Sandstone									
874	0.60	0.1216	0.1246	0.0847	0.1478	0.1478	0.1203	0.1298	0.262
875	0.65	0.2369	0.2391	0.3000	0.2525	0.2478	0.2520	0.2500	0.244
876	0.25	0.1910	0.1923	0.1994	0.1946	0.1933	0.1937	0.1868	0.209
877	0.35	0.1146	0.1164	0.1224	0.1306	0.1268	0.1429	0.1193	0.169
878	0.65	-0.0147	-0.0113	0.0082	0.0402	0.0302	0.0721	0.0186	0.113
879	1.00	-0.0422	-0.0369	-0.0567	-0.0073	-0.0045	0.0000	-0.0367	0.171
880	0.80	0.0434	0.0478	-0.0065	0.0576	0.0582	0.0523	0.0339	0.229
881	0.70	0.1161	0.1198	0.0476	0.1085	0.1168	0.0864	0.0899	0.144
882	0.70	0.0261	0.0298	-0.0111	0.0940	0.0715	0.0818	0.0685	0.124

Table 3.10: Results of regression analyses by the least-squares method to establish the dependence of log-derived porosities on core based porosity (independent variable)

Dependent Variable (p.u.)	05-07-017-07W4M			06-35-017-09W4M		
	R-squared (fractional)	y-Intercept (p.u.)	Slope (fractional)	R-squared (fractional)	y-Intercept (p.u.)	Slope (fractional)
<i>Bar Island Formation Interval</i>						
PHMEDA	0.7140	-0.1022	1.5115	0.0593	0.0981	-0.3530
PHMEDC	0.7132	-0.1064	1.5250	0.0607	0.0954	-0.3637
PHMES	0.5635	-0.2021	1.9439	0.1089	0.0916	-0.7627
PHMED2	0.8687	-0.0980	1.3631	0.0848	0.1169	-0.4784
PHMED3	0.8446	-0.1030	1.4338	0.0801	0.1102	-0.4463
PHMED5	0.8726	-0.0494	1.1436	0.0811	0.1179	-0.4331
PHMEDVW	0.7864	-0.0663	1.2721	0.0872	0.1263	-0.4959
<i>Basal Colerado Sandstone Interval</i>						
PHMEDA	0.0306	0.0039	0.4945	0.3445	-0.1004	1.0198
PHMEDC	0.0394	0.0049	0.4616	0.3473	-0.0954	1.0088
PHMES	0.0746	-0.0662	1.1305	0.2739	-0.1306	1.1191
PHMED2	0.0638	-0.0035	0.6768	0.2892	-0.0348	0.8003
PHMED3	0.0724	0.0063	0.6000	0.3386	-0.0510	0.8692
PHMED5	0.1079	-0.0165	0.8200	0.2126	-0.0102	0.6567
PHMEDVW	0.0692	-0.0176	0.6604	0.2847	-0.0665	0.8761
<i>Basal Colerado Sandstone Interval*</i>						
PHMEDA	* improved correlation after omission of unreliable core data (at 874, 879 and 880 m)			0.9310	-0.1908	1.8115
PHMEDC				0.9272	-0.1839	1.7843
PHMES				0.9819	-0.2820	2.3514
PHMED2				0.9700	-0.1078	1.4634
PHMED3				0.9723	-0.1254	1.5342
PHMED5				0.9796	-0.0973	1.4082
PHMEDVW				0.9831	-0.1505	1.6314

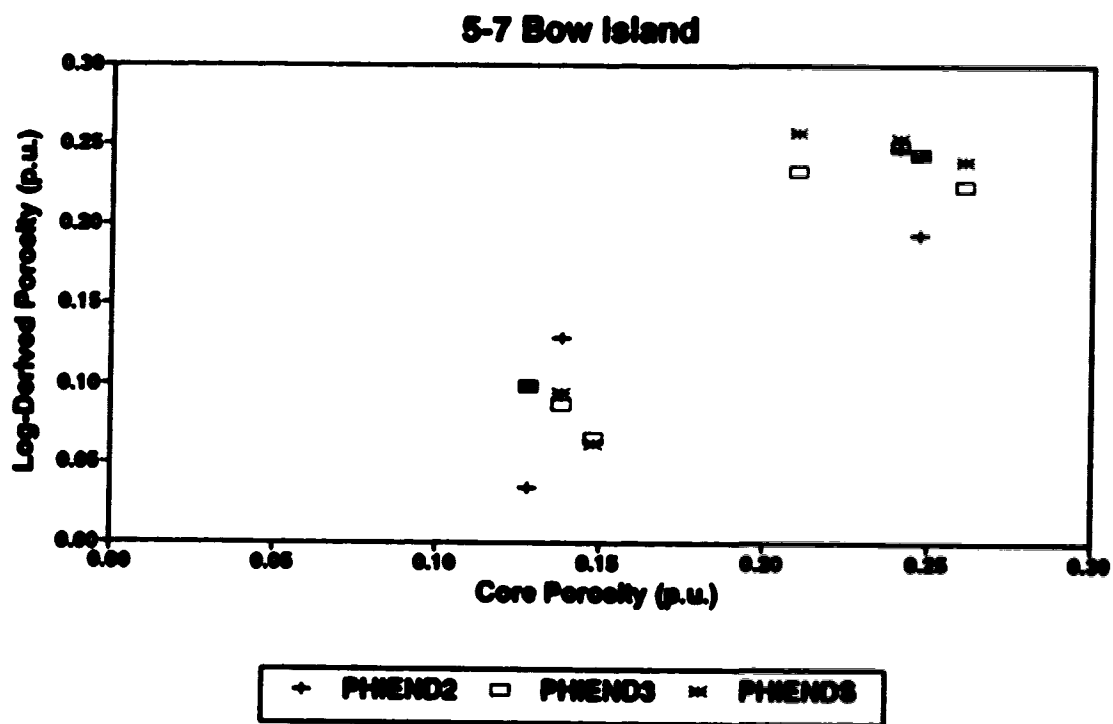
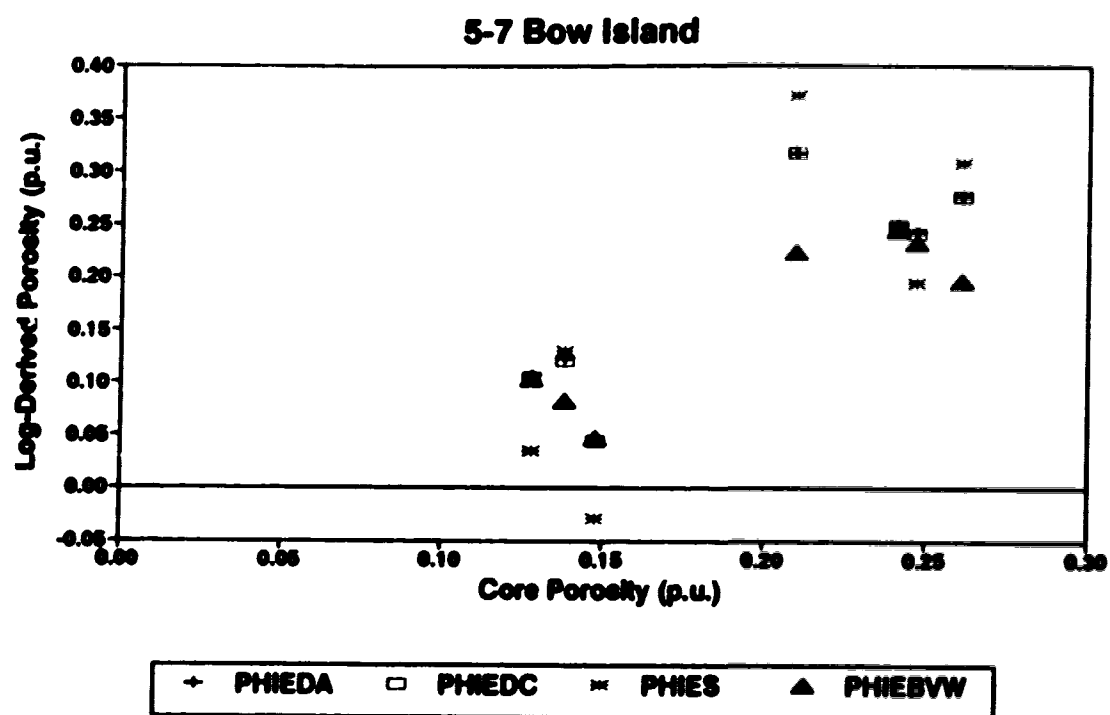


Figure 3.8: Cross plots of core based porosity versus log-derived porosities for the cored interval of the Bow Island Formation of 5-7.

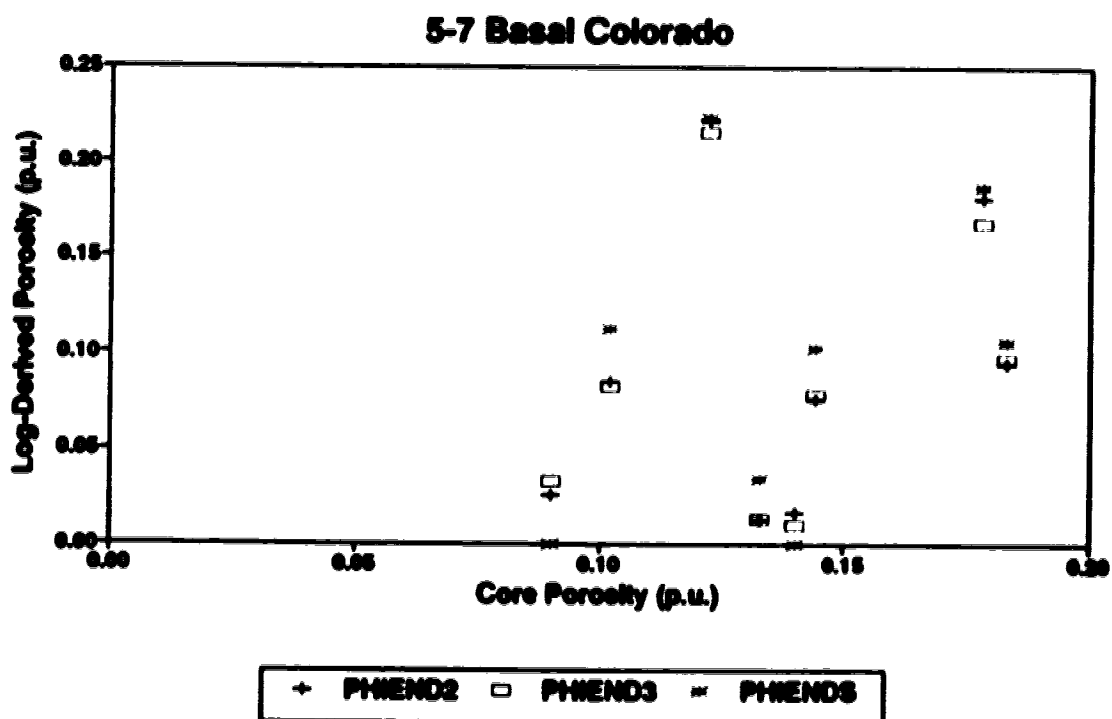
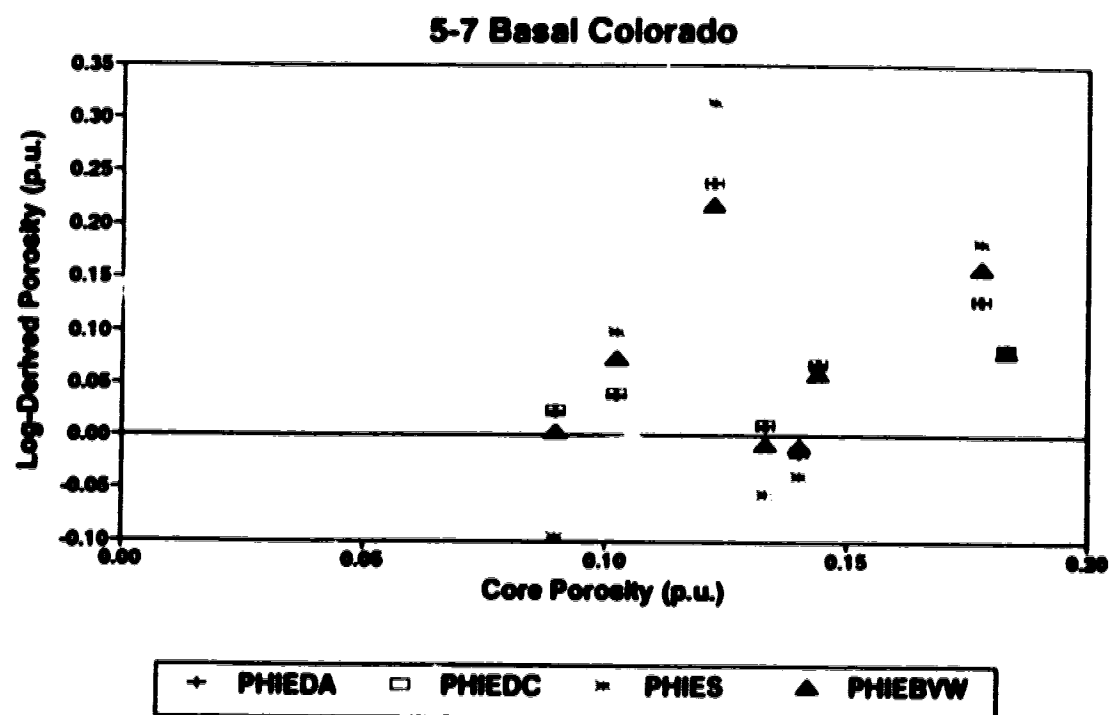


Figure 3.9: Cross plots of core based porosity versus log-derived porosities for the cored interval of the Basal Colorado Sandstone of 5-7.

the cored section, for which no porosity measurements are available. The lack of porosity measurements may not pose a problem in a homogeneous formation, but is a serious problem in a laminated sequence. Difficulties arise from the fact that the available core is sandstone; according to the lithology description in the original core analysis report the missing part is shale. At the depth of 874 m, 0.82 m of the one metre of core represented by one average porosity value was identified as calcitic or sideritic unit on logs. No other causes for the scatter, such as rough borehole walls, were observed in the log suites.

The graphs for the Bow Island Formation of 6-35 (Figure 3.10) do show a linear trend. It does not represent correlation, however, because a spread of about 0.10 p.u. in each of the log-derived porosities corresponds to a spread of less than 0.03 p.u. in the core based porosity. The low R^2 's also do not indicate any correlation. Again, numerous shale laminae were omitted in the core analysis resulting in a bias in the distribution and range of core porosities, while no apparent causes of uncertainty were found in the log suite.

Bimodal distributions are apparent for the Basal Colorado Sandstone core interval of 6-35 (Figure 3.11). The original core analysis report shows that the value of porosity for the depth of 874 m was averaged over only 0.47 m of sandstone in the one-metre interval. The remaining 0.53 m of shale are not incorporated in the analysis. Since lithology may influence porosity, the data pair for 874 m is considered unreliable. Similar conditions are found at 879 m. Merely 0.35 m were available for analysis. In addition, the measurements are marked as affected by fracturing. The core based porosity value for a depth of 880 m was computed from only 0.09 m. The data points corresponding to these three depths of 874, 879 and 880 m were identified as those points falling below the imaginary trendline connecting the remaining points in Figure 3.11. All three were omitted from the data set because of the unreliable and non-

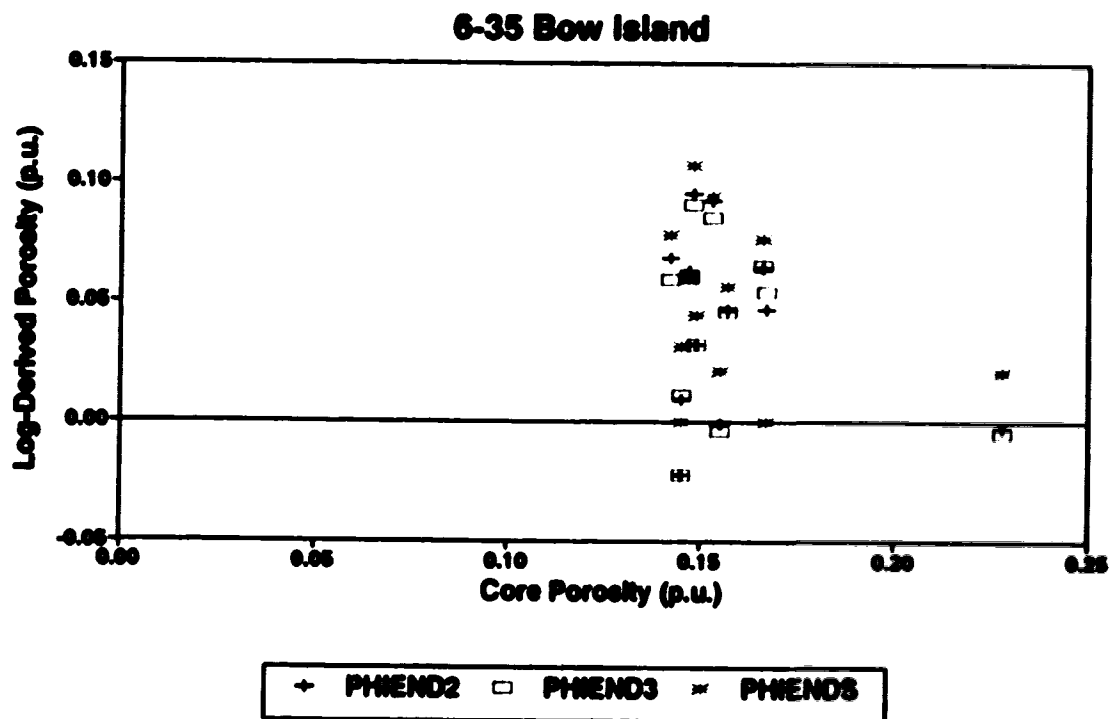
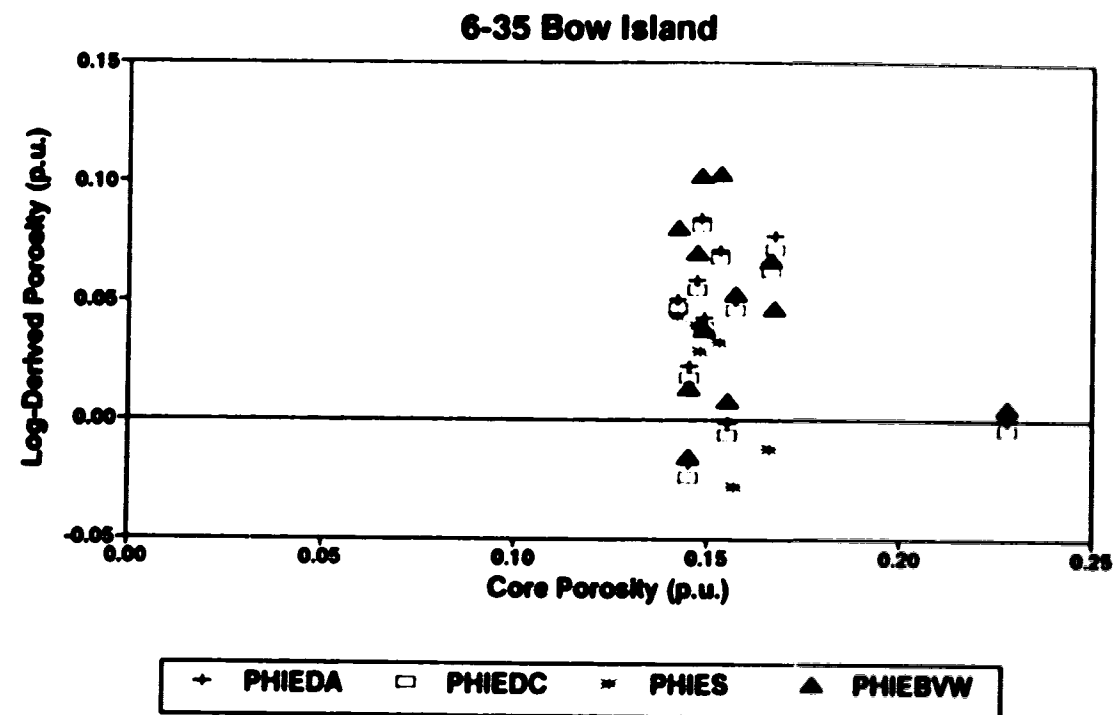


Figure 3.10: Cross plots of core based porosity versus log-derived porosities for the cored interval of the Bow Island Formation of 6-35.

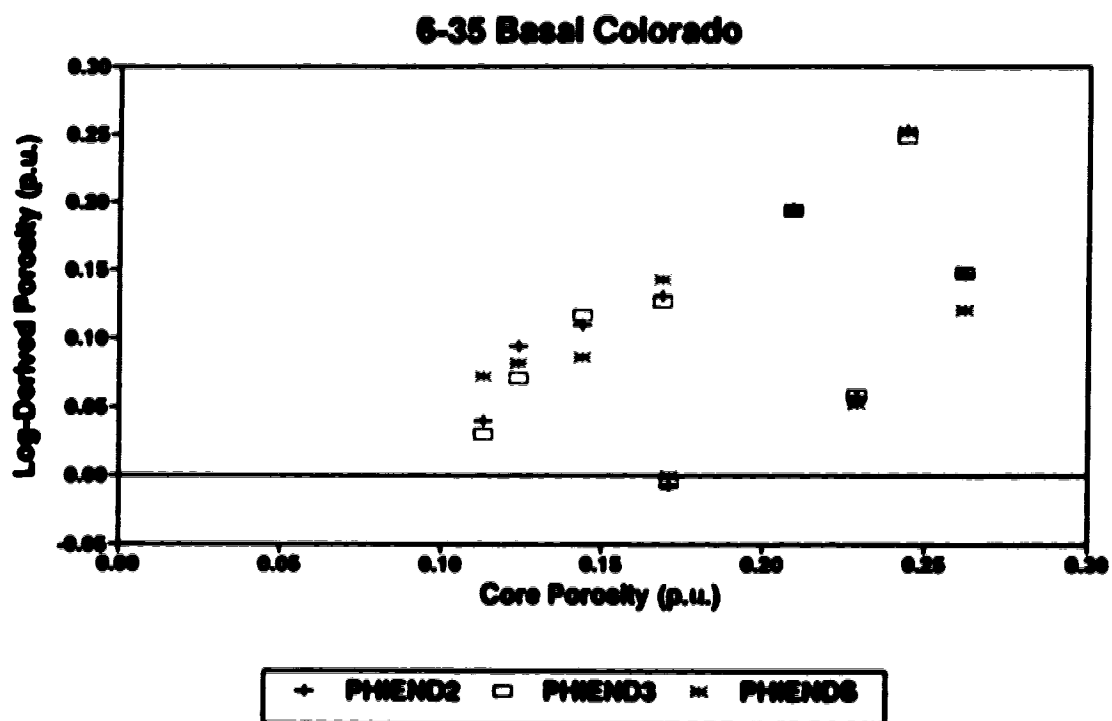
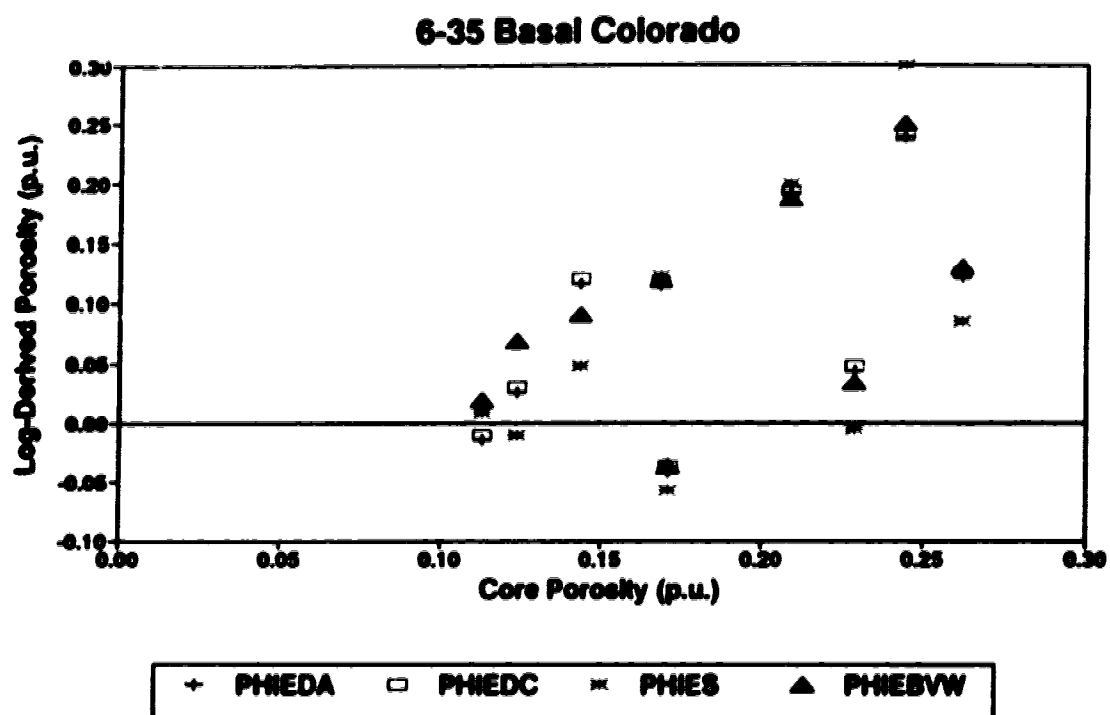


Figure 3.11: Cross plots of core based porosity versus log-derived porosities for the cored interval of the Basal Colorado Sandstone of 6-35.

representative nature of the core based porosities. The repeated regression analysis resulted in significantly enhanced R^2 's (Table 3.10).

The degree of correlation between the log-derived porosities and the core based porosities was used as criterion to choose regression equations from Table 3.10 for the calibration of the computed porosity series. The correlation was believed to be too low in the Basal Colorado Sandstone section of 5-7 to allow reliable calibration. The regression analysis in the Bow Island Formation interval of 6-35 was considered inconclusive for the purpose because the spread of the core porosity is insufficient for the definition of a best-fit line. The results of the regression analyses of the Bow Island Formation core interval of 5-7 and the Basal Colorado Sandstone interval of 6-35, however, indicate good correlation.

With the statistics being derived from data sets containing merely seven and six data pairs, respectively, the allowable depth ranges and lithological make-ups of the intervals to be calibrated are of concern. The calculated shale volume in the Bow Island Formation interval of 5-7 is relatively low, i.e., 0.10 to 0.55, compared to the remaining log interval which is shale dominated, with shale volumes of 0.80 or greater (VSH logs of Sets B1 and B2). The Basal Colorado sandstone interval of 6-35 includes a more favorable (0.05 to 1.00) spread of shale volumes.

Equation 3.5.22 was rearranged to solve for x , in order to calibrate the log-derived porosities (y) using the statistical constants listed in Table 3.10:

$$x = \frac{y - c}{m} = \frac{y}{m} - \frac{c}{m} \quad (3.5.23)$$

where c is the y -intercept and m is the slope. The log-derived porosity for every one-metre interval was substituted as variable y corresponding to the set of

constants. The results are listed in Appendix C and plotted as porosity against depth in Log Sets B1 and B2.

Regression analysis was employed to compare the calibrated log-derived porosities to each other (Table 3.11). With respect to the analysis previously applied to the uncalibrated log-derived porosities (Table 3.7), the y-intercepts and slopes of the best-fit lines changed for respective pairs of log-derived porosity to accommodate the adjustment of the individual log-derived porosity curves to the core porosity. The curves were shifted laterally on the scale grid by an amount equal to the ratio of the y-intercept to the slope of the best-fit line. The magnitude of their deflections were altered by a factor equal to the inverse of the slope of the best-fit line (see equation 3.5.23).

The R^2 's of the respective pairs of log-derived porosity remained identical. It may be deduced that, overall, the calibration preserved the signature character of the individual log-derived porosity curves and the correlation between the curves derived from different algorithms. The observations and conclusions made about the correlation of the initial, log-derived porosity curves are, therefore, still valid in the context of calibrated log-derived porosities.

The accuracy of the calibrated log-derived porosities was checked by comparing these to porosity measurements available from core analyses in boreholes located in townships bordering on those containing 5-7 and 6-35 (Table 3.12). Where possible, logs were compared to ensure similarity of signatures, and therefore, of approximate lithology. For the purpose of comparison, ranges of porosity were favoured over average values of porosity for individual stratigraphic units to lessen the influence of the high-grading bias

Table 3.11: Results of regression analyses by the least-squares method for calibrated log-derived porosities, expressed in terms of the correlation statistic R-squared, and the y-intercept and slope of the best-fit straight line

Independent Variable (p.u.)	Dependent Variable (p.u.)	06-07-017-07W4M			06-08-017-08W4M		
		R-squared (fractional)	y-Intercept (p.u.)	Slope (fractional)	R-squared (fractional)	y-Intercept (p.u.)	Slope (fractional)
PND2	PND3	0.9916	0.0047	0.9501	0.9832	0.0106	0.9523
PND2	PND6	0.8203	-0.0115	0.9539	0.7239	0.0244	0.7491
PND2	PS	0.7317	0.0597	0.6355	0.6316	0.0884	0.5056
PND2	PDA	0.9021	0.0112	0.8724	0.8043	0.0584	0.7302
PND2	PDC	0.9082	0.0085	0.8931	0.8340	0.0440	0.7969
PND2	PBVW	0.9959	-0.0054	1.0678	0.9939	0.0279	0.8965
PND3	PND6	0.8060	-0.0146	0.9909	0.6583	0.0210	0.7438
PND6	PDA	0.7982	0.0368	0.7494	0.4482	0.0703	0.6192
PND6	PDC	0.7322	0.0353	0.7811	0.4665	0.0590	0.6770
PND6	PBVW	0.8180	0.0257	0.9190	0.6976	0.0350	0.8436
PS	PBVW	0.7189	-0.0467	1.2195	0.5951	-0.0307	1.0787
PDA	PDC	0.9925	-0.0021	1.0160	0.9722	-0.0128	1.0567
PDC	PBVW	0.9024	-0.0041	1.0852	0.8528	0.0014	0.9411
PDC	PS	0.6889	0.0603	0.6477	0.4065	0.0828	0.4617

Table 3.12: Collection of porosity and permeability measurements available from core analyses conducted for boreholes in townships adjacent to 017-07W4M and 017-08W4M, and ranges of the log-derived PND2, PND3, PDA, PDC and PBVW (one enveloping range)

Stratigraphic Unit	Well location	Cored interval (m below KB)	Range of measured porosity (fractional)	Range of measured permeability (md)	Lithology	Approx. log-derived porosity (fractional)
Milk River Formation	16-07-017-06W4M	344-379	0.110-0.106	0.14-2.50, 58-484	shaly siltstone, mudstone, shale	5-7: 0.07-0.20 6-35: 0.06-0.16
	14-28-018-07W4M	388-433	0.141-0.240	0.01-0.79, 45.8		
	11-02-017-10W4M	344-382	0.103-0.148	0.05-0.08		
	03-28-017-10W4M	318-354	0.006-0.177	0.01-1438		
Medicine Hat Sandstone	16-07-017-06W4M	452-457	0.102-0.146	131-286	sandstone, siltstone, mudstone	5-7: 0.10-0.15 6-35: 0.10-0.12
	03-28-017-10W4M	432-436.5	0.104-0.147	0.55-0.80, 134-239		
Second White Speckled Sandstone	16-07-017-06W4M	641-644	0.041-0.058, 0.118-0.145	0.01-0.05, 196, 1076	calcareous sandstone, siltstone	5-7: 0.12-0.19 6-35: 0.12-0.18
Second White Speckled Shale	16-07-017-06W4M	644-649	0.087-0.130	0.01-51.0	shale, siltstone	5-7: 0.03-0.10 6-35: 0.03-0.08
	03-28-017-10W4M	625	0.036	0.09		
Bow Island Formation	11-30-017-06W4M	756-759	0.178-0.219	4.71-118	sandstone, shale laminae	5-7: 0.03-0.25 6-35: 0.05-0.27
	07-31-017-07W4M	739-743	0.142-0.202	0.54-50.6		
	11-04-018-06W4M	766-762	0.124-0.236	0.99-443		
	12-07-018-06W4M		0.171-0.211	5.49-88.5		
Basal Colorado Sandstone	11-30-017-06W4M	861-869	0.133-0.243	1.20-80.4	shaly sandstone	5-7: 0.07-0.24 6-35: 0.07-0.24
	12-07-018-06W4M	577-884.5	0.137-0.249	0.27-34.7, 87.2-337		

introduced into core measurements by selective sampling with emphasis on core intervals with the highest potential for reservoir quality porosity. Overall, the porosity ranges determined for PDA, PDC, PND2, PND3 and PBVW agreed well with the corresponding core analysis porosity ranges for the Milk River Formation, the Medicine Hat Sandstone, the Second White Speckled Sandstone and Shale, the Bow Island Formation and the Basal Colorado Sandstone. This observation is encouraging and provides support for the validity of the calibration procedure with small training sets of core based porosity. However, a more in-depth examination with a broader independent data base would be required to determine the quantitative accuracy of the log-derived porosity profiles for the full lithology spectrum and continuously over the entire section.

The core analysis report for the Milk River Formation of 14-28-018-07W4M contains measurements for anomalous lithologies. Two shaly streaks of siderite of 0.16 m and 0.21 m thickness are recorded with porosities of 6.8 % and 9.4 %, respectively. Three streaks of shaly sandstone with siderite content are listed with thicknesses of 0.06 to 0.24 m and corresponding porosities of 9.3 to 15.3 %. Although no special provisions were included in the analysis, the log-derived porosity profiles do, in general, show a distinct deflection to lower porosity relative to the adjacent lithology. This trend is not based on physical principles; however, it is more likely an artifact of mathematical manipulations. It would be unrealistic to expect the absolute values of the core porosities to be matched, since the thickness of the streaks is below the limit of vertical resolution of measurements and no special provisions for mineralogy other than that of shale and sandstone were incorporated into the analysis.

Thus far it may be concluded that PDA, PDC, PND2, PND3 and PBVW are in sufficient concordance for the formation and borehole conditions of 5-7 and 6-35 to permit the computation of only one porosity profile with the method of choice without loss of essential signature character or accuracy of the final porosity profile. PND5 of 5-7 and PND5 of 6-35 show merely weak tendencies toward lower values than any of PDA, PDC, PND2, PND3 or PBVW. As such, PND5 may serve satisfactorily as a first approximation without the necessity of defining shale base values. P3 exceeds all other porosities in overall absolute magnitude. The discrepancy appears to be largest (up to about 0.05 p.u.) in intervals with shale volume content of greater than 0.85. Based on a different type of physical measurement, it may be advisable to compute PS as the only porosity approximation only if no neutron porosity and bulk density or density porosity data are available.

3.6. Permeability

Without prior computation of a continuous profile of irreducible water saturation, traditional approaches of permeability determination from well logs are reduced to the single method of the transformation of log-derived porosity using a semi-logarithmic equation expressing the dependence of permeability on porosity. This, and a not yet well established method involving the nuclear magnetism log, have been applied here.

Crain (1966) stated a commonly applied, generic equation representing a semi-logarithmic relationship between effective porosity (PHie) and the logarithm of permeability (PERMp):

$$\log (\text{PERMp}) = \text{HPERM} \cdot \text{PHie} + \text{JPERM} , \quad (3.6.1)$$

the antilog of which solves for permeability:

$$\text{PERMp} = 10 (\text{HPERM} \cdot \text{PHie} + \text{JPERM}) \quad (3.6.2)$$

where HPERM and JPERM are constants related to lithology for which recommended ranges of values are listed in the reference.

To evaluate the applicability of the method for the data sets of 5-7 and 6-35, the correlation between core porosity and the logarithm of core permeability was investigated. The regression analysis was performed twice for each core interval. Set A in Table 3.13 contains the statistics R^2 , and y-intercept and slope of the best-fit line obtained for the porosity (P_{avg}) and permeability (K_{avg}) measurements averaged over one-metre intervals (Table 3.1). Set B in Table 3.13 was calculated using the original porosity (P_i) and permeability ($K_{\text{max}i}$) measurements of Appendix B. The two sets were computed to ensure that the averaging process of core measurements representing intervals of irregular thickness, to one-metre intervals corresponding to the digitizing interval of logs did not adversely affect the correlation. The opposite effect was recognized in the slightly higher R^2 's for Set A with respect to Set B. Set A is, therefore, favorable for the transformation of log-derived porosities to permeabilities. Further, it was noted that R^2 's were highest for the Bow Island Formation core of 5-7 and the Basal Colorado Sandstone core of 6-35; the same intervals also resulted in the highest R^2 's for regression analyses of log-derived versus core based porosities (Table 3.10). The R^2 's for Set A indicate a definite correlation between core porosity and the logarithm of core permeability. Even the R^2 of 0.4181 for the Bow Island Formation interval of 6-35 is acceptable when viewed as a correlation coefficient (R) of 0.6466. The principle of the transformation method was adopted as a result.

The constants HPERM and JPERM of equation 3.6.2 were replaced by the appropriate values of slope (S) and y-intercept (Y) from Table 3.13,

Table 3.13: Results of regression analyses by the least-squares method to establish the dependence of the logarithm of the maximum value of core permeability on the core porosity (independent variable), expressed in terms of the correlation statistic R-squared, and the y-intercept and slope of the best-fit straight line

Stratigraphic Unit	05-07-017-07W4M				06-35-017-09W4M			
	R-squared (fractional)	y-Intercept (md)	Slope (md/p.u.)		R-squared (fractional)	y-Intercept (md)	Slope (md/p.u.)	
Set A - using maximum permeability averaged over one-meter intervals								
Bow Island Formation	0.9884	-1.1851	15.7614	0.4181	-2.0629	15.9246		
Basal Colorado Sandstone	0.7676	-0.5440	14.0008	0.8820	-2.4399	19.1869		
Set B - using permeability for original analysis spacings								
Bow Island Formation	0.9263	-0.9637	15.0990	0.3541	-2.1849	16.1164		
Basal Colorado Sandstone	0.5007	-0.6376	14.2701	0.6739	-1.9758	16.6058		

respectively, and the log-derived porosity PND2 was substituted for PHie to compute permeability KCN in md:

$$\text{KCN} = 10 (S \cdot \text{PND2} + Y) \quad . \quad (3.6.3)$$

The substitution of PND2 for core porosity was justified by the previous calibration of the log-derived porosity by the latter. Because of the high correlation between the log-derived porosities (Table 3.11), PND3, PDA, PDC or PBVW could have been chosen instead of PND2 without significantly influencing the final permeability profile.

To generate a continuous permeability profile for the entire log interval, the established semi-logarithmic relationships for the Bow Island Formation and Basal Colorado Sandstone core intervals were extrapolated. Considering the relatively high R^2 's, all four intervals were used; in contrast to the calibration of log-derived porosity with core porosity, where only one interval for each well contributed to the process. For the final computation of permeability, the sets of constants for the Bow Island Formation core were substituted into equation 3.6.3 along with PND2 for the depth interval spanning from the bottom of the Bow Island Formation to the top of the log. The sets of constants derived for the Basal Colorado Sandstone core were used for the remaining log interval from the bottom of the Basal Colorado Sandstone to the top of the Joli Fou Formation. The resulting permeability values (KCN) for the one-metre intervals are listed in Appendix C and plotted against depth in Log Sets B1 and B2.

The second method of permeability determination is independent of core measurements and log-derived porosity profiles. Instead, it is based on an equation relating the free fluid index and the density porosity to permeability. Logan (1969) derived the equation for shaly sandstone lithology with the

objective of matching core permeability. Relying on previous work by Timur (1969) and extensive core and log data the result was:

$$KNML = \frac{(PHID \cdot 100)^5 \cdot (FFI \cdot 100)}{[(PHID \cdot 100) - (FFI \cdot 100)] \cdot 10^5} \quad (3.6.4)$$

KNML is the permeability derived from the nuclear magnetism log, PHID is the density porosity, and FFI is the free fluid index. The multiplications by factors of 100 are required to transform fractional porosity units to percentages. Even though PHID and FFI are input in porosity units, KNML is given units of md. Considering the empirical derivation of the relationship, inverse permeability units may be ascribed to the constant 10^5 in the denominator. Equation 3.6.4 was applied to the data sets of 5-7 and 6-35. The results are contained in Appendix C and Log Sets B1 and B2. Because of the discontinuous FFI curve, KNML of 5-7 is available only from 332 to 547 m, 631 to 709 m, and 740 to 877 m.

The qualitative and quantitative evaluation of the KCN and KNML profiles is difficult due to the lack of comparative data.

As may be expected from the algorithm used for the computation of KCN, the visual comparison of KCN and PND2 confirms the close resemblance of the profiles. PND2 is practically the only variable in equation 3.6.3 with Y and S being constant over large depth intervals. PND2, therefore, strongly influences the character of the signature of KCN. The magnitude of the deflections is controlled by Y and S, which reflects the dependence of the logarithm of core permeability on core porosity. By entering fictitious porosity values into equation 3.6.3, it becomes apparent that an increase in porosity of 5% raises permeability by 0.70 to 0.79 of a log cycle. Overall KCN of 5-7 is higher than KCN of 6-35. The difference is attributed to the relative values of Y and S in

equation 3.6.3. While S is higher for both intervals of 6-35, i.e., causing higher KCN values, its effect is opposed more strongly by negative Y's of greater magnitude than those of 5-7. Also expected, core intervals which displayed a high R² in the correlation of core porosity to core permeability show a good overlap of core permeability (KCA) and KCN.

Equation 3.6.4 for the determination of KNML may be reduced to

$$KNML = \left(\frac{PHID^5 \cdot FFI}{PHID - FFI} \right) \cdot 10^5 . \quad (3.6.5)$$

PHID dominates the denominator because it is generally one to two orders of magnitude larger than FFI. FFI is the more influential factor in the numerator since PHID is a decimal number raised to the power of 5. Therefore, both FFI and PHID contribute significantly to the character and magnitude of the KNML curve. As a result, uncertainties introduced to PHID by borehole rugosity may adversely affect KNML and cause differences between the KNML profiles of 5-7 and 6-35. Different ranges of grid scales on the original nuclear magnetism log may have also caused inconsistencies in the digitizing process of the two FFI curves.

It is somewhat puzzling that KNML is unexpectedly high in the massive shale section of the Milk River Formation, and the Colorado Shale and the Second White Speckled Shale. Both increased PHID and FFI values contribute to permeabilities exceeding those of the surrounding sandstones or more sandy shales. A possible explanation is the presence of magnetic ions associated with minerals contained in the rock mass. Examples of such minerals are siderite or calcite cement, which may attract various cations (Mottana et al., 1978). The added density may enhance PHID, while the obscured measurements of spin-lattice and thermal relaxation times may affect FFI either positively or negatively. Similarly to KCN, the correlation between

KNML and KCA is best for the Bow Island Formation interval of 5-7 and the Basal Colorado Sandstone interval of 6-35.

The accuracy of the absolute magnitudes of the KNML and KCN profiles can be evaluated only by comparison to the permeability data, though sparse, available from core analyses in nearby townships (Table 3.12). In addition, KNML may be compared to the core permeabilities of 5-7 and 6-35. The core permeabilities indicate wide ranges of values within any one stratigraphic unit, which erratic character is also observed in the profiles. The spreads of permeability match as well. In general this agreement is encouraging. However, the overlap of ranges of values over entire stratigraphic units rather than short, well defined intervals provides little indication of the accuracy of KNML and KCN because of the erratic nature of the data.

Analyses of core in the Milk River Formation of 14-28-018-07W4M provide permeability measurements of 0.04 md and 0.05 md for siderite streaks in a sandstone matrix. Permeabilities for shaly siderite streaks were lower than the 0.01 md, which is the limit of measurement for conventional core analysis apparatus. Similarly to the previously discussed porosity measurements, both KCN and KNML show the trend of low permeability without true reflection of the absolute magnitude.

The ratios of K_v to K_{med} were calculated from the original core measurements of 5-7 and 6-35 and are listed in Appendix B. The wide spread of ratios from 0.02 to 0.68 indicates vertical permeability anisotropy and heterogeneity within cored intervals of the Bow Island Formation and Basal Colorado Sandstone. All values are less than one, i.e., permeability is lower in the vertical than in the horizontal direction. No trend can be recognized which

would allow a meaningful statistical transformation of log-derived permeabilities to a profile of vertical permeability.

Neither the method involving core calibrated log-derived porosity, nor that based on the free fluid index of the nuclear magnetism log could be proven or disproven to be reliable for the determination of permeability.

Recommendations for their usage are limited to considerations of the availability of the required data sets. If possible, it may be advisable to employ both algorithms in the hope of comparing and complementing the results for a less uncertain final permeability approximation.

4. Discussion

The algorithms applied in this study originated in the petroleum industry and are, with the exception of the permeability determination from the nuclear magnetism log, still widely used by geologists, geophysicists and log analysts involved in hydrocarbon exploration. They are employed mainly for stratigraphic correlation, the detection or delineation of zones of high porosity and permeability, evaluation of water and hydrocarbon saturations, estimation of recoverable reserves, etc.. The thorough evaluation of a reservoir or cap-rock formation generally requires a team of analysts covering several earth science and engineering disciplines. Such integrative studies are of considerably larger scale than this thesis study and require a broad data base. Core analysis may include detailed mineralogical investigations such as thin section, scanning electron microscope and X-ray diffraction analysis (Sneider et al., 1984), advanced permeability testing using pressure-decay profile-permeameter equipment (Jones, 1992; Georgi et al., 1993), measurements of capillary pressure characteristics and electrical properties like the cation exchange capacity (Luffel and Guidry, 1989; Guidry et al., 1990), etc.. The conventional log suite of spontaneous potential, gamma radiation, bulk density, neutron porosity, sonic traveltime, deep and shallow resistivity may be expanded to include logs of photoelectric cross-section index, natural gamma ray spectroscopy, nuclear magnetic properties, array sonic traveltimes, electromagnetic propagation, aluminum activation, geochemistry and so on (Shen et al., 1984; Burns and Cheng, 1986; Cheruvier and Winkler, 1987; Herron, 1987; Morris and Laverdiere, 1988; Cannon and Coates, 1990; Goldberg et al., 1990; Miller et al., 1990; van den Oord, 1990; Gwinner et al., 1991; Klimentos, 1991; Serra et al., 1993; Wyatt et al., 1993). Fluid and fluid

flow characteristics may be measured or deduced from drill stem tests and repeat formation tester data (Yildiz and Desbrandes, 1989; Cannon and Coates, 1990; Badry et al., 1993), transient-pressure-buildup tests (Ahmed et al., 1987), the analysis of production records (Cheng, 1986; Crain, 1986), etc.. Measurement While Drilling (MWD) may contribute quantitative and qualitative information on permeability (Dewan and Chenevert, 1993). Theoretical and practical approaches to integrative studies were demonstrated by Connolly and Reed (1983), Sneider et al. (1984), and Serra et al. (1993). Technological progress is ongoing and experience is collected most prominently by petroleum explorationists in the application of new tools and the integration of comprehensive data bases.

Hydrogeologists should take advantage of already proven knowledge and expand it to suit their wider ranges of application. Unfortunately, publications on the application of geophysical well logs for hydrogeological or geotechnical investigations, in general, are sparse; some examples are Speelman and Breunese (1985); Daniels and Keys (1990); Howard (1990a); Howard (1990b); Soonawala et al. (1990); de Lima (1993); Molz and Young (1993); and Paillet et al. (1993).

As far as the scope of this study is concerned, several of the conventional log analysis algorithms were applied outside the limits of shaly sandstone reservoir specifications for which they were developed by petroleum explorationists. The methodology was also modified as necessary to meet the requirements of the thesis objectives.

The following is a comparison of the approaches and considerations taken by the hydrogeologist in the analysis and interpretation of the specific data set of this thesis project, as opposed to those taken by a petroleum

explorationist conducting a reservoir or "play"-study. The reader is asked to excuse the generalized address of the two professional groups for the sake of discussion.

1) The zones of interest are more narrowly defined for the petroleum explorationist. He/she focuses on potential reservoir rocks, usually sandstones which contain little or no shales and clays, and possibly indicate promising porosity and permeability. The hydrogeologist does not regard lithology or first indications of formation properties as discriminating factors once a particular stratigraphic section has been selected for analysis and interpretation.

2) The petroleum explorationist subdivides the identified zones of interest into horizontal layers, the thicknesses of which are determined mostly by changes in porosity and resistivity readings. The hydrogeologist divides the entire section into horizontal layers of uniform interval thickness, e.g., one metre.

3) The volume of data contributed to the data base by a single well is likely to be larger in the case of the hydrogeologist as a result of items 1) and 2).

4) Although both interpreters require hard copies of the logs for visual inspection, the hydrogeologist needs, in addition, a digitized version of the logs to be used in spreadsheet manipulations and calculations on the computer. The analog version alone may be sufficient for the petroleum explorationist to pick parameters for calculations.

5) Depending on the number and the heterogeneity of the zones of interest, the quantitative analysis for petroleum exploration may often be carried out efficiently with the aid of manually generated tables of log parameters, a basic or programmable hand calculator and interpretation charts provided by service companies, or readily available computer software packages. The hydrogeologist must resort to computer spreadsheet facilities to cope effectively

with the volume of data. Chart book methods are, therefore, vastly replaced by numerical algorithms.

6) The base values in shales and sandstone are picked manually in similar fashion by both interpreters. However, the values of the individual parameters in each horizontal layer are picked manually only by the petroleum explorationist. In doing so, personal bias and judgment enter the process, and may either lessen or enhance the quality of the analysis. For the hydrogeologist this step of the analysis is not necessary; the representative values of the log readings are those recorded at the preset depths defined by the digitizing interval.

7) The petroleum explorationist and hydrogeologist may choose from a multitude of methods of analysis considering the availability of various logs, range of shale content, borehole and drilling conditions, presence of hydrocarbons and heavy mineral deposits, etc., and personal preference. The petroleum explorationist may base his/her choice on previous personal or other interpreters' experience in terms of the expectable quality of the results from any one line of methods. The hydrogeologist may or may not have the opportunity to refer to past applications of methods, which may be strained by excessive clay content, and may be advised to implement the maximum possible number of algorithms. He/she may more successfully inspect the quality of the results for individual parameters if several log-derived values are available for comparison.

8) The parameters determined by the petroleum explorationist from quantitative analysis include several of lithology, shale volume, porosity, water resistivity, water saturation, permeability, hydrocarbon content and a type of productivity index. The quantitative analyses of properties like shale volume and water resistivity are frequently viewed by the petroleum explorationist

exclusively as necessary steps in the derivation of permeability or hydrocarbon content. By contrast, every single factor may contribute individually to hydrogeological studies, e.g., as input parameter for computer models, qualitative interpretation for characteristics of the flow domain, etc..

9) The presentation of the final results is influenced by the initial subdivision of the curves into horizontal layers. The petroleum explorationist may resort to various forms of presentation such as tables listing the determined values for each property for each individual subdivision, or a representative (e.g., average, maximum, minimum) value for each zone. The contents of such a table may also be plotted in log form against depth for each zone. Because of the continuous, thicker sections being analysed, the hydrogeologist prefers the form of logs. For subsequent interpretation it may be advantageous to plot values of one property as determined with different equations on one scale grid.

The differences between the approaches taken by hydrogeologists and petroleum explorationists, as discussed in these nine points, tend to dissipate when professional log analysts are called upon by the petroleum explorationist to aid in thorough evaluations of lithologically complex zones, or in large-scale hydrocarbon pool or basin studies.

As mentioned, the algorithms applied in this study were selected on the basis of generality. No examples were found in literature of methods which were developed specifically for shales or applied in massive shales. The chosen ones are classified as shaly sandstone methods. Extensive collections of algorithms were presented by Atlas Wireline Services (1965, pp. 183 to 186) for the estimation of shale volume and the approximation of permeability from logging data. Those implemented here share at least the one common characteristic that they do not contain any numerical constants which serve as

empirical calibration or correction factors defined on the basis of location-specific field data analysis, or mineralogy- and fluid-specific experimental work.

The relative simplicity of the individual algorithms or of the overall methodology may have adversely influenced the final results of the analysis. For some specific points, possible means of improvement are suggested.

The digitization of all logs involved in computations was proven invaluable for spreadsheet data-manipulations. The digitizing process with the fixed interval of one metre was, however, insensitive to the data character. Manual editing was required to increase some deflections to their full magnitude. A flexible digitizing interval, determined by an automated process, may improve the sensitivity of the analysis. The "filter" may be designed as the second derivative of a parameter curve to place digitizing breaks at the inflection points of the curve. The appropriate parameter should portray good vertical resolution with respect to the remaining logs in the suite. It must also be sensitive to clay content in the formation, since the shale volume is an essential parameter for the majority of shaly sandstone algorithms. The total gamma radiation curve could be used as such a parameter.

Two independent algorithms, based on different physical measurements, were applied for the approximation of shale volume. The discrepancies between the resulting series of values varied unpredictably with depth. Hand-picking of representative shale volumes was required for which VSHG and VSHND served as guide values. A third independent algorithm, such as one based on the spontaneous potential or the natural gamma spectroscopy curves, could have resolved some ambiguity and aided or replaced the manual, biased procedure.

Three types of shale distribution were introduced in Section 2.3. The schematic models of these (Figure 2.9) may be expressed mathematically in

terms of shale volume, and total and effective porosities (Fertl, 1987). Bateman (1985) even presented equations solving for shale volume and effective porosity for each of the three types of distribution from neutron porosity and density porosity. They could not be implemented in this study since the analysis of distribution type in Section 3.3 was not sufficiently detailed and conclusive. Equation 3.4.2 for VSHND corresponds to the dispersed shale distribution, while the porosity equations involving the combination of neutron porosity and density porosity are not associated with any one model.

Mineralogical impurities such as calcite cement and pyrite were also ignored in the analysis. Matrix parameters such as DENSMA and DELTMA were approximated by the density of and sonic traveltime in quartz, and opposed to shale parameters DENSSH and DELTSH without consideration for cement or mineral inclusions. Partial compensation for these approximations may be achieved by close calibration with core porosity and permeability. Unfortunately, the limited core available for 5-7 and 6-35 for calibration of log-derived porosities could not possibly have rectified inaccuracies resulting from the omission of minerals other than quartz and clays from the computational processes.

Another short-coming of the methodology is recognized indirectly in the high correlation between the log-derived porosities PHIEDA, PHIEDC, PHIEND2, PHIEND3 and PHIEBVW before and after calibration with core values. Despite different equations with some different additional input parameters, all five algorithms are based on the same shale volume, neutron porosity, density porosity or bulk density, from which density porosity is computed, with constant conversion factors. On one hand, the exercise may be viewed as a type of error analysis of the algorithms, in which case it may be interpreted as encouraging that five different algorithms produce such similar

porosity profiles. On the other hand, the high correlation may signal the necessity for a large suite of logs from which porosities may be determined independently. Only then may the generated profiles be compared for the purpose of quality evaluation with respect to each other. For example, problems caused by borehole rugosity in the bulk density measurement will become most apparent when the bulk-density derived porosity is compared to the sonic-traveltime derived porosity.

The calibrations of log-derived porosities and the subsequent approximation of permeability through core statistics are vulnerable techniques. They rely on a series of assumptions such as the compatibility of data sets in the senses of scale and location of the volume of investigation, and the representativity of point measurements over sample intervals, etc.. In this study, particular difficulties arose from the lack of porosity and permeability measurements in shale strata of the available core, as well as in bentonite and calcareous streaks. In addition, only two, less than 15 m-long cores from sections near the bottom of the logged interval were analysed for each location. The core data as a whole are, therefore, not truly representative of the entire log interval of nearly 700 m. Nevertheless, the core porosity and permeability data were extrapolated with log-derived porosities to the uncored intervals. The final porosities PDA, PDC, PND2, PND3 and PBVW of 5-7 and 6-35 did, however, compare well in ranges of absolute values with core porosities of corresponding stratigraphic units in nearby wells. Problems associated with the physical log measurements or the analytical procedures of PS and PNDS, rather than inappropriate calibration with core values are thought to be responsible for the lower degree of correlation with core porosities.

The comparison of KCN, the permeability profile obtained from the transformation of the log-derived porosity profile with a core based expression

of dependence between porosity and the logarithm of maximum permeability, with permeability measurements from nearby well locations was less conclusive. The results do not warrant earnest speculations about the reliability of the technique for this data set.

The comparison of KNML, the permeability derived from the free fluid index and density porosity curves, with core permeabilities from nearby well locations was equally ambiguous. Without regarding the results, the algorithm for KNML appears more favorable than that of KCN. Through the direct computation of permeability from original logs, no uncertainties are introduced by intermittent computational steps involving approximations and assumptions.

At the outset of this study, the dominating challenge to the methods of analysis adopted from petroleum explorationists was expected to be the excessive clay content in the formation. It may be argued that certain porosity algorithms lose validity with the correction for extremely high shale volumes of, say, greater than 0.80. The reader is reminded, however, that the approximated parameter, VSH, is not strictly the volume or weight portion of shale in a formation, but a quantity representing the sum of the effects of several formation characteristics, most prominently clay content and bound water, on well logs. Even in massive shales, it is highly unlikely that the entire response recorded on logs of bulk density, neutron porosity and sonic traveltime is prompted exclusively by clay minerals and other factors influencing VSH. Bentonite beds may pose a greater challenge to the concept since clay minerals are its primary constituents, while, as mentioned, clay minerals normally make up an average of only about 60 % of the volume of shales (Kukul and Hill, 1966). As a result, a component of the signal remains after shale correction for further analysis and interpretation. In fact, the log-derived porosity may possibly be a conservative

figure if the assumption of zero porosity association with clay mineralogy is incorrect. The computed porosity profiles may certainly not be rendered invalid on the basis of extremely high VSH values. The effect of large correction factors on the accuracy of the final log-derived porosity cannot be evaluated appropriately in this study because of insufficient comparative data. In general terms, the range of uncertainty tolerable in the quantitative results must be judged based on the purpose of the study. For preliminary investigations over a large areal extent, the porosity profiles of this project may be satisfactory. Detailed studies directed toward the accurate numerical evaluation of specific conditions or processes will require logging methods of higher quality.

The methodology developed in this study lends itself well to semi-automated analysis. The initial log measurements may be obtained in digital format from the acquisition company, rendering the labour-intensive manual digitizing procedure unnecessary. With the proposed third method of shale volume determination, an automated picking criterion or averaging function could possibly replace the hand picking or assigning of values. All constants involved in the approximation of porosity and permeability would have to be estimated manually and be input in spreadsheet format similar to Tables 3.5 and 3.6. The equations, including the substitutions of constants, and the order of calculations could be programmed once and implemented with an unlimited number of sets of logging data provided the input format is honored.

The potential for enhanced quality of results, and increased cost and labour efficiency grows with the number of wells included in the project. If the geology is approximately homogeneous in the study area for example, certain matrix constants may have to be assigned only once for the entire series of calculations. Also, core control could be extrapolated throughout the area.

Rather than cutting core in the same stratigraphic units in several wells, resources could be allocated to the cutting and analysis of one or a small number of cores covering the entire log section. This would improve the overall core control, and reduce the amount of statistical analysis involved in the calibration of log-derived porosities and the derivation of porosity versus permeability relationships.

The results of this thesis project do warrant the application of geophysical well logs in hydrogeological investigations in shaly sandstones. The adaptability of a selection of methods of analysis and interpretation was proven to various degrees. Additional logs and analytical methods may be incorporated into the established methodology.

Furthermore, the methodology is not restricted to stratigraphically deep investigations. As discussed in Section 3.2, shallow logs recorded from the surface to depths of less than 350 m, tied in well with the deeper logs of 5-7 and 6-35. With necessary adjustments to drilling and recording equipment, comprehensive suites of logs may become more readily available for shallow intervals. Additional considerations for effects of unsaturated and unconsolidated zones may be required.

Qualitatively, logs may be used for stratigraphic correlation, e.g., to establish the geological framework of a flow domain or to map the areal extent and thickness of a particular aquifer or aquitard. Generated profiles of shale volume, porosity and permeability may aid in the definition of the areal hydrostratigraphy.

Quantitatively, the profiles may serve as input parameters for computer programmes or manual calculations of hydraulic conductivity, specific discharge, chemical water quality parameters, storativity, transmissivity and so

on. They may also be incorporated into computer simulations of fluid flow systems for the investigation of cross-formational hydraulic communication, petroleum accumulations, contaminant transport and dissipation, etc..

It may be inferred from this study that hydrogeologists may safely overstep the boundaries traced by petroleum explorationists, who developed the majority of technical devices involved in the acquisition of well logs and the methods of log analysis. The empirical nature of the analytical algorithms for shaly sandstone appears to provide a variable degree of leeway for excessive clay content. In addition, the conventional methodology is adaptable to the special needs of hydrogeological investigations. An aggressive approach to analysis is necessary, however, to draw the maximum possible quantitative and qualitative results from well logs.

5. Conclusions

Several conclusions may be drawn from the theoretical and applied studies, conducted as a result of the objectives stated in the Introduction.

1) The qualitative interpretation of lithology was successful in the recognition of shale, shaly sandstone, sandstone, bentonite and calcareous streaks in the 700 m long sections of interest of wells 5-7 and 6-35. Cross-plot analyses for clay type involving the photoelectric cross-section index, and the potassium content and thorium to potassium ratio, were interpreted as mixed layer clays or combinations of clay types which change with depth. Cross plots for the approximation of the type of shale distribution indicated mostly disseminated and laminated shales in shaly sandstone.

2) A multitude of numerical methods is available in literature for the analysis of geophysical well logs recorded in shaly sandstone lithology. The profiles of shale volume calculated from the total gamma radiation curve, and the combination of the neutron porosity and density porosity curves were ambiguous. Hand-picking of values was necessary, with the profiles serving as guidelines.

3) The results computed with a selection of empirical algorithms for the approximation of porosity, were found to remain meaningful even in extremely shaly lithology. From statistical and visual comparisons of the profiles generated with algorithms involving the bulk density curve, the sonic traveltime curve, and the combination of the neutron porosity and density porosity curves, it was concluded that empirically derived algorithms based on the same physical measurements of formation properties tend to produce closely related profiles of porosity. Further, accuracy of log-derived porosity profiles is attained only through calibration with core porosity measurements. The degree to which

the calibrated log-derived porosity profiles of 5-7 and 6-35 represent the actual effective porosity of the stratigraphic section in relative and absolute terms could not be evaluated reliably given the insufficient volume of comparative data from core analyses in nearby wells.

4) The permeability profiles generated from an algorithm based on statistical correlation of core porosity and the logarithm of core permeability as well as log-derived porosity, and an equation involving the free fluid index and density porosity, vary from each other by as much as one-and-a-half log cycles. Theoretically, the algorithm involving the free fluid index is favoured, because it is a direct method of computation with less potential for recurring uncertainties introduced in intermittent data manipulations in the other method. The signature characters and the wide range of values corresponding to small changes in lithology or porosity rendered any evaluation of the accuracy of the permeability profiles ambiguous.

5) Overall, it may be concluded that the analysis and interpretation of geophysical well logs may contribute qualitative and quantitative information with respect to lithology, shale volume, porosity and permeability of the rock formation to hydrogeological investigations in shaly sandstone. A selection of algorithms developed for the purposes of petroleum exploration is applicable and the methodology of implementation adaptable.

References

- Ahmed, U., F. Kuchuk, and L. Ayestaran. 1987. Short-term transient rate and pressure-buildup analysis of low-permeability reservoirs. *Formation Evaluation*, 2(4), pp. 611-617.
- American Geological Institute. 1976. *Dictionary of Geological Terms*. Anchor Books, 472 pp.
- Asquith, G.B. 1982. *Basic Well Log Analysis For Geologists*. AAPG, Tulsa, Oklahoma, USA, 216 pp.
- Asquith, G.B. 1990. *Log Evaluation of Shaly Sandstones: A Practical Guide*. Continuing Education Course Note Series #31, Amer. Assoc. Petrol. Geol., Tulsa, Oklahoma, 59 pp.
- Atlas Wireline Services. 1985. *Log Interpretation Charts*. Atlas Wireline Services, Western Atlas International, Inc., 203 pp.
- Badry, R.B., E. Head, C. Morris, and I. Traboulay. 1993. New wireline formation tester techniques and applications. *Trans. 34th Annual Logging Symposium*, Soc. Prof. Well Log Analysts, ZZ1-ZZ15.
- Barton, R.H., E.A. Christiansen, W.O. Kupech, W.H. Mathews, C.P. Gravenor, and L.A. Bayrock. 1970. Quaternary. *Geological History of Western Canada*, eds. R.G. McGrossan and R.P. Gleister, Alberta Soc. Petrol. Geol., pp. 195-200.
- Bateman, R.M. 1985. *Open-hole log analysis and formation evaluation*. D. Reidel Publishing Company, 647 pp.
- Bateman, R.M. 1990. Thinbed analysis with conventional log suites. *Trans. 31st Annual Logging Symposium*, Soc. Prof. Well Log Analysts, 111-1124.
- Borland, 1991. *Quattro Pro Version 3.0 User's Guide*. Borland International, 807 pp.
- Brock, J. 1986. *Applied Open Hole Log Analysis: A step-by-step course in well log interpretation - from fundamentals to advanced concepts*. Contributions in Petroleum Geology & Engineering, Gulf Publishing Company, 2, 284 pp.
- Burns, D.R., and C.H. Cheng. 1986. Determination of in-situ permeability from tube wave velocity and attenuation. *Trans. 27th Annual Logging Symposium*, Soc. Prof. Well Log Analysts, KK1-KK15.
- Busch, J.M., W.G. Fortney, and L.N. Berry. 1987. Determination of lithology from well logs by statistical analysis. *Formation Evaluation*, 2(4), pp. 412-418.

Cannon, D.E., and G.R. Coates. 1990. Applying mineral knowledge to standard log interpretation. *Trans. 31st Annual Logging Symposium*, Soc. Prof. Well Log Analysts, V1-V24.

Cant, D.J. 1969. Zuni Sequence: The Foreland Basin - Lower Zuni Sequence: Middle Jurassic to Middle Cretaceous. *Western Canada Sedimentary Basin - A Case History*, ed. B.D. Ricketts, Can. Soc. Petrol. Geol., pp. 251-267.

Carlson, V.A. 1970. Bedrock Topography, Medicine Hat map area. NTS 72L, 1:250000, Alberta Research Council.

Cheng, A.M. 1986. Calibrating log-derived permeability by well system analysis. *Trans. 27th Annual Logging Symposium*, Soc. Prof. Well Log Analysts, Q1-Q9.

Cheruvier, E., and K.W. Winkler. 1987. Field example of in-situ permeability indication from full acoustic wavetrains. *Trans. 28th Annual Logging Symposium*, Soc. Prof. Well Log Analysts, NN1-NN15.

Clavier, C., G. Coates, and J. Dumanoir. 1984. Theoretical and experimental bases for the dual-water model for interpretation of shaly sands. *J. Soc. Petrol. Eng.*, 24(2), pp. 153-168.

Connolly, E.T., and P.A. Reed. 1983. Full spectrum formation evaluation. *J. Can. Well Logging Soc.*, 12(1), pp. 23-69.

Crain, E.R. 1986. *The Log Analysis Handbook - Quantitative Log Analysis Methods*. PennWell Publishing Company, Tulsa, Oklahoma, 684 pp.

Crain, E.R. 1990. *The Log Analysis Handbook*. Vol. 2, Chapter 3, E.R. Crain, Rocky Mountain House, Alberta, Canada.

Daniels, J.J., and W.S. Keys. 1990. Geophysical well logging for evaluating hazardous waste sites. *Geotechnical and environmental geophysics*, ed. S.H. Ward, Investigations in Geophysics No. 5, Vol. I, Soc. Explor. Geophys., pp. 263-286.

Darcy, H. 1856. *Les fontaines publiques de la ville de Dijon*; Victor Dalmont, Paris, 647 pp. Translated excerpt of pp. 590-594: The public fountains of the city of Dijon - Determination of the laws of the flow of water through sand. In: *Physical Hydrogeology*, eds. R.A. Freeze and J.W. Back, Benchmark Papers in Geology, 72, Hutchinson Ross Publishing Company, 1983, 431 pp.

Davis, J.C. 1986. *Statistics and data analysis in geology*. John Wiley & Sons, Inc., 646 pp.

de Marsily, G. 1986. *Quantitative Hydrogeology*. Academic Press, Inc., 440 pp.

de Lima, O.A.L. 1993. Geophysical evaluation of sandstone aquifers in the Recôncavo-Tucano Basin, Bahia - Brazil. *Geophysics*, 58(11), pp. 1689-1702.

Dewan, J.T., and M.E. Chenevert. 1993. Mudcake buildup and invasion in low permeability formations; Application to permeability determination by Measurement While Drilling. *Trans. 34th Annual Logging Symposium, Soc. Prof. Well Log Analysts*, NN1-NN24.

Dickey, P.A. 1986. *Petroleum Development Geology*. PennWell Publishing Company, 530 pp.

Dresser Atlas. 1982. *Well Logging and Interpretation Techniques - The Course for Home Study*. Dresser Industries Inc., 211 pp.

Edmundson, H. and L.L. Raymer. 1979. Radioactive logging parameters for common minerals. *Log Analyst*, 20(5), pp. 38-47.

Ellis, D. V. 1987. *Well Logging for Earth Scientists*. Elsevier Science Publishing Company, Inc., New York, 532 pp.

Etnyre, L.M. 1993. Comparative performance of a dual water model equation in laminar shaly sands. *Trans. 34th Annual Logging Symposium, Soc. Prof. Well Log Analysts*, I1-I25.

Fertl, W.H. 1987. Log-derived evaluation of shaly clastic reservoirs. *J. Petrol. Tech.*, 39(2), pp. 175-194.

Foster, N.H., and E.A. Beaumont, eds. 1990. *Formation Evaluation: 1. Log Evaluation, 2. Log Interpretation*. Treatise of Petroleum Geology Reprint Series, No. 16, Amer. Assoc. Petrol. Geol.

Freeze, R.A., and J.A. Cherry. 1979. *Groundwater*. Prentice-Hall, Inc., 604 pp.

Freund, J.E., and R.E. Walpole. 1980. *Mathematical Statistics*. Prentice-Hall, Inc., USA, 548 pp.

Georgi, D.T., D.G. Harville, C. Phillips, and G.M. Ostroff. 1993. Extrapolation of core permeability data with wireline logs to uncored intervals. *Trans. 34th Annual Logging Symposium, Soc. Prof. Well Log Analysts*, KK1-KK19.

Glass, D.J. ed. 1990. *Lexicon of Canadian Stratigraphy - Volume 4: Western Canada, including Eastern British Columbia, Alberta, Saskatchewan and Southern Manitoba*. Can. Soc. Petrol. Geol., 772 pp.

Goldberg, D., D. Speed, C. Wilkinson, and E. Scholz. 1990. A correlation of hydraulic conductivity from pulse tests with sonic log amplitudes. *Geological Applications of Wireline Logs*, eds. A. Hurst, M.A. Lovell and A.C. Morton, Geol. Soc. Special Publication No. 48, pp. 297-302.

Guidry, F.K., D.L. Luffel, and A.J. Olszewski. 1990. Devonian shale formation evaluation model based on logs, new core analysis methods, and production tests. *Trans. 31st Annual Logging Symposium*, Soc. Prof. Well Log Analysts, NN1-NN20.

Gwinner, D.M., L.S. Laude, J.L. Olmos, J.A. Quirein, and L.J. Reimer. 1991. Improved reservoir characterization by integration of petrophysics, geology and core analysis: an example from the Hugoton Field, Kansas. *Trans. 32nd Annual Logging Symposium*, Soc. Prof. Well Log Analysts, TT1-TT23.

Hankel, R.C., G.R. Davies, and H.R. Krouse. 1969. Eastern Medicine Hat gas field: a shallow, Upper Cretaceous, bacteriogenic gas reservoir of southeastern Alberta. *Bull. Can. Petrol. Geol.*, 37(1), pp. 96-112.

Hartmann, D.J. 1975. Effect of bed thickness and pore geometry on log response. *Trans. 16th Annual Logging Symposium*, Soc. Prof. Well Log Analysts, Y1-Y14.

Helander, D.P. 1983. *Fundamentals of formation evaluation*. Oil & Gas Consultants International, Inc. and Donald P. Helander, 332 pp.

Herron, M.M. 1967. Estimating the intrinsic permeability of clastic sediments from geochemical data. *Trans. 26th Annual Logging Symposium*, Soc. Prof. Well Log Analysts, HH1-HH23.

Hilchie, D.W. 1978. *Applied Openhole Log Interpretation for Geologists and Engineers*. D.W. Hilchie Inc., Golden, Colorado.

Howard, K.W.F. 1990a. Geophysical well logging methods for detection and characterization of fractures in hard rocks. *Geotechnical and environmental geophysics*, ed. S.H. Ward, Investigations in Geophysics No. 5, Vol. I, Soc. Explor. Geophys., pp. 287-308.

Howard, K.W.F. 1990b. The role of well logging in contaminant transport studies. *Geotechnical and environmental geophysics*, ed. S.H. Ward, Investigations in Geophysics No. 5, Vol. II, Soc. Explor. Geophys., pp. 289-302.

Hubbert, M.K. 1940. The theory of ground-water motion. The University of Chicago, J. Geology, 48, pp. 785-944. Excerpt of pp. 785-819. In: *Physical Hydrogeology*, eds. R.A. Freeze and W. Back, Benchmark Papers in Geology, 72, Hutchinson Ross Publishing Company, 1983, 431 pp.

Johnson, H.M. 1962. Review article: a history of well logging. *Geophysics*, 27 (4), pp. 507-527.

Jones, S.C. 1992. The profile permeameter -- A new, fast, accurate minipermeameter. Soc. Petrol. Eng. paper 24757, 11 pp.

Jorden, J.R., and F.L. Campbell. 1986. *Well Logging II - Electric and Acoustic Logging*. Monograph Vol. 10, Henry L. Doherty Series, Soc. Petrol. Eng., USA, 182 pp.

Klimentos, T. 1991. The effects of porosity-permeability-clay content on the velocity of compressional waves. *Geophysics*, 56(12), pp. 1930-1939.

Koster, E.H., P.J. Currie, D. Eberth, D. Brinkman, P. Johnston, and D. Braman. 1987. *Sedimentology and Palaeontology of the Upper Cretaceous Judith River/Bearpaw Formations at Dinosaur Provincial Park, Alberta. Field Trip Guidebook: Trip 10*, Geol. Assoc. Can., Mineral. Assoc. Can., 112 pp.

Kukul, G.C., and R.E. Hill. 1986. Log analysis of clay volume: An evaluation of techniques and assumptions used in an Upper Cretaceous sand-shale sequence. *Trans. 27th Annual Logging Symposium*, Soc. Prof. Well Log Analysts, RR1-RR22.

Leckie, D.A. 1989. Upper Zuni Sequence: Upper Cretaceous to Lower Tertiary. *Western Canada Sedimentary Basin - A Case History*, ed. B.D. Ricketts, Can. Soc. Petrol. Geol., pp. 269-284.

Logan, W.D. 1989. Bridging the gap between core permeability and log-derived permeability. *Trans. 30th Annual Logging Symposium*, Soc. Prof. Well Log Analysts, V1-V23.

Luffel, D.L., and F.K. Guidry. 1989. Reservoir rock properties of Devonian shale from core and log analysis. *Soc. Core Analysts Conf.*, Paper Nr. 8910 (J), 15 pp.

Malikem, W.R. 1982. *Clay Minerals from some Upper Cretaceous Bentonites, Southwestern Alberta*. Unpublished M.Sc. Thesis, University of Alberta, 72 pp.

Male, W.H., and R.R. Pacholko. 1982. Upper Cretaceous Gas Reservoirs of the Suffield Military Range - Southeastern Alberta. *Canada's Giant Hydrocarbon Reservoirs*, ed. W.G. Cutler, Can. Soc. Petrol. Geol., pp. 95-106.

Martin, I., and G.C. Yeung. 1991. The Medicine Hat gas field - 100 years after discovery. *J. Can. Petrol. Tech.*, 30(5), pp. 66-73.

McQuillin, R., M. Bacon, and W. Barclay. 1984. *An Introduction to Seismic Interpretation*. Gulf Publishing Company, Houston, Texas, USA, 287 pp.

Merkel, R.H. 1983. *Well Log Formation Evaluation*. Continuing Education Course Note Series #14, Amer. Assoc. Petrol. Geol., Tulsa, Oklahoma, 82 pp.

Miller, M.N., Z. Paliel, M.E. Gillen, J. Granot, and J.C. Bouton. 1990. Spin echo magnetic resonance logging: porosity and free fluid index determination. *Trans. 65th Ann. Tech. Conf. and Exhib. of Soc. Petrol. Eng.*, Paper 20561, pp. 321-334.

Moinard, L.L., R.L. Jones, and D.J. Gawick. 1983. Evaluation of the Milk River sand in the Suffield Block. *Trans. 24th Annual Logging Symposium*, Soc. Prof. Well Log Analysts, HH1-HH17.

Molz, F.J., and S.C. Young. 1993. Development and application of borehole flowmeters for environmental assessment. *Log Analyst*, 34(1), pp. 13-23.

Morriss, C.E., and L. Laverdiere. 1988. Nuclear magnetism log interpretation in shaly sand formations. *Trans. 29th Annual Logging Symposium*, Soc. Prof. Well Log Analysts, EE1-EE23.

Mottana, A., R. Crespi, and G. Liborio. 1978. *Simon and Schuster's Guide to Rocks and Minerals*. Simon and Schuster, New York, 607 pp.

Nelson, S.J., R.P. Glaister, and R.G. McGrossan. 1970. Introduction. *Geological History of Western Canada*, eds. R.G. McGrossan and R.P. Glaister, Alberta Soc. Petrol. Geol., pp. 1-13.

Oord, van den R.J. 1990. Experience with geochemical logging. *Trans. 31st Annual Logging Symposium*, Soc. Prof. Well Log Analysts, T1-T25.

Paillet, F.L., and R.E. Crowder. 1993. Environmental applications of logging: Introduction to special issue. *Log Analyst*, 34 (1), pp. 11-12.

Paillet, F.L., R.T. Kay, D. Yeskis, and W. Pedler. 1993. Integrating well logs into a multiple-scale investigation of a fractured sedimentary aquifer. *Log Analyst*, 34(1), pp. 24-40.

Press, F., and R. Siever. 1982. *Earth*. W.H. Freeman and Company, USA, 613 pp.

Rudkin, R.A. 1970. Lower Cretaceous. *Geological History of Western Canada*, eds. R.G. McGrossan and R.P. Glaister, Alberta Soc. Petrol. Geol., pp. 156-168.

Sah, R.C. 1977. Shaly sand evaluation with total water. *Proc. Annual Logging Symposium*, Canadian Well Logging Society.

Schlumberger. 1985. *Open Hole - Basics*. Schlumberger Educational Services, Houston, Texas.

Schlumberger. 1988. *Log Interpretation Charts*. Schlumberger Educational Services, Houston, Texas.

Schlumberger. 1989. *Log Interpretation Principles/Applications*. Schlumberger Educational Services, Houston, Texas.

Serra, O., I. Stowe, and D. Motet. 1993. True integrated interpretation. *Trans. 34th Annual Logging Symposium*, Soc. Prof. Well Log Analysts, Z1-Z25.

Shen, L.C., M.J. Manning, and J.M. Price. 1984. Application of electromagnetic propagation tool in formation evaluation. *Trans. 25th Annual Logging Symposium*, Soc. Prof. Well Log Analysts, J1-J15.

Shepard, W., and B. Bartow. 1986. Tectonic history of the Sweetgrass Arch, a key to finding new hydrocarbons, Montana and Alberta. *Wyoming Geological Association Symposium, Rocky Mountain Oil and Gas Fields*, pp. 9-19.

Sheriff, R.E. 1991. *Encyclopedic Dictionary of Exploration Geophysics*, Soc. Exploration Geophysicists, 376 pp.

Sneider, R.M., H.R. King, R.W. Hietala, and E.T. Connolly. 1984. Integrated rock-log calibration in the Elsworth Field - Alberta, Canada. *Elsworth - Case Study of a Deep Basin Gas Field*, ed. J.S. Masters, Memoir 38, Amer. Assoc. Petro. Geol., pp. 205-282.

Soonawala, N.M., A.L. Holloway, and D.K. Tomsons. 1990. Geophysical methodology for the Canadian nuclear fuel waste management program. *Geotechnical and environmental geophysics*, ed. S.H. Ward, Investigations in Geophysics No. 5, Vol. I, Soc. Explor. Geophys., pp. 309-332.

Speelman, H., and J.N. Breunese. 1985. Determination of porosity and permeability of low-permeable unconsolidated marine Tertiary deposits in the Netherlands. *Proc. Intern. Assoc. of Hydrogeol., Memoirs - Tucson Congress*, Vol. XVII, Part 1, pp. 198-208.

Stott, D.F. 1984. Cretaceous sequences of the foothills of the Canadian Rocky Mountains. *The Mesozoic of Middle North America*, eds. D.F. Stott and D.J. Glass, Memoir 9, Can. Soc. Petrol. Geol., pp. 85-107.

Straley, C., C.E. Morris, W.E. Kenyon, and J.J. Howard. 1991. NMR in partially saturated rocks: laboratory insights on free fluid index and comparison with borehole logs. *Trans. 32nd Annual Logging Symposium*, Soc. Prof. Well Log Analysts, CC1-CC17.

Suau, J., P. Grimaldi, A. Poupon, and P. Souhailte. 1972. The dual laterolog-R_{xo} tool. Soc. Petrol. Eng. Paper 4018, American Institute of Mining, Metallurgical, and Petroleum Engineers, Inc., 12 pp.

Taylor, R.S., W.H. Mathews, and W.O. Kupech. 1970. Tertiary. *Geological History of Western Canada*, eds. R.G. McGrossan and R.P. Glaister, Alberta Soc. Petrol. Geol., pp. 190-194.

Telford, W.M., L.P. Geldart, R.E. Sheriff, and D.A. Keys. 1976. *Applied Geophysics*. Cambridge University Press, 880 pp.

Timur, A. 1969. Pulsed nuclear magnetic resonance studies of porosity, moveable fluid and permeability in sandstones. *J. Petrol. Tech.*, 21, pp. 775-786.

- Tittman, J. 1986. *Geophysical Well Logging*. Excerpted from: *Methods in Experimental Physics*, Vol. 24: Geophysics, Academic Press, Inc., Orlando, Florida, 175 pp.**
- Tizzard, P.G. 1974. Viking Deposition in the Suffield Area, Alberta. Unpublished M.Sc. Thesis, University of Alberta, 126 pp.**
- Tokarsky, O. 1986. Hydrogeologic Cross-Sections A-A' and M-M', Medicine Hat 72 L. Alberta Environment, Earth Sciences Division for Water Resources Management Services.**
- Tóth, J. 1984. The role of regional gravity flow in the chemical and thermal evolution of ground water. *Proc. First Can./Amer. Conf. on Hydrogeology*, Banff, Alberta, Canada, June 22-26; National Water Well Assoc., Worthington, Ohio, USA.**
- Tóth, J. 1990. Hydraulic Continuity in Large Sedimentary Basins; Keynote Address. *Proc. Intern. Conf. on Groundwater in Large Sedimentary Basins*, Perth, Australia.**
- Wessels, N.K., and J.L. Hopson. 1988. *Biology*. Random House, Inc., 1251 pp.**
- Williams, G.D., and C.F. Burk. 1970. Upper Cretaceous. *Geological History of Western Canada*, eds. R.G. McGrossan and R.P. Glaister, Alberta Soc. Petrol. Geol., pp. 169-189.**
- Wyatt, D.F., L.A. Jacobson, and K. Hashmy. 1993. Elemental yields and complex lithology analysis from the pulsed spectral gamma log. *Trans. 34th Annual Logging Symposium*, Soc. Prof. Well Log Analysts, UU1-UU25.**
- Wyllie, M.R.J., A.R. Gregory, and L.W. Gardner. 1956. Elastic wave velocities in heterogeneous and porous media. *Geophysics*, 21(1), pp. 41-70.**
- Yildiz, T., and R. Desbrandes. 1989. A new model to determine permeability from wireline formation testing. *Trans. 28th Annual Logging Symposium*, Soc. Prof. Well Log Analysts, T1-T25.**

APPENDICES

Appendix A: List of well log parameters for 5-7 and 6-35 as digitized in one-metre depth intervals

Legend for Column Headers:

DEPTH = depth below KB (m)
 PHID = density porosity (fractional porosity units - p.u.)
 DENS = bulk density (kg/m³)
 PHIN = neutron porosity (fractional porosity units - p.u.)
 GR = total gamma radiation (API units)
 PEF = photoelectric cross-section index (barne/electron)
 LLD = deep laterolog (Ω.m)
 LLS = shallow laterolog (Ω.m)
 SP = spontaneous potential (mV)
 DTL = sonic traveltime (μs/m)
 FFI = free fluid index (fractional porosity units - p.u.)

05-07-017-07W-001										
DEPTH	PHID	DENS	PHIN	GR	PEF	LLD	LLS	SP	DTL	FFI
188	0.118	2488	0.309	48.38	2.87	18.88	12.88	-38.38	288.38	-888.888
189	0.308	2548	0.318	48.38	2.88	8.88	8.88	-38.17	378.88	-888.888
190	0.384	2188	0.388	48.18	2.81	8.88	8.88	-31.34	418.88	-888.888
191	0.388	2188	0.388	48.38	2.88	7.88	8.18	-38.38	488.88	-888.888
192	0.388	2178	0.387	88.38	2.88	8.84	8.78	-38.88	418.88	-888.888
193	0.384	2801	0.318	88.48	2.84	8.87	7.88	-37.81	388.88	-888.888
194	-0.010	2888	0.888	84.88	4.88	178.18	181.81	-38.34	387.87	-888.888
195	0.388	2188	0.381	48.88	2.48	8.88	7.88	-34.78	387.18	-888.888
196	0.388	2808	0.318	88.71	2.84	8.88	7.88	-38.88	488.88	-888.888
197	0.388	2188	0.388	47.48	2.48	8.47	8.44	-31.88	384.88	-888.888
198	0.188	2848	0.278	48.88	3.88	14.88	8.88	-38.88	388.88	-888.888
199	0.387	2188	0.388	81.88	2.88	8.48	8.48	-31.88	388.88	-888.888
200	0.381	2188	0.384	88.88	2.78	8.88	8.78	-38.38	384.88	-888.888
201	0.388	2188	0.388	84.48	2.71	8.87	8.88	-38.88	381.41	-888.888
202	0.388	2171	0.378	88.88	2.88	8.88	8.88	-38.88	388.88	-888.888
203	0.277	2188	0.388	88.11	2.78	8.47	8.88	-48.88	388.88	-888.888
204	0.388	2187	0.388	81.81	2.88	8.88	8.88	-44.87	381.87	-888.888
205	0.388	2187	0.378	81.88	2.71	7.88	8.88	-48.48	388.88	-888.888
206	0.348	2837	0.348	88.88	2.88	7.18	4.87	-38.88	388.18	-888.888
207	0.278	2188	0.488	88.48	2.88	4.88	8.18	-38.88	488.87	-888.888
208	0.277	2187	0.348	87.84	3.88	8.11	8.88	-48.88	378.88	-888.888
209	0.381	2848	0.388	84.78	2.88	8.18	8.88	-48.48	384.88	-888.888
210	0.388	2884	0.488	84.84	3.88	8.88	3.88	-48.88	488.88	-888.888
211	0.384	2888	0.471	88.48	3.81	8.88	4.18	-38.88	488.88	-888.888
212	0.348	2888	0.448	84.88	2.88	8.18	8.88	-38.88	484.88	-888.888
213	0.388	2884	0.418	88.48	2.88	7.88	8.88	-48.88	481.88	-888.888
214	0.347	2847	0.488	81.87	2.88	8.48	4.84	-34.88	488.78	-888.888
215	0.388	2888	0.518	78.88	2.88	4.88	8.48	-34.84	488.88	-888.888
216	0.218	2888	0.348	88.18	2.88	7.88	8.18	-37.88	381.87	-888.888
217	0.344	2181	0.448	88.88	2.88	7.18	8.88	-44.88	487.88	-888.888
218	0.318	2888	0.388	88.47	2.88	8.78	4.88	-31.88	418.77	-888.888
219	0.388	2188	0.488	88.81	2.88	7.88	8.84	-48.87	488.88	-888.888
220	0.388	2884	0.488	84.88	2.88	8.88	4.88	-48.78	418.88	-888.888
221	0.388	2188	0.388	88.88	3.18	8.88	7.81	-37.88	381.88	-888.888
222	0.318	2148	0.488	81.78	3.88	8.88	8.87	-38.41	381.88	-888.888
223	-0.018	2888	0.881	38.88	4.17	388.48	388.11	-38.88	187.88	-888.888
224	-0.088	2788	0.148	38.88	8.88	188.48	88.88	-34.18	188.18	-888.888
225	0.384	2888	0.388	48.78	3.87	18.78	18.88	-38.88	387.88	-888.888
226	0.388	2188	0.378	88.18	2.88	8.88	8.88	-17.88	387.81	-888.888
227	0.387	2147	0.387	81.17	2.87	8.88	8.88	-18.88	387.88	-888.888
228	0.318	2188	0.388	88.48	2.81	18.88	8.88	-18.88	388.88	-888.888
229	0.388	2188	0.388	88.44	2.88	18.88	8.78	-18.88	384.88	-888.888
230	0.318	2118	0.388	47.88	2.47	8.88	7.84	-18.81	388.88	-888.888

05-07-017-07W4M										
DEPTH	PHD	DENS	PHIN	GR	PEF	LLD	LLS	SP	DTL	FFI
231	0.307	2135	0.362	51.34	2.81	10.80	8.83	-18.68	385.07	-888.000
232	0.180	2560	0.300	48.00	3.48	13.00	8.90	-30.48	382.34	-888.000
233	0.312	2142	0.368	56.80	2.30	8.32	6.30	-18.22	388.82	-888.000
234	0.314	2138	0.343	54.02	2.84	8.80	6.84	-30.22	388.88	-888.000
235	0.288	2160	0.388	48.00	2.72	13.80	8.10	-22.87	378.38	-888.000
236	0.288	2230	0.378	54.44	3.17	11.02	8.40	-28.34	371.20	-888.000
237	0.308	2174	0.388	88.18	2.78	9.08	6.91	-28.18	387.38	-888.000
238	0.230	2260	0.367	54.82	3.86	8.87	6.84	-28.81	384.38	-888.000
239	0.288	2161	0.372	54.88	2.84	8.78	7.88	-38.44	378.82	-888.000
240	0.281	2173	0.382	88.87	2.81	8.48	6.78	-30.88	383.88	-888.000
241	0.282	2178	0.381	88.78	2.83	8.87	7.88	-34.28	388.38	-888.000
242	0.308	2280	0.388	83.87	3.78	8.17	7.21	-32.88	381.38	-888.000
243	0.308	2140	0.367	88.88	2.86	8.04	7.18	-34.88	388.01	-888.000
244	0.288	2203	0.407	82.88	3.88	8.84	7.88	-38.82	388.78	-888.000
245	0.282	2174	0.388	88.88	2.88	8.88	6.78	-48.78	387.71	-888.000
246	0.283	2218	0.438	88.77	3.23	6.48	8.88	-51.88	388.88	-888.000
247	0.288	2287	0.438	81.17	2.88	8.27	4.88	-47.88	418.88	-888.000
248	0.228	2278	0.384	71.07	3.18	8.33	4.78	-57.18	418.14	-888.000
249	0.232	2288	0.484	73.18	3.02	4.83	4.08	-48.23	428.87	-888.000
250	0.213	2300	0.380	70.88	3.08	6.38	6.34	-57.47	404.88	-888.000
251	0.210	2307	0.413	77.38	3.11	6.18	6.81	-48.81	388.88	-888.000
252	0.211	2308	0.421	88.82	3.08	8.80	8.28	-48.71	407.87	-888.000
253	0.202	2380	0.438	78.18	3.14	8.78	6.88	-48.77	418.88	-888.000
254	0.211	2303	0.438	78.37	3.10	8.38	4.88	-48.82	418.21	-888.000
255	0.204	2311	0.483	71.88	3.27	8.18	4.88	-48.88	421.71	-888.000
256	0.213	2300	0.448	67.88	3.18	8.72	6.14	-48.30	417.30	-888.000
257	0.218	2384	0.437	82.88	3.28	8.88	8.13	-48.48	417.88	-888.000
258	0.218	2384	0.488	74.81	3.34	8.41	4.88	-48.37	424.88	-888.000
259	0.218	2384	0.488	72.38	3.18	8.78	6.38	-48.34	428.81	-888.000
260	0.207	2388	0.488	77.38	3.18	8.88	4.88	-48.48	418.48	-888.000
261	0.217	2388	0.487	78.38	3.08	4.88	4.84	-48.38	428.21	-888.000
262	0.217	2388	0.488	88.88	2.97	8.27	8.11	-47.88	418.38	-888.000
263	0.208	2388	0.487	78.32	3.28	4.34	4.88	-48.88	428.88	-888.000
264	0.234	2384	0.484	78.87	3.18	4.27	4.88	-48.41	428.84	-888.000
265	0.238	2278	0.487	72.78	3.08	4.41	4.88	-48.44	428.78	-888.000
266	0.217	2384	0.472	78.88	3.11	4.88	4.48	-44.38	427.38	-888.000
267	0.217	2388	0.437	78.88	3.21	8.88	4.81	-48.82	421.88	-888.000
268	0.231	2274	0.488	78.18	3.48	4.88	4.81	-48.82	428.38	-888.000
269	0.234	2383	0.488	88.88	3.12	8.18	4.88	-48.78	428.84	-888.000
270	0.227	2278	0.388	88.81	2.88	8.72	4.88	-48.84	418.84	-888.000
271	0.282	2188	0.407	88.88	3.18	7.18	8.84	-38.47	388.81	-888.000
272	0.301	2148	0.438	88.84	2.88	7.88	6.32	-38.38	387.88	-888.000
273	0.308	2147	0.438	88.88	2.78	7.88	6.38	-34.18	387.17	-888.000
274	0.318	2138	0.482	87.88	2.88	8.44	7.18	-38.88	408.88	-888.000
275	0.881	2848	0.388	48.88	3.88	38.88	38.88	-38.87	388.88	-888.000
276	0.387	2307	0.438	88.38	3.18	7.88	8.84	-38.38	388.38	-888.000
277	0.301	2188	0.384	88.88	3.88	7.22	6.48	-38.82	388.21	-888.000
278	0.387	2181	0.438	82.12	2.88	7.88	6.71	-38.87	384.84	-888.000
279	0.388	2844	0.407	87.27	3.27	8.88	6.78	-38.88	378.88	-888.000
280	0.388	2188	0.388	82.88	2.88	7.78	6.84	-34.88	378.44	-888.000
281	0.384	2178	0.488	88.38	3.18	7.88	8.88	-38.88	378.78	-888.000
282	0.381	2188	0.378	88.48	3.84	7.13	6.38	-38.38	388.88	-888.000
283	0.388	2182	0.407	88.87	3.88	7.22	6.21	-41.77	388.87	-888.000
284	0.388	2288	0.378	88.87	2.88	6.88	6.88	-48.87	387.88	-888.000
285	0.382	2284	0.388	88.88	2.88	6.48	6.88	-51.88	388.18	-888.000
286	0.382	2278	0.388	87.88	2.81	8.11	8.88	-38.88	388.18	-888.000
287	0.388	2388	0.488	88.11	3.88	4.88	4.48	-38.88	418.81	-888.000
288	0.317	2388	0.488	88.18	3.13	4.88	4.81	-48.81	418.88	-888.000
289	0.388	2388	0.488	78.38	3.88	4.88	4.84	-48.88	418.47	-888.000
290	0.312	2388	0.488	88.87	3.18	4.88	4.78	-48.88	428.84	-888.000
291	0.314	2388	0.488	78.84	3.18	8.84	8.18	-38.11	428.11	-888.000
292	0.388	2388	0.487	88.88	3.18	4.88	4.27	-48.87	428.61	-888.000
293	0.388	2387	0.381	88.81	3.87	3.88	3.78	-41.78	428.87	-888.000
294	0.388	2388	0.484	82.88	3.88	8.34	8.17	-34.84	428.78	-888.000
295	0.388	2388	0.488	88.48	3.88	6.88	8.88	-38.18	428.88	-888.000
296	0.347	2384	0.388	87.71	3.14	8.11	4.88	-38.88	421.88	-888.000

03-07-017-07W4M										
DEPTH	PHID	DENS	PHIN	GR	PEF	LLD	LLS	SP	DTL	FFI
297	0.220	2309	0.438	65.81	3.14	5.35	4.83	-55.88	404.02	-888.000
298	0.217	2294	0.414	65.75	3.08	4.98	4.89	-55.89	406.38	-888.000
299	0.211	2314	0.478	66.68	3.11	4.14	3.82	-57.15	414.47	-888.000
300	0.200	2318	0.411	72.08	3.15	4.10	3.50	-57.57	414.13	-888.000
301	0.204	2325	0.448	67.08	3.13	3.08	2.55	-58.82	415.07	-888.000
302	0.216	2302	0.463	69.40	3.23	5.00	4.10	-58.85	414.57	-888.000
303	0.188	2340	0.438	72.84	3.38	3.08	2.80	-57.38	414.88	-888.000
304	0.208	2318	0.457	68.01	3.19	1.80	1.40	-57.82	418.53	-888.000
305	0.208	2312	0.480	67.33	3.08	2.80	2.70	-57.18	411.83	-888.000
306	0.184	2330	0.477	71.43	3.15	4.34	3.70	-57.85	405.82	-888.000
307	0.184	2329	0.484	73.29	3.35	4.70	4.37	-58.04	408.89	-888.000
308	0.188	2338	0.388	68.89	3.29	4.54	4.28	-57.77	399.43	-888.000
309	0.204	2323	0.440	68.44	3.18	4.38	4.14	-57.91	414.76	-888.000
310	0.188	2340	0.432	71.38	3.23	4.80	4.80	-58.07	413.57	-888.000
311	0.200	2334	0.488	68.89	3.22	4.82	4.71	-57.76	415.49	-888.000
312	0.188	2332	0.488	73.32	3.10	4.88	4.74	-58.23	418.23	-888.000
313	0.201	2321	0.488	73.10	3.11	4.14	4.28	-58.48	404.88	-888.000
314	0.203	2314	0.488	78.48	3.18	3.88	3.88	-58.48	408.34	-888.000
315	0.204	2317	0.442	73.08	3.12	3.94	3.88	-58.57	405.28	-888.000
316	0.215	2303	0.488	70.81	3.22	4.13	4.01	-58.18	405.91	-888.000
317	0.274	2200	0.380	61.35	3.14	3.43	3.35	-58.22	441.28	-888.000
318	0.217	2286	0.407	71.80	2.88	5.02	4.80	-57.51	405.88	-888.000
319	0.238	2272	0.488	78.33	2.92	2.90	2.70	-58.88	402.08	-888.000
320	0.283	2180	0.572	82.80	2.78	4.01	3.97	-58.38	415.67	-888.000
321	0.230	2288	0.444	78.13	3.21	3.30	3.10	-58.17	401.57	-888.000
322	0.223	2285	0.488	78.34	2.98	3.99	4.10	-58.61	408.22	-888.000
323	0.312	2180	0.541	84.05	2.88	2.70	2.80	-58.84	402.08	-888.000
324	0.239	2288	0.488	88.78	3.08	3.80	3.90	-58.67	443.38	-888.000
325	0.270	2280	0.478	78.84	3.12	2.80	2.80	-57.72	402.23	-888.000
326	0.308	2318	0.484	78.84	3.08	4.82	4.48	-57.38	411.57	-888.000
327	0.304	2320	0.418	81.48	3.14	4.88	4.88	-57.18	411.07	-888.000
328	0.308	2319	0.488	84.05	3.08	4.84	4.39	-58.85	412.88	-888.000
329	0.283	2345	0.537	88.08	3.07	4.38	4.38	-57.91	415.88	-888.000
330	0.199	2338	0.418	88.14	3.08	4.48	4.48	-58.38	410.31	-888.000
331	0.178	2383	0.488	88.08	3.28	5.11	5.14	-58.88	399.28	-888.000
332	0.180	2380	0.488	88.08	3.28	5.78	5.42	-58.34	399.78	-888.000
333	0.177	2388	0.414	87.80	2.80	6.98	7.11	-58.88	394.18	-888.000
334	0.081	2800	0.328	81.88	4.10	8.81	8.88	-51.87	348.88	-888.000
335	0.132	2488	0.388	100.81	2.88	8.31	8.38	-48.88	398.88	-888.000
336	0.148	2421	0.388	82.27	3.02	8.74	8.89	-48.48	398.81	-888.000
337	0.148	2409	0.388	85.77	3.04	8.84	8.81	-48.54	319.54	-888.000
338	0.480	1888	0.888	82.81	2.74	3.70	3.70	-48.88	408.38	-888.000
339	0.184	2400	0.388	88.87	2.88	10.34	10.88	-47.88	348.34	-888.000
340	0.182	2401	0.318	82.18	2.80	10.48	8.87	-48.38	398.88	-888.000
341	0.188	2388	0.312	88.81	2.88	11.48	10.88	-44.38	348.31	-888.000
342	0.147	2411	0.388	84.83	2.74	10.88	10.38	-44.17	348.74	-888.000
343	0.161	2387	0.388	82.78	2.88	10.88	10.44	-48.78	344.81	-888.000
344	0.138	2422	0.388	88.18	2.80	11.38	10.88	-48.84	348.84	-888.000
345	0.141	2421	0.388	80.17	2.88	11.71	11.38	-44.48	348.54	-888.000
346	0.148	2408	0.388	81.88	3.18	11.48	10.88	-44.88	348.81	-888.000
347	0.144	2408	0.327	87.88	2.88	10.88	10.38	-48.84	348.18	-888.000
348	0.142	2407	0.317	88.88	3.13	10.48	8.78	-48.78	348.53	-888.000
349	0.188	2401	0.388	88.13	2.88	11.88	11.13	-48.47	341.88	-888.000
350	0.144	2418	0.318	82.38	2.87	11.88	11.88	-48.84	348.88	-888.000
351	0.137	2434	0.301	88.87	2.88	12.88	12.31	-48.88	354.13	-888.000
352	0.138	2418	0.388	88.88	2.88	14.14	13.18	-48.88	357.87	-888.000
353	0.138	2408	0.318	88.88	2.88	12.84	12.18	-44.38	348.38	-888.000
354	0.142	2418	0.318	81.88	2.87	12.71	11.87	-44.13	348.18	-888.000
355	0.134	2408	0.388	88.48	3.88	12.48	11.84	-44.38	348.54	-888.000
356	0.181	2411	0.318	82.71	2.88	13.14	12.18	-48.44	357.88	-888.000
357	0.131	2408	0.314	87.13	2.88	13.87	12.77	-48.38	357.88	-888.000
358	0.167	2370	0.312	81.11	3.88	12.88	11.88	-44.81	344.18	-888.000
359	0.188	2388	0.327	82.88	2.74	11.74	11.38	-48.81	348.48	-888.000
360	0.141	2408	0.327	88.38	2.88	12.88	12.38	-48.38	341.44	-888.000
361	0.138	2408	0.388	100.88	2.78	13.77	12.48	-44.48	351.11	-888.000
362	0.181	2407	0.388	83.88	2.88	13.88	14.84	-48.48	358.88	-888.000

03-07-017-07W4M										
DEPTH	PHO	DENS	PHN	GR	PEF	LLD	LLS	SP	DTL	FFI
363	0.143	2419	0.303	78.81	2.63	15.88	14.27	-48.38	338.88	0.008
364	0.135	2425	0.318	80.43	3.02	13.25	12.38	-48.88	339.28	0.008
365	0.147	2411	0.311	86.27	2.77	13.80	12.75	-48.38	334.62	0.004
366	0.148	2416	0.313	88.35	2.83	13.18	12.05	-48.31	333.91	0.004
367	0.147	2412	0.307	83.00	2.88	12.34	11.54	-47.32	340.75	0.008
368	0.141	2419	0.322	88.01	2.83	11.82	10.85	-48.54	341.47	0.008
369	0.183	2408	0.300	82.10	2.80	12.79	11.83	-48.38	335.30	0.008
370	0.142	2420	0.319	88.78	2.88	12.08	11.18	-48.13	338.34	0.008
371	0.138	2431	0.344	82.08	3.05	11.01	10.82	-48.88	343.84	0.008
372	0.147	2407	0.308	88.48	2.88	11.38	10.43	-48.13	348.31	0.004
373	0.160	2380	0.328	88.07	3.17	12.21	11.21	-44.35	348.70	0.008
374	0.167	2382	0.323	91.45	2.71	13.41	12.17	-44.30	347.40	0.008
375	0.164	2387	0.387	88.71	2.88	12.48	11.61	-44.88	344.88	0.008
376	0.188	2403	0.327	82.83	2.84	11.48	10.88	-44.84	348.78	0.004
377	0.188	2318	0.338	82.87	2.88	10.88	9.78	-43.82	357.34	0.008
378	0.243	2280	0.383	88.81	2.78	10.88	10.88	-48.88	388.88	0.001
379	0.132	2418	0.334	77.88	2.88	13.38	12.42	-38.48	387.88	0.008
380	0.248	2288	0.318	88.82	2.78	14.27	13.04	-48.88	384.88	0.018
381	0.180	2480	0.381	87.81	3.00	13.40	12.78	-40.71	388.84	0.011
382	0.237	2280	0.388	80.88	2.88	11.48	10.80	-41.84	347.88	0.012
383	0.188	2488	0.341	84.88	3.40	11.48	10.81	-43.78	341.18	0.007
384	0.188	2325	0.307	77.88	2.78	12.48	11.40	-43.88	383.78	0.008
385	0.082	2510	0.280	81.88	3.18	12.38	11.88	-43.88	341.27	0.008
386	0.188	2388	0.318	82.88	2.87	12.18	11.48	-43.88	343.74	0.008
387	0.178	2380	0.327	81.88	2.88	11.78	10.88	-43.40	348.81	0.008
388	0.184	2480	0.338	87.88	2.87	11.88	11.13	-44.81	348.88	0.007
389	0.283	2348	0.330	88.88	2.81	10.88	9.87	-42.37	382.88	0.017
390	0.188	2388	0.340	108.88	2.88	10.88	9.87	-42.88	347.18	0.008
391	0.118	2488	0.284	88.88	3.48	10.88	9.88	-48.88	344.78	0.013
392	0.188	2380	0.284	88.88	2.88	10.71	9.87	-48.88	383.34	0.008
393	0.184	2382	0.380	81.88	2.87	10.84	10.22	-44.88	388.88	0.008
394	0.218	2380	0.348	88.88	2.88	10.34	9.88	-44.44	387.78	0.007
395	0.138	2414	0.314	88.81	3.02	12.88	11.88	-42.17	381.48	0.018
396	0.212	2314	0.387	82.88	2.71	10.18	9.48	-41.81	388.88	0.008
397	0.288	2380	0.382	82.48	2.88	9.78	8.18	-43.81	384.88	0.008
398	0.178	2384	0.388	88.87	2.88	11.18	10.88	-48.87	348.48	0.008
399	0.188	2381	0.388	102.88	3.07	11.88	10.48	-48.41	348.38	0.008
400	0.200	2341	0.372	87.88	2.78	11.88	10.87	-44.74	388.74	0.007
401	0.211	2380	0.340	88.88	2.78	12.38	11.88	-48.18	341.17	0.018
402	0.218	2380	0.321	88.48	2.77	11.38	11.88	-48.84	341.88	0.018
403	0.188	2384	0.388	88.78	3.88	11.81	11.87	-41.42	347.81	0.018
404	0.137	2421	0.382	74.88	2.88	18.88	18.88	-41.81	388.81	0.004
405	0.248	2388	0.384	88.88	2.88	13.48	12.38	-48.88	347.88	0.008
406	0.188	2377	0.380	87.88	2.88	14.88	11.88	-41.88	348.88	0.018
407	0.188	2388	0.384	87.87	2.88	8.88	7.84	-48.88	344.88	0.008
408	0.272	2380	0.482	88.88	3.31	4.88	4.88	-48.42	388.88	0.018
409	0.217	2388	0.388	87.88	2.77	12.88	11.88	-48.84	348.18	0.008
410	0.187	2388	0.388	88.41	2.78	14.84	12.31	-48.11	388.78	0.008
411	0.171	2448	0.314	88.88	2.88	13.88	12.88	-38.88	344.88	0.008
412	0.281	2183	0.318	88.87	2.78	12.48	11.88	-38.84	388.88	0.008
413	0.288	2183	0.384	108.88	2.88	11.48	11.48	-48.18	388.87	0.008
414	0.330	2388	0.388	88.87	2.88	14.38	12.88	-38.88	344.88	0.018
415	0.182	2381	0.388	88.87	2.88	14.72	13.28	-38.48	388.38	0.007
416	0.188	2413	0.382	88.88	2.88	14.78	13.84	-38.37	387.88	0.008
417	0.178	2383	0.388	108.88	2.81	14.77	13.48	-38.88	388.87	0.018
418	0.132	2488	0.388	81.88	2.88	14.81	13.41	-38.48	387.78	0.011
419	0.143	2388	0.382	88.48	2.81	14.14	12.87	-38.48	388.88	0.008
420	0.178	2388	0.318	88.88	2.88	13.21	12.81	-37.34	384.38	0.008
421	0.174	2378	0.381	88.88	2.91	13.11	11.88	-38.48	388.88	0.008
422	0.148	2181	0.318	88.87	3.38	11.88	11.18	-38.48	387.87	0.018
423	0.288	2388	0.388	102.87	2.74	10.78	9.88	-48.88	388.88	0.008
424	0.288	2344	0.487	88.88	2.88	10.88	9.88	-37.18	381.81	0.008
425	0.248	2388	0.318	108.88	2.88	8.88	8.48	-48.88	388.87	0.007
426	0.188	2388	0.388	102.81	2.84	18.18	8.88	-48.88	388.84	0.012
427	0.218	2388	0.388	88.88	2.88	8.88	8.48	-48.78	381.88	0.018
428	0.212	2384	0.381	102.44	2.88	11.88	11.12	-41.87	388.88	0.011

05-07-017-07W4M

DEPTH	PHO	DENS	PHN	GR	PEF	LLD	LLS	SP	DTL	FFI
429	0.187	2345	0.360	108.66	3.12	12.52	11.93	-43.78	384.87	0.004
430	0.148	2410	0.360	112.79	3.08	11.52	11.19	-46.85	388.98	0.010
431	0.168	2384	0.421	134.00	3.40	10.56	10.17	-48.63	378.21	0.001
432	0.151	2440	0.357	117.00	3.79	14.00	14.00	-48.24	367.88	0.002
433	0.158	2355	0.418	136.00	3.44	11.07	10.62	-48.64	370.82	0.000
434	0.165	2379	0.372	120.47	3.52	11.08	10.42	-48.08	367.38	0.001
435	0.168	2384	0.360	136.00	3.41	10.88	10.62	-48.48	373.85	0.001
436	0.174	2386	0.419	116.05	3.34	8.20	8.20	-48.31	386.41	0.003
437	0.083	2510	0.314	97.00	4.00	14.00	14.00	-48.38	331.51	0.002
438	0.162	2365	0.383	127.01	3.24	10.34	10.34	-48.82	370.80	0.006
439	0.165	2440	0.382	125.37	3.43	9.31	8.61	-51.43	373.53	0.005
440	0.188	2275	0.443	86.00	2.85	5.10	5.10	-53.18	336.34	0.005
441	0.174	2400	0.388	136.00	3.68	15.80	15.80	-48.61	376.54	0.008
442	0.180	2348	0.408	118.88	3.51	8.65	8.64	-50.86	388.36	0.005
443	0.178	2384	0.442	122.73	3.35	8.52	8.64	-51.30	378.83	0.005
444	0.185	2362	0.362	127.02	3.38	13.80	13.80	-50.68	388.04	0.005
445	0.184	2351	0.438	133.20	3.18	9.70	9.37	-50.53	372.23	0.005
446	0.128	2445	0.368	117.82	3.33	8.05	8.95	-52.04	355.83	0.005
447	0.178	2381	0.382	114.46	3.01	10.33	10.12	-51.13	374.08	0.005
448	0.184	2380	0.405	120.81	3.42	10.01	9.32	-48.48	380.61	0.005
449	0.174	2368	0.425	110.00	3.30	8.05	8.15	-48.67	354.31	0.005
450	0.179	2367	0.371	126.00	3.52	8.22	8.00	-51.11	376.04	0.005
451	0.181	2368	0.403	115.67	3.28	8.22	8.07	-50.97	378.33	0.004
452	0.180	2365	0.413	108.85	3.18	8.48	8.18	-48.52	380.18	0.004
453	0.198	2387	0.377	114.41	3.20	8.31	8.82	-47.47	380.32	0.013
454	0.180	2364	0.431	114.42	3.22	8.67	8.64	-47.82	387.01	0.012
455	0.174	2386	0.428	117.85	3.21	8.88	8.81	-48.65	384.88	0.005
456	0.178	2380	0.400	120.00	3.38	8.04	8.68	-47.67	388.80	0.005
457	0.108	2470	0.313	110.00	3.67	12.88	12.68	-48.14	394.18	0.005
458	0.173	2387	0.380	117.40	3.41	8.17	8.25	-48.80	378.00	0.005
459	0.171	2370	0.380	118.14	3.23	8.48	8.88	-47.58	371.71	0.005
460	0.178	2388	0.373	107.00	3.18	8.38	8.38	-47.71	376.54	0.005
461	0.188	2376	0.378	116.88	3.68	8.88	8.88	-48.43	378.27	0.002
462	0.188	2386	0.333	84.00	2.87	12.48	11.31	-42.61	382.88	0.008
463	0.183	2388	0.318	84.04	2.87	12.18	11.43	-38.48	388.48	0.007
464	0.188	2331	0.388	102.00	3.08	11.27	10.88	-48.67	382.12	0.005
465	0.211	2300	0.330	83.77	2.87	13.67	12.36	-48.51	348.75	0.017
466	0.178	2372	0.337	108.78	2.83	13.34	12.34	-41.10	388.77	0.012
467	0.183	2405	0.311	105.40	2.84	11.88	11.38	-42.11	382.51	0.003
468	0.184	2382	0.388	108.70	3.10	10.88	10.48	-40.72	371.88	0.018
469	0.187	2328	0.388	101.18	2.97	10.18	8.77	-41.14	371.78	0.005
470	0.188	2335	0.385	102.88	2.85	11.68	10.38	-41.43	388.88	0.021
471	0.188	2371	0.338	108.00	2.88	13.84	12.70	-41.77	348.83	0.011
472	0.178	2388	0.331	101.81	3.00	13.88	11.84	-41.38	348.61	0.014
473	0.178	2382	0.331	88.88	2.81	12.72	12.08	-40.88	348.07	0.018
474	0.172	2364	0.351	102.88	3.14	12.38	11.28	-40.28	383.88	0.018
475	0.184	2344	0.357	104.00	2.85	10.75	8.64	-38.28	381.88	0.021
476	0.178	2388	0.351	103.88	2.74	10.38	10.88	-38.78	387.78	0.004
477	0.188	2331	0.375	88.88	2.78	10.27	10.48	-37.83	382.88	0.005
478	0.344	2250	0.417	88.38	2.80	8.71	8.47	-38.54	380.78	0.022
479	0.200	2321	0.488	111.88	2.88	8.82	8.68	-38.68	372.38	0.022
480	0.221	2291	0.357	107.88	2.87	7.88	7.58	-37.67	378.54	0.005
481	0.228	2276	0.438	108.28	2.87	8.25	7.84	-37.88	373.88	0.005
482	0.243	2244	0.388	108.00	2.88	8.88	8.68	-38.88	388.78	0.005
483	0.342	2101	0.378	108.00	2.84	8.18	8.67	-38.57	387.18	0.027
484	0.388	2219	0.384	104.54	2.75	8.62	8.67	-38.42	384.21	0.021
485	0.388	2533	0.382	108.87	2.83	10.11	8.88	-38.34	388.18	0.018
486	0.388	2308	0.438	102.82	2.78	8.48	8.68	-38.18	383.23	0.018
487	0.187	2368	0.388	88.74	3.05	8.73	8.10	-38.81	344.88	0.018
488	0.107	2475	0.358	88.88	3.78	8.88	8.62	-37.11	344.82	0.002
489	0.228	2233	0.388	108.88	2.78	8.18	8.77	-38.28	348.81	0.005
490	0.344	2275	0.374	101.52	2.88	8.38	8.48	-38.41	381.47	0.005
491	0.187	2320	0.418	88.82	3.18	12.88	12.88	-38.88	344.88	0.017
492	0.351	2220	0.383	102.51	2.88	8.38	8.68	-38.64	388.47	0.018
493	0.222	2320	0.381	108.51	2.85	8.67	8.38	-38.85	387.34	0.017
494	0.233	2238	0.348	101.87	2.80	8.67	8.64	-38.27	383.37	0.022

05-07-017-07W4M										
DEPTH	PHD	DENS	PHIN	GR	PEF	LLD	LLS	SP	DTL	FFI
496	0.206	2189	0.426	102.82	2.75	9.84	9.11	-37.48	361.78	0.031
496	0.236	2246	0.360	106.60	2.88	10.39	9.43	-37.89	366.72	0.019
497	0.213	2263	0.383	98.86	2.81	11.10	11.00	-38.71	363.25	0.028
498	0.219	2276	0.385	98.86	2.70	9.81	9.13	-38.82	366.86	0.038
499	0.227	2297	0.382	103.47	3.02	9.20	8.80	-38.82	368.28	0.023
500	0.216	2318	0.361	100.88	2.87	9.71	9.28	-38.82	369.96	0.021
501	0.190	2367	0.327	102.64	3.15	11.45	10.84	-41.02	346.71	0.010
502	0.278	2190	0.417	98.86	2.70	9.88	9.04	-40.30	366.86	0.034
503	0.186	2340	0.383	106.00	2.80	9.88	9.18	-41.88	366.83	0.023
504	0.202	2323	0.398	101.82	2.87	9.78	9.11	-41.81	366.83	0.034
505	0.238	2268	0.318	108.00	2.88	8.43	8.04	-41.82	361.38	0.024
506	0.182	2363	0.410	102.07	2.80	8.80	8.20	-43.18	367.38	0.034
507	0.329	2110	0.384	98.42	2.78	8.88	8.01	-38.80	347.70	0.016
508	0.188	2313	0.312	98.42	2.78	10.80	9.40	-43.38	361.84	0.018
509	0.178	2342	0.408	108.78	2.84	8.10	8.10	-48.38	370.48	0.010
510	0.138	2408	0.371	107.18	2.88	9.10	9.10	-48.48	348.88	0.014
511	0.183	2328	0.384	108.08	2.88	8.00	8.00	-44.70	364.31	0.018
512	0.217	2270	0.438	113.11	3.04	7.88	8.80	-42.88	361.70	0.080
513	0.322	2120	0.430	107.68	2.94	8.37	8.38	-42.88	363.41	0.018
514	0.218	2382	0.408	106.48	2.82	8.18	8.13	-43.88	378.02	0.025
515	0.188	2314	0.388	118.00	3.24	10.88	10.48	-48.48	374.18	0.017
516	0.182	2380	0.438	108.08	3.40	8.82	8.78	-47.78	362.48	0.018
517	0.148	2410	0.407	117.00	3.43	10.30	10.88	-47.38	368.84	0.012
518	0.188	2348	0.408	107.88	3.18	8.88	8.14	-48.00	367.81	0.002
519	0.182	2381	0.404	108.78	3.10	8.78	8.88	-48.38	367.38	0.017
520	0.187	2361	0.378	108.38	3.23	8.88	8.82	-48.48	368.84	0.008
521	0.174	2348	0.381	113.82	3.18	8.84	8.44	-48.44	364.87	0.008
522	0.188	2380	0.418	111.40	2.97	8.08	7.88	-48.88	367.11	0.008
523	0.308	2314	0.418	131.00	3.01	4.88	4.38	-54.27	368.47	0.008
524	0.340	2288	0.808	118.88	2.88	3.84	3.84	-65.88	408.81	0.008
525	0.188	2382	0.381	108.88	2.88	8.80	8.80	-54.10	377.38	0.010
526	0.188	2388	0.382	117.21	3.18	7.21	6.87	-51.88	377.38	0.013
527	0.188	2378	0.380	104.88	2.82	8.42	8.13	-47.88	373.41	0.008
528	0.178	2382	0.438	114.37	2.87	8.38	8.31	-48.34	378.82	0.018
529	0.181	2388	0.408	118.48	2.88	7.82	7.48	-50.87	378.81	0.008
530	0.188	2378	0.388	116.44	2.88	8.48	8.48	-50.34	378.38	0.007
531	0.188	2380	0.348	104.17	3.22	10.18	9.30	-51.88	368.14	0.008
532	0.380	2382	0.478	132.88	2.81	3.78	3.37	-68.87	364.88	0.008
533	0.230	2381	0.488	132.82	2.74	3.88	3.14	-68.88	364.88	0.008
534	0.344	2344	0.438	147.88	2.88	3.14	3.88	-51.34	364.78	0.007
535	0.182	2380	0.384	101.38	2.81	9.84	8.88	-48.34	368.14	0.018
536	0.231	2388	0.381	108.08	2.81	10.88	8.88	-38.77	364.84	0.008
537	0.231	2322	0.388	98.77	2.77	11.17	10.10	-37.07	368.88	0.008
538	0.348	2180	0.388	101.88	2.88	9.78	8.88	-38.48	368.38	0.008
539	0.342	2227	0.388	108.88	2.70	9.71	8.84	-38.12	418.78	0.008
540	0.280	2380	0.314	104.88	2.88	12.00	12.00	-38.81	361.88	0.008
541	0.284	2340	0.388	98.00	2.78	8.88	8.88	-38.38	361.84	0.004
542	0.218	2348	0.348	108.88	2.78	8.17	8.00	-38.34	364.21	0.004
543	0.211	2348	0.388	98.81	2.78	10.38	8.88	-38.38	364.44	0.001
544	0.212	2340	0.388	108.88	2.88	10.18	8.77	-38.77	368.88	0.008
545	0.284	2318	0.378	108.81	2.82	9.88	9.78	-38.78	368.18	0.004
546	0.304	2388	0.418	108.07	2.83	10.88	8.84	-38.78	368.88	0.018
547	0.187	2388	0.388	108.82	2.87	10.88	10.88	-38.31	367.88	0.008
548	0.280	2322	0.418	108.81	3.08	10.84	10.38	-37.38	364.18	0.008
549	0.217	2388	0.388	108.07	3.08	10.78	10.38	-37.84	368.88	0.008
550	0.270	2388	0.487	108.27	2.78	10.87	8.88	-37.88	368.88	0.008
551	0.184	2388	0.378	108.38	3.04	10.17	8.88	-38.78	378.14	0.008
552	0.238	2380	0.384	104.81	2.84	9.88	8.43	-38.10	364.48	0.008
553	0.231	2388	0.488	98.88	2.88	8.88	8.88	-38.48	368.18	0.008
554	0.248	2344	0.377	101.41	3.38	8.48	8.87	-37.81	377.88	0.008
555	0.288	2380	0.382	108.88	2.88	8.47	8.17	-38.87	378.88	0.008
556	0.288	2388	0.388	108.88	2.81	9.78	9.47	-37.88	368.38	0.008
557	0.188	2318	0.381	108.31	2.81	8.88	8.78	-38.88	372.84	0.008
558	0.280	2381	0.414	138.88	2.88	8.47	8.38	-41.18	368.88	0.008
559	0.188	2381	0.388	108.41	2.88	8.88	8.88	-38.78	378.48	0.008
560	0.080	2380	0.388	78.88	4.12	22.22	20.88	-38.78	368.38	0.008

05-07-017-07W4M										
DEPTH	PHID	DENS	PHIN	GR	PEF	LLD	LLS	SP	DTL	FFI
561	0.180	2355	0.401	105.90	2.88	9.15	9.08	-38.82	373.32	-688.000
562	0.187	2400	0.404	127.00	2.93	8.75	9.03	-42.11	370.11	-688.000
563	0.184	2330	0.398	115.04	2.87	9.88	9.81	-40.11	374.78	-688.000
564	0.182	2370	0.420	111.38	2.92	9.78	9.83	-38.85	371.23	-688.000
565	0.180	2350	0.387	107.18	2.72	10.38	9.90	-38.48	367.91	-688.000
566	0.220	2261	0.348	108.13	2.84	10.88	10.22	-38.27	364.14	-688.000
567	0.267	2225	0.360	104.82	2.89	10.62	10.21	-38.40	360.18	-688.000
568	0.185	2373	0.404	102.71	2.84	11.08	10.87	-38.80	363.15	-688.000
569	0.184	2334	0.398	105.93	2.88	10.33	10.14	-38.83	366.40	-688.000
570	0.184	2348	0.398	108.44	2.88	10.18	10.07	-38.83	368.43	-688.000
571	0.179	2364	0.421	108.88	2.82	10.08	9.88	-40.17	368.84	-688.000
572	0.217	2301	0.429	105.48	2.88	10.27	10.11	-38.88	368.34	-688.000
573	0.188	2378	0.408	118.00	2.88	10.82	10.88	-38.82	368.76	-688.000
574	0.180	2383	0.381	111.83	2.79	11.00	10.88	-38.80	363.38	-688.000
575	0.185	2378	0.435	104.91	2.85	10.30	10.08	-40.00	366.27	-688.000
576	0.179	2385	0.389	114.00	3.05	10.83	10.48	-38.87	368.51	-688.000
577	0.188	2388	0.430	104.00	3.01	10.10	10.07	-38.44	368.48	-688.000
578	0.175	2361	0.380	121.30	2.88	9.80	10.14	-38.30	373.91	-688.000
579	0.173	2383	0.407	111.18	2.90	10.00	9.87	-38.88	367.66	-688.000
580	0.141	2408	0.408	120.04	3.13	11.11	10.82	-37.88	368.40	-688.000
581	0.183	2382	0.380	107.00	2.87	10.00	9.82	-38.88	368.54	-688.000
582	0.171	2387	0.382	122.00	2.88	9.87	9.72	-38.30	371.14	-688.000
583	0.188	2330	0.340	104.78	2.88	10.04	9.78	-38.84	363.86	-688.000
584	0.202	2388	0.401	118.00	2.88	9.82	9.82	-38.47	372.88	-688.000
585	0.285	2247	0.441	107.72	2.84	9.71	9.31	-37.48	368.47	-688.000
586	0.188	2321	0.387	108.90	3.10	9.70	9.31	-38.83	368.38	-688.000
587	0.214	2273	0.388	117.78	2.88	8.80	8.88	-38.40	375.73	-688.000
588	0.223	2234	0.388	118.38	3.08	8.01	7.88	-38.88	360.88	-688.000
589	0.247	2244	0.387	108.38	2.88	12.80	12.80	-34.80	368.72	-688.000
590	0.232	2290	0.381	108.74	2.72	10.80	10.80	-34.88	361.88	-688.000
591	0.107	2470	0.383	82.00	2.78	14.80	13.80	-38.02	368.82	-688.000
592	0.300	2184	0.401	108.47	2.80	9.80	9.88	-38.88	368.84	-688.000
593	0.341	2288	0.387	117.88	2.88	9.88	8.72	-38.48	367.54	-688.000
594	0.341	2275	0.372	108.38	2.88	10.41	9.82	-38.07	361.76	-688.000
595	0.218	2288	0.343	108.88	2.77	10.82	9.18	-38.31	364.67	-688.000
596	0.188	2380	0.382	114.00	2.88	10.82	9.43	-38.88	368.84	-688.000
597	0.244	2180	0.388	88.00	2.88	10.10	9.41	-38.02	368.38	-688.000
598	0.238	2330	0.344	108.34	2.88	10.88	10.12	-38.82	368.27	-688.000
599	0.308	2380	0.381	118.00	2.88	10.88	10.11	-38.48	378.88	-688.000
600	0.232	2381	0.388	111.88	2.71	9.78	9.31	-38.18	368.76	-688.000
601	0.238	2338	0.372	118.00	2.78	8.48	7.81	-37.88	343.42	-688.000
602	0.212	2234	0.402	124.00	2.80	8.80	8.34	-38.18	368.88	-688.000
603	0.210	2308	0.378	107.82	2.82	8.30	7.88	-38.72	368.12	-688.000
604	0.238	2388	0.388	108.88	2.82	9.81	8.48	-38.81	348.88	-688.000
605	0.188	2348	0.348	97.38	2.81	10.12	8.97	-38.88	362.88	-688.000
606	0.188	2380	0.380	102.78	2.81	10.88	9.81	-38.88	361.30	-688.000
607	0.188	2332	0.388	102.87	2.81	10.81	9.48	-38.08	368.88	-688.000
608	0.223	2270	0.388	104.81	2.88	9.88	9.78	-38.88	377.88	-688.000
609	0.213	2288	0.380	104.78	2.88	8.78	8.17	-38.88	368.78	-688.000
610	0.228	2301	0.388	100.82	2.78	8.71	8.43	-38.88	347.88	-688.000
611	0.264	2237	0.384	107.38	2.88	8.88	8.88	-38.78	368.38	-688.000
612	0.223	2300	0.388	107.43	2.80	8.84	8.87	-38.82	362.82	-688.000
613	0.236	2267	0.408	108.88	2.78	8.88	8.78	-38.81	368.88	-688.000
614	0.232	2381	0.374	111.88	2.78	8.88	8.88	-38.78	368.88	-688.000
615	0.218	2380	0.410	108.87	2.78	8.88	8.80	-37.48	368.11	-688.000
616	0.232	2321	0.388	108.88	2.88	8.88	8.78	-38.78	368.88	-688.000
617	0.232	2347	0.408	108.38	2.84	8.48	8.88	-40.88	371.88	-688.000
618	0.230	2261	0.388	108.88	2.88	8.84	8.48	-41.48	374.78	-688.000
619	0.238	2338	0.384	110.84	2.88	8.31	8.48	-42.82	378.81	-688.000
620	0.237	2381	0.380	102.42	2.48	8.30	8.31	-43.80	377.88	-688.000
621	0.218	2382	0.408	108.88	2.88	8.87	8.84	-44.84	373.48	-688.000
622	0.188	2388	0.384	104.48	2.87	8.78	8.81	-44.88	368.84	-688.000
623	0.188	2378	0.408	117.40	2.77	8.88	8.18	-48.30	368.48	-688.000
624	0.188	2382	0.430	113.88	2.88	7.87	8.41	-51.14	368.88	-688.000
625	0.188	2380	0.438	121.17	2.88	7.88	7.87	-51.78	368.87	-688.000
626	0.181	2348	0.441	118.88	3.08	7.88	7.88	-53.81	367.14	-688.000

03-07-017-07W4M										
DEPTH	PHD	DENS	PHIN	GR	PEF	LLD	LLS	SP	DTL	FFI
627	0.186	2336	0.483	116.78	2.82	6.80	6.81	-34.03	389.82	-888.000
628	0.186	2340	0.486	114.38	3.14	6.87	6.23	-34.44	381.34	-888.000
629	0.186	2338	0.427	111.88	2.87	6.48	6.86	-33.88	380.11	-888.000
630	0.186	2326	0.425	119.26	3.20	6.07	6.08	-34.27	388.80	-888.000
631	0.200	2324	0.482	117.44	3.01	6.88	6.88	-34.51	386.97	0.018
632	0.184	2322	0.423	111.46	3.08	6.73	6.83	-33.83	383.81	0.018
633	0.207	2318	0.422	119.78	3.03	6.34	6.30	-34.21	379.86	0.018
634	0.188	2338	0.401	112.10	3.04	6.84	6.10	-33.88	378.11	0.018
635	0.201	2318	0.436	117.33	2.91	6.10	6.04	-33.74	377.01	0.018
636	0.210	2283	0.411	160.12	3.02	4.80	4.80	-34.48	373.80	0.017
637	0.277	2200	0.388	100.20	3.81	13.18	12.43	-31.84	342.38	0.018
638	0.222	2370	0.388	84.00	4.80	18.17	17.88	-38.88	311.81	0.018
639	0.217	2338	0.344	88.00	3.80	14.88	15.18	-38.88	328.10	0.012
640	0.448	1830	0.348	208.00	1.80	2.80	1.80	-32.41	400.18	0.014
641	0.210	2344	0.388	102.80	3.70	14.80	14.80	-37.77	388.48	0.000
642	0.183	2382	0.348	79.78	2.91	18.30	18.61	-41.28	322.30	0.008
643	0.173	2330	0.388	88.88	3.80	20.38	19.88	-40.88	308.38	0.044
644	0.147	2470	0.291	108.80	2.78	14.88	14.38	-40.88	381.78	0.084
645	0.134	2428	0.322	122.80	3.13	12.34	11.88	-42.88	381.30	0.013
646	0.137	2428	0.338	88.00	2.88	11.47	11.38	-42.78	342.84	0.014
647	0.188	2388	0.341	100.88	2.88	11.88	10.81	-42.71	381.88	0.014
648	0.148	2407	0.388	118.38	3.22	8.88	6.71	-41.71	388.48	0.012
649	0.188	2380	0.438	138.31	3.18	8.87	8.84	-41.84	388.82	0.088
650	0.188	2377	0.384	138.80	3.34	8.81	8.82	-42.18	378.38	0.044
651	0.180	2401	0.388	108.88	3.12	10.88	10.88	-41.88	381.84	0.018
652	0.182	2418	0.378	110.27	3.34	10.17	8.88	-41.88	388.11	0.088
653	0.148	2407	0.388	117.10	3.38	10.88	10.88	-42.88	388.81	0.018
654	0.138	2438	0.388	108.88	3.47	10.81	10.87	-41.84	347.88	0.018
655	0.188	2388	0.371	100.88	3.30	8.78	8.88	-41.88	381.88	0.088
656	0.148	2421	0.408	112.78	3.42	8.22	8.30	-48.88	387.84	0.044
657	0.128	2430	0.373	118.88	3.88	8.47	8.18	-44.38	388.72	0.088
658	0.138	2438	0.374	141.88	4.88	12.88	12.88	-44.77	381.38	0.018
659	0.137	2418	0.402	118.84	3.88	8.88	8.30	-44.88	378.12	0.088
660	0.188	2382	0.438	119.14	3.48	8.88	8.88	-48.88	378.88	0.088
661	0.182	2388	0.427	127.12	3.87	8.81	8.78	-47.88	378.88	0.018
662	0.187	2378	0.438	138.88	3.72	8.82	8.80	-47.88	388.10	0.017
663	0.184	2387	0.438	122.81	4.01	8.73	8.88	-48.88	381.88	0.018
664	0.187	2373	0.438	142.88	3.82	12.88	12.88	-47.77	377.88	0.018
665	0.172	2387	0.427	134.88	4.38	8.88	8.88	-48.48	388.18	0.018
666	0.177	2382	0.488	131.88	3.88	8.88	8.38	-48.77	388.88	0.018
667	0.188	2381	0.388	148.88	3.88	8.14	8.48	-48.88	372.84	0.018
668	0.181	2384	0.388	131.88	3.47	8.87	8.48	-48.81	378.88	0.014
669	0.188	2388	0.417	143.38	3.47	8.84	8.38	-48.78	388.81	0.012
670	0.188	2388	0.437	148.38	3.78	8.88	10.38	-48.48	388.27	0.088
671	0.188	2382	0.448	148.78	3.88	10.48	11.88	-48.84	378.88	0.088
672	0.188	2388	0.427	138.88	3.88	10.47	11.17	-48.88	388.81	0.088
673	0.138	2448	0.388	131.48	3.44	10.78	11.84	-44.81	387.14	0.088
674	0.147	2430	0.388	148.78	3.88	8.81	10.88	-48.88	387.18	0.018
675	0.140	2380	0.388	188.88	2.88	4.88	4.88	-34.81	378.81	0.018
676	0.188	2388	0.488	181.88	3.81	8.11	8.88	-44.88	378.88	0.088
677	0.188	2388	0.488	172.88	3.48	8.88	8.81	-48.78	378.87	0.088
678	0.184	2388	0.488	141.88	3.37	8.88	7.18	-48.84	388.48	0.088
679	0.184	2388	0.488	118.78	2.97	8.88	8.88	-48.88	388.88	0.088
680	0.148	2422	0.381	111.88	3.88	8.88	8.88	-48.87	384.14	0.088
681	0.078	2388	0.311	187.88	3.88	8.88	8.88	-47.78	388.88	0.018
682	0.342	2380	0.488	138.88	2.88	3.88	3.88	-37.44	388.14	0.011
683	0.182	2384	0.487	138.88	2.88	3.42	3.42	-37.81	388.18	0.018
684	0.178	2384	0.478	132.82	2.88	3.38	3.48	-38.48	481.38	0.088
685	0.188	2384	0.447	127.11	3.88	3.38	3.48	-37.84	481.44	0.088
686	0.188	2383	0.478	131.38	2.91	3.88	3.48	-38.88	488.48	0.011
687	0.384	2388	0.388	137.88	2.81	3.38	3.38	-37.48	488.84	0.018
688	0.148	2410	0.388	118.88	3.88	8.78	8.78	-48.48	388.88	0.018
689	0.347	2388	0.488	188.88	2.87	3.88	4.27	-44.88	388.88	0.011
690	0.178	2388	0.388	138.32	3.88	8.88	8.88	-38.71	388.88	0.018
691	0.188	2382	0.388	121.34	2.88	8.88	8.48	-38.78	388.84	0.088
692	0.181	2387	0.371	118.88	2.78	7.88	7.88	-34.87	388.48	0.087

05-07-017-07W4M										
DEPTH	PHID	DENS	PHIN	GR	PEF	LLD	LLS	SP	DTL	FFI
693	0.253	2240	0.466	182.00	2.81	2.80	2.80	-53.15	318.77	0.008
694	0.163	2362	0.312	109.00	2.81	9.10	9.10	-53.44	327.50	0.008
695	0.236	2260	0.462	156.00	2.57	3.20	3.20	-53.67	333.67	0.011
696	0.170	2365	0.300	103.92	2.82	12.00	12.00	-51.84	321.42	0.008
697	0.244	2250	0.500	183.00	2.46	3.00	3.00	-53.23	336.20	0.008
698	0.174	2363	0.330	146.67	2.67	12.00	12.00	-51.80	330.66	0.008
699	0.177	2361	0.338	144.01	2.66	6.88	6.77	-53.11	331.72	0.008
700	0.178	2364	0.330	168.00	2.98	10.71	10.73	-52.40	342.80	0.008
701	0.178	2362	0.362	162.00	3.12	7.00	7.00	-52.38	338.66	0.008
702	0.180	2360	0.338	127.00	3.35	10.15	9.93	-52.78	340.41	0.010
703	0.181	2346	0.466	167.00	3.32	5.98	6.52	-56.60	375.98	0.007
704	0.189	2325	0.428	140.62	2.98	4.01	4.19	-56.40	376.64	0.008
705	0.170	2377	0.388	96.00	2.94	4.66	4.98	-56.92	386.64	0.010
706	0.166	2372	0.412	115.36	3.11	5.30	5.30	-56.68	373.48	0.010
707	0.178	2363	0.388	100.38	2.97	3.91	3.91	-57.35	380.66	0.010
708	0.168	2367	0.418	101.83	3.01	3.80	3.82	-57.00	384.68	0.010
709	0.163	2369	0.414	104.01	2.81	3.84	3.88	-56.88	382.13	0.011
710	0.170	2364	0.442	106.54	2.81	4.66	3.97	-56.72	381.23	-999.000
711	0.178	2367	0.361	113.36	2.96	4.34	4.38	-54.88	370.68	-999.000
712	0.141	3420	0.388	108.88	2.86	4.38	4.51	-56.62	388.62	-999.000
713	0.181	3408	0.383	96.62	2.96	6.00	6.00	-56.68	386.68	-999.000
714	0.180	3404	0.388	101.20	3.00	4.73	4.84	-56.68	387.70	-999.000
715	0.187	2397	0.388	97.10	2.72	4.80	4.96	-56.68	386.64	-999.000
716	0.117	3475	0.388	98.30	2.86	3.92	3.96	-56.47	386.30	-999.000
717	0.181	3415	0.367	100.14	2.78	4.17	4.19	-56.39	370.68	-999.000
718	0.180	3408	0.373	102.88	2.64	4.38	4.63	-56.37	388.68	-999.000
719	0.180	2347	0.318	98.78	3.16	5.90	5.90	-54.88	347.27	-999.000
720	0.147	3436	0.388	96.00	2.76	4.88	4.84	-54.36	381.68	-999.000
721	0.180	2368	0.388	108.88	2.84	4.12	4.38	-56.14	376.37	-999.000
722	0.171	2372	0.408	104.88	2.72	4.38	4.32	-55.88	382.31	-999.000
723	0.177	2368	0.388	108.41	2.88	5.00	5.00	-54.18	383.18	-999.000
724	0.182	2362	0.374	100.38	2.88	4.38	4.38	-54.78	382.62	-999.000
725	0.108	3467	0.361	96.00	3.80	4.48	4.82	-54.96	388.64	-999.000
726	0.163	2363	0.416	114.00	2.88	3.88	4.13	-56.18	373.62	-999.000
727	0.238	2260	0.467	136.00	2.80	2.80	2.80	-54.48	388.68	-999.000
728	0.080	3600	0.388	102.88	3.76	3.98	3.92	-53.62	376.62	-999.000
729	0.308	2360	0.478	116.70	2.88	3.48	3.51	-53.68	383.13	-999.000
730	0.178	2367	0.378	118.88	2.94	3.48	3.88	-56.48	384.18	-999.000
731	0.180	2363	0.367	121.51	2.88	3.62	3.78	-56.38	382.38	-999.000
732	0.188	2363	0.401	113.63	2.90	3.88	3.90	-56.10	380.48	-999.000
733	0.077	3625	0.413	108.00	3.76	5.00	5.00	-54.71	348.62	-999.000
734	0.183	3403	0.407	110.64	2.73	4.48	4.78	-54.38	382.34	-999.000
735	0.171	2371	0.414	122.00	3.00	4.30	4.41	-56.68	388.68	-999.000
736	0.080	3600	0.388	96.00	3.68	4.64	4.74	-56.32	347.51	-999.000
737	0.148	3407	0.378	113.00	2.98	4.11	4.38	-56.68	371.14	-999.000
738	0.163	2367	0.348	96.00	2.88	4.62	4.27	-54.37	378.62	-999.000
739	0.182	3405	0.388	108.47	2.92	4.38	4.71	-54.68	386.64	-999.000
740	0.184	2366	0.378	101.30	2.76	4.88	4.84	-54.11	382.38	0.008
741	0.084	3485	0.378	97.88	3.13	4.51	4.38	-56.62	371.78	0.008
742	0.174	2369	0.418	106.88	2.80	3.97	3.78	-56.61	386.67	0.008
743	0.178	2363	0.408	97.34	2.88	3.48	3.88	-56.68	384.38	0.008
744	0.188	2365	0.388	101.38	3.18	3.88	3.91	-56.27	384.38	0.011
745	0.088	3485	0.384	94.64	3.80	6.38	6.38	-56.48	314.78	0.008
746	0.178	2363	0.310	98.44	2.88	5.88	5.88	-56.18	384.38	0.010
747	0.181	2367	0.388	96.11	2.88	6.38	6.32	-51.38	341.11	0.010
748	0.178	2363	0.348	100.38	2.81	4.64	4.78	-56.62	386.68	0.011
749	0.180	2362	0.348	100.40	2.80	4.87	4.97	-51.82	381.88	0.011
750	0.172	2368	0.327	90.60	2.81	5.38	5.32	-53.18	348.38	0.013
751	0.177	2363	0.311	94.88	2.77	6.17	6.38	-56.78	386.13	0.011
752	0.178	2364	0.388	96.18	2.88	5.38	5.30	-56.38	381.47	0.012
753	0.108	3461	0.348	92.38	3.32	5.11	5.38	-52.38	382.27	0.016
754	0.171	2370	0.348	96.88	2.94	5.07	5.16	-51.38	348.38	0.018
755	0.188	2365	0.342	106.88	2.72	4.88	5.18	-52.68	386.38	0.012
756	0.174	2363	0.348	94.88	2.71	4.88	5.88	-52.38	384.68	0.012
757	0.167	2364	0.414	108.88	2.88	4.41	4.88	-52.68	382.42	0.012
758	0.188	2404	0.384	108.00	3.10	4.43	4.48	-51.88	381.88	0.011

05-07-017-07W4M										
DEPTH	PHD	DENS	PHN	GR	PEF	LLD	LLS	SP	DTL	FFI
759	0.164	2383	0.374	81.00	2.72	4.88	5.30	-50.30	337.74	0.018
760	0.177	2360	0.285	98.11	2.83	7.00	7.00	-47.67	327.88	0.036
761	0.100	2460	0.373	120.00	3.70	5.30	5.30	-47.48	302.08	0.013
762	0.150	2413	0.316	104.72	2.77	7.80	7.80	-44.93	314.20	0.011
763	0.142	2425	0.281	98.40	2.53	9.20	9.11	-43.54	296.84	0.008
764	0.132	2431	0.251	104.88	2.80	8.90	9.17	-41.88	303.86	0.032
765	0.165	2380	0.288	98.18	2.80	8.77	8.98	-38.68	307.32	0.016
766	0.073	2525	0.301	82.42	2.92	9.19	9.19	-38.81	306.11	0.010
767	0.138	2410	0.307	87.00	2.80	8.94	9.15	-38.43	308.28	0.010
768	0.128	2437	0.285	93.83	2.72	9.11	9.38	-33.10	298.84	0.007
769	0.128	2460	0.288	84.48	2.48	9.51	9.85	-30.37	298.28	0.008
770	0.168	2368	0.285	77.00	2.48	8.81	9.38	-28.23	296.53	0.040
771	0.138	2428	0.280	90.00	2.51	11.17	11.80	-28.04	291.80	0.012
772	0.178	2363	0.211	77.84	2.88	17.82	17.31	-18.38	284.88	0.087
773	0.322	2130	0.181	88.78	2.28	34.00	28.00	-14.13	283.80	0.148
774	0.288	2182	0.225	84.78	2.18	18.48	12.82	-18.88	276.40	0.181
775	0.288	2205	0.288	88.08	2.34	7.48	8.80	-14.80	248.08	0.188
776	0.271	2257	0.312	87.84	2.32	6.31	8.48	-18.91	288.84	0.178
777	0.261	2220	0.308	88.18	2.45	6.42	8.22	-18.87	328.88	0.188
778	0.288	2224	0.300	73.88	2.25	6.85	8.77	-30.34	283.84	0.188
779	0.218	2283	0.302	78.47	2.41	7.38	6.23	-32.31	317.48	0.138
780	0.248	2248	0.312	73.88	2.25	7.28	6.27	-38.85	316.18	0.138
781	0.213	2288	0.307	80.25	2.40	7.70	7.00	-38.47	314.48	0.180
782	0.232	2285	0.300	78.88	2.25	8.22	7.31	-31.31	288.83	0.112
783	0.173	2267	0.288	81.28	2.58	8.77	8.31	-38.88	303.17	0.044
784	0.178	2287	0.302	84.87	2.78	8.84	8.27	-42.85	304.28	0.087
785	0.148	2413	0.308	88.80	2.83	8.80	8.34	-47.88	302.48	0.088
786	0.138	2438	0.308	87.80	2.78	7.28	7.13	-31.41	288.28	0.088
787	0.168	2384	0.308	101.82	2.73	8.88	8.88	-38.88	313.88	0.088
788	0.188	2388	0.308	88.78	2.81	8.87	8.78	-48.17	288.88	0.084
789	0.178	2380	0.302	88.78	2.81	7.27	7.28	-38.88	308.28	0.081
790	0.160	2287	0.284	88.88	2.88	8.78	8.48	-31.28	312.77	0.014
791	0.161	2288	0.318	84.28	2.74	8.88	8.81	-38.43	318.47	0.070
792	0.142	2418	0.307	100.87	2.80	8.78	8.88	-44.38	281.88	0.088
793	0.184	2408	0.313	88.17	2.77	8.73	8.88	-32.77	318.77	0.088
794	0.188	2418	0.308	88.88	2.78	8.88	8.28	-31.48	288.88	0.088
795	0.228	2278	0.438	120.00	2.72	2.80	2.80	-51.80	282.88	0.088
796	0.188	2388	0.308	88.88	2.88	8.40	8.40	-48.88	308.81	0.087
797	0.188	2408	0.317	88.88	2.72	4.88	4.88	-31.88	281.84	0.087
798	0.180	2388	0.308	108.84	2.73	4.88	4.84	-31.88	288.88	0.088
799	0.184	2408	0.308	88.88	2.83	4.82	4.78	-31.88	287.71	0.088
800	0.160	2388	0.304	108.48	2.83	4.78	4.87	-48.88	241.78	0.087
801	0.182	2388	0.308	108.34	2.78	4.41	4.28	-48.88	280.88	0.070
802	0.208	2311	0.318	88.88	2.81	8.88	8.88	-38.42	288.88	0.118
803	0.208	2218	0.318	88.88	2.88	8.22	8.88	-38.84	288.31	0.187
804	0.227	2283	0.288	78.81	2.88	8.81	8.88	-38.88	312.88	0.088
805	0.178	2384	0.302	81.28	2.78	8.40	7.88	-38.28	304.28	0.088
806	0.181	2381	0.302	88.88	2.88	8.27	7.78	-48.44	288.48	0.078
807	0.188	2388	0.308	78.88	2.88	8.14	7.88	-38.88	288.48	0.088
808	0.188	2402	0.308	88.88	2.88	8.88	8.88	-38.18	288.28	0.088
809	0.218	2388	0.308	84.88	2.88	8.88	8.44	-31.81	314.11	0.088
810	0.228	2388	0.317	72.28	2.88	8.28	8.48	-38.88	318.18	0.088
811	0.088	2488	0.317	77.84	3.40	12.88	12.88	-38.12	288.28	0.040
812	0.180	2347	0.302	78.78	2.87	8.28	8.01	-41.17	288.88	0.088
813	0.180	2388	0.308	84.87	2.81	8.88	7.88	-48.88	282.43	0.047
814	0.184	2388	0.308	87.88	2.78	7.27	7.28	-44.28	288.27	0.078
815	0.188	2388	0.312	88.48	2.88	7.88	7.88	-48.78	288.28	0.074
816	0.132	2408	0.308	84.84	2.78	8.32	8.87	-48.78	318.28	0.078
817	0.218	2388	0.302	88.78	2.48	8.88	8.78	-38.88	318.22	0.084
818	0.188	2380	0.278	78.87	2.88	7.28	8.88	-48.28	288.24	0.088
819	0.184	2408	0.307	81.88	2.88	7.88	7.88	-48.87	288.18	0.088
820	0.148	2481	0.302	82.84	2.78	8.72	8.28	-38.78	288.88	0.088
821	0.138	2488	0.302	81.87	2.87	4.78	4.88	-38.48	287.28	0.071
822	0.148	2418	0.308	108.88	2.88	4.44	4.28	-38.88	288.48	0.078
823	0.144	2413	0.302	88.41	2.74	4.88	4.81	-38.18	241.88	0.072
824	0.188	2400	0.301	101.88	2.78	3.87	3.88	-44.28	288.24	0.078

05-07-017-07W4M										
DEPTH	PHD	DENS	PHN	GR	PEF	LLD	LLS	SP	DTL	FFI
825	0.153	2360	0.361	86.00	2.81	3.78	3.81	-54.65	361.35	0.014
826	0.153	2365	0.346	83.20	2.86	3.57	3.57	-54.14	367.53	0.014
827	0.151	2366	0.401	89.32	2.89	3.29	3.29	-55.07	365.11	0.012
828	0.168	2377	0.364	86.00	2.84	3.25	3.21	-54.28	362.82	0.010
829	0.175	2367	0.258	78.16	2.86	5.50	5.50	-51.07	343.56	0.040
830	0.235	2260	0.480	100.15	2.78	2.10	2.10	-52.21	400.46	0.023
831	0.197	2322	0.470	108.28	2.83	2.52	2.51	-51.70	366.33	0.019
832	0.147	2407	0.363	100.32	2.86	3.34	3.48	-52.71	369.60	0.010
833	0.153	2366	0.362	105.58	3.04	2.88	3.07	-52.09	373.48	0.010
834	0.189	2363	0.363	110.78	2.87	2.63	2.86	-50.53	362.33	0.018
835	0.175	2367	0.474	102.03	3.05	2.71	2.87	-49.84	363.12	0.034
836	0.141	2408	0.364	86.00	2.72	4.24	4.70	-48.77	334.97	0.023
837	0.077	2520	0.268	63.20	3.28	7.50	7.50	-43.43	305.50	0.033
838	0.189	2340	0.368	77.16	2.84	6.51	6.31	-38.48	318.48	0.048
839	0.211	2305	0.313	61.00	2.80	6.00	5.89	-32.38	365.62	0.166
840	0.239	2255	0.309	61.01	2.82	4.83	4.80	-44.12	333.78	0.080
841	0.164	2385	0.408	97.17	2.86	3.16	3.10	-50.48	363.56	0.030
842	0.189	2350	0.454	91.54	2.89	3.09	3.08	-49.86	360.79	0.028
843	0.182	2367	0.423	80.00	3.07	2.88	2.70	-52.80	365.18	0.010
844	0.209	2230	0.308	84.73	3.00	2.10	2.10	-50.08	406.43	0.081
845	0.170	2380	0.436	88.27	3.05	2.63	2.88	-52.02	364.86	0.013
846	0.188	2317	0.438	88.78	2.86	2.86	2.86	-50.68	368.68	0.041
847	0.188	2338	0.412	100.72	2.80	2.71	2.73	-50.44	362.86	0.034
848	0.185	2355	0.404	97.43	2.67	2.76	2.88	-49.84	361.70	0.036
849	0.164	2400	0.433	88.38	2.88	3.08	3.22	-50.77	370.74	0.013
850	0.129	2445	0.385	101.07	3.12	3.80	3.82	-50.48	360.62	0.015
851	0.163	2398	0.398	82.00	2.80	4.22	4.36	-49.60	344.53	0.086
852	0.188	2304	0.379	100.30	2.87	3.61	3.78	-49.88	362.78	0.018
853	0.167	2374	0.440	88.80	2.80	3.15	3.18	-49.89	365.89	0.034
854	0.088	2488	0.334	88.70	3.40	2.97	3.30	-48.82	373.78	0.023
855	0.205	2333	0.435	100.09	2.87	2.80	3.01	-48.80	378.33	0.025
856	0.180	2351	0.385	101.38	2.89	2.64	2.64	-48.71	365.78	0.035
857	0.185	2350	0.372	84.89	2.84	2.84	2.82	-50.00	377.55	0.030
858	0.176	2390	0.438	82.89	2.82	2.83	2.87	-50.88	375.82	0.014
859	0.208	2334	0.419	97.88	2.78	2.67	2.88	-50.48	379.60	0.012
860	0.188	2350	0.388	97.82	2.77	3.00	3.00	-50.63	367.48	0.030
861	0.222	2300	0.448	88.88	2.83	2.30	2.30	-50.88	374.80	0.038
862	0.161	2385	0.351	87.31	2.80	3.00	3.00	-52.11	365.83	0.007
863	0.174	2373	0.484	78.89	2.88	2.30	2.30	-52.22	375.61	0.019
864	0.207	2216	0.487	83.48	3.01	2.73	2.67	-48.34	378.18	0.011
865	0.173	2333	0.382	82.38	2.77	3.80	3.80	-47.28	341.57	0.011
866	0.181	2360	0.351	82.49	2.72	2.83	2.87	-48.30	374.88	0.011
867	0.174	2348	0.417	101.17	3.07	2.80	2.80	-48.02	368.38	0.015
868	0.176	2361	0.394	83.38	2.82	5.98	6.08	-38.80	389.93	0.051
869	0.161	2364	0.277	62.00	2.57	6.48	6.39	-34.79	314.48	0.051
870	0.141	2415	0.267	61.54	2.81	7.97	7.97	-33.82	310.19	0.013
871	0.210	2358	0.380	86.00	2.43	7.83	7.70	-38.27	363.80	0.082
872	0.130	2488	0.344	70.80	3.25	7.30	7.35	-38.60	389.64	0.038
873	0.130	2423	0.330	84.00	2.82	5.70	5.84	-40.08	318.53	0.030
874	0.134	2438	0.408	128.00	2.72	3.88	3.88	-43.48	354.86	0.035
875	0.189	2364	0.378	88.00	2.38	7.80	7.80	-32.00	385.01	0.048
876	0.131	2488	0.382	114.00	4.45	4.80	4.84	-44.88	388.53	0.039
877	0.131	2434	0.382	122.00	2.85	2.80	2.80	-43.61	380.78	0.010

06-35-017-00W4M										
DEPTH	PHD	DENS	PHN	GR	PEF	LLD	LLS	SP	DTL	FFI
193	0.242	2264	0.484	70.26	2.86	3.56	3.41	-38.24	438.66	-888.000
194	0.252	2253	0.404	64.51	2.85	5.51	4.86	-27.71	432.37	-888.000
195	0.226	2311	0.376	67.36	2.82	7.36	6.34	-23.60	385.71	-888.000
196	0.240	2248	0.386	69.83	2.72	7.83	6.53	-24.31	380.24	-888.000
197	0.226	2277	0.382	63.76	2.72	7.33	5.97	-25.14	384.36	-888.000
198	0.224	2262	0.400	66.36	2.82	7.84	5.78	-25.29	380.57	-888.000
199	0.238	2256	0.421	70.04	2.83	6.80	5.74	-26.73	406.87	-888.000
200	0.251	2237	0.480	70.70	2.85	6.72	5.79	-25.80	406.87	-888.000
201	0.238	2280	0.481	77.16	2.87	3.32	3.23	-29.88	486.38	-888.000
202	0.212	2286	0.483	63.88	3.26	4.14	3.88	-29.88	442.91	-888.000
203	0.180	2303	0.386	67.64	3.46	20.88	18.28	-27.10	387.88	-888.000
204	0.023	2630	0.136	28.00	4.20	40.00	40.00	-29.36	284.00	-888.000
205	0.223	2266	0.386	62.82	2.86	6.57	7.76	-25.87	373.77	-888.000
206	0.234	2283	0.419	57.44	2.83	7.82	6.84	-24.72	371.72	-888.000
207	0.228	2247	0.414	63.86	2.88	7.11	5.88	-22.88	387.40	-888.000
208	0.236	2276	0.431	72.88	2.70	5.97	4.37	-25.88	413.57	-888.000
209	0.238	2263	0.436	70.57	3.04	7.84	5.97	-26.12	400.56	-888.000
210	0.216	2298	0.378	70.97	2.76	6.86	5.31	-26.76	406.83	-888.000
211	0.214	2268	0.402	60.67	2.84	6.30	5.06	-24.73	404.35	-888.000
212	0.222	2267	0.438	68.88	2.83	5.51	4.46	-26.86	416.14	-888.000
213	0.236	2262	0.488	70.33	3.12	4.98	4.07	-27.40	438.38	-888.000
214	0.264	2200	0.482	68.84	2.72	3.06	2.80	-28.02	488.00	-888.000
215	0.180	2406	0.372	61.78	3.86	6.38	5.08	-23.88	386.00	-888.000
216	0.231	2276	0.436	68.36	2.86	6.46	5.14	-21.76	416.83	-888.000
217	0.238	2251	0.400	68.67	2.80	6.84	5.30	-18.82	381.26	-888.000
218	0.232	2268	0.418	68.88	2.73	6.42	5.17	-20.16	401.80	-888.000
219	0.246	2229	0.431	70.01	2.86	6.23	5.14	-20.82	416.18	-888.000
220	0.264	2218	0.401	63.61	2.74	6.86	5.80	-18.47	370.80	-888.000
221	0.263	2220	0.388	67.61	2.88	6.83	5.57	-18.30	383.41	-888.000
222	0.241	2254	0.471	68.31	3.13	4.42	3.78	-23.70	443.77	-888.000
223	0.267	2258	0.476	64.16	2.57	4.96	4.10	-21.29	486.00	-888.000
224	0.286	2187	0.388	68.37	2.47	6.57	5.15	-10.46	376.30	-888.000
225	0.288	2180	0.284	68.16	2.43	7.08	5.80	-11.88	380.88	-888.000
226	0.288	2206	0.388	64.88	2.62	7.34	5.89	-12.48	387.57	-888.000
227	0.288	2215	0.376	68.02	2.80	7.44	5.82	-14.62	376.38	-888.000
228	0.272	2207	0.370	64.78	2.44	7.42	5.72	-17.71	370.83	-888.000
229	0.251	2238	0.388	64.80	2.51	7.51	5.94	-20.28	372.88	-888.000
230	0.202	2230	0.377	62.42	3.34	7.88	6.04	-18.16	344.88	-888.000
231	0.248	2228	0.370	62.88	2.74	7.88	5.89	-20.88	373.40	-888.000
232	0.288	2228	0.384	62.88	2.88	6.41	5.18	-20.47	388.48	-888.000
233	0.247	2248	0.470	61.88	3.08	5.82	4.28	-24.88	482.00	-888.000
234	0.251	2286	0.388	68.67	2.88	6.84	5.44	-20.28	388.08	-888.000
235	0.238	2271	0.436	67.82	3.01	5.31	4.82	-22.88	414.42	-888.000
236	0.210	2287	0.400	73.88	2.88	6.88	4.94	-23.82	482.48	-888.000
237	0.217	2206	0.436	68.73	2.88	5.38	4.86	-24.26	411.14	-888.000
238	0.288	2200	0.438	68.88	2.78	5.34	4.84	-20.40	410.86	-888.000
239	0.237	2261	0.438	70.67	2.80	5.82	4.71	-21.14	407.83	-888.000
240	0.226	2264	0.488	68.37	2.84	5.15	4.67	-21.26	416.70	-888.000
241	0.254	2260	0.486	73.48	2.87	4.88	4.27	-24.26	422.48	-888.000
242	0.286	2273	0.482	71.70	2.88	5.88	4.76	-23.20	411.73	-888.000
243	0.236	2267	0.488	72.88	2.84	5.88	5.32	-21.47	387.31	-888.000
244	0.214	2286	0.448	74.34	3.03	5.82	4.76	-23.06	384.12	-888.000
245	0.217	2286	0.444	73.86	3.08	4.76	4.27	-24.16	388.82	-888.000
246	0.217	2291	0.436	70.88	2.91	4.34	3.81	-23.88	488.31	-888.000
247	0.234	2280	0.436	72.34	2.88	5.31	4.88	-20.46	486.81	-888.000
248	0.234	2288	0.414	67.18	2.86	6.34	5.38	-14.73	384.88	-888.000
249	0.228	2276	0.472	70.86	3.02	5.48	4.88	-18.70	414.57	-888.000
250	0.215	2288	0.476	75.08	2.88	4.82	4.18	-20.88	486.88	-888.000
251	0.223	2282	0.436	68.88	3.02	5.80	4.45	-18.17	411.88	-888.000
252	0.215	2283	0.443	76.08	2.91	4.84	3.82	-20.86	481.88	-888.000
253	0.218	2287	0.487	76.37	2.89	4.67	3.88	-18.46	486.38	0.001
254	0.221	2276	0.447	71.91	3.16	3.80	2.88	-18.88	481.38	0.002
255	0.251	2270	0.481	67.88	2.89	4.82	4.38	-18.88	386.34	0.001
256	0.188	2286	0.416	66.37	3.48	7.97	7.88	1.51	-888.00	0.000
257	0.188	2480	0.247	61.14	4.86	10.46	10.10	5.88	-888.00	0.001
258	0.277	2246	0.414	61.08	3.08	7.88	5.51	5.86	-888.00	0.000

06-35-017-00W4M										
DEPTH	PHD	DENS	PHIN	GR	PEF	LLD	LLS	SP	DTL	FFI
250	0.298	2186	0.400	58.77	3.05	6.88	5.58	4.27	-888.00	0.012
260	0.278	2205	0.383	60.97	2.84	6.83	5.15	3.27	-888.00	0.011
261	0.308	2142	0.388	65.28	2.81	7.38	5.30	3.97	-888.00	0.008
262	0.310	2133	0.388	65.24	2.82	7.54	5.47	2.15	-888.00	0.003
263	0.238	2270	0.419	64.75	3.48	7.54	5.83	0.73	-888.00	0.004
264	0.282	2180	0.428	65.88	2.87	6.50	5.08	-0.56	-888.00	0.004
265	0.087	2503	0.378	59.00	4.00	4.55	4.00	-12.21	418.98	0.003
266	0.302	2187	0.408	62.80	2.88	6.27	5.18	-0.38	412.37	0.005
267	0.288	2188	0.419	63.51	3.02	6.58	4.81	-5.38	387.85	0.004
268	0.278	2191	0.423	62.70	2.80	5.87	4.42	-4.57	387.58	0.007
269	0.283	2215	0.438	58.48	2.87	5.57	4.37	-11.07	400.08	0.008
270	0.282	2188	0.413	58.83	2.88	5.88	4.75	-4.78	388.18	0.008
271	0.278	2185	0.388	64.88	2.83	5.84	4.81	-13.80	388.84	0.008
272	0.287	2237	0.434	67.44	2.87	5.54	4.88	-18.57	408.88	0.002
273	0.288	2238	0.464	61.78	2.85	5.43	4.72	-18.88	384.88	0.002
274	0.238	2259	0.431	68.08	2.78	5.85	4.88	-18.22	388.88	0.001
275	0.175	2344	0.388	61.07	3.12	5.54	5.08	-17.82	383.00	0.002
276	0.248	2250	0.448	67.18	2.88	5.15	4.88	-17.88	408.17	0.002
277	0.237	2262	0.441	68.88	3.01	4.84	4.18	-19.38	403.33	0.002
278	0.280	2280	0.387	68.88	2.81	5.78	5.10	-13.80	382.00	0.002
279	0.174	2385	0.388	63.88	3.05	5.88	5.33	-18.80	382.00	0.002
280	0.204	2288	0.438	68.78	3.01	4.88	4.48	-22.44	411.31	0.002
281	0.215	2298	0.480	63.74	3.07	5.05	4.88	-21.82	410.34	0.001
282	0.188	2338	0.435	68.91	2.88	5.88	5.43	-18.72	388.57	0.001
283	0.180	2378	0.381	54.00	3.21	7.38	6.48	-18.80	382.14	0.002
284	0.241	2288	0.387	68.67	2.78	6.84	5.77	-17.84	378.88	0.011
285	0.208	2814	0.438	67.74	3.04	4.84	4.88	-22.88	408.88	0.001
286	0.201	2818	0.444	70.08	3.25	5.14	4.88	-22.13	408.18	0.001
287	0.208	2808	0.448	71.44	3.12	5.18	4.88	-22.12	408.88	0.001
288	0.200	2818	0.448	71.88	2.88	5.08	4.88	-22.18	408.78	0.002
289	0.197	2834	0.484	78.41	3.10	4.88	4.31	-22.81	417.88	0.002
290	0.197	2828	0.488	78.88	2.88	4.31	4.12	-22.84	415.37	0.001
291	0.201	2828	0.481	71.70	3.02	3.87	3.88	-22.87	415.10	0.002
292	0.194	2834	0.448	71.74	3.04	3.82	3.78	-22.14	413.13	0.008
293	0.188	2838	0.480	74.22	3.04	3.01	2.87	-22.88	414.88	0.002
294	0.187	2844	0.488	72.82	3.18	4.38	4.38	-22.48	418.11	0.002
295	0.181	2843	0.488	71.32	3.17	2.44	2.41	-28.87	404.88	0.002
296	0.188	2832	0.477	77.84	3.21	2.88	2.77	-22.88	411.74	0.002
297	0.188	2838	0.442	78.72	3.18	4.88	4.88	-22.18	415.18	0.002
298	0.208	2818	0.488	68.88	3.08	2.78	2.78	-22.18	417.88	0.002
299	0.180	2833	0.481	73.91	3.18	3.88	3.88	-22.21	418.78	0.001
300	0.208	2812	0.488	71.88	3.07	3.34	3.38	-22.34	402.34	0.001
301	0.208	2812	0.477	71.88	3.08	3.87	3.48	-28.87	408.34	0.002
302	0.217	2808	0.488	67.88	3.08	3.82	3.84	-22.38	402.88	0.001
303	0.208	2808	0.480	71.48	3.17	3.38	3.38	-22.78	411.88	0.001
304	0.188	2822	0.412	74.01	3.15	4.48	4.38	-22.88	414.88	0.001
305	0.188	2838	0.488	74.38	2.97	4.21	4.08	-22.18	418.88	0.001
306	0.200	2822	0.448	80.51	3.08	5.88	5.88	-28.78	412.11	0.008
307	0.208	2811	0.488	74.70	3.18	5.84	5.84	-24.84	408.88	0.008
308	0.188	2821	0.438	74.38	2.88	4.88	3.74	-24.87	408.84	0.001
309	0.188	2823	0.488	81.88	3.08	4.84	3.88	-28.18	408.71	0.008
310	0.208	2811	0.481	81.27	2.88	3.88	3.77	-24.88	408.88	0.001
311	0.208	2818	0.488	78.88	3.08	3.78	3.88	-28.87	404.17	0.001
312	0.218	2808	0.438	81.88	2.88	5.88	5.88	-28.88	408.88	0.001
313	0.213	2808	0.438	74.38	2.88	4.84	3.78	-24.88	417.87	0.008
314	0.218	2148	0.448	81.72	2.84	3.88	3.48	-24.88	408.88	0.001
315	0.248	2848	0.888	81.88	2.72	3.88	3.88	-24.88	408.88	0.001
316	0.213	2808	0.474	81.38	2.88	3.82	3.88	-24.11	407.87	0.008
317	0.180	1838	0.888	88.84	2.15	2.78	2.78	-28.88	407.48	0.002
318	0.281	2848	0.478	88.88	2.88	3.78	3.78	-24.87	408.13	0.001
319	0.200	2188	0.488	84.78	2.78	2.88	2.88	-24.88	407.88	0.001
320	0.202	2821	0.488	78.38	2.97	4.38	4.08	-22.38	413.34	0.001
321	0.188	2827	0.447	88.48	2.88	4.78	4.38	-22.88	418.84	0.001
322	0.188	2832	0.481	88.73	3.08	4.88	4.34	-22.88	418.18	0.002
323	0.184	2848	0.488	88.48	3.88	4.88	4.88	-22.78	413.88	0.008
324	0.218	2808	0.488	81.88	2.88	3.88	3.78	-22.78	408.38	0.002

06-35-017-00W4M										
DEPTH	PHO	DENS	PHN	GR	PEF	LLD	LLS	SP	DTL	FFI
325	0.224	2280	0.450	80.28	2.88	4.18	4.08	-22.20	417.72	0.002
326	0.180	2353	0.430	88.85	3.20	4.91	4.74	-21.23	409.27	0.002
327	0.183	2350	0.422	84.00	2.88	5.23	4.88	-21.28	403.41	0.001
328	0.179	2354	0.478	87.00	3.02	5.15	4.85	-20.45	400.47	0.002
329	0.174	2350	0.458	100.56	2.82	5.82	5.27	-18.86	388.20	0.001
330	0.140	2418	0.338	98.17	2.78	6.50	6.50	-15.98	383.38	0.000
331	0.156	2386	0.344	98.02	2.80	6.05	6.03	-15.51	388.86	0.000
332	0.347	2075	0.481	90.00	2.83	5.30	5.30	-15.53	386.00	0.008
333	0.184	2335	0.382	98.27	2.72	7.19	6.48	-14.88	373.57	0.002
334	0.130	2436	0.336	98.82	2.78	10.97	10.38	-13.32	341.18	0.001
335	0.182	2400	0.318	98.38	2.75	10.07	9.88	-13.35	380.88	0.008
336	0.145	2419	0.328	93.82	2.88	10.64	10.14	-11.42	344.31	0.002
337	0.188	2416	0.338	87.88	2.70	10.61	9.78	-8.84	343.10	0.001
338	0.137	2438	0.331	92.18	2.84	11.05	10.18	-10.82	342.37	0.002
339	0.132	2438	0.318	87.72	2.78	11.13	10.38	-11.47	348.86	0.000
340	0.130	2439	0.322	87.32	2.73	11.18	10.27	-11.31	344.38	0.001
341	0.145	2416	0.335	98.70	2.87	10.80	10.38	-11.14	343.41	0.000
342	0.138	2430	0.329	88.85	2.71	10.41	9.84	-10.77	346.48	0.001
343	0.141	2420	0.341	98.67	2.80	10.18	9.79	-11.34	348.47	0.001
344	0.137	2424	0.308	93.44	2.80	12.38	10.95	-10.14	341.93	0.001
345	0.133	2427	0.322	87.18	2.80	11.45	10.88	-10.38	342.14	0.001
346	0.140	2421	0.325	96.42	2.78	12.34	11.88	-10.31	338.84	0.002
347	0.078	2517	0.308	88.85	3.80	18.80	13.80	-8.33	314.00	0.002
348	0.127	2400	0.325	105.80	2.78	12.57	12.38	-8.48	348.00	0.002
349	0.143	2418	0.330	87.41	2.78	11.82	10.61	-8.48	348.78	0.002
350	0.131	2430	0.312	95.67	2.88	12.42	11.44	-10.22	340.78	0.002
351	0.138	2423	0.308	98.11	2.88	11.82	10.91	-10.88	343.88	0.002
352	0.140	2421	0.322	83.48	2.88	12.38	11.88	-8.88	338.08	0.001
353	0.138	2422	0.304	98.82	2.81	12.38	11.38	-8.71	338.81	0.002
354	0.145	2410	0.304	98.78	2.72	12.11	11.88	-10.18	344.48	0.002
355	0.145	2410	0.318	98.82	2.72	10.87	10.88	-8.80	344.78	0.002
356	0.138	2419	0.308	94.82	2.78	12.02	11.47	-10.38	342.17	0.001
357	0.135	2427	0.313	84.78	2.83	14.08	12.88	-8.34	318.00	0.001
358	0.144	2414	0.305	88.48	2.77	14.08	13.18	-8.04	334.38	0.002
359	0.147	2414	0.305	81.67	2.78	14.88	13.48	-7.83	328.48	0.002
360	0.138	2438	0.320	81.80	2.88	12.41	11.57	-8.17	338.81	0.001
361	0.134	2438	0.311	81.72	2.84	13.81	12.88	-8.88	330.27	0.001
362	0.138	2433	0.308	82.88	2.84	12.88	11.88	-8.88	314.88	0.002
363	0.140	2421	0.301	88.48	2.78	11.78	11.38	-10.18	334.12	0.001
364	0.138	2428	0.304	82.12	2.88	11.74	10.88	-10.88	343.88	0.002
365	0.144	2413	0.347	88.21	2.84	10.38	9.44	-11.27	348.88	0.008
366	0.140	2422	0.304	87.88	2.81	12.88	11.47	-8.88	340.88	0.008
367	0.140	2423	0.302	88.88	2.78	11.97	11.88	-10.17	338.38	0.008
368	0.148	2418	0.305	88.88	3.80	11.13	10.07	-8.83	344.88	0.008
369	0.144	2414	0.348	88.38	2.78	10.48	9.88	-10.27	332.14	0.002
370	0.141	2421	0.302	88.88	2.88	11.38	10.78	-8.88	341.57	0.008
371	0.140	2423	0.308	88.88	2.88	11.18	10.13	-8.97	331.27	0.002
372	0.148	2414	0.340	87.38	2.71	10.87	10.88	-10.21	348.38	0.008
373	0.138	2417	0.304	102.88	2.72	11.82	10.48	-8.88	347.88	0.008
374	0.148	2378	0.305	88.42	2.84	10.91	9.88	-10.51	333.88	0.008
375	0.177	2388	0.308	81.88	2.78	9.88	9.18	-7.88	331.18	0.018
376	0.188	2331	0.384	87.88	2.83	10.81	10.81	-7.41	338.88	0.011
377	0.184	2387	0.348	88.88	2.88	10.81	10.17	-4.38	348.88	0.008
378	0.181	2384	0.305	88.88	2.88	12.78	11.88	-4.88	348.88	0.001
379	0.184	2342	0.348	88.48	2.84	11.87	10.88	-4.38	332.47	0.008
380	0.113	2482	0.308	84.87	3.13	13.88	12.88	-7.88	333.84	0.004
381	0.173	2367	0.321	83.47	2.72	12.82	11.81	-8.87	341.87	0.018
382	0.148	2408	0.348	84.42	2.88	10.78	10.13	-7.81	348.48	0.008
383	0.188	2388	0.305	88.88	2.84	11.17	10.88	-7.38	343.38	0.004
384	0.188	2378	0.367	88.84	2.78	10.84	10.38	-4.48	338.57	0.008
385	0.137	2438	0.305	88.48	2.88	11.78	10.87	-7.48	341.51	0.007
386	0.181	2402	0.308	88.37	2.88	11.38	10.87	-4.91	338.88	0.018
387	0.138	2430	0.327	88.88	2.78	11.87	10.37	-7.82	348.88	0.012
388	0.122	2480	0.305	102.88	2.71	11.18	10.38	-4.88	348.88	0.008
389	0.184	2384	0.348	81.81	2.82	10.71	9.84	-4.44	348.38	0.007
390	0.184	2388	0.337	81.88	2.72	10.37	9.88	-4.30	332.88	0.017

06-35-017-00W4M										
DEPTH	PHID	DENS	PHIN	GR	PEF	LLD	LLS	SP	DTL	FFI
301	0.155	2402	0.328	104.00	2.81	10.03	9.38	-8.25	357.80	0.005
302	0.151	2399	0.351	97.41	2.77	12.00	11.00	-6.18	345.71	0.006
303	0.109	2467	0.308	91.16	2.75	9.80	9.00	-7.64	320.00	0.007
304	0.172	2364	0.408	95.00	2.62	12.50	11.00	-7.67	363.00	0.012
305	0.150	2408	0.330	92.45	2.68	11.71	10.87	-5.96	329.00	0.006
306	0.086	2505	0.320	91.08	3.20	11.54	10.46	-5.00	342.25	0.006
307	0.138	2426	0.347	101.70	2.65	9.57	9.20	-5.34	343.30	0.008
308	0.147	2403	0.382	103.12	2.68	9.79	9.14	-4.90	388.83	0.006
309	0.142	2415	0.392	84.84	2.60	14.78	13.80	-4.75	315.00	0.010
400	0.144	2414	0.321	83.77	3.30	13.43	12.41	-4.68	388.32	0.008
401	0.141	2421	0.313	89.48	2.68	12.39	11.11	-5.25	388.84	0.006
402	0.148	2403	0.338	85.88	2.67	11.78	10.48	-4.30	340.13	0.010
403	0.153	2398	0.347	92.89	2.78	10.83	10.20	-4.15	385.38	0.015
404	0.155	2351	0.335	98.95	2.72	10.40	9.95	-4.89	385.15	0.022
405	0.178	2361	0.357	91.75	2.62	11.68	10.38	-4.48	345.61	0.017
406	0.140	2432	0.327	90.19	2.70	12.35	11.15	-4.49	342.88	0.018
407	0.155	2337	0.342	89.08	2.68	11.70	10.85	-4.13	345.88	0.021
408	0.163	2380	0.333	92.75	3.00	12.12	11.34	-4.38	383.03	0.008
409	0.170	2380	0.340	94.54	2.57	11.30	10.80	-4.13	388.30	0.010
410	0.221	2282	0.334	91.48	2.77	14.00	13.00	-4.88	388.08	0.010
411	0.141	2417	0.311	91.38	2.68	13.75	12.83	-4.50	385.22	0.008
412	0.133	2437	0.307	92.72	2.63	13.87	13.07	-4.32	351.52	0.008
413	0.184	2388	0.384	92.43	2.85	12.16	11.38	-3.44	384.78	0.010
414	0.144	2419	0.302	93.10	2.68	13.82	12.88	-4.57	382.85	0.008
415	0.163	2405	0.343	93.78	2.63	12.18	10.88	-3.84	386.62	0.009
416	0.235	2280	0.338	98.13	2.40	12.98	11.42	-1.87	382.37	0.011
417	0.388	2145	0.388	105.98	2.64	10.38	9.88	-1.35	388.75	0.014
418	0.237	2225	0.388	104.35	2.62	10.10	9.51	-2.60	351.48	0.022
419	0.254	2225	0.387	98.48	2.64	10.48	9.84	-3.13	383.75	0.020
420	0.382	2185	0.387	104.41	2.85	10.00	9.88	-2.88	357.92	0.018
421	0.155	2340	0.384	105.85	2.71	10.17	9.15	-3.43	383.85	0.008
422	0.382	2200	0.402	107.18	2.85	9.98	9.07	-4.80	354.88	0.016
423	0.235	2254	0.379	111.58	2.83	8.10	7.80	-4.80	371.54	0.014
424	0.155	2300	0.383	110.48	2.77	9.57	8.90	-4.88	357.47	0.014
425	0.123	2480	0.372	108.44	2.88	11.88	10.67	-4.37	386.88	0.008
426	0.138	2435	0.378	114.42	2.93	11.88	10.88	-4.45	385.64	0.008
427	0.187	2378	0.378	130.97	3.01	10.80	10.22	-4.88	371.88	0.008
428	0.163	2379	0.454	132.64	3.08	9.38	9.21	-10.85	351.58	0.008
429	0.122	2447	0.345	138.88	3.48	12.80	12.88	-10.77	344.88	0.009
430	0.165	2381	0.385	138.82	3.18	9.78	10.17	-10.38	376.30	0.008
431	0.161	2383	0.385	138.38	3.17	8.80	8.98	-10.80	372.80	0.008
432	0.161	2382	0.382	127.64	3.18	10.78	10.51	-10.38	373.88	0.008
433	0.175	2351	0.408	127.85	3.00	8.05	8.88	-11.38	371.88	0.008
434	0.173	2389	0.388	118.74	3.13	11.34	11.38	-10.78	354.18	0.004
435	0.163	2378	0.402	131.07	3.02	9.91	9.72	-12.02	372.43	0.008
436	0.188	2348	0.401	132.72	3.18	9.08	8.93	-13.14	350.47	0.001
437	0.211	2351	0.408	121.47	2.78	8.70	8.70	-14.30	372.37	0.001
438	0.082	2500	0.317	95.00	3.75	15.00	15.00	-12.88	315.00	0.002
439	0.170	2388	0.410	135.00	3.33	9.73	9.78	-12.41	388.33	0.001
440	0.172	2388	0.417	143.00	3.34	9.68	9.88	-13.37	388.67	0.002
441	0.182	2385	0.441	135.48	3.11	9.78	9.85	-12.51	382.51	0.006
442	0.177	2357	0.389	131.17	3.07	11.80	11.68	-12.85	372.85	0.001
443	0.184	2351	0.484	127.72	3.08	8.88	9.08	-14.18	374.18	0.001
444	0.148	2407	0.388	135.01	3.38	10.57	11.18	-13.44	347.80	0.002
445	0.181	2388	0.488	112.00	3.38	9.68	9.57	-13.18	377.53	0.001
446	0.185	2370	0.418	138.80	3.03	9.83	9.91	-12.18	351.83	0.001
447	0.184	2382	0.488	138.82	3.32	9.19	9.38	-12.80	388.80	0.001
448	0.161	2382	0.488	121.21	3.08	8.84	8.21	-13.88	388.84	0.001
449	0.188	2371	0.438	108.00	2.67	8.37	8.41	-12.38	351.43	0.005
450	0.185	2378	0.382	118.32	3.22	9.68	9.17	-12.82	382.82	0.008
451	0.173	2383	0.388	114.88	3.02	8.67	8.67	-12.38	357.31	0.008
452	0.172	2367	0.488	125.67	3.11	8.83	8.43	-11.84	385.48	0.008
453	0.177	2388	0.484	121.32	3.05	7.64	7.38	-12.88	388.51	0.008
454	0.172	2388	0.482	130.81	3.13	8.85	9.21	-12.13	385.83	0.001
455	0.087	2485	0.318	114.00	3.60	9.90	10.73	-12.78	388.88	0.001
456	0.172	2382	0.434	130.48	3.07	9.33	9.42	-12.83	375.83	0.001

00-35-017-00W4M

DEPTH	PHO	DENS	PHN	GR	PEF	LLD	LLS	SP	DTL	FFI
457	0.157	2388	0.383	127.53	3.00	8.54	8.73	-12.08	377.55	0.001
458	0.165	2378	0.410	118.57	2.98	8.10	8.10	-11.68	380.32	0.002
459	0.161	2376	0.383	118.57	2.95	8.07	8.42	-10.08	383.24	0.003
460	0.179	2362	0.378	108.82	2.91	8.44	8.51	-9.02	376.70	0.005
461	0.147	2406	0.342	102.04	2.74	11.84	11.35	-7.41	380.58	0.018
462	0.144	2410	0.300	97.00	2.76	13.87	12.74	-8.94	388.78	0.015
463	0.144	2410	0.348	101.38	2.78	12.88	12.38	-8.43	381.71	0.007
464	0.188	2387	0.380	103.84	2.77	11.38	10.88	-8.15	388.57	0.007
465	0.187	2377	0.383	100.57	2.78	10.41	10.25	-8.50	382.22	0.008
466	0.188	2380	0.400	105.63	2.74	9.88	9.81	-8.85	388.88	0.008
467	0.180	2387	0.388	102.43	2.80	12.04	11.82	-8.50	348.31	0.008
468	0.134	2438	0.318	97.15	2.78	13.44	12.41	-8.83	340.73	0.008
469	0.138	2435	0.323	101.77	2.72	13.48	12.42	-8.51	341.00	0.008
470	0.138	2440	0.341	102.35	2.67	12.88	11.38	-8.38	347.18	0.008
471	0.188	2380	0.418	102.37	2.88	10.17	9.88	-4.41	348.43	0.017
472	0.121	2378	0.388	104.78	2.80	10.12	9.97	-4.88	388.80	0.008
473	0.173	2387	0.384	105.88	2.78	9.78	9.97	-4.54	388.88	0.021
474	0.188	2348	0.388	108.83	2.67	9.88	8.88	-4.38	388.33	0.024
475	0.308	2318	0.381	111.51	2.82	9.38	8.82	-4.51	383.48	0.018
476	0.212	2288	0.410	104.88	2.78	7.38	6.82	-4.28	382.78	0.018
477	0.308	2331	0.388	108.82	3.08	8.84	7.87	-3.71	381.18	0.014
478	0.180	2383	0.381	113.34	2.61	10.88	10.88	-2.88	348.88	0.018
479	0.304	2314	0.388	104.77	2.70	9.88	9.84	-2.41	384.88	0.020
480	0.288	2228	0.447	107.88	2.51	9.18	8.82	-2.38	380.01	0.008
481	0.308	2301	0.407	118.88	2.78	9.38	8.88	-1.88	384.18	0.021
482	0.288	2388	0.388	108.78	2.70	9.38	8.81	-3.78	388.73	0.021
483	0.308	2314	0.418	102.48	2.82	9.48	8.88	-2.78	388.37	0.021
484	0.188	2313	0.387	112.78	2.77	9.32	8.48	-2.88	388.14	0.022
485	0.187	2321	0.388	108.88	2.74	8.78	8.18	-2.88	388.88	0.020
486	0.228	2388	0.387	102.11	2.88	8.84	8.17	-2.48	388.88	0.027
487	0.181	2400	0.372	108.78	3.18	8.34	8.88	-2.88	384.78	0.018
488	0.218	2384	0.402	108.38	2.78	8.51	7.88	-2.48	382.88	0.018
489	0.308	2388	0.388	102.88	2.78	8.27	8.77	-2.48	388.88	0.018
490	0.148	2408	0.382	108.38	3.38	8.87	8.88	-3.12	382.88	0.018
491	0.348	2348	0.431	108.88	2.78	8.34	7.91	-2.78	388.78	0.017
492	0.188	2347	0.382	108.88	2.88	8.48	8.38	-3.18	382.78	0.018
493	0.288	2278	0.417	108.48	2.88	8.44	8.18	-3.88	388.87	0.021
494	0.288	2278	0.491	107.84	2.88	8.38	7.88	-3.88	387.88	0.018
495	0.148	2408	0.381	108.88	3.01	10.88	10.88	-2.38	388.88	0.011
496	0.254	2278	0.488	108.88	2.78	8.88	8.88	-3.34	372.88	0.008
497	0.188	2388	0.388	108.88	2.84	10.88	10.88	-2.88	388.88	0.018
498	0.218	2388	0.407	108.84	2.88	8.88	8.78	-3.88	388.81	0.021
499	0.188	2388	0.482	108.88	2.88	8.48	8.41	-3.88	388.88	0.020
500	0.118	2488	0.388	118.48	2.87	10.88	10.88	-4.88	388.88	0.020
501	0.188	2348	0.484	102.78	2.88	8.88	8.57	-4.88	382.38	0.022
502	0.174	2388	0.388	108.78	2.88	8.88	8.31	-4.88	388.31	0.011
503	0.288	2278	0.388	110.34	2.81	8.88	7.88	-4.38	388.31	0.018
504	0.187	2373	0.488	118.88	2.88	8.88	8.88	-7.74	378.88	0.018
505	0.174	2381	0.378	101.14	2.88	8.88	8.88	-4.78	388.88	0.017
506	0.188	2342	0.387	101.38	2.88	8.88	7.78	-4.51	388.88	0.018
507	0.181	2341	0.388	102.37	3.04	8.88	7.88	-4.34	384.38	0.018
508	0.181	2391	0.488	108.88	2.78	8.88	7.81	-4.91	388.88	0.017
509	0.182	2408	0.388	118.88	2.88	8.88	8.88	-7.88	388.88	0.008
510	0.388	2213	0.488	108.82	2.78	8.71	8.28	-4.94	388.38	0.018
511	0.187	2388	0.411	118.48	3.04	7.88	7.88	-4.88	387.18	0.020
512	0.188	2318	0.418	108.88	3.18	8.88	8.81	-7.88	384.48	0.018
513	0.278	2218	0.481	117.18	3.48	8.81	8.38	-4.88	378.18	0.027
514	0.188	2372	0.488	112.87	3.12	8.88	8.88	-7.78	488.82	0.008
515	0.388	2328	0.317	78.88	4.88	13.48	13.48	-8.37	313.18	0.021
516	0.188	2384	0.482	108.88	3.18	8.88	7.88	-4.88	387.81	0.020
517	0.188	2387	0.488	112.78	3.38	8.48	8.88	-8.87	388.88	0.022
518	0.254	2388	0.488	117.48	2.88	7.38	7.38	-4.38	387.38	0.018
519	0.178	2388	0.448	111.88	3.84	7.87	7.72	-8.38	384.37	0.008
520	0.178	2382	0.478	108.88	2.84	8.88	8.27	-8.88	388.31	0.011
521	0.188	2388	0.488	114.88	3.88	8.88	8.88	-10.88	388.34	0.022
522	0.188	2381	0.488	108.88	2.88	8.88	8.87	-10.81	381.38	0.018

06-35-017-00W4M										
DEPTH	PHO	DENS	PHN	GR	PEF	LLD	LLS	SP	DTL	FFI
523	0.168	2342	0.411	124.00	2.84	6.53	6.68	-13.15	385.78	0.004
524	0.168	2388	0.425	120.19	3.14	7.40	7.40	-17.50	383.90	0.008
525	0.127	2440	0.380	105.00	3.80	9.40	9.40	-14.84	378.02	0.008
526	0.207	2510	0.488	125.81	3.08	3.80	3.80	-18.00	344.00	0.002
527	0.195	2320	0.477	124.91	2.84	3.88	3.81	-14.84	388.85	0.005
528	0.143	2411	0.380	117.00	2.81	5.97	5.42	-12.21	377.77	0.005
529	0.148	2410	0.425	121.25	2.81	5.88	5.18	-12.84	378.40	0.004
530	0.165	2388	0.438	134.00	2.88	6.80	6.30	-15.85	375.25	0.008
531	0.147	2415	0.388	112.00	3.40	5.00	5.00	-17.22	384.00	0.002
532	0.238	2280	0.501	131.94	2.40	2.40	2.40	-19.17	388.00	0.001
533	0.168	2345	0.388	141.81	2.84	3.44	3.18	-18.13	372.75	0.001
534	0.280	2288	0.471	133.34	2.81	3.42	3.25	-14.84	388.55	0.010
535	0.208	2308	0.388	105.15	2.88	6.30	6.30	-8.42	388.73	0.004
536	0.134	2440	0.381	112.00	2.78	8.30	8.30	-4.25	388.38	0.018
537	0.137	2438	0.388	108.38	2.85	10.85	8.85	-3.82	388.25	0.005
538	0.244	2280	0.387	102.88	2.81	8.88	8.14	-1.37	347.88	0.008
539	0.210	2308	0.430	108.38	2.78	10.40	10.00	-2.22	348.88	0.013
540	0.171	2388	0.388	108.88	2.88	9.97	8.31	-2.27	344.27	0.018
541	0.283	2253	0.380	108.88	2.70	8.82	8.30	-2.32	348.18	0.025
542	0.197	2313	0.387	87.08	2.85	8.88	8.11	-1.78	348.78	0.025
543	0.213	2284	0.388	108.88	2.88	8.48	8.38	-2.88	388.87	0.027
544	0.302	2314	0.388	108.07	3.08	8.87	8.38	-3.87	387.88	0.018
545	0.214	2280	0.388	118.00	2.83	8.12	8.74	-1.72	388.88	0.014
546	0.188	2313	0.387	107.78	3.00	8.85	8.80	-1.78	384.32	0.011
547	0.215	2288	0.372	108.88	2.88	10.31	10.05	-3.81	388.74	0.008
548	0.388	2214	0.388	108.48	2.83	8.88	8.88	-2.87	388.48	0.005
549	0.388	2178	0.488	112.88	2.87	8.27	8.88	-4.78	388.88	0.018
550	0.308	2148	0.438	98.88	2.72	8.88	8.14	0.38	377.88	0.014
551	0.384	2238	0.487	114.88	2.88	8.18	8.88	-1.88	388.88	0.018
552	0.348	2243	0.427	108.82	2.88	8.72	8.88	-3.87	387.88	0.018
553	0.328	2272	0.488	108.78	2.87	8.78	8.88	-3.12	371.78	0.018
554	0.278	2200	0.488	107.38	2.81	8.84	8.81	-3.88	388.88	0.012
555	0.228	2278	0.388	112.17	2.81	8.38	8.88	-3.81	387.27	0.018
556	0.188	2345	0.414	138.78	2.78	8.88	7.85	-4.88	388.88	0.014
557	0.213	2288	0.488	114.48	3.08	8.74	8.88	-3.71	388.78	0.005
558	0.217	2288	0.432	113.18	2.88	8.88	8.48	-3.84	384.37	0.008
559	0.080	2310	0.188	88.00	4.88	48.88	48.88	-3.88	388.88	0.008
560	0.282	2288	0.431	111.81	2.88	8.88	8.88	-3.21	388.87	0.018
561	0.388	2210	0.448	128.88	2.88	8.78	8.78	-4.11	378.88	0.018
562	0.382	2207	0.388	118.88	2.81	8.18	8.88	-3.88	378.17	0.014
563	0.342	2288	0.488	118.88	2.88	8.44	8.41	-4.81	388.78	0.005
564	0.388	2223	0.388	138.88	2.78	8.88	8.78	-3.88	388.88	0.008
565	0.388	2125	0.488	108.87	2.48	8.38	8.48	-2.71	387.78	0.018
566	0.212	2288	0.388	117.48	2.78	8.88	8.88	-2.87	388.88	0.018
567	0.218	2200	0.388	117.88	2.82	8.41	8.88	-2.81	388.78	0.008
568	0.288	2203	0.372	118.74	2.84	8.88	8.18	-3.88	387.88	0.014
569	0.228	2278	0.370	112.84	2.81	10.88	8.88	-2.81	384.88	0.018
570	0.284	2188	0.388	111.31	2.88	10.38	8.74	-2.78	387.88	0.008
571	0.348	2280	0.438	108.88	2.81	8.12	8.82	-2.87	388.31	0.018
572	0.380	2203	0.388	114.88	2.88	8.38	8.88	-2.27	388.84	0.014
573	0.388	2278	0.481	114.48	2.88	8.12	8.83	-3.88	388.21	0.012
574	0.214	2284	0.388	112.38	2.72	8.27	8.38	-3.88	388.84	0.012
575	0.214	2281	0.488	111.48	2.78	8.38	8.18	-3.88	371.88	0.011
576	0.272	2280	0.388	113.14	2.78	8.48	8.18	-2.88	388.88	0.013
577	0.228	2280	0.387	113.18	2.84	8.78	8.88	-2.88	388.12	0.018
578	0.188	2315	0.388	114.78	2.88	8.78	8.97	-2.78	381.18	0.015
579	0.281	2218	0.378	113.88	2.87	8.18	8.38	-2.88	388.88	0.014
580	0.181	2348	0.484	118.27	2.88	10.38	10.38	-2.48	387.88	0.008
581	0.288	2218	0.488	113.81	2.81	8.88	8.88	-2.81	388.88	0.018
582	0.288	2218	0.388	113.87	2.84	8.87	8.88	-2.88	378.88	0.011
583	0.188	2288	0.388	118.18	2.88	8.17	8.87	-2.81	384.18	0.013
584	0.288	2278	0.413	112.82	2.72	8.88	8.78	-2.87	384.87	0.018
585	0.288	2217	0.421	113.81	2.88	8.88	8.88	-2.88	371.38	0.011
586	0.188	2284	0.388	118.48	2.71	8.84	8.81	-2.88	384.71	0.011
587	0.228	2284	0.488	111.72	2.88	8.88	8.41	-1.88	388.74	0.018
588	0.228	2287	0.432	112.73	2.71	8.78	8.38	-2.87	388.88	0.018

02-35-017-00W4M										
DEPTH	PHD	DENS	PHN	GR	PEF	LLD	LLS	SP	DTL	FFI
588	0.313	2148	0.408	107.40	2.81	8.88	8.44	-0.83	388.18	0.018
589	0.240	2250	0.444	122.31	3.01	8.11	7.83	-0.97	385.00	0.011
591	0.284	2214	0.418	120.48	2.78	8.83	8.74	-0.83	388.83	0.004
592	0.278	2178	0.422	118.88	2.78	7.12	8.83	-0.20	387.00	0.020
593	0.282	2178	0.380	114.81	2.34	8.80	8.88	0.67	388.87	0.020
594	0.237	2238	0.348	107.82	2.48	10.00	8.88	1.41	318.00	0.030
595	0.244	2238	0.380	108.77	2.83	8.88	8.88	0.87	384.88	0.017
596	0.208	2284	0.372	128.00	2.83	8.82	8.08	-0.38	342.88	0.007
597	0.173	2388	0.312	118.88	2.88	10.30	8.80	0.81	301.00	0.008
598	0.270	2238	0.384	110.47	2.41	8.82	8.88	1.21	388.88	0.021
599	0.223	2128	0.388	108.88	2.32	8.27	8.71	1.28	387.84	0.008
600	0.210	2300	0.388	107.48	2.87	8.81	8.18	2.18	382.87	0.013
601	0.212	2300	0.388	108.88	2.83	8.82	8.10	1.82	388.81	0.023
602	0.247	2288	0.388	113.88	2.88	10.14	8.88	0.44	318.17	0.007
603	0.277	2180	0.384	108.88	2.88	8.87	8.18	1.18	382.48	0.022
604	0.188	2378	0.384	118.87	3.38	8.87	8.88	0.72	387.88	0.008
605	0.241	2280	0.388	117.40	2.81	7.08	8.88	0.88	384.84	0.027
606	0.240	2281	0.410	128.88	2.87	7.74	7.44	-0.18	388.00	0.018
607	0.233	2282	0.388	118.88	2.87	7.88	7.21	0.77	384.00	0.018
608	0.238	2278	0.407	108.81	2.84	8.88	7.77	2.88	348.88	0.018
609	0.188	2301	0.388	108.82	2.88	10.10	8.88	2.38	387.80	0.011
610	0.184	2380	0.342	88.88	2.81	8.21	8.44	3.40	388.81	0.088
611	0.208	2328	0.374	107.88	2.81	8.08	8.84	2.10	387.88	0.080
612	0.114	3488	0.388	110.84	3.02	8.18	8.22	2.31	382.47	0.014
613	0.201	2387	0.388	110.88	2.88	8.04	8.18	2.88	341.21	0.088
614	0.188	2330	0.348	118.88	2.78	8.41	7.74	2.80	348.88	0.027
615	0.211	2307	0.402	117.88	2.84	8.88	7.88	2.88	388.78	0.013
616	0.182	2341	0.381	114.78	2.88	8.31	8.08	2.78	387.72	0.017
617	0.200	2327	0.388	108.88	2.88	8.31	7.81	2.48	388.81	0.021
618	0.238	2388	0.408	111.81	2.81	8.88	7.88	2.81	388.81	0.018
619	0.212	2308	0.488	114.88	2.88	8.88	7.81	1.78	388.84	0.018
620	0.207	2308	0.488	108.88	2.88	7.88	7.78	0.12	374.88	0.018
621	0.218	2307	0.488	112.88	2.88	7.84	7.84	-0.88	378.81	0.018
622	0.178	2380	0.418	117.88	2.88	7.84	7.88	-0.38	377.88	0.012
623	0.208	2312	0.388	113.87	2.88	8.02	7.88	-0.87	378.88	0.011
624	0.213	2314	0.408	113.78	2.48	8.88	8.84	-1.87	388.88	0.010
625	0.188	2378	0.372	104.18	2.82	8.88	8.88	-2.32	387.88	0.018
626	0.208	2318	0.417	118.88	2.84	7.81	8.12	-3.38	387.18	0.007
627	0.178	2388	0.442	128.88	2.81	7.78	7.88	-0.38	388.81	0.001
628	0.188	2388	0.488	121.48	2.87	7.84	7.88	-0.88	388.81	0.001
629	0.182	2381	0.414	118.87	2.84	8.88	8.12	-0.48	384.88	0.002
630	0.188	2378	0.488	122.88	2.78	8.88	8.87	-11.88	384.88	0.001
631	0.177	2381	0.432	121.84	2.88	8.88	8.87	-12.18	387.18	0.001
632	0.188	2348	0.488	127.88	2.77	8.88	8.82	-12.81	381.88	0.001
633	0.188	2388	0.488	127.88	2.88	8.78	8.88	-11.88	388.84	0.001
634	0.188	2381	0.487	128.18	2.71	8.18	8.18	-11.81	381.18	0.001
635	0.184	2384	0.488	122.47	2.88	8.97	8.88	-11.88	388.88	0.001
636	0.188	2348	0.448	121.88	3.88	8.88	8.88	-12.88	388.14	0.188
637	0.181	2382	0.418	113.88	2.88	8.18	8.18	-18.88	388.48	0.001
638	0.181	2388	0.488	128.88	3.81	8.82	8.88	-11.81	388.88	0.002
639	0.188	2342	0.488	128.88	2.88	8.81	8.88	-18.87	378.41	0.002
640	0.177	2381	0.488	108.88	3.14	8.48	8.48	-11.41	388.84	0.002
641	0.182	2348	0.388	128.48	3.07	8.88	8.88	-11.88	384.88	0.008
642	0.248	2380	0.348	88.88	3.88	13.88	13.88	-8.84	388.84	0.004
643	0.218	2388	0.372	88.88	3.81	12.88	12.88	-4.18	388.88	0.002
644	0.240	2380	0.388	88.88	3.88	10.88	10.88	-4.41	387.81	0.008
645	0.238	2188	0.388	288.88	2.88	1.88	1.88	-8.88	487.88	0.008
646	0.273	2380	0.418	138.88	3.88	12.88	13.88	-4.88	381.88	0.034
647	0.208	2341	0.381	84.88	3.88	10.88	12.88	-3.88	384.81	0.008
648	0.288	2388	0.347	87.88	3.18	21.88	21.88	-4.88	381.88	0.004
649	0.137	3444	0.388	118.88	3.81	12.88	12.48	1.88	381.87	0.008
650	0.131	3488	0.318	128.88	3.14	8.88	18.87	8.82	342.18	0.008
651	0.138	3488	0.348	102.17	3.18	18.18	18.87	-0.88	388.41	0.008
652	0.131	3444	0.388	121.88	3.81	8.87	8.42	-1.81	388.81	0.004
653	0.138	3447	0.378	118.88	3.81	8.82	8.78	0.48	378.88	0.008
654	0.148	3418	0.438	138.88	3.17	8.88	8.18	-0.18	388.81	0.007

03-35-017-00W4M										
DEPTH	PHD	DENS	PHN	GR	PEF	LLD	LLS	SP	DTL	FFI
655	0.132	2433	0.363	115.00	3.22	9.44	9.38	-0.78	357.78	0.006
656	0.144	2412	0.367	118.44	3.12	9.43	9.34	-0.28	358.30	0.006
657	0.141	2421	0.366	121.88	2.96	9.48	9.34	1.00	355.65	0.004
658	0.112	2457	0.338	116.82	3.23	10.34	10.14	0.38	347.40	0.003
659	0.132	2436	0.334	110.71	3.18	10.04	9.98	0.86	341.85	0.003
660	0.141	2412	0.379	113.28	3.36	8.58	8.11	0.92	354.90	0.017
661	0.188	2388	0.411	118.60	3.17	8.02	8.12	0.50	354.24	0.008
662	0.123	2455	0.385	116.44	3.30	8.08	8.17	-0.79	355.94	0.003
663	0.162	2401	0.387	141.00	3.73	9.07	9.11	-2.18	355.22	0.002
664	0.184	2377	0.441	122.63	3.37	7.88	7.87	-0.17	372.08	0.017
665	0.174	2370	0.468	124.87	2.98	7.71	7.86	-0.38	379.01	0.012
666	0.154	2383	0.443	130.81	3.74	8.22	8.40	-1.81	362.08	0.004
667	0.185	2373	0.440	141.28	3.80	8.70	8.67	-3.08	375.87	0.002
668	0.152	2403	0.404	132.48	3.73	9.85	9.18	-2.82	375.43	0.002
669	0.188	2389	0.418	144.80	3.67	9.38	9.08	-2.87	381.45	0.002
670	0.170	2373	0.483	140.00	4.30	9.83	9.40	-3.48	379.89	0.002
671	0.184	2379	0.437	183.00	3.63	8.43	8.32	-4.08	385.74	0.002
672	0.183	2347	0.481	140.00	3.88	8.08	8.48	-4.28	387.70	0.003
673	0.148	2401	0.445	162.00	3.38	8.82	8.86	-5.88	375.85	0.002
674	0.147	2425	0.418	138.04	3.80	8.83	8.48	-2.11	388.86	0.002
675	0.140	2411	0.432	148.82	3.11	8.88	8.34	-2.43	375.23	0.002
676	0.188	2375	0.434	164.00	3.42	8.38	8.54	-4.57	388.05	0.002
677	0.148	2408	0.384	180.32	3.67	11.00	11.00	-4.28	383.00	0.002
678	0.147	2414	0.440	183.00	3.68	9.40	9.40	-4.81	381.00	0.001
679	0.088	2480	0.338	148.81	3.75	13.30	13.30	-5.01	318.00	0.001
680	0.135	2457	0.400	137.00	3.30	9.80	9.28	-7.38	357.73	0.002
681	0.188	2380	0.467	175.00	3.38	7.38	6.87	-6.44	370.21	0.003
682	0.284	2180	0.882	185.00	2.80	3.00	3.00	-8.18	402.00	0.003
683	0.181	2387	0.484	171.00	3.34	8.22	8.88	-7.88	378.85	0.003
684	0.188	2341	0.484	184.00	3.38	7.47	7.88	-8.18	379.43	0.002
685	0.180	2338	0.480	174.00	3.12	6.88	6.78	-8.80	374.88	0.004
686	0.147	2411	0.412	138.44	2.74	8.18	8.18	-8.00	373.18	0.003
687	0.088	2500	0.318	148.88	4.40	12.80	12.80	-4.88	391.88	0.018
688	0.148	2403	0.448	142.13	2.85	4.88	4.74	-10.88	388.84	0.003
689	0.182	2381	0.488	148.38	2.88	3.88	3.88	-13.38	408.38	0.003
690	0.181	2388	0.478	138.47	2.88	3.48	3.48	-13.48	402.48	0.004
691	0.172	2388	0.488	138.88	2.88	3.34	3.38	-18.88	404.88	0.003
692	0.182	2382	0.478	148.38	2.88	3.18	3.18	-12.18	407.31	0.002
693	0.184	2388	0.448	138.88	2.88	3.88	3.18	-13.88	414.41	0.002
694	0.188	2400	0.342	138.00	2.78	7.80	7.80	-8.18	388.84	0.004
695	0.388	2180	0.801	174.00	2.38	2.78	2.78	-7.88	388.00	0.003
696	0.188	2387	0.388	138.88	2.88	7.88	7.88	-7.88	348.88	0.002
697	0.188	2371	0.347	132.97	2.82	6.88	6.88	-8.97	384.88	0.003
698	0.381	2388	0.482	188.88	2.41	2.38	2.38	-6.18	388.88	0.003
699	0.188	2343	0.330	138.87	2.88	7.48	7.48	-7.38	388.91	0.003
700	0.184	2383	0.367	134.88	2.87	6.88	6.87	-4.12	381.22	0.001
701	0.188	2322	0.418	187.00	2.88	4.38	4.38	-4.88	382.88	0.004
702	0.187	2371	0.380	111.00	2.82	18.10	18.10	-4.88	317.88	0.004
703	0.387	2380	0.417	188.88	2.85	3.88	3.88	-7.88	388.88	0.003
704	0.188	2388	0.341	148.88	2.81	18.88	18.88	-4.88	388.88	0.003
705	0.171	2381	0.378	174.88	2.78	6.88	6.88	-3.88	381.88	0.003
706	0.178	2388	0.330	181.88	2.88	18.18	18.18	-3.88	388.88	0.004
707	0.184	2388	0.388	181.88	2.88	7.18	7.18	-4.31	387.31	0.003
708	0.182	2383	0.348	178.88	3.18	8.61	8.78	-4.37	388.88	0.004
709	0.188	2382	0.418	172.88	3.13	8.38	8.38	-7.81	388.88	0.003
710	0.194	2388	0.381	144.14	2.88	4.88	4.88	-8.31	387.88	0.003
711	0.188	2378	0.414	112.74	2.84	4.47	4.88	-11.88	378.84	0.003
712	0.188	2371	0.408	113.10	2.84	3.78	3.88	-12.88	388.22	0.003
713	0.181	2381	0.408	110.21	2.88	3.84	3.84	-11.38	387.88	0.002
714	0.181	2381	0.408	110.88	2.88	3.71	3.88	-10.88	388.88	0.003
715	0.188	2388	0.408	112.88	2.88	3.88	3.78	-10.91	378.84	0.003
716	0.181	2382	0.414	114.12	2.88	3.88	3.88	-11.81	378.81	0.002
717	0.188	2381	0.431	128.88	2.88	8.88	8.88	-18.77	388.88	0.003
718	0.181	2388	0.408	188.81	2.84	4.81	3.88	-18.77	381.88	0.003
719	0.141	2415	0.384	181.87	3.81	4.88	4.27	-11.31	384.88	0.002
720	0.188	2388	0.412	188.40	2.81	4.88	4.18	-18.38	377.88	0.003

06-35-017-09W4M

DEPTH	PHID	DENS	PHIN	GR	PEF	LLD	LLS	SP	DTL	FFI
721	0.288	2170	0.388	108.87	2.88	3.78	3.57	-8.48	378.88	0.003
722	0.183	2383	0.407	108.84	2.81	4.03	3.82	-8.48	378.43	0.002
723	0.183	2408	0.408	99.31	2.88	4.08	4.03	-7.88	370.27	0.004
724	0.084	2540	0.383	102.83	3.80	4.87	4.51	-7.12	381.00	0.003
725	0.118	2433	0.388	103.48	3.07	5.32	5.30	-7.80	381.00	0.006
726	0.188	2388	0.383	100.88	2.78	4.77	4.88	-7.88	385.80	0.007
727	0.188	2388	0.411	108.88	2.81	3.84	3.88	-8.17	378.22	0.002
728	0.188	2374	0.408	108.47	2.71	3.80	3.88	-8.18	378.27	0.003
729	0.273	2200	0.482	123.00	2.83	2.80	2.80	-7.73	408.00	0.003
730	0.130	2480	0.383	88.00	2.83	4.10	4.10	-7.88	387.00	0.004
731	0.384	2010	0.388	111.82	2.83	4.11	3.88	-8.28	388.84	0.004
732	0.287	2182	0.411	117.10	2.73	4.28	4.18	-8.13	370.81	0.004
733	0.177	2382	0.387	117.31	2.80	4.78	4.70	-4.11	384.88	0.008
734	0.080	2800	0.387	118.48	2.78	5.01	4.87	-4.73	348.00	0.004
735	0.407	1880	0.488	123.88	2.41	3.80	3.80	-3.23	372.87	0.008
736	0.434	1810	0.388	120.80	2.88	4.04	3.83	-3.18	377.34	0.004
737	0.382	2047	0.438	121.88	2.83	3.88	3.87	-2.80	378.88	0.008
738	0.844	1780	0.422	118.48	2.47	3.80	3.80	-3.42	378.08	0.008
739	0.442	1800	0.438	128.08	2.38	3.83	3.80	-3.84	384.80	0.004
740	0.288	2280	0.447	128.73	2.88	3.88	3.82	-4.70	378.78	0.004
741	0.128	2480	0.438	118.42	3.31	4.78	4.82	-4.10	384.83	0.008
742	0.333	2100	0.438	114.88	2.78	4.18	4.03	-2.80	370.88	0.004
743	0.138	2440	0.384	112.88	3.08	4.81	4.48	-3.81	388.13	0.008
744	0.181	2800	0.378	117.88	2.78	4.08	4.12	-2.74	378.48	0.008
745	0.184	2880	0.418	114.14	2.82	4.42	4.37	-3.88	387.81	0.008
746	0.188	2882	0.378	117.00	2.74	4.88	4.38	-3.38	388.23	0.008
747	0.138	2421	0.401	108.80	2.88	5.28	5.18	-4.38	348.00	0.004
748	0.118	2488	0.388	88.00	3.08	5.38	5.08	-4.83	348.00	0.004
749	0.807	2810	0.418	118.00	2.74	3.77	3.80	-8.03	378.14	0.008
750	0.182	2880	0.378	112.88	2.84	3.88	3.80	-8.30	382.81	0.008
751	0.188	2888	0.438	110.78	2.84	3.88	3.88	-7.82	382.88	0.002
752	0.087	2488	0.380	100.00	3.88	6.18	6.18	-4.88	388.00	0.008
753	0.180	2884	0.384	101.28	2.88	5.88	5.88	-3.12	388.88	0.004
754	0.188	2878	0.318	100.71	2.73	5.38	5.12	-3.84	380.08	0.004
755	0.181	2882	0.344	88.70	2.88	5.10	4.87	-3.84	342.81	0.004
756	0.188	2888	0.340	108.22	2.73	5.10	4.88	-3.88	347.88	0.004
757	0.180	2878	0.388	101.78	2.81	5.84	5.88	-1.88	387.48	0.008
758	0.123	2480	0.348	108.18	2.88	5.88	5.44	-1.88	388.80	0.008
759	0.184	2843	0.382	88.00	2.81	5.88	5.88	-0.84	348.88	0.008
760	0.272	2800	0.438	117.00	3.30	3.78	3.78	-1.88	388.21	0.012
761	0.188	2888	0.348	88.88	2.83	5.27	5.08	-3.00	348.88	0.008
762	0.182	2888	0.340	100.28	2.82	4.88	4.88	-4.88	348.81	0.007
763	0.183	2888	0.348	108.08	2.88	4.88	4.88	-4.88	344.88	0.008
764	0.182	2884	0.387	111.00	3.08	4.38	4.38	-4.00	388.18	0.002
765	0.183	2888	0.318	81.87	2.78	5.08	4.87	-0.88	388.84	0.011
766	0.138	2423	0.388	88.72	2.88	5.87	5.88	-1.88	382.18	0.004
767	0.184	2401	0.274	78.00	2.48	6.80	6.80	1.27	387.00	0.007
768	0.182	2887	0.278	80.82	2.38	5.82	5.88	1.88	384.88	0.007
769	0.213	2800	0.388	111.00	2.84	3.88	3.88	2.80	388.00	0.012
770	0.182	2400	0.388	81.82	2.48	7.07	7.33	2.80	384.88	0.010
771	0.148	2400	0.287	88.10	2.88	7.83	7.88	2.80	388.88	0.008
772	0.138	2423	0.384	108.82	2.88	8.23	8.07	2.80	381.00	0.004
773	0.138	2448	0.382	108.88	2.88	8.00	7.88	2.00	388.88	0.004
774	0.122	2448	0.380	108.88	2.82	7.80	7.33	1.80	388.78	0.007
775	0.188	2400	0.313	78.88	2.72	7.84	7.88	8.33	387.88	0.008
776	0.148	2418	0.318	82.78	2.71	8.23	8.00	8.00	387.88	0.013
777	0.121	2448	0.388	88.84	2.78	8.40	7.81	8.00	388.87	0.008
778	0.123	2488	0.388	108.00	2.88	7.88	7.78	7.88	387.88	0.008
779	0.107	2488	0.388	108.88	2.83	8.11	7.88	8.00	388.77	0.007
780	0.138	2448	0.382	88.88	2.88	8.88	8.88	8.88	388.84	0.008
781	0.138	2400	0.388	88.88	2.88	8.71	8.23	7.80	388.78	0.008
782	0.578	2828	0.388	88.87	2.80	8.88	8.23	7.88	388.88	0.017
783	0.138	2432	0.384	88.88	2.38	8.13	8.78	8.88	384.97	0.008
784	0.144	2484	0.388	88.87	2.84	7.81	7.78	8.88	388.88	0.008
785	0.288	2800	0.388	48.88	2.48	3.78	3.78	18.88	388.88	0.188
786	0.181	2388	0.331	108.88	2.80	6.38	6.71	3.82	317.73	0.010

00-35-017-09W4M										
DEPTH	PHD	DENS	PHIN	GR	PEF	LLD	LLS	SP	DTL	FFI
787	0.161	2387	0.308	98.61	2.58	7.79	7.08	2.93	307.08	0.007
788	0.162	2384	0.309	98.77	2.63	7.34	6.98	1.08	305.17	0.008
789	0.160	2402	0.317	101.17	2.62	6.89	6.84	-0.42	307.66	0.004
790	0.138	2438	0.327	100.67	2.98	6.38	6.23	-1.50	308.61	0.008
791	0.138	2418	0.298	98.89	2.55	6.77	6.67	0.00	308.08	0.008
792	0.147	2410	0.301	102.28	2.61	6.47	6.48	-2.00	310.98	0.008
793	0.148	2405	0.320	102.71	2.67	6.42	6.34	-0.50	312.88	0.008
794	0.138	2418	0.330	97.63	2.62	6.31	6.01	-2.50	315.94	0.010
795	0.143	2413	0.334	98.77	2.70	6.21	6.28	-4.50	322.52	0.004
796	0.144	2418	0.318	100.11	2.68	6.94	6.70	-4.50	318.27	0.003
797	0.144	2410	0.318	98.68	2.67	6.56	6.44	-3.00	318.78	0.004
798	0.208	2305	0.440	123.00	2.47	2.80	2.80	-4.00	365.00	0.009
799	0.192	2433	0.333	98.85	2.68	5.00	5.00	-5.00	327.02	0.008
800	0.148	2414	0.340	108.41	2.68	4.98	4.78	-5.00	333.50	0.002
801	0.148	2410	0.330	107.71	2.68	4.67	4.80	-5.50	335.15	0.003
802	0.182	2400	0.314	98.38	2.60	3.08	3.08	-4.01	329.00	0.003
803	0.173	2380	0.298	90.70	2.63	6.00	6.00	-3.48	312.08	0.008
804	0.288	2225	0.802	129.00	2.58	1.73	1.73	-5.29	388.00	0.004
805	0.147	2383	0.315	98.61	2.65	6.67	6.50	-3.03	319.62	0.002
806	0.131	2431	0.337	98.42	2.72	4.78	4.80	-0.79	320.46	0.005
807	0.151	2398	0.303	98.74	2.54	6.58	6.46	2.51	302.88	0.014
808	0.173	2375	0.295	87.45	2.67	6.64	6.70	2.25	295.50	0.010
809	0.131	2425	0.309	90.35	2.98	6.77	6.84	0.67	298.81	0.007
810	0.188	2403	0.308	92.00	2.65	6.18	6.20	3.58	305.43	0.010
811	0.138	2419	0.308	90.31	2.48	6.83	6.70	2.21	314.18	0.008
812	0.138	2422	0.318	102.08	2.67	6.38	6.18	0.28	318.67	0.008
813	0.182	2384	0.405	105.02	3.02	3.68	3.72	-1.30	385.90	0.008
814	0.288	2348	0.310	48.01	2.17	4.08	3.70	10.00	385.08	0.183
815	0.282	2180	0.315	51.12	2.30	3.78	3.53	12.80	383.85	0.188
816	0.248	2348	0.307	85.47	2.37	4.18	3.85	14.80	387.58	0.084
817	0.288	2210	0.488	90.38	2.38	2.98	2.54	2.75	378.28	0.018
818	0.187	2385	0.380	88.08	2.44	3.85	3.62	6.31	343.29	0.064
819	0.201	2351	0.311	98.77	2.80	6.80	6.44	10.89	312.39	0.078
820	0.208	2300	0.302	70.88	2.44	5.91	5.54	10.12	318.77	0.080
821	0.180	2330	0.308	78.68	2.62	5.88	5.88	6.58	314.77	0.087
822	0.213	2302	0.367	69.41	2.67	3.83	3.41	2.21	348.04	0.088
823	0.288	2080	0.481	119.00	2.51	1.88	1.88	2.40	408.00	0.008
824	0.181	2318	0.388	88.28	2.68	3.88	4.01	6.80	381.80	0.112
825	0.248	2380	0.328	67.54	2.68	4.78	4.38	18.47	318.28	0.185
826	0.247	2238	0.321	74.48	2.38	4.87	4.41	17.41	319.51	0.190
827	0.220	2305	0.322	70.88	2.78	5.10	4.78	18.48	314.58	0.188
828	0.238	2385	0.387	72.12	2.48	5.15	4.88	19.80	327.25	0.110
829	0.244	2280	0.338	60.88	2.38	4.74	4.63	13.37	312.80	0.188
830	0.138	2440	0.385	68.85	3.30	7.78	7.70	14.68	274.00	0.111
831	0.222	2308	0.315	70.84	2.31	5.34	5.01	11.63	310.78	0.070
832	0.218	2304	0.333	71.84	2.42	5.21	5.15	9.22	312.85	0.088
833	0.223	2385	0.322	68.18	2.48	4.83	5.00	9.57	315.53	0.115
834	0.187	2318	0.312	72.88	2.37	5.82	5.91	7.80	310.75	0.080
835	0.187	2378	0.301	82.34	2.37	6.18	6.10	3.00	308.18	0.088
836	0.187	2385	0.288	83.34	2.37	6.04	5.75	3.30	308.57	0.080
837	0.124	2480	0.283	78.88	2.62	6.67	6.08	1.78	290.78	0.017
838	0.182	2380	0.422	98.80	2.68	2.75	2.75	0.12	388.57	0.008
839	0.188	2385	0.302	85.82	2.51	5.25	5.25	0.88	318.15	0.017
840	0.181	2388	0.385	85.64	2.68	3.85	3.67	2.34	384.88	0.018
841	0.178	2381	0.444	94.61	2.65	2.30	2.30	2.10	400.00	0.018
842	0.228	2385	0.497	91.67	2.67	2.48	2.41	1.97	387.72	0.017
843	0.188	2387	0.373	80.38	2.74	3.10	3.13	0.97	380.88	0.007
844	0.188	2383	0.483	85.83	2.73	2.75	2.75	0.18	378.82	0.008
845	0.188	2384	0.485	88.15	2.73	2.80	2.61	1.01	387.94	0.008
846	0.213	2385	0.518	95.04	2.67	2.31	2.34	1.88	388.78	0.010
847	0.188	2384	0.447	98.12	2.70	2.55	2.55	1.25	377.48	0.007
848	0.210	2388	0.504	98.28	2.63	2.44	2.55	2.01	384.57	0.008
849	0.187	2480	0.330	84.48	2.80	6.00	5.88	4.75	311.28	0.047
850	0.171	2372	0.321	84.85	2.48	5.80	5.78	7.08	312.88	0.042
851	0.180	2384	0.307	78.80	2.67	5.88	5.75	6.88	311.78	0.054
852	0.138	2414	0.322	78.08	2.47	6.03	5.87	6.21	307.38	0.008

06-36-017-09W4M										
DEPTH	PHI	DENS	PHIN	GR	PEF	LLD	L.S	SP	DTL	FFI
853	0.176	2363	0.308	71.27	2.42	5.66	5.48	8.59	317.12	0.085
854	0.185	2368	0.310	72.38	2.42	5.66	5.56	7.71	319.34	0.080
855	0.113	2452	0.318	73.61	3.45	6.25	6.01	8.98	312.30	0.088
856	0.187	2365	0.318	73.19	2.48	5.58	5.36	9.41	314.80	0.078
857	0.327	2115	0.332	84.38	2.54	4.28	4.23	4.92	308.38	0.523
858	0.285	2180	0.443	83.88	2.48	2.80	2.80	1.79	308.12	0.008
859	0.212	2267	0.382	88.30	2.64	3.40	3.40	1.38	304.70	0.008
860	0.314	2140	0.480	87.88	2.68	2.70	2.68	2.10	303.88	0.010
861	0.333	2100	0.384	84.87	2.82	2.58	2.61	1.90	304.08	0.014
862	0.241	2250	0.438	83.88	2.65	2.81	2.71	2.22	378.38	0.008
863	0.280	2178	0.407	104.88	2.63	2.71	2.88	0.49	378.08	0.004
864	0.343	2088	0.418	88.08	2.63	2.73	2.78	0.55	378.48	0.004
865	0.248	2253	0.408	87.88	2.68	2.87	2.82	0.70	371.18	0.004
866	0.240	2242	0.408	81.32	2.68	2.78	2.83	-0.68	388.88	0.002
867	0.218	2281	0.433	88.02	2.62	2.83	2.81	-1.18	384.78	0.001
868	0.234	2298	0.388	84.22	2.68	2.87	2.84	-0.81	388.88	0.002
869	0.402	1888	0.688	78.88	2.18	1.80	1.80	-1.25	402.88	0.002
870	0.313	2138	0.416	80.57	2.48	2.17	2.00	-0.48	381.17	0.008
871	0.237	2280	0.402	88.70	2.80	2.82	2.38	1.01	377.88	0.003
872	0.388	2038	0.448	88.18	2.80	2.80	2.48	3.41	388.00	0.008
873	0.167	2375	0.348	88.84	2.83	3.21	3.08	6.34	388.88	0.008
874	0.228	2288	0.373	91.38	2.41	4.88	4.84	10.08	384.00	0.042
875	0.348	2250	0.388	87.01	2.41	6.42	6.00	18.08	341.48	0.088
876	0.228	2273	0.382	88.88	2.88	6.80	6.04	13.00	387.42	0.088
877	0.188	2388	0.274	74.82	2.42	6.72	6.80	12.00	308.88	0.088
878	0.088	2488	0.314	82.23	2.78	6.30	6.17	8.91	304.41	0.011
879	0.138	2443	0.388	118.00	2.85	4.34	4.83	7.98	308.34	0.008
880	0.170	2380	0.383	103.83	2.64	4.12	4.34	7.82	304.73	0.018
881	0.238	2270	0.380	87.38	2.80	3.80	3.88	8.48	308.88	0.021
882	0.121	2418	0.434	87.00	2.78	3.97	3.81	8.53	308.87	0.008

Appendix B: Core analysis porosity and permeability measurements for 5-7 and 6-35 as obtained from the Energy Resources Conservation Board (depth corrected as indicated to match log depths), and computed ratio of Kv to Kmaxi

Depth (m below KB)	Thickness of core interval (m) - Di	Porosity (fractional) Pi	Permeability (md)			Kv / Kmaxi
			Kmaxi (horizontal)	K90 (horizontal)	Kv (vertical)	
65-67-617-671401						
Bow Island Formation Core (subtracted 1.00 m from original core depth)						
769.50	0.44	NA	NA	NA	NA	NA
769.94	0.56	0.128	6.00	5.44	0.75	0.11
770.50	0.17	0.128	6.00	5.44	0.75	0.11
770.67	0.75	0.153	24.90	21.50	2.55	0.10
771.42	0.06	0.145	8.48	7.05	3.99	0.47
771.50	0.43	0.145	8.48	7.05	3.99	0.47
771.93	0.57	0.132	22.70	22.60	0.51	0.02
772.50	0.23	0.132	22.70	22.60	0.51	0.02
772.73	0.31	0.239	1074.00	1048.00	726.00	0.69
773.04	0.21	0.224	439.00	344.00	134.00	0.31
773.25	0.25	0.233	626.00	590.00	239.00	0.39
773.50	0.03	0.233	626.00	590.00	239.00	0.39
773.53	0.41	0.250	908.00	592.00	353.00	0.59
773.94	0.41	0.280	1375.00	NA	NA	NA
774.35	0.01	NA	NA	NA	NA	NA
774.38	0.14	0.244	485.00	450.00	139.00	0.30
774.50	0.24	0.244	485.00	450.00	139.00	0.30
774.74	0.52	0.237	227.00	214.00	89.90	0.39
775.28	0.24	0.247	373.00	NA	NA	NA
775.50	0.20	0.247	373.00	NA	NA	NA
775.70	0.80	NA	NA	NA	NA	NA
Basal Colorado Sandstone Core (no depth correction)						
867.50	0.52	NA	NA	NA	NA	NA
868.02	0.48	0.183	147.00	117.00	19.10	0.13
868.50	0.10	NA	NA	NA	NA	
868.60	0.26	0.142	98.10	55.90	13.20	0.19
868.86	0.02	NA	NA	NA	NA	
868.88	0.48	0.200	99.90	67.00	16.30	0.16
869.26	0.14	0.167	30.00	28.40	3.77	0.13
869.50	0.18	0.167	30.00	28.40	3.77	0.13
869.66	0.25	0.130	3.03	2.98	0.34	0.11
869.93	0.02	NA	NA	NA	NA	NA
869.95	0.33	NA	NA	NA	NA	NA
870.28	0.06	NA	NA	NA	NA	NA
870.34	0.16	0.138	8.13	7.83	0.94	0.12
870.50	0.46	0.138	8.13	7.83	0.94	0.12
870.66	0.50	0.110	311.00	179.00	123.00	0.40
871.46	0.04	0.098	1.25	1.17	0.08	0.06
871.50	0.76	0.098	1.25	1.17	0.08	0.06
872.26	0.13	NA	NA	NA	NA	NA
872.39	0.11	0.142	45.90	27.70	3.64	0.08
872.50	0.65	0.142	45.90	27.70	3.64	0.08
873.15	0.35	0.117	23.50	9.70	0.63	0.03
873.50	0.14	0.117	23.50	9.70	0.63	0.03

Depth (m below KB)	Thickness of core interval (m) - Di	Porosity (fractional) Pi	Permeability (md)			Kv / Kmaxi
			Kmaxi (horizontal)	K90 (horizontal)	Kv (vertical)	
873.64	0.82	NA	NA	NA	NA	NA
874.46	0.04	0.220	392.00	349.00	126.00	0.32
874.50	0.41	0.220	392.00	349.00	126.00	0.32
874.91	0.59	NA	NA	NA	NA	NA
66-35-017-001W-001						
Bow Island Formation Core (added 8.59 m to original core depth)						
764.41	0.18	0.202	18.10	NA	NA	NA
764.59	0.52	0.132	86.00	NA	NA	NA
765.11	0.26	0.152	0.54	NA	NA	NA
765.37	0.13	0.119	0.41	0.32	0.17	0.41
765.50	0.13	0.119	0.41	NA	NA	NA
765.63	0.10	0.146	0.18	NA	NA	NA
765.73	0.30	0.105	0.56	0.44	0.03	0.05
766.03	0.22	0.156	12.60	NA	NA	NA
766.25	0.18	0.197	75.60	NA	NA	NA
766.43	0.07	0.150	0.26	NA	NA	NA
766.50	0.03	0.180	0.26	NA	NA	NA
766.53	0.08	0.148	0.49	NA	NA	NA
766.61	0.25	0.122	1.45	1.43	0.26	0.18
766.86	0.21	0.150	2.86	NA	NA	NA
767.07	0.19	0.162	3.47	NA	NA	NA
767.26	0.11	0.170	2.86	NA	NA	NA
767.37	0.13	0.159	17.30	NA	NA	NA
767.50	0.13	0.159	17.30	NA	NA	NA
767.63	0.18	0.162	48.40	NA	NA	NA
767.81	0.10	0.168	2.28	NA	NA	NA
767.91	0.30	0.157	13.40	13.20	4.00	0.30
768.21	0.24	0.171	7.63	NA	NA	NA
768.45	0.05	NA	NA	NA	NA	NA
768.50	0.10	NA	NA	NA	NA	NA
768.60	0.31	0.155	26.80	26.70	2.32	0.09
768.91	0.29	0.189	3.62	NA	NA	NA
769.20	0.28	0.161	0.96	NA	NA	NA
769.48	0.02	0.184	4.04	3.99	0.44	0.11
769.50	0.20	0.184	4.04	3.99	0.44	0.11
769.70	0.32	0.149	0.44	NA	NA	NA
770.02	0.28	0.184	1.86	NA	NA	NA
770.26	0.22	0.141	0.36	NA	NA	NA
770.50	0.02	0.141	0.36	NA	NA	NA
770.52	0.30	0.165	2.32	NA	NA	NA
770.62	0.29	0.127	1.46	1.44	0.22	0.15
771.11	0.39	0.154	0.60	NA	NA	NA
771.44	0.06	0.151	0.21	NA	NA	NA
771.50	0.24	0.151	0.21	NA	NA	NA
771.74	0.15	0.136	0.22	NA	NA	NA
771.89	0.61	NA	NA	NA	NA	NA
772.50	1.00	NA	NA	NA	NA	NA
773.50	0.64	NA	NA	NA	NA	NA
774.34	0.09	0.230	35.60	NA	NA	NA
774.43	0.04	NA	NA	NA	NA	NA

Depth (m below KB)	Thickness of core interval (m) - Di	Porosity (fractional) Pi	Permeability (md)			Kv / Kmaxi
			Kmaxi (horizontal)	K90 (horizontal)	Kv (vertical)	
774.47	0.03	0.221	16.40	15.80	1.71	0.10
774.50	0.09	0.221	16.40	15.80	1.71	0.10
774.59	0.19	0.218	6.43	NA	NA	NA
774.78	0.14	0.174	5.02	NA	NA	NA
774.92	0.03	NA	NA	NA	NA	NA
774.95	0.06	0.212	22.50	NA	NA	NA
775.01	0.24	NA	NA	NA	NA	NA
775.25	0.09	0.149	1.86	NA	NA	NA
775.34	0.16	NA	NA	NA	NA	NA
775.50	1.00	NA	NA	NA	NA	NA
776.50	0.18	NA	NA	NA	NA	NA
776.68	0.10	0.155	1.89	NA	NA	NA
776.78	0.72	NA	NA	NA	NA	NA
777.50	0.13	NA	NA	NA	NA	NA
777.63	0.12	0.145	1.92	NA	NA	NA
777.75	0.75	NA	NA	NA	NA	NA
Basal Colorado Sandstone Core (added 6.29 m to original core depth)						
873.50	0.53	NA	NA	NA	NA	NA
874.03	0.09	0.254	135.00	NA	NA	NA
874.12	0.19	0.289	188.00	NA	NA	NA
874.31	0.17	0.256	299.00	290.00	118.00	0.39
874.48	0.02	0.275	295.00	NA	NA	NA
874.50	0.09	0.275	295.00	NA	NA	NA
874.59	0.13	0.248	167.00	NA	NA	NA
874.72	0.20	0.246	118.00	NA	NA	NA
874.92	0.16	0.238	80.40	NA	NA	NA
875.08	0.15	0.233	231.00	207.00	78.70	0.34
875.23	0.12	0.236	87.10	NA	NA	NA
875.36	0.09	0.249	91.10	NA	NA	NA
875.44	0.08	0.222	81.80	81.30	21.50	0.26
875.50	0.17	0.222	81.80	NA	NA	NA
875.67	0.16	0.224	31.70	NA	NA	NA
875.83	0.10	0.241	58.10	NA	NA	NA
875.93	0.15	0.205	15.30	NA	NA	NA
876.08	0.28	0.201	15.40	NA	NA	NA
876.36	0.14	0.173	4.80	NA	NA	NA
876.50	0.06	0.173	4.80	NA	NA	NA
876.56	0.10	0.242	43.30	NA	NA	NA
876.66	0.21	0.161	18.30	12.60	2.62	0.14
876.87	0.16	0.161	3.67	NA	NA	NA
877.03	0.14	0.154	2.53	NA	NA	NA
877.17	0.15	0.196	63.20	51.10	4.47	0.06
877.32	0.16	0.117	1.01	NA	NA	NA
877.50	0.17	0.117	1.01	NA	NA	NA
877.67	0.21	0.129	4.23	NA	NA	NA
877.86	0.11	0.144	1.45	NA	NA	NA
877.99	0.21	0.079	0.16	NA	NA	NA
878.20	0.30	NA	NA	NA	NA	NA
878.50	0.07	0.144	15.30	NA	NA	NA
878.57	0.63	NA	NA	NA	NA	NA

Depth (m below KB)	Thickness of core interval (m) - DI	Porosity (fractional) Pi	Permeability (md)			Kv / Kmaxi
			Kmaxi (horizontal)	K90 (horizontal)	Kv (vertical)	
879.20	0.28	0.178	18.60	NA	NA	NA
879.48	0.02	NA	NA	NA	NA	NA
879.50	0.28	NA	NA	NA	NA	NA
879.78	0.08	0.229	312.00	NA	NA	NA
879.86	0.64	NA	NA	NA	NA	NA
880.50	0.82	NA	NA	NA	NA	NA
881.32	0.16	0.146	0.49	NA	NA	NA
881.48	0.02	0.130	4.08	3.84	0.98	0.24
881.50	0.20	0.130	4.08	3.84	0.98	0.24
881.70	0.22	0.083	0.03	NA	NA	NA
881.82	0.26	0.056	NA	NA	NA	NA
882.18	0.15	0.091	0.35	0.34	NA	NA
882.33	0.14	0.141	0.45	NA	NA	NA
882.47	0.03	0.136	2.55	1.97	0.59	0.23
882.50	0.14	0.136	2.55	1.97	0.59	0.23
882.64	0.60	0.146	1.01	NA	NA	NA
883.33	0.17	0.151	4.05	4.04	1.38	0.34
883.50	0.02	0.151	4.05	4.04	1.38	0.34
883.52	0.36	0.141	4.78	4.58	0.75	0.16
883.88	0.62	NA	NA	NA	NA	NA

[illegible]

[illegible]

[illegible]

ITEM	W1	W2	W3	W4	W5	W6	W7	W8	W9	W10	W11	W12	W13	W14	W15	W16	W17	W18	W19	W20	W21	W22	W23	W24	W25	W26	W27	W28	W29	W30	W31	W32	W33	W34	W35	W36	W37	W38	W39	W40	W41	W42	W43	W44	W45	W46	W47	W48	W49	W50	W51	W52	W53	W54	W55	W56	W57	W58	W59	W60	W61	W62	W63	W64	W65	W66	W67	W68	W69	W70	W71	W72	W73	W74	W75	W76	W77	W78	W79	W80	W81	W82	W83	W84	W85	W86	W87	W88	W89	W90	W91	W92	W93	W94	W95	W96	W97	W98	W99	W100	W101	W102	W103	W104	W105	W106	W107	W108	W109	W110	W111	W112	W113	W114	W115	W116	W117	W118	W119	W120	W121	W122	W123	W124	W125	W126	W127	W128	W129	W130	W131	W132	W133	W134	W135	W136	W137	W138	W139	W140	W141	W142	W143	W144	W145	W146	W147	W148	W149	W150	W151	W152	W153	W154	W155	W156	W157	W158	W159	W160	W161	W162	W163	W164	W165	W166	W167	W168	W169	W170	W171	W172	W173	W174	W175	W176	W177	W178	W179	W180	W181	W182	W183	W184	W185	W186	W187	W188	W189	W190	W191	W192	W193	W194	W195	W196	W197	W198	W199	W200	W201	W202	W203	W204	W205	W206	W207	W208	W209	W210	W211	W212	W213	W214	W215	W216	W217	W218	W219	W220	W221	W222	W223	W224	W225	W226	W227	W228	W229	W230	W231	W232	W233	W234	W235	W236	W237	W238	W239	W240	W241	W242	W243	W244	W245	W246	W247	W248	W249	W250	W251	W252	W253	W254	W255	W256	W257	W258	W259	W260	W261	W262	W263	W264	W265	W266	W267	W268	W269	W270	W271	W272	W273	W274	W275	W276	W277	W278	W279	W280	W281	W282	W283	W284	W285	W286	W287	W288	W289	W290	W291	W292	W293	W294	W295	W296	W297	W298	W299	W300	W301	W302	W303	W304	W305	W306	W307	W308	W309	W310	W311	W312	W313	W314	W315	W316	W317	W318	W319	W320	W321	W322	W323	W324	W325	W326	W327	W328	W329	W330	W331	W332	W333	W334	W335	W336	W337	W338	W339	W340	W341	W342	W343	W344	W345	W346	W347	W348	W349	W350	W351	W352	W353	W354	W355	W356	W357	W358	W359	W360	W361	W362	W363	W364	W365	W366	W367	W368	W369	W370	W371	W372	W373	W374	W375	W376	W377	W378	W379	W380	W381	W382	W383	W384	W385	W386	W387	W388	W389	W390	W391	W392	W393	W394	W395	W396	W397	W398	W399	W400	W401	W402	W403	W404	W405	W406	W407	W408	W409	W410	W411	W412	W413	W414	W415	W416	W417	W418	W419	W420	W421	W422	W423	W424	W425	W426	W427	W428	W429	W430	W431	W432	W433	W434	W435	W436	W437	W438	W439	W440	W441	W442	W443	W444	W445	W446	W447	W448	W449	W450	W451	W452	W453	W454	W455	W456	W457	W458	W459	W460	W461	W462	W463	W464	W465	W466	W467	W468	W469	W470	W471	W472	W473	W474	W475	W476	W477	W478	W479	W480	W481	W482	W483	W484	W485	W486	W487	W488	W489	W490	W491	W492	W493	W494	W495	W496	W497	W498	W499	W500	W501	W502	W503	W504	W505	W506	W507	W508	W509	W510	W511	W512	W513	W514	W515	W516	W517	W518	W519	W520	W521	W522	W523	W524	W525	W526	W527	W528	W529	W530	W531	W532	W533	W534	W535	W536	W537	W538	W539	W540	W541	W542	W543	W544	W545	W546	W547	W548	W549	W550	W551	W552	W553	W554	W555	W556	W557	W558	W559	W560	W561	W562	W563	W564	W565	W566	W567	W568	W569	W570	W571	W572	W573	W574	W575	W576	W577	W578	W579	W580	W581	W582	W583	W584	W585	W586	W587	W588	W589	W590	W591	W592	W593	W594	W595	W596	W597	W598	W599	W600	W601	W602	W603	W604	W605	W606	W607	W608	W609	W610	W611	W612	W613	W614	W615	W616	W617	W618	W619	W620	W621	W622	W623	W624	W625	W626	W627	W628	W629	W630	W631	W632	W633	W634	W635	W636	W637	W638	W639	W640	W641	W642	W643	W644	W645	W646	W647	W648	W649	W650	W651	W652	W653	W654	W655	W656	W657	W658	W659	W660	W661	W662	W663	W664	W665	W666	W667	W668	W669	W670	W671	W672	W673	W674	W675	W676	W677	W678	W679	W680	W681	W682	W683	W684	W685	W686	W687	W688	W689	W690	W691	W692	W693	W694	W695	W696	W697	W698	W699	W700	W701	W702	W703	W704	W705	W706	W707	W708	W709	W710	W711	W712	W713	W714	W715	W716	W717	W718	W719	W720	W721	W722	W723	W724	W725	W726	W727	W728	W729	W730	W731	W732	W733	W734	W735	W736	W737	W738	W739	W740	W741	W742	W743	W744	W745	W746	W747	W748	W749	W750	W751	W752	W753	W754	W755	W756	W757	W758	W759	W760	W761	W762	W763	W764	W765	W766	W767	W768	W769	W770	W771	W772	W773	W774	W775	W776	W777	W778	W779	W780	W781	W782	W783	W784	W785	W786	W787	W788	W789	W790	W791	W792	W793	W794	W795	W796	W797	W798	W799	W800	W801	W802	W803	W804	W805	W806	W807	W808	W809	W810	W811	W812	W813	W814	W815	W816	W817	W818	W819	W820	W821	W822	W823	W824	W825	W826	W827	W828	W829	W830	W831	W832	W833	W834	W835	W836	W837	W838	W839	W840	W841	W842	W843	W844	W845	W846	W847	W848	W849	W850	W851	W852	W853	W854	W855	W856	W857	W858	W859	W860	W861	W862	W863	W864	W865	W866	W867	W868	W869	W870	W871	W872	W873	W874	W875	W876	W877	W878	W879	W880	W881	W882	W883	W884	W885	W886	W887	W888	W889	W890	W891	W892	W893	W894	W895	W896	W897	W898	W899	W900	W901	W902	W903	W904	W905	W906	W907	W908	W909	W910	W911	W912	W913	W914	W915	W916	W917	W918	W919	W920	W921	W922	W923	W924	W925	W926	W927	W928	W929	W930	W931	W932	W933	W934	W935	W936	W937	W938	W939	W940	W941	W942	W943	W944	W945	W946	W947	W948	W949	W950	W951	W952	W953	W954	W955	W956	W957	W958	W959	W960	W961	W962	W963	W964	W965	W966	W967	W968	W969	W970	W971	W972	W973	W974	W975	W976	W977	W978	W979	W980	W981	W982	W983	W984	W985	W986	W987	W988	W989	W990	W991	W992	W993	W994	W995	W996	W997	W998	W999	W1000	W1001	W1002	W1003	W1004	W1005	W1006	W1007	W1008	W1009	W1010	W1011	W1012	W1013	W1014	W1015	W1016	W1017	W1018	W1019	W1020	W1021	W1022	W1023	W1024	W1025	W1026	W1027	W1028	W1029	W1030	W1031	W1032	W1033	W1034	W1035	W1036	W1037	W1038	W1039	W1040	W1041	W1042	W1043	W1044	W1045	W1046	W1047	W1048	W1049	W1050	W1051	W1052	W1053	W1054	W1055	W1056	W1057	W1058	W1059	W1060	W1061	W1062	W1063	W1064	W1065	W1066	W1067	W1068	W1069	W1070	W1071	W1072	W1073	W1074	W1075	W1076	W1077	W1078	W1079	W1080	W1081	W1082	W1083	W1084	W1085	W1086	W1087	W1088	W1089	W1090	W1091	W1092	W1093	W1094	W1095	W1096	W1097	W1098	W1099	W1100	W1101	W1102	W1103	W1104	W1105	W1106	W1107	W1108	W1109	W1110	W1111	W1112	W1113	W1114	W1115	W1116	W1117	W1118	W1119	W1120	W1121	W1122	W1123	W1124	W1125	W1126	W1127	W1128	W1129	W1130	W1131	W1132	W1133	W1134	W1135	W1136	W1137	W1138	W1139	W1140	W1141	W1142	W1143	W1144	W1145	W1146	W1147	W1148	W1149	W1150	W1151	W1152	W1153	W1154	W1155	W1156	W1157	W1158	W1159	W1160	W1161	W1162	W1163	W1164	W1165	W1166	W1167	W1168	W1169	W1170	W1171	W1172	W1173	W1174	W1175	W1176	W1177	W1178	W1179	W1180	W1181	W1182	W1183	W1184	W1185	W1186	W1187	W1188	W1189	W1190	W1191	W1192	W1193	W1194	W1195	W1196	W1197	W1198	W1199	W1200	W1201	W1202	W1203	W1204	W1205	W1206	W1207	W1208	W1209	W1210	W1211	W1212	W1213	W1214	W1215	W1216	W1217	W1218	W1219	W1220	W1221	W1222	W1223	W1224	W1225	W1226	W1227	W1228	W1229	W1230	W1231	W1232	W1233	W1234	W1235	W1236	W1237	W1238	W1239	W1240	W1241	W1242	W1243	W1244	W1245	W1246	W1247	W1248	W1249	W1250	W1251	W1252	W1253	W1254	W1255	W1256	W1257	W1258	W1259	W1260	W1261	W1262	W1263	W1264	W1265	W1266	W1267	W1268	W1269	W1270	W1271	W1272	W1273	W1274	W1275	W1276	W1277	W1278	W1279	W1280	W1281	W1282	W1283	W1284	W1285	W1286	W1287	W1288	W1289	W1290	W1291	W1292	W1293	W1294	W1295	W1296	W1297	W1298	W1299	W1300	W1301	W1302	W1303	W1304	W1305	W1306	W1307	W1308	W1309	W1310	W1311	W1312	W1313	W1314	W1315	W1316	W1317	W1318	W1319	W1320	W1321	W1322	W1323	W1324	W1325	W1326	W1327	W1328	W1329	W1330	W1331	W1332	W1333	W1334	W1335	W1336	W1337	W1338	W1339	W1340	W1341	W1342	W1343	W1344	W1345	W
------	----	----	----	----	----	----	----	----	----	-----	-----	-----	-----	-----	-----	-----	-----	-----	-----	-----	-----	-----	-----	-----	-----	-----	-----	-----	-----	-----	-----	-----	-----	-----	-----	-----	-----	-----	-----	-----	-----	-----	-----	-----	-----	-----	-----	-----	-----	-----	-----	-----	-----	-----	-----	-----	-----	-----	-----	-----	-----	-----	-----	-----	-----	-----	-----	-----	-----	-----	-----	-----	-----	-----	-----	-----	-----	-----	-----	-----	-----	-----	-----	-----	-----	-----	-----	-----	-----	-----	-----	-----	-----	-----	-----	-----	-----	-----	-----	------	------	------	------	------	------	------	------	------	------	------	------	------	------	------	------	------	------	------	------	------	------	------	------	------	------	------	------	------	------	------	------	------	------	------	------	------	------	------	------	------	------	------	------	------	------	------	------	------	------	------	------	------	------	------	------	------	------	------	------	------	------	------	------	------	------	------	------	------	------	------	------	------	------	------	------	------	------	------	------	------	------	------	------	------	------	------	------	------	------	------	------	------	------	------	------	------	------	------	------	------	------	------	------	------	------	------	------	------	------	------	------	------	------	------	------	------	------	------	------	------	------	------	------	------	------	------	------	------	------	------	------	------	------	------	------	------	------	------	------	------	------	------	------	------	------	------	------	------	------	------	------	------	------	------	------	------	------	------	------	------	------	------	------	------	------	------	------	------	------	------	------	------	------	------	------	------	------	------	------	------	------	------	------	------	------	------	------	------	------	------	------	------	------	------	------	------	------	------	------	------	------	------	------	------	------	------	------	------	------	------	------	------	------	------	------	------	------	------	------	------	------	------	------	------	------	------	------	------	------	------	------	------	------	------	------	------	------	------	------	------	------	------	------	------	------	------	------	------	------	------	------	------	------	------	------	------	------	------	------	------	------	------	------	------	------	------	------	------	------	------	------	------	------	------	------	------	------	------	------	------	------	------	------	------	------	------	------	------	------	------	------	------	------	------	------	------	------	------	------	------	------	------	------	------	------	------	------	------	------	------	------	------	------	------	------	------	------	------	------	------	------	------	------	------	------	------	------	------	------	------	------	------	------	------	------	------	------	------	------	------	------	------	------	------	------	------	------	------	------	------	------	------	------	------	------	------	------	------	------	------	------	------	------	------	------	------	------	------	------	------	------	------	------	------	------	------	------	------	------	------	------	------	------	------	------	------	------	------	------	------	------	------	------	------	------	------	------	------	------	------	------	------	------	------	------	------	------	------	------	------	------	------	------	------	------	------	------	------	------	------	------	------	------	------	------	------	------	------	------	------	------	------	------	------	------	------	------	------	------	------	------	------	------	------	------	------	------	------	------	------	------	------	------	------	------	------	------	------	------	------	------	------	------	------	------	------	------	------	------	------	------	------	------	------	------	------	------	------	------	------	------	------	------	------	------	------	------	------	------	------	------	------	------	------	------	------	------	------	------	------	------	------	------	------	------	------	------	------	------	------	------	------	------	------	------	------	------	------	------	------	------	------	------	------	------	------	------	------	------	------	------	------	------	------	------	------	------	------	------	------	------	------	------	------	------	------	------	------	------	------	------	------	------	------	------	------	------	------	------	------	------	------	------	------	------	------	------	------	------	------	------	------	------	------	------	------	------	------	------	------	------	------	------	------	------	------	------	------	------	------	------	------	------	------	------	------	------	------	------	------	------	------	------	------	------	------	------	------	------	------	------	------	------	------	------	------	------	------	------	------	------	------	------	------	------	------	------	------	------	------	------	------	------	------	------	------	------	------	------	------	------	------	------	------	------	------	------	------	------	------	------	------	------	------	------	------	------	------	------	------	------	------	------	------	------	------	------	------	------	------	------	------	------	------	------	------	------	------	------	------	------	------	------	------	------	------	------	------	------	------	------	------	------	------	------	------	------	------	------	------	------	------	------	------	------	------	------	------	------	------	------	------	------	------	------	------	------	------	------	------	------	------	------	------	------	------	------	------	------	------	------	------	------	------	------	------	------	------	------	------	------	------	------	------	------	------	------	------	------	------	------	------	------	------	------	------	------	------	------	------	------	------	------	------	------	------	------	------	------	------	------	------	------	------	------	------	------	------	------	------	------	------	------	------	------	------	------	------	------	------	------	------	------	------	------	------	------	------	------	------	------	------	------	------	------	------	------	------	------	------	------	------	------	------	------	------	------	------	------	------	------	------	------	------	------	------	------	------	------	------	------	------	------	------	------	------	------	------	------	------	------	------	------	------	------	------	------	------	------	------	------	------	------	------	------	------	------	------	------	------	------	------	------	------	------	------	------	------	------	------	------	------	------	------	------	------	------	------	------	------	------	------	------	------	------	------	------	------	------	------	------	------	------	------	------	------	------	------	------	-------	-------	-------	-------	-------	-------	-------	-------	-------	-------	-------	-------	-------	-------	-------	-------	-------	-------	-------	-------	-------	-------	-------	-------	-------	-------	-------	-------	-------	-------	-------	-------	-------	-------	-------	-------	-------	-------	-------	-------	-------	-------	-------	-------	-------	-------	-------	-------	-------	-------	-------	-------	-------	-------	-------	-------	-------	-------	-------	-------	-------	-------	-------	-------	-------	-------	-------	-------	-------	-------	-------	-------	-------	-------	-------	-------	-------	-------	-------	-------	-------	-------	-------	-------	-------	-------	-------	-------	-------	-------	-------	-------	-------	-------	-------	-------	-------	-------	-------	-------	-------	-------	-------	-------	-------	-------	-------	-------	-------	-------	-------	-------	-------	-------	-------	-------	-------	-------	-------	-------	-------	-------	-------	-------	-------	-------	-------	-------	-------	-------	-------	-------	-------	-------	-------	-------	-------	-------	-------	-------	-------	-------	-------	-------	-------	-------	-------	-------	-------	-------	-------	-------	-------	-------	-------	-------	-------	-------	-------	-------	-------	-------	-------	-------	-------	-------	-------	-------	-------	-------	-------	-------	-------	-------	-------	-------	-------	-------	-------	-------	-------	-------	-------	-------	-------	-------	-------	-------	-------	-------	-------	-------	-------	-------	-------	-------	-------	-------	-------	-------	-------	-------	-------	-------	-------	-------	-------	-------	-------	-------	-------	-------	-------	-------	-------	-------	-------	-------	-------	-------	-------	-------	-------	-------	-------	-------	-------	-------	-------	-------	-------	-------	-------	-------	-------	-------	-------	-------	-------	-------	-------	-------	-------	-------	-------	-------	-------	-------	-------	-------	-------	-------	-------	-------	-------	-------	-------	-------	-------	-------	-------	-------	-------	-------	-------	-------	-------	-------	-------	-------	-------	-------	-------	-------	-------	-------	-------	-------	-------	-------	-------	-------	-------	-------	-------	-------	-------	-------	-------	-------	-------	-------	-------	-------	-------	-------	-------	-------	-------	-------	-------	-------	-------	-------	-------	-------	-------	-------	-------	-------	-------	-------	-------	-------	-------	-------	-------	-------	-------	-------	-------	-------	-------	-------	-------	-------	-------	-------	-------	-------	-------	-------	-------	-------	-------	-------	-------	-------	-------	-------	-------	-------	-------	-------	-------	-------	---

[illegible]

[illegible]

[illegible]

[illegible]

[illegible]

[illegible]